UCRL-10706
c.2

University of California

Ernest O. Lawrence Radiation Laboratory

INORGANIC MATERIALS RESEARCH DIVISION

ANNUAL REPORT, 1962

Berkeley, California

DISCLAIMER

UCRL-10706
UC-2 General Misc.
and Progress Report
TID-4500 (19th Ed.)

UNIVERSITY OF CALIFORNIA

Lawrence Radiation Laboratory
Berkeley, California

Contract No. W-7405-eng-48

INORGANIC MATERIALS RESEARCH DIVISION
ANNUAL REPORT, 1962

February 28, 1963

Printed in USA. Price $3.00. Available from the
Office of Technical Services
U. S. Department of Commerce
Washington 25, D.C.

INORGANIC MATERIALS RESEARCH DIVISION ANNUAL REPORT, 1962

Leo Brewer, Division Head
Alan W. Searcy, Associate Division Head

Lawrence Radiation Laboratory, Department of Chemistry,
Department of Mineral Technology, and Department of Nuclear Engineering
University of California, Berkeley, California

February 28, 1963

GENERAL INTRODUCTION

This third annual report of the Inorganic Materials Research Division follows the same general pattern as the report published last year as UCRL-10119. The material presented consists of brief research reports on studies that have been completed or that have yielded significant new information during 1962, and of statements from each investigator on research currently in progress. A list of those publications by staff members of the Division which appeared in 1962 is included as Section IV of this report.

The various programs described in this report demonstrate a fair degree of success toward the prime objectives of the Inorganic Materials Research program: (1) to provide fertile interdisciplinary atmosphere for basic research accomplishment, and (2) to prepare and train new talent in broad areas of fundamental research. More than two-thirds of the research staff is derived from student research assistantships and temporary post-doctoral appointments of one to three years.

During the year, two internal symposia--one on Metals and another on Superconductivity--were held in cooperation with the solid-state physics group of the University Physics Department. These interdisciplinary symposia were well attended and have inspired new efforts in several research areas. The Division co-hosted, with the University College of Chemistry, the 1962 meeting of the Calorimetry Conference in August.

This summary report is organized into three main sections--Chemistry, Metallurgy and Ceramics, and Reactor Materials Engineering--to be consistent with the AEC organizational branches from which funds are budgeted. Each of the sections is further divided into a number of research areas. The work of each investigator has been grouped, in general, under the most appropriate single heading in order to give a view of the breadth of the research interest of each principal investigator.

STAFF MEMBERS

Leo Brewer	Division Head
Alan Searcy	Associate Division Head
Ira Pratt	Assistant Division Head
T. H. Chenoweth	Business Officer

Robert E. Connick
John E. Dorn
Richard M. Fulrath
Dudley R. Herschbach
Laurence Himmel
Ralph Hultgren
William L. Jolly
George Jura
Bruce N. Mahan
Rolf H. Muller
Rollie J. Myers
Donald R. Olander
Edwin F. Orlemann
Earl R. Parker
Joseph A. Pask
Norman E. Phillips
Thomas H. Pigford
Otto Redlich
Charles H. Sederholm
Gareth Thomas
Charles W. Tobias
Jack Washburn
Victor F. Zackay

UCRL-10706*

INORGANIC MATERIALS RESEARCH DIVISION
ANNUAL REPORT, 1962

Contents

*Preceding Annual Reports: UCRL-9579, UCRL-10119

I. CHEMISTRY

A. INORGANIC CHEMISTRY

1. HYDROLYSIS AND POLYMERIZATION IN SOLUTIONS OF CHROMIC ION

Sister Gertrude Thompson and Robert E. Connick

A blue species isolated from refluxed solutions of Cr(III) has been identified as a dimer of the form $Cr_2(OH)_2^{+4}$ or Cr_2O^{+4}.[1,2,3] Rate studies of the decomposition of this species have been carried out in acid solutions of varying concentration at 25.0(± 0.1)°C and, for the lower acid concentrations, at constant ionic strength of $\mu = 2$. Concentrated solutions of the blue species prepared by evaporation under vacuum were used to follow its decomposition at low acid concentrations. Large quantities of the dimer can be conveniently prepared by using a modification of the method of Ardon and Plane[3] and subsequent separation on a cation-exchange column.

The kinetics of the decomposition indicate a two-step process and point to the existence of an intermediate complex. It is postulated that this species is a singly bridged complex Cr_2OH^{+5}. Behavior on a resin indicates a higher charge than that characteristic of either the monomer, $Cr(H_2O)_6^{3+}$, or the dimer, $Cr_2(OH)_2^{4+}$. If one allows the blue species to remain for several half-lives in concentrated acid to form the intermediate and then dilutes the solution, one can follow the rate at which the intermediate reforms the dimer. A color change from a light green to the blue color of the dimer can be followed visually over a period of about 2 hours.

Spectra of the intermediate in concentrated perchloric acid show a slight shift in maxima and minima from those of monomer and dimer, and enchancement of absorbance per Cr. Exact values cannot as yet be reported, since it has not been possible to isolate the material.

There is some evidence for the presence of the intermediate as a first species in the preparation of the dimer by oxidation of Cr^{2+} in acid solution by molecular oxygen. Dilutions of Cr^{2+} oxidation product have been made at varying times in the course of oxidation, and spectra have been followed over the visible and ultraviolet ranges. Spectra show maxima and minima in the same positions as for the intermediate, but still larger values for the absorbance per Cr.

---

[1] James E. Finholt, Chemistry of Some Hydrolyzed Cr(III) Polymers (thesis), UCRL-8879, April 1960.

[2] J. A. Laswick and R. A. Plane, J. Am. Chem. Soc. 81, 3564 (1959).

[3] M. Ardon and R. A. Plane, J. Am. Chem. Soc. 81, 3197 (1959).

Two other approaches are being used to obtain information on the change from dimer to intermediate: freezing-point lowering, as carried out by Ardon and Linenberg,[4] and magnetic susceptibility measurements of the two species on cation-exchange beads. Quoy-type measurements will also be made on the dimer and on a second green species believed to be a trimer, $Cr_3(OH)_4^{5+}$.

[4] M. Ardon and A. Linenberg, J. Phys. Chem. 65, 1443 (1961).

2. STUDIES ON THE RUTHENIUM(III) CHLORIDE SYSTEMS

Robert A. Hasty and Robert E. Connick

The identification of the chloride complexes of ruthenium(III) discussed in preceding annual reports has been continued and an additional paper is in preparation.[1] Determination of the composition of ruthenium(III) solutions in terms of the various chloride complexes as a function of the free chloride concentration has been continued in order to give more exact values of the equilibrium quotients.

Measurements have been made of the rates of interconversion of $RuCl_6^{3-}$, $RuCl_5^{2-}$, and the two isomers of $RuCl_4^-$. An isomerization of the $RuCl_4^-$ isomers is observed in some cases, apparently caused by catalytic action. Although the catalyst has not been identified, it is thought to be a species involving a lower oxidation state of ruthenium. Studies are being continued to identify the catalyst.

[1] R. Hasty, R. Connick, and D. Fine, Identification of Anionic Ruthenium Species, UCRL-10605, Dec. 1962, to be presented at the 144th meeting of the American Chemical Society, Los Angeles, April 1963.

3. DETERMINATION OF THE NUMBER OF WATER MOLECULES IN THE HYDRATION SPHERE OF DIAMAGNETIC IONS IN AQUEOUS SOLUTIONS

Daniel Fiat and Robert E. Connick

Jackson, Lemons, and Taube [J. Chem. Phys. 32, 553 (1960)] showed that if cobaltous perchlorate is added to solutions of some diamagnetic salts it is possible to distinguish separate O^{17} nmr signals corresponding to the water bound to the diamagnetic ions, and to the free water. The paramagnetic salt shifts the free-water signal to a lower field, whereas the signal of the bound water is not shifted. Using water that contains only low concentrations of O^{17} made very high rf power necessary, and in order to avoid saturation the dispersion mode was detected by the derivative method. Consequently the number of water molecules in the hydration sphere, the width of the lines,

and the relaxation times could not be determined.

In the work reported here a modification of the above method of detection and higher concentrations of O^{17} were used, yielding accurate hydration numbers and relaxation times. Instead of the usual derivative method the side-band technique for the detection of the nmr signals was employed. As the width of the lines exceeded the highest modulation frequency (400 cps) of the Varian sweep unit, the Varian integrator was used for modulating the magnetic field at the frequency of 2088 cps.

It was found that the absorption curves were perfectly Lorentzian, thereby facilitating to a large extent the separation of the overlapping portions of the absorption signals. The true width of the lines as well as the ratio of the populations in the two different environments could then be calculated very accurately. A hydration number of 6.0±0.2 was obtained for Al^{+++} ions. For a solution of the composition (expressed in millimoles) $AlCl_3$, 2.60: H_2O, 91.0; $HClO_4$, 0.812; $Co(ClO_4)_2$, 0.396 at a frequency of 5.415 Mc, the widths of lines were: $\Delta f_{\text{bound water}} = 650 \pm 5$ cps; $\Delta f_{\text{free water}} = 580 \pm 5$ cps. The chemical shift between the bound and free water (the bound water at a higher field than the free) was: $\Delta f_{\text{bound water/free water}} = 2330 \pm 10$ cps.

The signal of the bound water was broader than the signal of pure water, presumably as a result of the additional quadrupole mechanism of relaxation of the O^{17} in the electric field gradient of the ions. It is interesting that the signal of the bound water is even broader than the signal of the free water that was broadened by the presence of the paramagnetic ions.

4. NUCLEAR MAGNETIC RESONANCE STUDIES OF COMPLEX IONS

Elaine C. Blatt and Robert E. Connick

The rate of exchange of water molecules from the first coordination sphere of some paramagnetic transition metal ions in the first transition series has recently been measured by nuclear resonance techniques in this Laboratory [T. J. Swift and R. E. Connick, J. Chem. Phys. 37, 307 (1962)]. The addition of a paramagnetic ion to water decreases the transverse relaxation time of the oxygen-17 nucleus. A temperature-dependence study reveals whether the transverse relaxation rate is a measure of the chemical exchange rate or merely a lower limit.

By use of the same technique, measurements have been made of the rate of exchange of waters from the bulk of the solution to the first coordination sphere of complex ions, with their coordination spheres filled partly by molecules other than water. A typical series that was studied in preliminary work is the $FeCl(H_2O)_5^{2+}$, $FeCl_2(H_2O)_4^{+}$, etc., system. The addition of each chloride ion appeared to increase the rate of exchange of water. Preliminary work also showed the following order of influence in increasing the rate of exchange of water in the mono-ligand complex ions of Fe(III) and Ni(II): $OH^- > SCN^- > F^- > SO_4 = \sim H_2O$.

5. RESEARCH IN PROGRESS: ROBERT E. CONNICK

Projects now under way include the following.

a. Isolation and identification of additional hydrolyzed polymers of Cr(III) (with Sister Gertrude Thompson).

b. Kinetics and mechanisms of the interconversion of the lower Ru(III) chloride complexes (with Dr. Robert A. Hasty).

c. Studies of water exchange of additional inorganic complex ions, using nuclear magnetic resonance (with Elaine Blatt).

d. Determination of hydration numbers of metal ions, using nuclear magnetic resonance (with Dr. Daniel Fiat).

e. Extension of temperature range of nuclear magnetic resonance so as to yield additional information on rates of exchange of water molecules on paramagnetic cations (with Charles W. Meredith).

6. THE EXCHANGE OF DEUTERIUM WITH SOLID POTASSIUM HYDROBORATE*

Robert E. Mesmer† and William L. Jolly

Potassium deuteroborate has been prepared by reaction of deuterium gas with potassium hydroborate at temperatures near 500°. The proportions of the anions BH_4^-, BH_3D^-, $BH_2D_2^-$, BHD_3^-, and BD_4^- in partially deuterated samples have been deduced from the composition of the hydrogen evolved upon hydrolysis, from proton magnetic resonance spectra, and from the magnitude of the equilibrium constant for exchange.

---

*Abstract of paper in J. Am. Chem. Soc. 84, 2039 (1962).

†Now at Monsanto Chemical Co., St. Louis, Missouri.

7. THE HYDROLYSIS OF AQUEOUS HYDROBORATE*

Robert E. Mesmer† and William L. Jolly

The kinetics of the hydrolysis of hydroborate has been studied over the pH range 3.8 to 14. The rate may be represented by the expression

$$-d(BH_4^-)/dt = k_1(H^+)(BH_4^-) + k_2(BH_4^-),$$

where $k_1 = 2.18\times10^{11}T[\exp(-4000/T)]\ M^{-1}\ min^{-1}$,

and $k_2 = 1.72\times10^{7}\ T[\exp(-10,380/T)]\ min^{-1}$.

*Abstract of paper in Inorg. Chem. 1, 608 (1962).

†Now at Monsanto Chemical Co., St. Louis, Missouri.

8. THE CHEMISTRY OF DIGERMANIUM HEXACHLORIDE*

Richard W. Kopp† and William L. Jolly

The vapor pressure of Ge_2Cl_6 has been determined over the range 24.7 to 59.7°. The vapor pressure in this range may be calculated from the equation

$$\log P_{mm} = -2801/T + 9.29.$$

In diglyme solutions, Ge_2Cl_6 reacts with $NaBH_4$ to form GeH_4, B_2H_6, and only small amounts of Ge_2H_6. When the remaining solution is treated with aqueous acid, hydrogen, germane, and a trace of digermane are evolved. Tentatively, we suggest that the reaction of Ge_2Cl_6 and $NaBH_4$ proceed as follows:

$$Ge_2Cl_6 + 7\ NaBH_4 \rightarrow GeH_4 + 6\ NaCl + Na^+(H_3GeBH_3)^- + 3\ B_2H_6.$$

If the species $Na^+(H_3GeBH_3)^-$ is indeed formed, it is the first example of a compound with a Ge-B bond. Further work will be done on this reaction.

*Abstract of Richard Wilhelm Kopp, The Chemistry of Hexachlorogermane (thesis), UCRL-10437, Sept. 1962. Some of the preparative aspects, discussed in ID. 5 in the 1961 annual report, have been published: Inorg. Chem. 1, 958 (1962).

†Now at Chemistry Depart., University of Michigan, Ann Arbor, Michigan.

When Si_2Cl_6 is treated with water, the water is reduced to hydrogen.[1] However, Ge_2Cl_6 and water react with evolution only of HCl and with the formation of a white non-volatile residue. This residue turns yellow when heated or treated with base. Perhaps the white residue is "germano-oxalic acid" which decomposes, on heating, to yellow GeO and GeO_2.

$$Ge_2Cl_6 + 4H_2O \rightarrow (GeOOH)_2 + 6HCl$$

$$(GeOOH)_2 \rightarrow GeO + GeO_2 + H_2O.$$

This reaction will be studied further.

Like Si_2Cl_6, Ge_2Cl_6 reacts with liquid ammonia to form an imide:

$$Ge_2Cl_6 + 9\,NH_3 \rightarrow Ge_2(NH)_3 + 6\,NH_4Cl.$$

Excess HCl reacts with Ge_2Cl_6, cleaving the Ge-Ge bond:

$$Ge_2Cl_6 + HCl \rightarrow GeHCl_3 + GeCl_4.$$

[1] K. A. Andrianov, Organic Silicon Compounds (State Scientific Technical Publishing House for Chemical Literature, Moscow, 1955), p. 135.

9. PREPARATION OF MIXED HYDRIDES OF SILICON, GERMANIUM, PHOSPHORUS, AND ARSENIC*

John E. Drake† and William L. Jolly

The preparation of germanium hydrides, up to nonagermanes, by the decomposition of germane in an ozonizer-type silent electric discharge has previously been reported.[1] We report now the formation of "mixed" hydrides (hydrides containing more than one element in addition to hydrogen) by use of the same apparatus. An equimolar mixture of germane or silane

*Abstract of three papers: J. E. Drake and W. L. Jolly, Chem. and Ind. 1962, 1470; J. E. Drake and W. L. Jolly, High-Resolution Proton Magnetic Resonance Spectra of Silylphosphine, Silylarsine, Germylphosphine, and Germylarsine, UCRL-10422, Aug. 1962, and note accepted for J. Chem. Phys. (1963). Also see reference 1.

†Now at the Chemistry Department, Hull University, Hull, England.

[1] The material described in ID. 6 in the 1961 annual report has been published: J. Chem. Soc. 1962, 2807.

and either phosphine or arsine was circulated through the ozonizer system. In each case, the ozonizer temperature was -78° and the total gas pressure was 0.25 to 0.5 atmosphere. The following mixed hydrides were detected by mass spectroscopy: SiH_3PH_2, Si_2PH_7, SiH_3AsH_2, Si_2AsH_7, GeH_3PH_2, Ge_2PH_7, Ge_3PH_9, GeP_2H_6 and GeH_3AsH_2.

The infrared and proton magnetic resonance spectra of $H_3Si\text{-}PH_2$, $H_3Si\text{-}AsH_2$, $H_3Ge\text{-}PH_2$, and $H_3Ge\text{-}AsH_2$ were obtained. The infrared symmetrical deformation frequencies for the SiH_3- and GeH_3- groups in these molecules fall in line with the deformation frequencies for these groups observed in other molecules. The proton magnetic resonance spectra are completely consistent with the indicated structures for the compounds. The chemical shifts indicate that the order of electronegativities is P > As > Ge > Si.

10. ABSORPTION SPECTRA OF METAL-AMMONIA SOLUTIONS*

Marvin Gold† and William L. Jolly

The experimental results described in the 1961 annual report (UCRL-10119, pp. 67-72) have been used to support a revised model for metal-ammonia solutions. The important conclusion is that the electron-in-a-cavity and ammoniated metal ion are the principal species over the concentration range 0 to 0.1 molar metal content. Ion pairs and quadrupoles of the type $(M^+)(e^-)$ and $(M^+)_2(e^-)_2$ account for the conductivity and susceptibility properties.

Calcium was found to show negative deviations from Beer's Law, and it was suggested that the equilibrium

$$2Ca^{++} + 2e^- = Ca_2^{++}$$

might explain the data. However, the calcium runs were somewhat marred by experimental difficulties--in particular the formation of an immiscible, bronze-colored phase in the solutions--so further work is called for.

---

*Abstract of two papers: M. Gold, W. L. Jolly, and K. S. Pitzer, J. Am. Chem. Soc. 84, 2264 (1962) and M. Gold and W. L. Jolly, Inorg. Chem. 1, 818 (1962).

†Now at Electrochimica Corp., 1140 O'Brien Dr., Menlo Park, California.

11. SOME REACTIONS OF DIPHOSPHORUS TETRACHLORIDE*

Charles Lindahl and William L. Jolly

Diphosphorus tetrachloride, with a lone pair of electrons and low-energy d orbitals available on each phosphorus atom, can possibly act as a Lewis base and as a Lewis acid. Therefore the reactivities of P_2Cl_4 with the compounds BBr_3, BCl_3, BF_3, B_2H_6, $Ni(CO)_4$, and C_2H_4 have been investigated.

When an excess of BBr_3 is allowed to react with P_2Cl_4 at 0° or room temperature in a sealed tube, two molecules of BBr_3 react with each molecule of P_2Cl_4, forming a white volatile solid, mp 54°, and a yellow nonvolatile solid. These products are currently under investigation.

When an excess of BCl_3 is placed in a sealed tube with P_2Cl_4 at 0°, the reactants can be recovered unchanged even after two months. No change in pressure of BCl_3 vapor is observed when it is exposed to P_2Cl_4 at 0° or room temperature.

No change in pressure of BF_3 vapor is observed when it is exposed to P_2Cl_4 at 0° or room temperature.

When B_2H_6 is exposed to P_2Cl_4 at 0°, a slow increase in pressure, due primarily to evolution of H_2, continues over a long period of time. This experiment was terminated after 17 days of continuous H_2 evolution. Boron trichloride and $BHCl_2$ (identified by their infrared spectra) were also evolved.

Preliminary experiments show that when an excess of $Ni(CO)_4$ is allowed to react with P_2Cl_4 at room temperature, two molecules of CO are evolved for each molecule of P_2Cl_4. Investigation of this reaction is being continued.

No change in pressure of C_2H_4 vapor is observed when it is exposed to P_2Cl_4 at 0° or room temperature.

With P_2Cl_4 as a reference Lewis base, BBr_3 is a stronger Lewis acid than either BCl_3 or BF_3, in agreement with published thermodynamic data[1] and qualitative spectroscopic observations[2] which show the order of

---

*Material presented in ID. 8 in the 1961 Annual Report has been published: Inorg. Chem. 1, 958 (1962).

[1] H. C. Brown and R. R. Holmes, J. Am. Chem. Soc. 78, 2173 (1956).

[2] R. L. Amster, Ph. D. Thesis, University of Michigan, 1961.

acid strengths to be $BBr > BCl_3 > BF_3$.

The complex $PCl_3 \cdot BBr_3$,[3] and the probable nonexistence of the complexes $PCl_3 \cdot BCl_3$,[4] and $PCl_3 \cdot BF_3$,[4] also support this trend, which is contrary to previously reported statements.[5] Arguments based on inducting effects and on possible steric hindrance would predict the order of acid strengths to be $BF_3 > BCl_3 > BBr_3$. However, apparently the determining factor is the decreased overlap of the vacant pΠ orbital of the boron with the lone pairs on the heavier halogens. This decreased overlap makes the fourth orbital on the boron more able to accept an electron pair from a donor atom, causing the order of acid strength to be $BBr_3 > BCl_3 > BF_3$.

In the diborane experiment the P_2Cl_4 evidently reacts with B_2H_6, causing slow decomposition rather than complex formation.

Under the conditions of our experiment P_2Cl_4 did not react with C_2H_4, although it is known[6] that $P_2(CF_3)_4$ adds to ethylene at room temperature and that $P_2(CH_3)_4$ adds to ethylene at temperatures approaching 300°.

---

[3] E. Wiberg and K. Shuster, Z. anorg. Chem. 213, 94 (1933).

[4] P. Baumgarter and W. Bruns [Ber. Deut. Chem. Ges. 80, 517 (1947)] state they have isolated PCl_3BF_3 from petroleum ether, but R. R. Holmes [J. Inorg. Nucl. Chem. 12, 266 (1960)] found no interaction of gaseous BF_3 in liquid PCl_3. Holmes also showed the PCl_3BCl_3 complex reported by A. Stieber, [Compt. Rend. 195, 610 (1932)] to be $POCl_3BCl_3$.

[5] D. R. Martin, Chem. Rev. 34, 461 (1944); ibid 42, 581 (1948).

[6] A. B. Burg, J. Am. Chem. 83, 2226 (1961).

12. THE CHEMISTRY OF SULFUR-NITROGEN COMPOUNDS*

Jerry Smith, Keith Maguire, and William L. Jolly

The reaction of nitrogen "plasmas" with sulfur vapor has been studied by using a plasma jet and a low-pressure microwave discharge. Products from the plasma jet were quenched with a carbon tetrachloride bath. Products formed were hexachlorobenzene, C_6Cl_6, and sulfur monochloride, S_2Cl_2, via carbon tetrachloride pyrolysis. As yet, no sulfur nitrides have been obtained from the plasma jet.

The microwave discharge system has been investigated at nitrogen pressures between 0.1 and 200 mm Hg, with sulfur in excess. Tetrasulfur dinitride, S_4N_2, and polymeric sulfur nitride, $(SN)_x$, have both been observed as products. The maximum yield of S_4N_2 obtained to date is 0.8 mmole/h.

---

*See W. L. Jolly, The Synthesis of S_4N_4 and $S_2N_2O_2$, Inorg. Chem. 1, 76 (1962).

It has been found that when a mixture of ammonium chloride and S_2Cl_2 is heated under reflux, an orange sublimate forms which can be converted to S_4N_3Cl by treatment with hot dioxane. It is believed that this process may be developed into a useful method for syntheses of S_4N_3Cl.

13. RESEARCH IN PROGRESS: WILLIAM L. JOLLY

a. Several grams of a mixture of polysilanes (such as Si_2H_6, Si_3Hg, etc.) and silicon-phosphorus hydrides (such as SiH_3PH_2, Si_2PH_7, etc.) have been prepared by passing a mixture of SiH_4 and PH_3 through an ozonizer at -78°. The SiH_3PH_2 will be separated and its heat of decomposition to the elements will be measured. It is hoped that the two isomers of Si_2PH_7 (disilylphosphine and disilanylphosphine) can be separated and identified by infrared and nmr spectroscopy.

b. Investigations of the absorption spectra of calcium-ammonia solutions showed that an immiscible, bronze-colored phase formed in relatively dilute solutions (approx 0.01 M). Preliminary to repeating the spectral measurements, we are determining the Ca-NH_3 phase diagram in the NH_3-rich region. The formation of the bronze phase is readily detected by following the conductivity of the bulk of the solution as a function of concentration. The conductivity is relatively constant in the two-phase region. When these data are complete, we will know the temperatures and concentrations of calcium for which we can measure spectra without difficulty.

c. The chemistry of the unusual compound S_4N_3Cl and related compounds will be investigated.

14. RATE OF AQUATION OF DICHLOROCHROMIC ION AS A FUNCTION OF pH IN PERCHLORATE AND CHLORIDE MEDIA*

Wayne Mathews, Charles W. Merideth, and Edwin F. Orlemann

The rate of aquation of dichlorochromic and monochlorochromic ions are of concern in interpreting data for the electroreduction of chromic ions in chloride media. A survey of the literature revealed that widely varying values for these rates have been reported.[1,2,3,4,5] In view of this fact, a reinvestigation of these rates was undertaken.

*Summary of work to be submitted to J. Inorg. Chem.

[1] N. Bjerrium, Z. Physik. Chem. 59, 336, 581 (1907).

[2] J. Ibarz, J. Virgili, and J. M. Costa, Anales Fis. Quim. 58-B, 89 (1962).

[3] Ju. P. Nazarenko, Russian Journal of Inorganic Chemistry 4, 826 (1959).

[4] Hamm and Shull, J. Am. Chem. Soc. 73, 1240 (1951).

[5] Lamb and Fonda, J. Am. Chem. Soc. 43, 1154 (1921).

In this work solid $[CrCl_2(H_2O)_4]Cl \cdot 2H_2O$ was prepared by the method described by Elving and Zemal,[6] and characterized by analyses for percent of water and chloride. Weighed amounts of this salt were dissolved to yield solutions approximately 0.005 M in chromium chloride in either $HClO_4$ and $NaClO_4$ or NaCl and HCl solutions of total 0.5 M perchlorate or chloride ion concentration. The pH was determined by glass electrode measurements made at the beginning and at the end of each rate determination.

Solutions of $CrCl_2(H_2O)_4^+$ prepared in the above manner have been found to be predominantly the transisomer.[7] The rate of conversion of this species to the monochlorochromic ion was followed spectrophotometrically by recording the absorbance of the solution at 700 mμ as a function of time. Suitable analysis of these data gave the desired rate constants. The subsequent conversion of monochlorochromic ion to the aquo ion was also followed by recording the absorbance of the solutions at 660 mμ as a function of time after the bulk of the dichlorochromic ion had undergone conversion to the monochloro species. Since the rate of aquation is much greater for dichlorochromic ion than for monochloro ion, in the pH range studied, no difficulty was experienced in clearly separating the two reaction rates.

With the symbol $[H^+]'$ representing the antilog of the measured pH, our results for the aquation of dichlorochromic ion over the pH range from 1.0 to 3.8 can be summarized in

$$k(min^{-1}) = 0.0053 + \frac{1.18 \times 10^{-5}}{[H^+]'} .$$

The above equation yields values of the rate constants in reasonable agreement with Bjerrum's and Lamb's results.[1,5] Rate constants reported by Hamm and Shull[4] and Ibarz, Virgili, and Costa[2] differ from these values by a factor of nearly 20. In re-examining their work we conclude the polarographic method used in each case to follow the apparent decrease in dichlorochromic ion concentration was invalidated by the formation of chromous ion at the electrode surface. In effect the chromous ion catalyzed the conversion of dichlorochromic to monochlorochromic ion according to

$$Cr^*Cl_2^+ + Cr(II) = Cr^*(II) + CrCl^{++} + Cl^-,$$

which has an approximate specific rate constant at 2°C of about 10^4 liters $mole^{-1}$ min^{-1}.[8] Thus the rate constants reported in references 2 and 4 actually are those of the monochloro rather than the dichlorochromic ion.

---

[6] Elving and Zemel, J. Am. Chem. Soc. 79, 1281 (1957).

[7] King, Woods and Gates, J. Am. Chem. Soc. 80, 5015 (1958).

[8] H. Taub and J. Meyers, J. Am. Chem. Soc. 76, 2103 (1954).

15. RATE OF AQUATION OF MONOCHLOROCHROMIC ION AS A FUNCTION OF pH IN PERCHLORATE AND CHLORIDE MEDIA

Charles W. Merideth, Wayne Mathews, and E. F. Orlemann

The data available for the rate of conversion of the monochlorochromic ion to the aquochromic ion in the pH range from 2 to 4 as reported by Ibarz, Virgili, and Costa[1] and Nazarenko,[2] and data obtained by reinterpretation of the results of Hamm and Shull[3] are in marked disagreement at pH greater than 2. Specifically, the acidity is quite uncertain in Nazarenko's data; Hamm and Shull's data are fitted by an expression of the type

$$k = a + b/[H^+];$$

and Ibarz, Virgili, and Costa's data are best expressed by the relation

$$k = a + c/[H^+]^2 .$$

We have measured the rate of the reaction in the pH range 1.75 to 3.40 in solutions made as described in the preceding section. That is, approximately 0.005 M chromic ion in HCl, NaCl solution, with the total chloride ion concentration equal to 0.50 M. Suitable analysis of the absorbance of these solutions at 660 mμ as a function of time leads to rate data that fit the equation

$$k = a + \frac{b}{[H^+]} + \frac{c}{[H^+]^2} .$$

The term $b/[H^+]$ is essentially negligible and the results are in qualitative agreement with the data of Ibarz, Virgili, and Costa.[1]

---

[1] Ibarz, Virgili, and Costa, Anales Fis. Quim. 58-B, 89 (1962).
[2] Yu. P. Nazarenko, Russ. J. Inorg. Chem. (English Transl.) 4, 826 (1959).
[3] Hamm and Shull, J. Am. Chem. Soc. 73, 1240 (1951).

16. THE USE OF CONSTANT-CURRENT TECHNIQUES IN THE STUDY OF ELECTRODE REACTIONS

Wayne Mathews and E. F. Orlemann

One useful technique for study of electrode reactions involves recording the potential and time history of the working electrode when current is passed through the cell at various constant levels. Interpretation of these potential-time data in terms of electrode reaction mechanism is complicated at high current densities by the potential-time relation that derives from the need to charge the electrode interface as a condenser. At low current densities the interpretation is complicated by convection effects in the diffusion-

layer region. A program to determine empirical corrections for these effects has been partially completed. The general validity of these corrections has yet to be established.

17. RESEARCH IN PROGRESS: EDWIN F. ORLEMANN

a. The rates of interconversion of In^{+++} to $InOH^{++}$ and indium chloride species will be studied by chromopotentiometric techniques as part of a study of electrode reaction mechanisms in this system.

b. A study of the reduction of nickel, and of related first-transition-group metal ions is planned, using techniques designed to characterize unipositive intermediate oxidation states if they exist.

18. FLUORINE SPIN-SPIN COUPLING CONSTANTS

Charles H. Sederholm

We are interested in calculating nuclear magnetic resonance spectra for nuclei exchanging between different rotational isomers. If there is no coupling between nuclei, the Bloch equations, as modified by McConnell,[1] result in a set of simultaneous equations which can be solved by standard methods to give the absorbance at each frequency.[2] To take coupling into account for all possible exchange rates, it is convenient to use the density matrix of the molecular systems. Kaplan has given the self-consistent averaged density matrices for molecular systems with any number of spins.[3] The matrix equations (of which a second set is obtained by permuting A and B) are

$$\rho_A = \int_0^\infty dt \, \frac{e^{-t/\tau_A}}{A} \; S_A(t) \; Tr_B \left[R_{ij}^{AB} (\rho_A \times \rho_B)(R^{-1})_{ij}^{AB} \right] \; S_A^{-1}(t), \qquad (1)$$

---

[1] J. A. Pople, W. G. Schneider, and H. J. Bernstein, High Resolution Nuclear Magnetic Resonance (McGraw-Hill Book Company, Inc., New York, 1959), pp. 218 ff.

[2] D. S. Thompson, R. A. Newmark, and C. H. Sederholm, J. Chem. Phys. 37, 411 (1962).

[3] J. Kaplan, J. Chem. Phys. 28, 258 (1958).

where ρ_A is the density matrix of molecular species A, $\rho_A \times \rho_B$ is the direct product of two matrices, R_{ij}^{AB} is a unitary exchange operator for nuclei i and j between species A and B, $Tr_B(\rho_A \times \rho_B)$ means the trace over elements B of the direct product matrix, to yield a matrix whose dimensionality is the same as ρ_A; τ_A is the exchange rate; $S_A(t) = \exp(iH_A t/\hbar)$, and H_A is the usual spin Hamiltonian in the rotating coordinate system for system A,

$$\hbar^{-1} H_A = \sum_i S_{zi}(\gamma_i H_0 - w) + \sum_i \gamma_i S_{xi} H_1 + \sum_i J_{ij} \vec{S}_i \cdot \vec{S}_j .$$

These results have been extended to a system containing two spins exchanging between three molecular species--A, B, and C. The equations corresponding to (1) are

$$\rho_A = \frac{\tau_A}{\tau_{AB}} \int_0^\infty dt \, \frac{e^{-t/\tau_A}}{\tau_A} \, S_A(t) \, Tr_{BC} \left[R_{ij}^{AB} (\rho_A \times \rho_B \times \rho_C)(R^{-1})_{ij}^{AB} \right] S_A^{-1}(t)$$

$$+ \frac{\tau_A}{\tau_{AC}} \int_0^\infty dt \, \frac{e^{-t/\tau_A}}{\tau_A} \, S_A(t) \, Tr_{BC} \left[R_{ij}^{AC} (\rho_A \times \rho_B \times \rho_C)(R^{-1})_{ij}^{AC} \right] S_A^{-1}(t) \qquad (2)$$

(Two additional equations are obtained by permuting A, B, and C.) Here $\tau_A^{-1} = \tau_{AB}^{-1} + \tau_{AC}^{-1}$; τ_{AB}^{-1} is the rate of exchange between species A and B. The coefficients of the integrals in (2) are determined by requiring that the equation reduce to the Bloch equations, as modified for exchange, to zeroth order in H_1.

For a sufficiently weak radio-frequency field H_1, the diagonal elements of ρ_A are given, to first order, by the Boltzmann factors $(1 - \frac{\hbar M_\ell \omega_0}{kT})/N$, where M_ℓ is the total magnetization and N the dimensionality of ρ_A, and ω_0 is the resonant frequency. We have further approximated the diagonal elements by 1/N. The off-diagonal elements, proportional to H_1, are nonzero only for spin flips corresponding to a change of $M_\ell = \pm 1$.[4] Thus, for a two-spin molecule,

---

[4] S. Alexander, J. Chem. Phys. 37, 967 (1962).

$$\rho_A = \begin{pmatrix} \frac{1}{4} & \rho_{12}^{A} & \rho_{13}^{A} & 0 \\ \rho_{12}^{*A} & \frac{1}{4} & 0 & \rho_{24}^{A} \\ \rho_{13}^{*A} & 0 & \frac{1}{4} & \rho_{34}^{A} \\ 0 & \rho_{24}^{*A} & \rho_{34}^{*A} & \frac{1}{4} \end{pmatrix}$$

The absorbance is proportional to the imaginary part of ρ_{ij}, so only four numbers per molecule need be found. For the case of three molecules with two spins, Eq. (2) result in 12 simultaneous equations to be solved for the $\mathrm{Im}(\rho_{ij})$. A FORTRAN program has been written for the IBM 7090 which solves these 12 equations as a function of exchange rates, chemical shifts, coupling constants, and the frequency.

Spectra have been calculated for CFClBr-CFClBr which duplicate, within experimental error, the spectra obtained at low temperatures when the internal rotation no longer averages the spectrum over the rotamers. The previous calculations on this molecule did not show the doublets due to spin-spin coupling present in one of the rotamers.[2]

We hope to extend this FORTRAN program to larger spin systems, in which the number of simultaneous equations (45 for three molecules with three spins) becomes too large for an exact solution on the computer in a reasonable amount of time. However, a Gauss-Seidel iteration procedure may solve the equations sufficiently quickly.

$$\rho_A = \int_0^\infty dt \left[\exp(-t/\tau_A) \right] / A$$

$$\times \mathrm{Tr}_B \left[R_{ij}^{AB} (\rho_A \times \rho_B)(R^{-1})_{ij}^{AB} \right] S_A^{-1}(t) .$$

19. A NEW SPIN COUPLING MECHANISM IN NUCLEAR MAGNETIC RESONANCE

Charles H. Sederholm

In NMR spectroscopy an indirect dipole-dipole interaction between magnetic nuclei gives rise to a multiplet structure known as spin-spin splitting. It is generally thought that this spin-spin coupling is exerted through the bonding electrons and that the magnitude of the coupling, measured phenomenologically as coupling constants, attenuates rapidly with an increase in the number of bonds that separate the interacting nuclei.

Recently Sederholm et al have observed NMR spectra of fluorine compounds, however, in which some coupling constants are much larger than can be accounted for in terms of through-bond coupling and others are much too small.[1] Sederholm proposed that this anomaly is due to an alternative coupling "mechanism" in which the spin-spin coupling is direct through space. This through-space coupling may well involve nonbonding electrons in the fluorine atoms.

However, Sederholm's through-space coupling mechanism has not been completely substantiated. Research into this effect was therefore initiated. This research requires, in the first place, synthesizing some fluorine compounds in which the fluorine nuclei are separated by at least five bonds and yet physically are close to each other. Separation by five bonds between the coupling nuclei would reduce through-bond coupling to a minimum. Through-space coupling is postulated to be most effective when the nuclei are at close range. Below are shown some compounds that have been or are in the process of being synthesized.

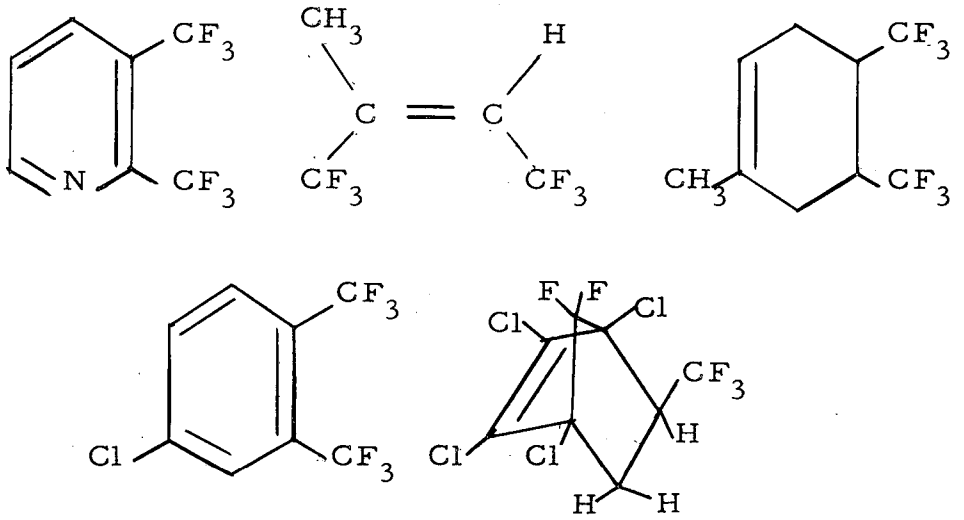

[1] L. Petrakis and C. H. Sederholm, J. C. P. 35, 1243 (1961).

Observed fluorine-fluorine coupling constants (between fluorine atoms in close proximity) are five to ten times as large as might be expected on the basis of through-bond coupling. These observations support the hypothesis of a through-space coupling mechanism.

20. RESEARCH IN PROGRESS: CHARLES H. SEDERHOLM

In an attempt to find supporting evidence for through-space fluorine-fluorine coupling, and to investigate barriers to internal rotation in halogen-substituted ethanes, we are measuring low-temperature spectra (150°K to 300°K) of several compounds, including CF_3-CFI-CF_2Cl, $CFBr_2$-CF_2Br, and CF_3-$CFBr_2$.

By observing how coupling constants vary with temperature in such model compounds, it should be possible to calculate or observe the coupling constants in the three rotamers and the barriers between the rotamers.

Geminal proton-proton coupling constants are of interest, since they have been calculated theoretically, but only few have been observed. These are expected to vary with the bond angle. Because of this expectation, we are attempting to interpret the spectrum of trimethylene oxide, a compound in which we expect this coupling constant to be observable.

B. CHEMICAL THERMODYNAMICS

1. THE VISIBLE SPECTRUM AND THE GROUND STATE OF Se_2

Leo Brewer, Beat Meyer, and R. F. Barrow*

Spectral analysis of the Se_2 molecule has given controversial results.[1, 2, 3] In an attempt to improve understanding of the system, the spectrum has been studied with separated isotopes, Se^{77}, Se^{78}, Se^{80}, both in absorption and in emission. The vibrational isotope shift and preliminary rotational analysis show that all bands in the complex visible region are part of one single band system. The transition seems to be $^3\Sigma$-$^3\Sigma$ and not $^1\Sigma$-$^1\Sigma$ as earlier authors have suggested.[2, 3] The Red system of Rosen[1] does not exist. The work was performed with the use of a high-dispersion grating (0.15 Å/mm in 16th order) of the spectroscopy group. Rotational analysis and study of the dissociation limits are under way.

*Physical Chemistry Laboratory, Oxford, England.

[1] B. Rosen, Physica 6, 205 (1939).

[2] E. Olsson, Thesis, Stockholm, 1938.

[3] S. P. Davis and F. A. Jenkins, Phys. Rev. 83, 1269 (1951).

2. THE VIBRATION SPECTRUM OF TRAPPED S_2

Beat Meyer and Leo Brewer

The infrared spectrum of trapped sulfur vapor has been studied systematically.[1] The band at 16.68 μ has been re-examined with the isotopes S^{32} and S^{34}. The shift and intensity relations indicate that this absorption is due to S_2 trapped in a matrix of sulfur chains which are formed by recombination of the S_2 molecules during the condensation process. Further work on trapping S_2 in different matrices is under way.

*Published in J. Chem. Phys. 37, 1577 (1962).

[1] B. Meyer, E. Schumacher, Helv. Chim. 43, 1333 (1960).

3. THE COMPOSITION OF ANTIMONY VAPOR*

Gerd M. Rosenblatt

Experiments on the vapor density of antimony carried out by Illarionov and Cherekanova[1] have been reinterpretated to show that the results are consistent with the accepted dissociation energy of Sb_4, contrary to the conclusions presented by the authors.

*Abstract of a note published in J. Phys. Chem. 66, 2259 (1962).

[1] V. V. Illarinovov and A. S. Cherekanova, Dokl. Akad. Nauk SSSR 133, 1086 (1960).

4. THERMODYNAMICS OF SUBOXIDE VAPORIZATION*

Leo Brewer and Gerd M. Rosenblatt

Thermodynamic calculations predict the species vaporizing from metal-oxide mixtures when reliable free energy functions, enthalpies of formation, and dissociation energies are available for the possible gaseous and condensed oxide components. The oxygen-to-metal ratio in the vapor phase compared with the oxygen-to-metal ratio in a liquid metal saturated with oxide impurity has been calculated for many metals. The results permit evaluation of the thermodynamic possibility of purifying metals contaminated with oxide by vacuum melting or by distillation. Kinetic effects have not been considered.

*Abstract of paper published in Trans. A. I. M. E. 224, 1268 (1962).

5. RADIATIVE LIFETIME OF I_2 FLUORESCENCE, $B^3\Pi_{0^+_u} \rightarrow X^1\Sigma_{0^+_g}$*

Leo Brewer, Robert A. Berg,† and Gerd M. Rosenblatt

The radiative lifetime of the fluorescence of molecular iodine vapor, $B^3\Pi_{0^+_u}$ ($v' = 26$) $\rightarrow X^1\Sigma_{0^+_g}$, has been determined to be $(7.2 \pm 1.0) \times 10^{-7}$ sec by use of a phase fluorometer. The result is in good agreement with absorption data, calculations of the transition probability, and data on vibrational energy transfer. Measurements on equilibrium vapor have been carried out over the pressure range 10^{-4} to 5 mm Hg. Results at the lowest pressures are considerably shorter than the true lifetime owing to mixing of scattered incident light with the fluorescence. This effect has been corrected analytically. At higher

*Abstract of paper to be published in J. Chem. Phys. (1963).

†Now at Department of Chemistry, Harvard University, Cambridge, Massachusetts.

pressures the measured lifetime is shortened by self-quenching. The slope of a Stern-Volmer plot of $1/\tau$ as a function of P yields a self-quenching collision diameter for I_2 of 11.3 Å. The diameter appears to be consistent with quenching by induced predissociation. Measurements have also been carried out with a molecular beam of iodine vapor.

6. PHASE FLUOROMETER TO MEASURE RADIATIVE LIFETIMES OF 10^{-5} TO 10^{-9} SECOND*

Leo Brewer, C. Geoffrey James†, Richard G. Brewer‡, Fred E. Stafford††, Robert A. Berg‡‡, and Gerd M. Rosenblatt

A rotating-wheel reflection grating modulates light at 60 kc for the measurement of lifetimes of 10^{-5} to 10^{-7} sec. An ultrasonic grating is used for modulation at 5.2 Mc to study lifetimes of 10^{-7} to 10^{-9} sec. Optical and electronic sources of error have been investigated. Procedures have been developed to minimize systematic errors in the lifetime measurements. Measurements have been carried out on $BaPt(CN)_4 \cdot 4H_2O$, I_2 vapor and on solutions of organic molecules.

---

*Abstract of paper published in Rev. Sci. Instr. 33, 1450 (1962).

†Now at Department of Mechanical Engineering, Imperial College of Science and Technology, London, S. W. 7, England.

‡Now at Department of Chemistry, University of California, Los Angeles, California.

††Now at Department of Chemistry, Northwestern University, Evanston, Illinois.

‡‡Now at Department of Chemistry, Harvard University, Cambridge, Massachusetts.

7. RADIATION TRANSITION PROBABILITY OF C_2

Leo Brewer and Lucy Hagan

The column of C_2 gas in a King furnace at temperatures of 2600 to 3000°K has been studied spectroscopically in absorption and emission to evaluate the transition probability of the Swan bands of C_2. Continuous light from a filament light source is passed through the C_2 gas, dispersed by a 3-meter grating, and then photographed. The filament temperature is varied over a range of temperatures starting well below the furnace temperature and ranging to well above the furnace temperature. Thus, the spectrum is first seen in emission and then passes through a reversal region where emission and absorption are exactly balanced, and finally the spectrum is seen in absorption. The reversal conditions are used to define the temperature of the

gas. Both the emission intersities corrected for absorption and the absorption intensities corrected for emission have been used to calculate f values or transition probabilities for the O-O Swan band of C_2. The f value is found to be 0.005±0.003.

8. PREDICTION OF ELECTRONIC STATES OF HIGH-TEMPERATURE DIATOMIC MOLECULES*

Leo Brewer

The prediction of high-temperature equilibrium concentrations of gaseous molecules requires knowledge of the entropies of these molecules. The calculation of the entropies requires, among other information, the knowledge of the types of low-lying electronic states.

A correlation of known electronic states of diatomic molecules with molecular orbital configurations allows the prediction of relative excitation energies of the low-lying electronic states of diatomic molecules bonded by means of s and p electrons. These correlations have been used to predict the ground electronic states for high-temperature gaseous molecules for which the ground states had not been previously established. In molecules such as MgO and CaO, the partition functions are found to be higher by a factor of ten than assumed in previous calculations of thermodynamic properties.

*Presented as a portion of a talk given at Robert Welch Foundation Conference on Modern Inorganic Chemistry, November 1962, and to be published in the Conference Report.

9. THERMODYNAMIC STABILITY AND BOND CHARACTER IN RELATION TO ELECTRONIC STRUCTURE AND CRYSTAL STRUCTURE*

Leo Brewer

The Engel theory of metals is used to relate structure and stability of elemental metals and intermetallic phases. The behavior of metallic systems can be described through use of the same bonding concepts as are successful in describing the chemical behavior of conventional materials.

*Published in Electronic Structure and Alloy Chemistry of Transitions Elements, edited by P. A. Beck (Interscience Publishers, division of John Wiley & Sons, New York, 1963).

10. APPARATUS FOR ABSORPTION SPECTROSCOPY AND DETERMINATION OF LIFETIMES IN MOLECULAR BEAMS

Leo Brewer, Beat Meyer, and Robert Walsh

A molecular beam apparatus has been built for optical observation of high-temperature molecules. The beam source is either a Knudsen cell heated by electron bombardment (temperatures up to 3200°K have been maintained over periods of one hour without fluctuations) or a resistance furnace with double heater. Absorption spectra of SnS, SnO, and I_2 have been photographed with a mirror system giving 21 absorption transits across the beam. Work is planned on LaO and other molecules.

11. INTERPRETATION OF KNUDSEN VAPOR-PRESSURE MEASUREMENTS ON POROUS SOLIDS*

Gerd M. Rosenblatt

A simple, steady-state model has been used to describe the vaporization, in a Knudsen cell, of a porous solid having a low vaporization coefficient. The description is in terms of the effective vaporizing area of the solid. The nature of the effective area and the assumptions in the model have been investigated. The model permits examination of vaporization processes in Knudsen cell studies and makes possible calculation of the equilibrium pressure and vaporization coefficient from vaporation rates measured with various Knudsen cells and simple geometries. A one-parameter empirical equation has been found to accurately represent measurements of the vaporization rates of arsenic taken over a large range of Knudsen-cell orifice areas.

*Abstract of Gerd M. Rosenblatt and Leo Brewer, Interpretation of Knudsen Measurements on Porous Solids, UCRL-10271, July 1962.

12. RESEARCH IN PROGRESS: LEO BREWER

a. Emission tubes containing C^{13} have been prepared and similar tubes with C^{14} are in preparation to allow study of the Deslandres-d'Azambuja bands of C_2 and a possible determination of the heat of formation of C_2 by establishment of a convergence limit in the spectrum. Owing to the overlapping of several band systems, comparisons of different isotopic spectra are necessary to separate rotational lines due to different bands. (Martin Shetlar)

b. Various sources of emission spectra of alkaline earth oxides are being investigated in preparation for an attempt to analyze several known but uncharacterized bands of MgO and CaO. (Robert Hauge)

c. Work is continuing on the consistent estimation of partition functions for the gaseous metal monoxides and thermodynamic evaluation of the high-temperature vaporization data for these molecules. (Gerd M. Rosenblatt)

d. High-temperature molecules and the reaction products of gas discharges are being trapped at low temperatures in different matrix materials. Work on visible and infrared spectra is in progress to characterize the species, their concentrations, and general matrix properties. (Beat Meyer)

e. Rotational analysis of the Se_2 spectrum is under way as a joint effort with Professor R. F. Barrow of Oxford University. (Beat Meyer).

f. A systematic survey of the O_2, S_2, Te_2, and Po_2 spectra is in progress. (Beat Meyer)

g. Work is in progress on the preparation of a LaO molecular beam which will be studied in absorption to fix the ground state and which will be excited to fluorescence with a sodium lamp so that the radiative lifetime of the excited electronic state can be determined. (Robert Walsh)

h. A paper is in preparation on the prediction of the types of phases and their composition ranges in the various multicomponent systems of 30 transition metals. The method of application of the Engel theory of bonding is described in detail, and the factors determining the stabilities of the body-centered cubic, hexagonal close-packed, cubic closed-packed, β-tungsten, sigma, α-manganese, and Laves phases are discussed. The final results are presented in the form of multicomponent phase diagrams. (Leo Brewer)

i. A paper is in preparation which discusses various methods of obtaining ultrapure metals by high-temperature purification processes. In particular, the removal of iron, cobalt, and nickel impurities is examined. Thermodynamic calculations are used to separate the metals into one group which can be distilled away from iron and another group from which iron can be vaporized by vacuum electron beam casting and by vacuum heating of filaments. The removal of iron from noble metals by heating filaments in a halide atmosphere is considered. (Leo Brewer)

13. PARAMAGNETIC RESONANCE OF METALS AND IONS IN MOLTEN SALTS AND SOLIDS*

Judith Brown† and Kenneth S. Pitzer‡

The observation of paramagnetic resonance absorption can be used as a microscopic tool for analysis of the nature of molten salts and their solids. A considerable amount of work has been done on molten salts, but most of this work has been concerned with macroscopic properties such as solubility, and the microscopic state of dissolved species has been unknown.

Paramagnetic resonance studies have been conducted from 25°C to 500° C on the systems $MnCl_2$, $MnCl_2 \cdot 4H_2O$, $MnCl_2$ in $ZnCl_2$, $MnCl_2$ in LiCl-KCl, $CrCl_3$, $CrCl_3$ in $ZnCl_2$, $CrCl_3$ in LiCl-KCl, $NiCl_2$ in LiCl-KCl, $FeCl_3$, $FeCl_3$ in LiCl-KCl, $VOCl_2$ in LiCl-KCl and Li in LiI. In the solids, resonance could be easily observed over a wide range of temperature. In the molten salts resonances could be observed only for the Mn(II) and Cr(III) systems.

Several microwave cavities were constructed for measurements on solids, but because of the high microwave losses in the molten systems a microwave cavity was not used. For the molten salts the sample was melted on the bottom of a terminated wave guide which was directly heated by an oven. The sample was either sealed in glass or melted directly in the wave guide, depending on the nature of the system.

In the case of Li in LiI it was hoped to determine the nature of the lithium metal that dissolves in LiI. Since no absorption could be observed in molten LiI, it can be concluded either that the system is not paramagnetic or that the line width is too large to allow detection. If the second conclusion is correct, we would estimate that $T_2 < 2 \times 10^{-10}$ sec. In light of our results for the transition metal ions in molten salts, a value of T_2 as small as this is not unexpected.

In the case of Mn(II) a variety of effects was observed and a summary of data for LiCl-KCl is given in Fig. IB. 13-1. In all the solutions (above 350°C) the line width increased with dilution. The total hyperfine line width expected for Mn(II) due to Mn^{55} is about 500 gauss. Since this value is approached by the most dilute solution, it might be expected that further dilution would reveal a hyperfine pattern. Because of experimental difficulties it was not possible to measure more dilute solutions. It is clear from the data that exchange interactions were important over the full range of concentrations studied, and future work should be designed for more dilute solutions.

In the case of $ZnCl_2$ all the line widths in the melt were determined by the high viscosity of this molten salt, and line widths changed little from solid to melt.

---

*Brief summary of work reported by Judith Brown, Magnetic Resonance of Metals and Paramagnetic Ions in Solution (thesis), UCRL-9944, Dec. 1961; a paper has been submitted to J. Phys. Chem.

†Now at Centre d'Etudes Nucléaire, Saclay (Seine et Oise), France.

‡Now President of Rice University, Houston, Texas.

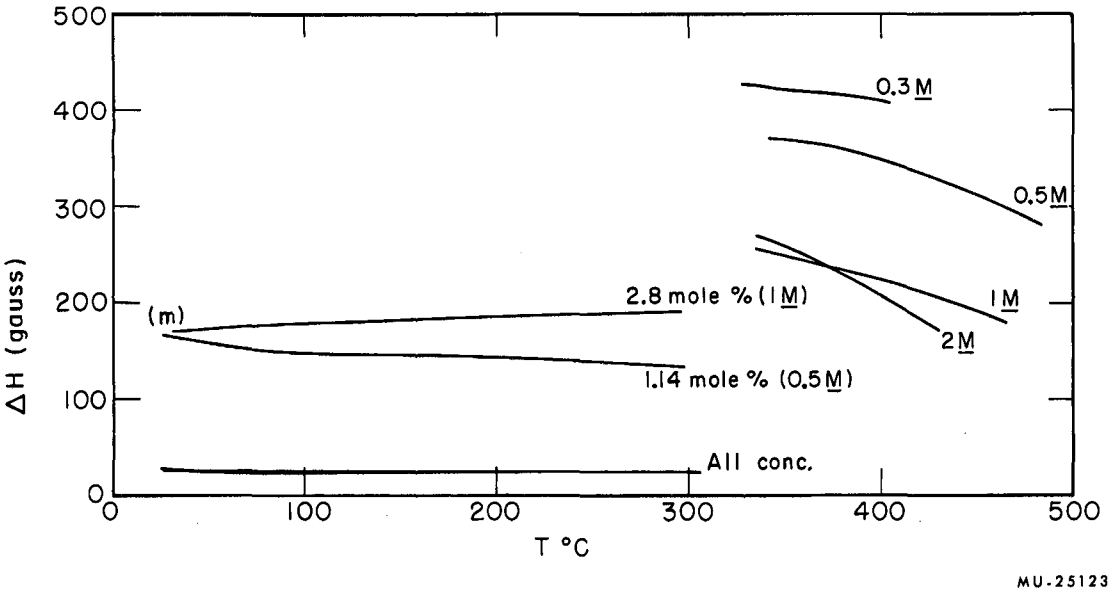

Fig. IB. 13-1. Summary of line widths of $MnCl_2$ in LiCl-KCl.

C. SOLID-STATE CHEMISTRY AND PHYSICS

1. THE PRESSURE GRADIENT IN LEAD BETWEEN BRIDGMAN ANVILS

Malcolm Nicol and George Jura

Since large pressure gradients have been demonstrated in materials between opposed anvils, it has been desirable to find better pressure-transmitting media than the usual silver chloride. Bridgman has studied various solids to pressures of 50 kbars. The techniques that he used would measure a value related to the average shear, but would give no information with respect to the pressure distribution within the sample. Phase transitions are the best and most reliable indicators for determining fixed pressure points. The small volumes in the anvils restrict the measurements to electrical resistivity. Most of Bridgman's measurements were on metals. There are obviously electrical problems in obtaining comparable measurements on poor conductors if the sample is to be immersed in a metal while the resistivity is determined at high pressures. This problem was solved in the following manner.

Lead was chosen as a pressure-transmitting medium for these experiments because it has the second lowest shear strength (thallium has the lowest). A lead disk for study between 0.5-in. -diameter anvils was prepared as follows:

A 0.020-in. hole was drilled in the lead. This hole was filled with silver chloride. Mylar tape, 0.0005 in. thick, was cemented to one side of the lead disk. A 0.006-in. hole was then drilled through the silver chloride and the Mylar tape. A 0.006-in. bismuth wire was forced through the center of this hole. The electrical-measuring connecting wires went through the anvils. In this manner the bismuth and the anvils were electrically isolated from the lead.

It was found that at low pressures, around the bismuth 1-2 transition, lead was a better pressure-transmitting medium than silver chloride in that the radial dependence was smaller. At the higher pressures, however, the silver chloride showed a smaller gradient. This was determined at the bismuth 6-8 transition, 88 kbars.

The silver chloride pressure distribution was measured, for comparison, both with and without Mylar tape. When the Mylar was used with the silver chloride, the pressure gradient became larger and, at the higher pressures, became nonlinear.

2. PHASE AND RESISTANCE CHANGES IN YTTERBIUM AT HIGH PRESSURES

George Jura and P. Clark Souers

The phase diagram of ytterbium was determined from 77 to 630°K. The transition pressure is 25 kbars at the highest temperature, and 55 kbars at the lowest. It has been shown by x-ray diffraction, by Hall and co-workers at Brigham Young University, that the transition is a change in structure from face-centered cubic at ordinary pressures to body-centered cubic at the higher pressures.

The important feature in the study of ytterbium is even more odd than the above unexpected change in crystal structure. It is the fact that ytterbium becomes a semiconductor before it undergoes this crystallographic change. Pressure is normally expected to enhance the metallic properties of any given material; at high enough pressures even insulators are expected to convert to metals. Such conversions have been demonstrated in this Laboratory for phosphorus and silver chloride. There is no published mechanism or calculation that would predict such a change.

Bridgman was the first investigator to observe a peculiarity in the electrical behavior of ytterbium. His investigations were carried out above room temperature and to pressures of 7 kbars. At the highest pressure he observed a reversal of the temperature coefficient of electrical resistivity. Our investigations were carried out at pressures ranging from 20 to 60 kbars, and at temperatures from 77 to more than 600°K, with both isothermal and isobaric measurements. The former were used primarily for the determination of the relative resistance and the latter for the determination of the energy gaps. Since the energy gaps are low, the isobaric measurements were all made below room temperature.

When ytterbium is compressed, there is an increase in resistance until the phase change occurs. At room temperature, the specific resistance increases by a factor of about 12, then falls by a factor of 14. The resistance in the β phase is practically independent of pressure to 200 kbars. At the higher temperatures the relative increase in resistance with pressure is less before the transition to the second phase occurs. As the temperature is lowered the resistance rises higher and higher. At 77°K the maximum measured resistance is almost 1000 times the resistance at room temperature and 1 atmosphere. The specific resistance at 77°K and a pressure of 50 kbars is 0.013 ohm cm. This resistance is roughly that of a heavily doped sample of germanium.

The isobaric determinations starting at 20 kbars all showed a temperature-resistance behavior characteristic of a semiconductor in that the resistance increased as the temperature was decreased. The energy gap was determined from the equation

$$R = P_{\infty} \exp(-E_G/2kT)$$

in the customary manner. The gap was 0.015 eV at 20 kbars, increased to

0.075 eV between 37.5 and 40 kbars, and then decreased to 0.04 eV at 45 kbars.

If this metal has been turned into a true semiconductor, then the observed values are not characteristic of intrinsic band gaps. The purity of the material used in these experiments was 99.8%. This is very impure for a semiconductor, and what probably has been observed are the impurity levels rather than the intrinsic gap. We are attempting to obtain purer material in an effort to determine the actual gap.

This unexpected behavior can be simply explained if certain assumptions are made with respect to relative shapes and positions of the various electronic bands.

The electronic configuration in the gas phase is $4f^{14}5s^{2}5p^{6}6s^{2}$. The chemistry indicates that the 4f band is not widely separated from the 5d band. The magnetic susceptibility measurements on 99.99% pure ytterbium by Locke indicate that in the solid about 1 in 250 of the 4f electrons are in the 5d state. This indicates that the binding in solid ytterbium is primarily due to the 6s electrons. With only two binding electrons ytterbium should be similar in properties to the alkaline earth metals. Bridgman has measured the compressibilities of most of the rare earths, including ytterbium, to 38 kbars. Ytterbium is much more compressible than any of the other rare earths. Indeed, its compressibility is almost the same as that of barium.

If ytterbium is indeed like barium, the electrical conductivity is due to the overlap of the 6p and 6s bands. If the bottom of the 6p band increases more rapidly with decrease in interatomic distance than the top of the 6s band, then the two bands will no longer overlap, and the material will become a semiconductor when compressed.

To explain the decrease in the gap it becomes necessary to assume that the 5d band lies above the 6s and 6p bands at the normal interatomic distance. The bottom of the band falls rapidly, and as the interatomic distance decreases, it first crosses the 6p band, and then should cross the 6s band. After the 5d band crosses the 6p band, the conduction band will be the 5d and not the 6p band. Lowering of energy of the 5d band, therefore, would account for the decrease in the gap. Furthermore, at a sufficiently high pressure the 5d band would intersect the 6s band, and when this occurred, the ytterbium would again become metallic. Metallic conductivity in the high-pressure modification of ytterbium measured at liquid nitrogen temperatures.

If these techniques could be applied to sufficiently low temperatures, then the return to the metallic state might be observed. Since the measurements are still somewhat uncertain at nitrogen temperatures, there is no immediate prospect of checking this last point.

3. THE INFLUENCE OF HIGH PRESSURES ON THE MÖSSBAUER EFFECT IN DYSPROSIUM-161

John A. Stone, Malcolm Nicol, John O. Rasmussen, and George Jura

An experimental study has been performed to determine the influence of pressures up to 100 kbar on the resonant absorption of gamma rays emitted without recoil.[1] The 25.6-keV γ ray of Dy^{161} from the decay of Tb^{161} situated in gadolinium metal was used with thin dysprosium absorbers.

The results of this work are summarized in Figs. IC. 3-1 through IC. 3-3 and in Table I. Figures IC. 3-1 and IC. 3-2 show the spectra of transmitted γ-ray intensity versus relative absorber velocity at pressures of approximately 30 kbar and 50 kbar, respectively. Considerable hyperfine structure is evident in these spectra. Figure IC. 3-3 is a comparison of spectrum envelopes, where the hyperfine structure has been smoothed and ignored, at 30 kbar, 50 kbar, and 100 kbar.

Table I gives several quantitative results derived from the experimental data. Because the absorption effect at atmospheric pressure was too small to be measured in these experiments, all quantities are quoted relative to the 30-kbar spectrum, for which the most precise data were obtained. The nomenclature used in Table I is defined as follows:

P = approximate pressure at which an experiment was performed;

x = ratio of the experimentally measured loading pressures on the oil in the hydraulic press, at pressure P and at 30 kbar; this is equal to the ratio of the pressures;

f_P/f_{30} = ratio of the fraction of γ rays emitted without recoil, at pressure P and at 30 kbar; this is equal to the ratio of the areas above the transmission curves at these pressures;

ΔE_P = energy difference between the highest- and lowest-energy components of the recoil-free γ-ray emission spectrum, at pressure P; the observed width of a velocity spectrum is the sum of this quantity and a corresponding quantity for the absorber, so that the difference between the observed widths at pressures P and 30 kbar is independent of the absorber and is equal to $\Delta E_P - \Delta E_{30}$; lower limits on $\Delta E_P \Sigma \Delta E_{30}$ may also be obtained;

$\bar{v}$ = velocity coordinate of the centroid of a velocity spectrum; this is related to the chemical shift between the source and the absorber.

Two qualitative conclusions may be drawn immediately from these comparisons. With increasing pressure:

(a) recoil-free fractions increase;

(b) hyperfine splittings increase.

---

[1] R. L. Mössbauer, Z. Physik 151, 125 (1958); Naturwiss. 45, 538 (1958); Z. Naturforsch. 14a, 211 (1959).

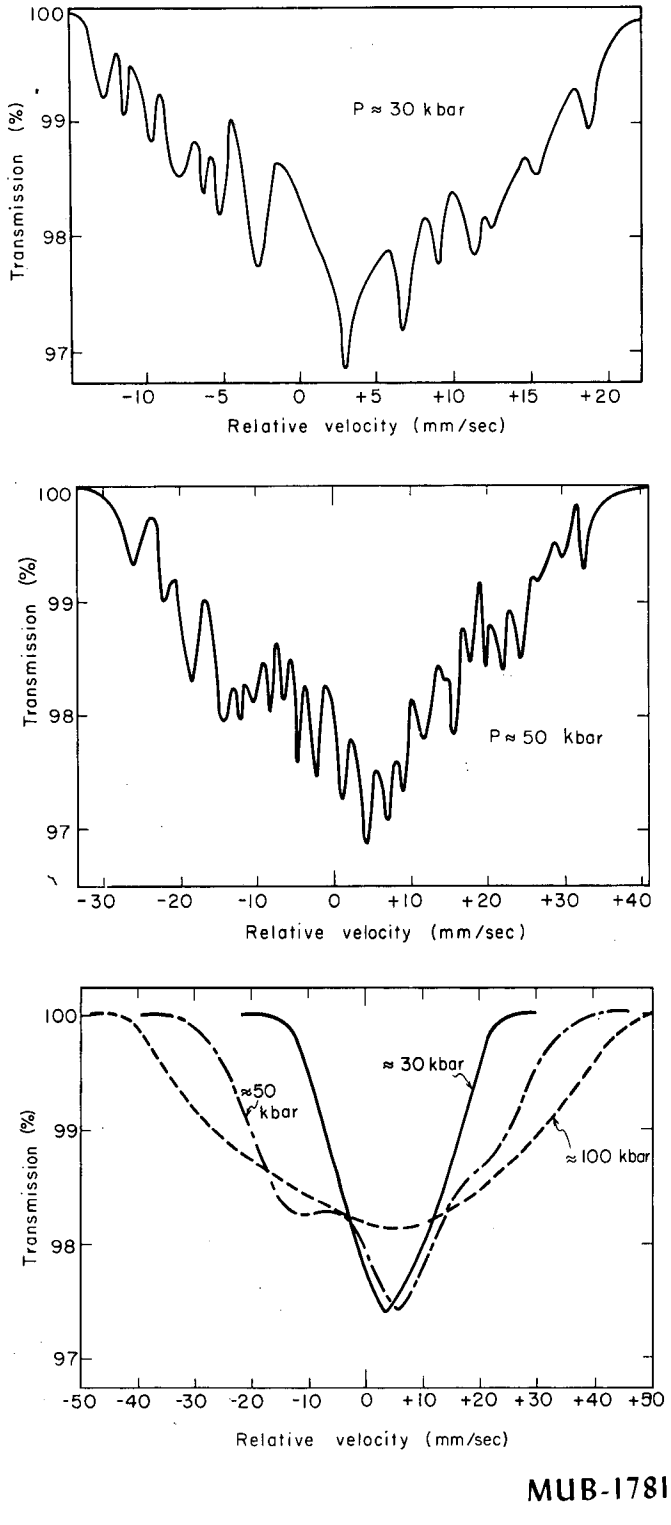

Figs. IC. 3-1 and IC. 3-2. Velocity spectrum of the 25.6-keV γ ray of Dy^{161} in Gd metal at approximately 30 and 50 kbar, respectively.

Fig. IC. 3-3. Comparison of envelopes of velocity spectra at several pressures for the 25.6-keV γ ray of Dy^{161} in Gd metal.

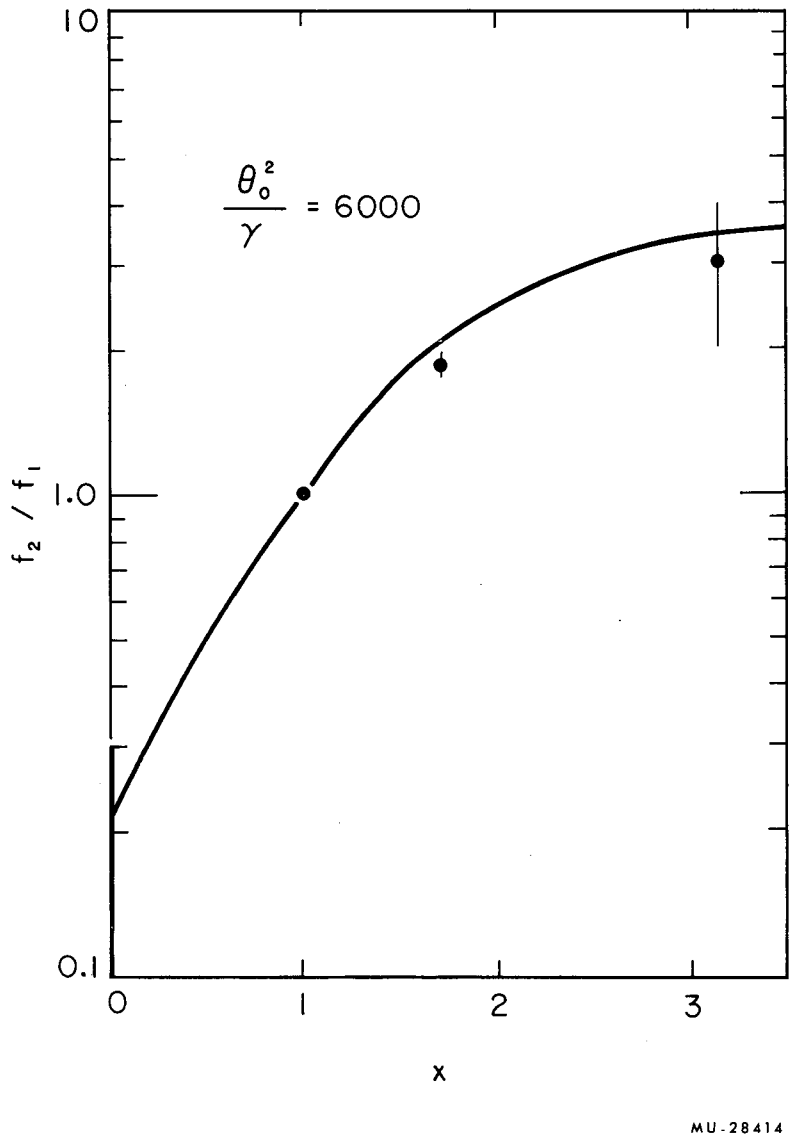

Fig. IC. 3-4. Comparison of calculated and experimental pressure dependence of recoil-free fraction ratios. —— calculated for $\theta_0^2/\gamma = 6000$; $\times \propto$ pressure.

Table I. Quantities measured in high-pressure Mössbauer absorption experiments.

P (kbar)	x	$\frac{f_P}{f_{30}}$	$\Delta E_P - \Delta E_{30}$ (cm/sec)	$\frac{\Delta E_P}{\Delta E_{30}}$	$\bar{v}$ (mm/sec)
0 (1 atm)	~0	≤0.3	---	---	---
30	1.00	1	0	1	4.0 ± 0.2
50	1.71	1.81 ± 0.05	2.67 ± 0.05	≥1.9	2.0 ± 0.4
100	3.14	3 ± 1	5.5 ± 0.2	≥2.8	---

An interpretation of the increase in recoil-free fractions with pressure may be made by use of a treatment similar to that by Hanks.[2] For this treatment it is necessary to derive equations for the case for which the ambient temperature T is greater than the Debye temperature θ. Starting with the expression for the recoil-free fraction f from the Debye model of lattice vibrations, one has

$$\ln f = -\frac{3}{2}\frac{R}{k\theta}\left[1 + 4\left(\frac{T}{\theta}\right)^2 \int_0^{\theta/T} \frac{t\,dt}{e^t - 1}\right], \tag{1}$$

where R is the normal recoil energy of an atom due to emission of the γ ray, and k is Boltzmann's constant, one may introduce the pressure dependence by the following series of approximations and assumptions:

(a) The volume dependence of θ is given by the Grüneisen relation,

$$\frac{d \ln \theta}{d \ln V} = -\gamma, \tag{2}$$

where γ is the Grüneisen constant for the material.

(b) Volume changes in the system are small.

(c) $T/\theta > 1.6$; this allows the use of the high-temperature approximation

$$4\left(\frac{T}{\theta}\right)^2 \int_0^{\theta/T} \frac{t\,dt}{e^t - 1} \approx 4\left(\frac{T}{\theta}\right) - 1. \tag{3}$$

(d) Volume changes can be expressed by

$$\frac{\Delta V}{V_0} \approx aP - bP^2, \tag{4}$$

where a and b are empirically determined coefficients.

[2] R. V. Hanks, Phys. Rev. 124, 1319 (1961).

(e) Pressure is proportional to loading.[3]

Using these assumptions, one obtains

$$\ln\frac{f_2}{f_1} = \frac{12\,RT\gamma}{k_{\theta_0}^2}\left(\frac{\Delta V_1}{V_0} - bP_1^2\,x\right)(x-1), \qquad (5)$$

where the subscript 1 refers to the reference state near 30 kbar, and the subscript 0 refers to the atmospheric pressure reference state. With θ_0^2/γ as an adjustable parameter, Fig. IC. 3-4 shows the fit of the calculated curve to the experimental points when $\theta_0^2/\gamma = 6000$. The experimental results appear to be consistent with values of θ_0 from 75 to 100 for a dysprosium impurity in gadolinium metal. This range is somewhat lower than the values for the pure metals, which are near 150.

[3]Peter W. Montgomery, Harold D. Stromberg, George H. Jura, and George Jura, Calibration of Bridgman Anvils, a Pressure Scale to 125 kbars UCRL-9807, Aug. 1961.

4. RESEARCH IN PROGRESS: GEORGE JURA

a. The Mössbauer spectrum of iron as a function of pressure is now under investigation. The "loud speaker" drive is being used for the determination of the entire spectrum. The present results indicate that only a small change, if any, occurs up to a nominal pressure of 120 kbars. At 140 kbars a line centering near zero velocity appears, and there is a strong perturbation of two other lines. There is a very sluggish phase change in iron which starts at about 160 to 170 kbars at room temperature. The new phase is hexagonal in structure. This structure would permit quadrupole-induced transitions. It is likely that the center line and the changes in the new lines result from the quadrupole transitions in the hexagonal form and quadrupole interaction. The present system does not permit investigation of this spectrum at higher pressures. Anvils with a different grade of carbide will be used in an attempt to determine the spectrum at higher pressures. (With Malcolm Nicol)

b. Work is proceeding on the apparatus for the determination of the magnetic permeability of solids as a function of pressure. The present sensitivity is sufficient to determine the Curie temperature of gadolinium as a function of pressure. At present the reproducibility of the Curie temperature of gadolinium at 1 atmosphere is about 0.5°. The electrical circuit is still faulty, however. When it is improved there should be a marked increase in the sensitivity. There are indications that further improvements can be made by changes in the coil design and in the shapes of the anvils. With the present apparatus the effect of pressure on the Curie temperature of gadolinium could be determined to pressures of about 100 x kbars. However, we feel that it would be wiser to spend time on the instrumentation to increase the overall usefulness of the apparatus. (With David Phillips)

c. Europium is now under investigation. There are two features of particular interest. First, the Neel point can be determined by the resistance change. Preliminary investigation shows that the temperature of the Neel point is independent or nearly independent of the pressure, and consequently of the molar volume. The full implications of this observation have not as yet been investigated. It seems strange that the antiferromagnetic-paramagnetic transition should be only temperature-dependent.

There is a phase transition that occurs at about 300 kbars at room temperature. The behavior of this transition will be studied as a function of temperature and pressure.

When the work on europium is completed, similar measurements will be undertaken on gadolinium and dysprosium. (With P. Clark Souers)

5. LATTICE HEAT CAPACITY, ISOTOPE EFFECT, AND SIMILARITY PRINCIPLE IN INDIUM

H. R. O'Neal, N. M. Senozan, and Norman E. Phillips

Bryant and Keesom[1] have reported heat capacity measurements on indium to 0.37°K which can be interpreted as showing that the lattice heat capacity is 40% less in the superconducting state than in the normal state. We have extended the heat capacity measurements to 0.08°K and have made critical field measurements on In^{113} and In^{115} between 1.1°K and T_c. The critical field measurements were suggested by the connection between the similarity principle and lattice heat capacity pointed out by Marcus and Maxwell[2] and by Chester.[3]

The temperature scale for the heat capacity measurements was based on an extrapolation of the susceptibility of a crystal of cerium magnesium nitrate according to the Curie law. Measurements on copper, for which the heat capacity is well known above 1°K, were used as a test of accuracy. Within the random error of about 1% they were in agreement with an extrapolation from above 1°K at temperatures above 0.5°K, 1% high at 0.3°, and 1.5% high at 0.09°.

In this temperature range the normal state heat capacity, C_N, can be expected to have the form.

$$C_N = C_Q + \gamma T + \alpha T^3 + \beta T^5 .$$

---

[1] C. A. Bryant and P. H. Keesom, Phys. Rev. Letters 4, 460 (1960); Phys. Rev. 123, 491 (1961).

[2] P. M. Marcus and E. Maxwell, Phys. Rev. 91, 1035 (1953).

[3] G. V. Chester, Phys. Rev. 104, 883 (1956).

Here C_Q is the heat capacity contribution associated with the nuclear quadrupole moment and is proportional to T^{-2}, γT is the conduction electron term, and the T^3 and T^5 terms represent the lattice heat capacity. The data are shown in Figs. IC. 5-1 and IC. 5-2. The experimental error prevents an unambigious evaluation of the parameter α, and would make a least-squares analysis misleading. We have obtained approximate values of C_Q and γ from the lowest temperature points and used these values to analyze the data in the region between 0.5° and 1°K, as shown in Fig. IC. 5-2. We have taken $\gamma = 1.68$ millijoules/mole deg^2 and $\alpha = 1.43$ millijoules/mole deg^4 as the most probable values. For this choice of γ the lattice heat capacity shows a pronounced deviation from the expected temperature dependence at low temperatures, but this behavior could be produced by a systematic error comparable to that found in the measurements on copper. Bryant and Keesom found α - 1.53 and elastic constants[4] give $\alpha = 1.41$. The values of γ and C_Q obtained in this way are in reasonable agreement with critical field measurements below 1°K,[5] and with nuclear resonance experiments,[6,7] respectively.

In the superconducting state no T^{-2} contribution to the heat capacity appears. We interpret this as showing that the nuclear spin-lattice relaxation time, T_1, is long compared with the 2 or 3 minutes required for a heat capacity measurement. As estimated T_1 of 8 seconds for normal indium at 0.1°K is obtained by application of the Korringa relation to Knight-shift data for liquid indium. The equality of the shift in solid and liquid has been discussed by Knight and Berger.[8] We could not detect relaxation effects in the normal-state measurements, and conclude that $T_1 \lesssim 5$ sec. The estimated increase in T_1 for the superconducting state[9] could explain our observations. As shown in Fig. IC.5-2, the total heat capacity in the superconducting state is as much as 10% less than the lattice heat capacity estimated for the normal state.

The larger size of the anomaly reported by Bryant and Keesom is partly a result of their subtraction of a calculated C_Q from the experimental data for both states. Our normal state measurements differ from theirs by at most 2%, but our analysis gives a 10% smaller T^3 term. In the superconducting state we find a heat capacity 10% higher than reported by Bryant and Keesom at their lowest temperature. Finally we note that our measurements do not by themselves completely exclude a value of approximately 1.3 for both states, but such an interpretation requires giving more weight to the lowest temperature points than we believe justified. In addition, the measured γ and α would not agree with those calculated from critical fields and elastic constants, and the lattice heat capacity would be approximated by $\alpha T^3 + \beta T^5$ only to 0.5°K, or approximately $\theta/200$.

---

[4] B. S. Chandrasekhar and J. A. Rayne, Phys. Rev. Letters 6, 3 (1961).

[5] D. K. Finnemore and Dillon E. Mapother (University of Illinois), private communication.

[6] R. R. Hewitt and W. D. Knight, Phys. Rev. Letters 3, 18 (1959).

[7] W. W. Simmons and C. P. Slichter, Phys. Rev. 121, 1580 (1961).

[8] W. D. Knight and A. G. Berger, Annals of Physics 8, 173 (1959).

[9] L. C. Hebel, Phys. Rev. 116, 79 (1959).

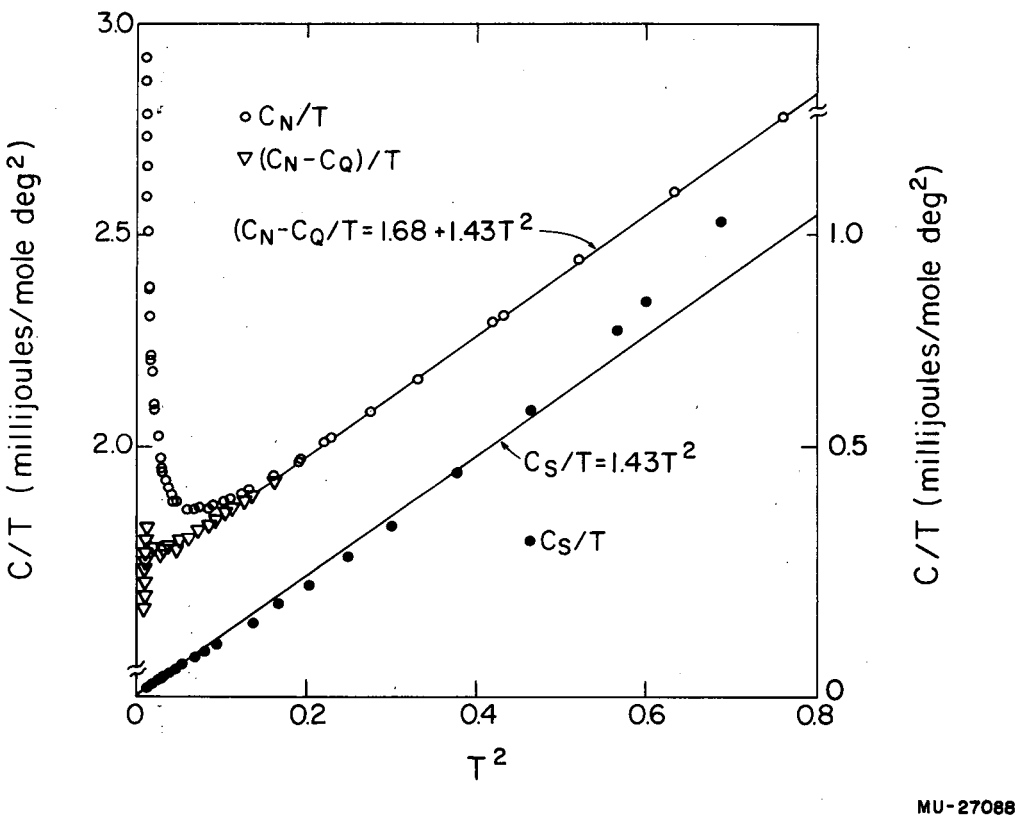

Fig. IC. 5-1. Heat capacity of indium.

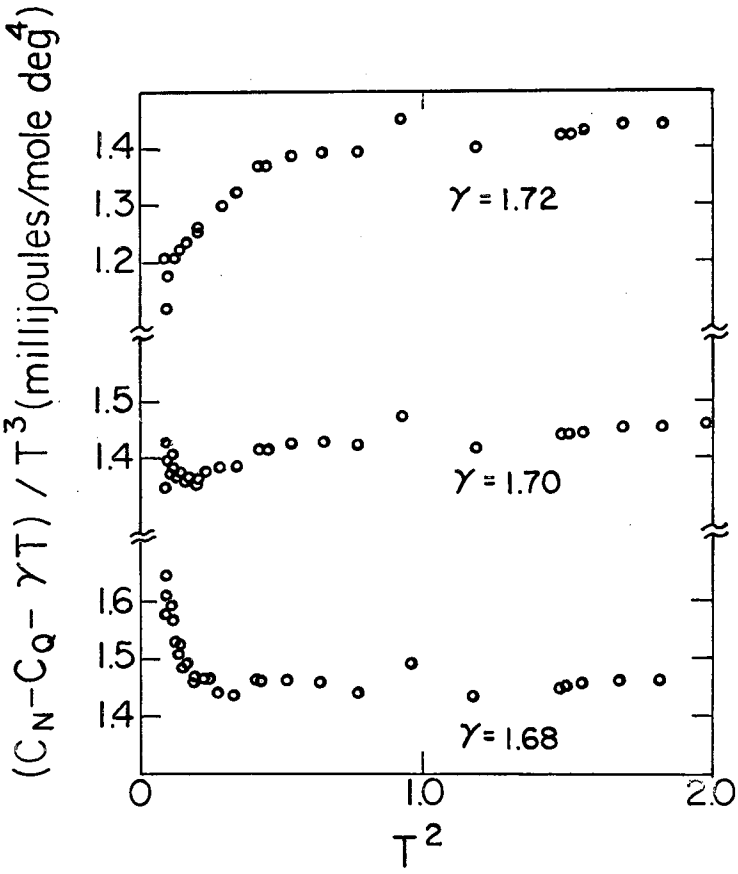

Fig. 2. Lattice heat capacity in the normal state the lowest points shown the lattice heat capacity is 5% of the total. MU-30319

Fig. IC. 5-2. Lattice heat capacity in the normal state. For the lowest points shown the lattice heat capacity is 5% of the total.

Preliminary critical field data are summarized in Figs. IC. 5-3 and IC. 5-4. We find that H_0 and T_c are proportional to $M^{-0.56}$ and that within the accuracy of the experiments the similarity principle is obeyed. It follows from the argument advanced by Chester[3] that the part of the heat capacity associated with the thermal excitation of lattice vibrations should be the same in the two states.

Several explanations of the difference in lattice heat capacity have been proposed. Ferrell has suggested that there is a dispersion of phonons in the superconducting state such that the important thermally excited modes have a velocity different from that observed in ordinary ultrasonic experiments.[10] Attempts to observe this dispersion have not been successful.[11] Daunt and Olsen have postulated that the whole frequency spectrum has a temperature dependence which is related to the temperature dependence of the elastic constants in the same way as expected for the low-frequency modes.[12] This temperature dependence is different in the normal and superconducting states, and although the usual heat capacity contribution is not significantly changed, there is an important contribution from the temperature dependent zero-point energy of the high frequency modes. An extension of this argument would give a readily observable latent heat at T_c related to the discontinuity in elastic constants, and would make measured lattice heat capacities generally differ from those calculated from elastic constants. It seems probable that if the lattice zero-point energy is involved it is the high-frequency modes which are important, but their frequencies are not related in such a simple way to the elastic constants.

[10] R. A. Ferrell, Phys. Rev. Letters 6, 541 (1961).

[11] K. Dransfeld (Ohio State University), private communication.

[12] J. G. Daunt and J. L. Olsen, Phys. Rev. Letters 6, 267 (1961).

6. LATTICE HEAT CAPACITY OF SUPERCONDUCTING TIN

Harry R. O'Neal and Norman E. Phillips

As part of a search for discrepancies in lattice heat capacities between the normal and superconducting states in metals other than indium we have made heat capacity measurements on normal and superconducting tin between 0.1°K and 1.1°K. The data, together with the measurements by Bryant and Keesom[1] at temperatures above 0.4°K, are shown in Fig. IC. 6-1 and have been analyzed as discussed in the accompanying report (IC. 5) on indium. In tin the lattice heat capacity is so small that it is not possible to obtain an accurate value calorimetrically in the normal state. The only meaningful comparison of the superconducting-state lattice heat capacity is with that calculated from

[1] C. A. Bryant and P. H. Keesom, Phys. Rev. 123, 491 (1961).

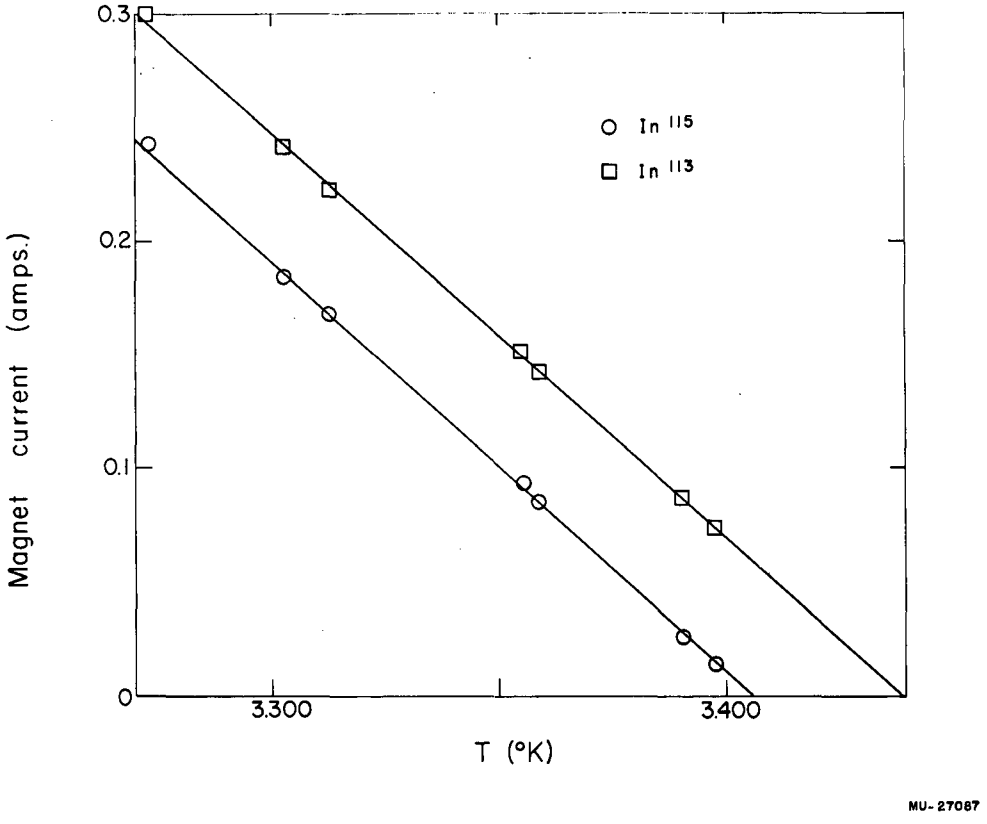

Fig. IC. 5-3. Isotope effect near T_c.

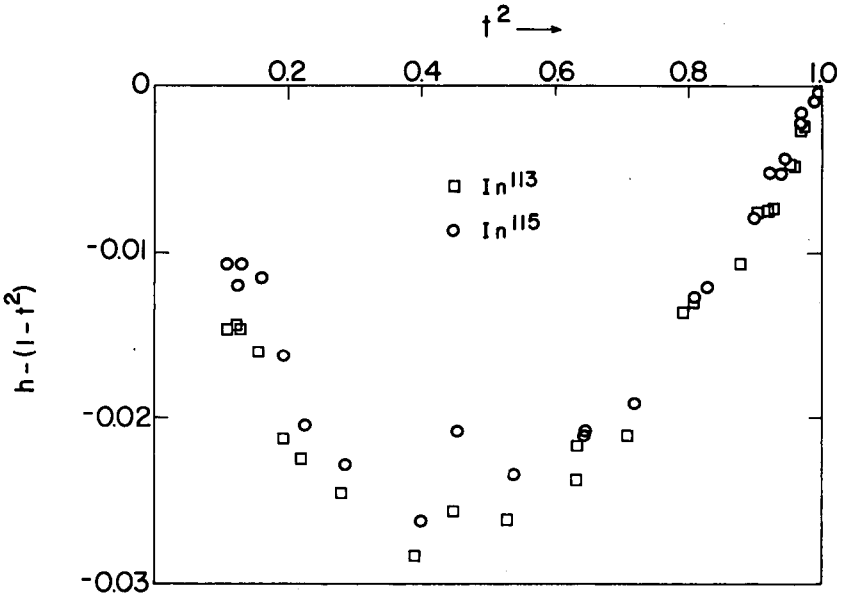

Fig. IC. 5-4. Demonstration of the similarity principle $h = H_c/H_o$, $t = T/T_c$.

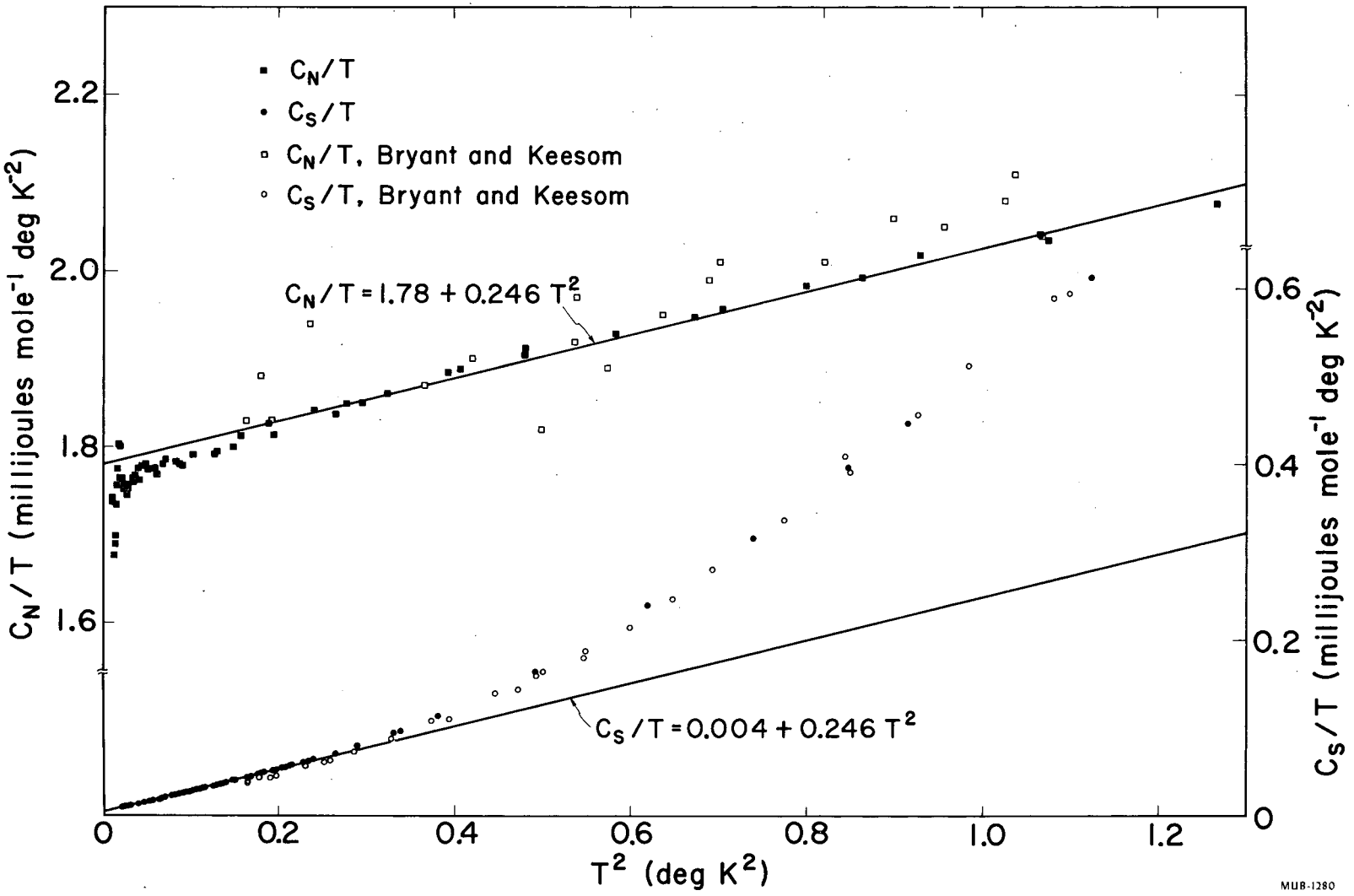

Fig. IC. 6-1. The heat capacity of tin.

the elastic constants. In contrast with the corresponding comparison for indium, the agreement is within the combined experimental errors. The calorimetric lattice heat capacity in the superconducting state is 0.246×10^{-3} T^3 joules $mole^{-1}$ deg^{-1}, and the value calculated from elastic constants[2] is 0.238×10^{-3} T^3 joules $mole^{-1}$ deg^{-1}.

[2] J. A. Rayne and B. S. Chandrasekhar, Phys. Rev. 120, 1658 (1960).

7. LATTICE HEAT CAPACITY OF LEAD AND MERCURY

William R. Gardner, Marcel Lambert, and Norman E. Phillips

The "strong-coupling" superconductors, lead and mercury, are logical choices for experiments designed to detect changes in properties of the lattice brought about by the transition to the superconducting state. From the experimental point of view the high transition temperatures and large lattice heat capacities make these metals attractive choices for calorimetric experiments. Since heat capacity measurements are at present the only method capable of detecting the effect,[1] it is particularly important that they be carried out on lead and mercury.

So far measurements have been made on normal and superconducting mercury between 1.2°K and 4.4°K and on superconducting lead between 0.3°K and 1.0°K. The mercury measurements show no obvious effect of the kind observed in indium, but do not extend to a low enough temperature to eliminate the possibility. They will shortly be extended to 0.1°K. The preliminary data on lead can be compared with elastic-constants measurements, and suggest that there is a difference in lattice heat capacity between the normal and superconducting states comparable in magnitude but opposite in sign to that in indium. It is planned to make normal-state measurements and to extend the temperature range of the measurements.

[1] One of us (N. E. P.) has developed an argument to show that the Mössbauer experiments, which have been suggested and used to search for a change in the frequency spectrum associated with the superconducting transition, are not sufficiently sensitive to show changes of the magnitude indicated by the calorimetric experiments on indium.

8. THERMAL PROPERTIES OF SOLID HYDROGEN AT SMALL MOLAR VOLUMES

Guenter Ahlers and Norman E. Phillips

Apparatus has been constructed for the measurement of thermal properties of solid hydrogen at small molar volumes. The accessible volume range is approximately 14 to 22.6 cc/mole. The temperature range is 1.4 to 25°K.

The heat capacity of parahydrogen has been measured at zero pressure and at a molar volume of 22.6 and 18.8 cc/mole. Apparent Debye θ values and Grüneisen γ values as calculated from the relation

$$\frac{d\ \ell n\,\theta}{d\ \ell n\,V} = -\gamma$$

are given in Table I.

Table I. Thermal data for solid parahydrogen.

T (°K)	θ (°K) 22.6 cc/mole	θ (°K) 18.7 cc/mole	γ	$\alpha \times 10^4$ (°K^{-1})
2	125.0	181	1.95	4
4	123.0	181	2.03	9
6	119.4	180	2.16	18
8	114.6	179	2.34	27
10	110.8	177	2.46	34
12	108.4	175	2.51	44
14	107.3	172	2.47	
16	107.1	168	2.36	
18		163		
20		157		

The heat capacity measurements at zero pressure, and at 22.6 cc/mole permit the calculation of the thermal expansion coefficient if the isothermal compressibility is known. Megaw's value[1] of the compressibility was used to calculate the thermal expansion. These results are also listed in the table. The calculated total volume change between 4.2°K and 13.8°K is 0.66 cc/mole, in agreement with the directly measured molar volumes.[1, 2] The thermal expansion at the triple point was found to be 48×10^{-4} °K^{-1}, to be compared with $(53 \pm 18) \times 10^{-4}$ °K^{-1} as obtained by Bartholomé.[2]

Measurements on the anomalous heat capacity in orthohydrogen due to the splitting of the $J=1$ rotational levels is now in progress. The theoretical work by Orttung[3] on this effect at low orthohydrogen concentrations has been somewhat extended.

[1] H. D. Megaw, Phil. Mag. 28, 129 (1939).

[2] E. Bartholomé, Z. Phys. Chem. B33, 387 (1936).

[3] William H. Orttung, Thermal Properties of Solid Hydrogen Under Pressure (thesis), UCRL-9388, Feb. 1961.

Some data have been obtained on the kinetics of the ortho-para conversion at small molar volumes. This work is also still in progress.

9. THE HEAT CAPACITY OF FERROMAGNETIC $CrBr_3$ BETWEEN 1°K AND 4°K

Lawrence Shen and Norman E. Phillips

The recently discovered insulating ferromagnet $CrBr_3$ provides an opportunity to test spin wave theory for a system of localized magnetic moments. We have measured the heat capacity between 1.2 and 4.2°K in zero magnetic and in fields to 13,000 Oe. These measurements were made as preliminary to a study over a wider temperature range and in higher fields. The measurements in sufficiently high fields are expected to provide an unambiguous separation of spin wave and lattice contributions, but the 13,000-Oe measurements have not proven helpful in this respect.

The present data in zero magnetic field could be fitted by the sum of a T^3 lattice term, a $T^{3/2}$ magnetic term, and a T^{-2} term due to magnetic hyperfine splitting.

The main contribution to the specific heat was from the ferromagnetic spin waves with which the $T^{3/2}$ term was associated. The exchange integral obtained from the coefficient of this term was close to that obtained from magnetic resonance experiments[1] and from the Curie temperature.[2] The dependence of spin-wave specific heat on external magnetic field was complicated by the anisotropy field of 6850 Oe.[3]

---

[1] A. C. Gossard, V. Jaccarino, and J. P. Remeika, Phys. Rev. Letters 7, 122 (1961).

[2] I. Tsubokawa, J. Phys. Soc. Japan 15, 1664 (1960).

[3] A. C. Gossard, V. Jaccarino, and J. P. Remeika, J. Appl. Phys. Suppl. 33, 1187 (1962).

10. CALORIMETER FOR THE REGION 0.25 TO 20°K

Russell H. Batt and Norman E. Phillips

Most low-temperature calorimetry has been confined to the temperature region 1 to 4°K, accessible with liquid helium, or to temperatures above 15°K, at which liquid hydrogen can be used. Only a few calorimeters for temperatures below 1°K or between 4° and 15°K have been used. On the other hand there are many materials for which heat capacity data over an extended low-temperature region from below 1°K to 20 or 30°K would be of great interest. These include ferromagnets, antiferromagnets, ferromagnetic superconductors, and superconductors with transition temperatures above 4°K.

This has led us to design and construct a calorimeter capable of operating between 0.25°K and 20°K or higher. The calorimeter consists of an inner vacuum-jacket heat shield which contains the sample and can be held at any temperature throughout the operating range, and an outer vacuum jacket which can be surrounded by a bath of liquid helium or liquid hydrogen. Mechanical thermal switches are used to make thermal contact between the sample and the heat shield and between the heat shield and the bath. The inner heat shield is in thermal contact with a magnetic thermometer, a gas thermometer, vapor-pressure thermometers, a calibrated platinum thermometer, and germanium thermometers. The gas thermometer is used to interpolate between the regions in which temperature can be determined from hydrogen or helium vapor-pressure measurements, and the magnetic thermometer is used to extrapolate below the helium region. The platinum thermometer provides a convenient check at the higher temperatures and the germanium thermometers are convenient secondary standards which are usable over the whole range and which retain their calibration from run to run. Temperature below 1°K are maintained by pumping a He^3 chamber attached to the heat shield, and regulated by controlling the pumping speed or by using a carbon thermometer in a bridge circuit as a sensing device to control a heat input to the shield. Between 1°K and the boiling point of liquid helium the heat shield is put in thermal contact with the helium bath, whose temperature is controlled by conventional methods. Between the boiling point of liquid helium and the triple point of hydrogen the heat shield is controlled at a temperature above that of the bath by the bridge circuit. Through the liquid hydrogen range the temperature of the outer bath is controlled and the heat shield is again placed in thermal contact with the bath.

Several preliminary runs on a copper sample have been made to test the operation of the apparatus. The results are in good agreement with other measurements between 1 and 4°K, and extrapolate in a reasonable way to higher and to lower temperature except near 0.3° and 10°K, where there is thought to be several percent error associated with the temperature measurements.

11. LOW-TEMPERATURE HEAT CAPACITIES OF CONSTANTAN AND MANGANIN

James C. Ho, Harry R. O'Neal, and Norman E. Phillips

Constantan and manganin wire are commonly used in the construction of heaters for calorimetric experiments. Each of these alloys has, at low temperatures, a heat capacity that is large compared with that of many materials on which calorimetric experiments are of interest. We present here the results of heat capacity measurements on constantan between 0.15°K and 4.2°K and on manganin between 0.2°K and 4.2°K. These data should be useful in the design of calorimetric experiments and, in some cases, in the correction of experimental data for the heat capacity of the heater.

Both metals were obtained from the Driver-Harris Company,[1] and were large cylindrical samples of the material used in the manufacture of

[1] Driver-Harris Company, Harrison, New Jersey.

resistance wire. The manganin was of stated composition 13% manganese and 87% copper. The constantan sample was of the material used in "Advance" wire, 43% nickel and 57% copper.

The measurements were made as described previously[2] except that above 1°K temperatures were measured on the 1958 He^4 scale and below 1°K the temperature was calculated from a different temperature-susceptibility relation which is believed to give heat capacities accurate to about 1%.[3]

Smooth curves giving heat capacity versus temperature are shown in Fig. IC. 11-1. With the exception noted below, the experimental points fell within 1% of the curves. For manganin the data between 0.2°K (the lowest temperature of measurement) and 2.5°K are given by

$$C = 0.0115T^{-2}+0.0595T+0.00294T^{3} \text{ millijoules } g^{-1} \text{ deg}^{-1} .$$

At temperatures above 2.5°K the data deviate from this equation, and smoothed values are given in Table I. For constantan, irreproducible heat capacities and spontaneous generation of heat in the sample were observed for temperatures between 0.3°K and 1.0°K. These effects may have been associated with the exposure of the sample to a magnetic field of several thousand oersteds on cooling. From 0.15°K, the lowest temperature at which measurements were made, to 0.3°K the data are given by

$$C = 0.00281T^{-2}+0.205T \text{ millijoules } g^{-1} \text{ deg}^{-1}.$$

Smoothed values of the heat capacity at higher temperatures are given in Table II. The experimental points in the region 0.3°K to 1.0°K deviated from the smoothed values by as much as 20%.

Table I. Heat capacity of manganin.

T (°K)	C (mJ/g. °K)
<2.50	$0.0115T^{-2}+0.0595T+0.00294T^{3}$
2.50	0.197
2.75	0.224
3.00	0.251
3.25	0.280
3.50	0.310
3.75	0.342
4.00	0.376

[2] N. E. Phillips, Phys. Rev. 114, 676 (1959).

[3] N. E. Phillips, unpublished data.

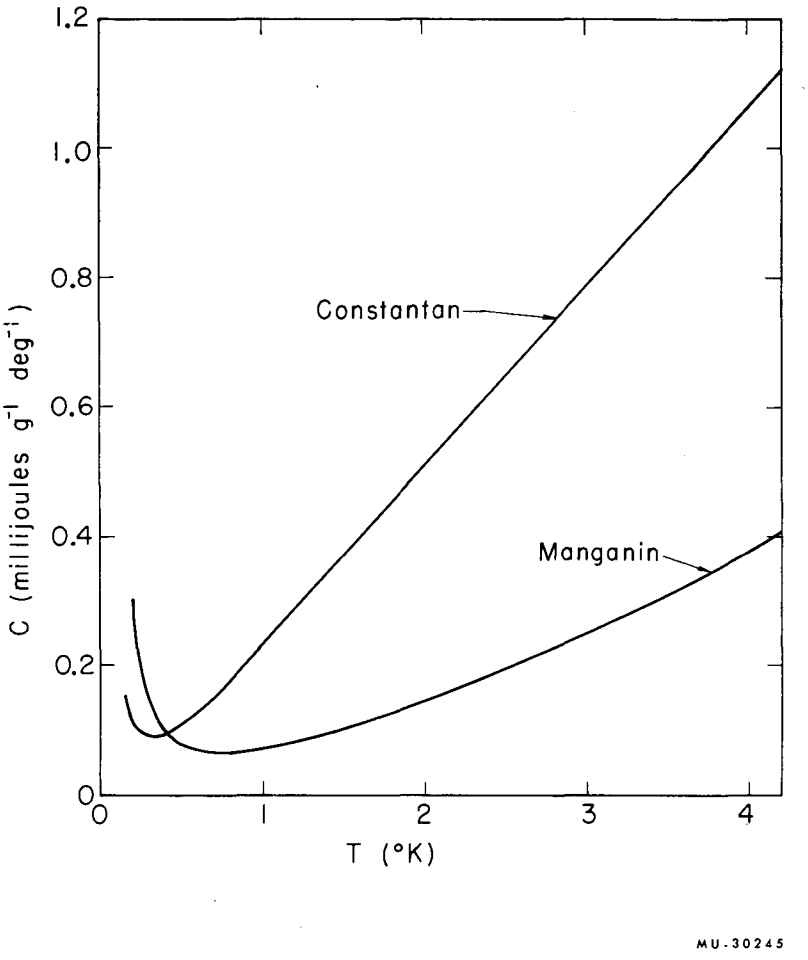

Fig. IC. 11-1. The heat capacities of constantan and manganin.

Table II. Heat capacity of constantan.

T (°K)	C (mJ/g. °K)
< 0.3	$0.00281T^{-2} + 0.205T$
0.30	0.0927
0.40	0.0960
0.50	0.107
0.75	0.163
1.00	0.233
1.25	0.303
1.50	0.372
1.75	0.442
2.00	0.511
2.25	0.580
2.50	0.649
2.75	0.715
3.00	0.786
3.25	0.853
3.50	0.923
3.75	0.991
4.00	1.060

12. HEAT CAPACITY OF KBr AT TEMPERATURES BELOW 1°K

Harry R. O'Neal and Norman E. Phillips

Recent improvements in low-temperature calorimetry and the development of the ultrasonic pulse technique for sound velocity measurements have made possible more exact comparisons of the Debye characteristic temperature obtained from heat-capacity experiments, θ_0^c, with that calculated from sound velocities, θ_0^s. At the same time theoretical developments have raised questions whether the two should be identical or not. Leibfried and Ludwig have suggested that anharmonic effects should introduce a discrepancy of several percent in certain cases.[1] Barron and Klein, on the other hand, find that θ_0^c and θ_0^s should be rigorously equal even in the presence of anharmonicity.[2] It is of considerable interest to test the equality of

[1] G. Leibfried and W. Ludwig, in Solid State Physics, edited by F. Seitz and D. Turnbull (Academic Press, Inc., New York, 1961), Vol. 12, p. 275.

[2] T. H. K. Barron and M. L. Klein, Phys. Rev. 127, 1997 (1962).

θ_0^c and θ_0^s, partly to answer the questions raised above and partly so that elastic-constants data can be used to calculate the lattice heat capacity in crystals in which it would otherwise be difficult to separate the lattice heat capacity from other contributions, e.g., spin wave effects.

For KBr the data previously available[3] did not extend to low enough temperatures to be in the T^3 region of lattice heat capacity, but an extrapolation to $T = 0$ gave a value of $\theta_0^c = 174°K$ in comparison with θ_0^s of 171.7,[4] and 172.8°K.[5] The present measurements extend to well below 1°K, where the heat capacity is accurately proportional to T^3, and give $\theta_0^c = 170.1 \pm 0.5°K$. This value of θ_0^c is more accurate than the available θ_0^s values, which have been obtained by extrapolation from 77°K, and the discrepancy must be considered as within the experimental error in θ_0^s.

---

[3] T. H. K. Barron, W. T. Berg, and J. A. Morrison, Proc. Phys. Soc. A242, 478 (1957); W. T. Berg and J. A. Morrison, ibid, p. 467.

[4] D. D. Betts, A. B. Bhatia, and M. Wyman, Phys. Rev. 104, 37 (1956).

[5] G. A. Alers and J. R. Neighbors, Rev. Mod. Phys. 31, 675 (1959).

13. RESEARCH IN PROGRESS: NORMAN E. PHILLIPS

a. Heat capacity measurements on superconducting alloys containing transition metals and lanthanide metals are being continued. The main interest is in connection with the various effects on the superconducting transition temperatures and the different kinds of magnetic behavior.

b. Work on solid hydrogen and solid helium under pressure is being continued and additional apparatus suitable for lower pressure measurements is being assembled.

c. The lattice heat capacity of superconducting lead and mercury is being measured to temperatures of 0.1°K and similar measurements on vanadium, niobium, and tantalum are planned.

d. Heat capacity measurements on several antiferromagnetic materials are in progress.

e. Heat capacity measurements designed to determine nuclear quadrupole coupling constants in several metals are planned.

f. Apparatus for heat capacity measurements to below 0.1°K is nearly complete and will be put into operation shortly.

g. Apparatus for elastic-constant measurements at low temperatures is being built and will be used to evaluate lattice heat capacities at low temperatures.

D. CHEMICAL KINETICS

1. ELASTIC SCATTERING OF MOLECULAR BEAMS

Philip R. Brooks and Dudley R. Herschbach

Studies of molecular beam scattering at thermal energies have mostly been confined to beams of alkali metals and their compounds, since these can be readily detected by surface ionization. In order to carry out measurements of collision cross sections for other molecules, we have constructed a space-charge detector, or "Kingdon Cage," which in principle should be capable of detecting any ionizable species. The operation of the detector is based on neutralizing part of the space charge within a diode by positive ions formed from the beam.[1] Details of the design and preliminary studies of the detector are described in a previous report.[2] In the original version of the detector,[1,2] the signal was obtained as the difference in plate currents of two identical diodes, one exposed to the beam, the other only to the background gas. A great increase in the convenience of operation has been obtained with a new, single diode model. The incident molecular beam is now mechanically modulated at 10 cycles per second and the AC signal from the detector is filtered and amplified by a phase sensitive lock-in amplifier.[3] Beam intensities of the order of 10^{10} molecules/sec can be detected. Compounds studied include argon, methyl iodide, ethane, heptane, and nitrogen.

In order to be useful for scattering experiments, the detector must be metrical and must detect the beam itself, rather than any general increase in background pressure. Both of these requirements are satisfied, as shown in Fig. ID. 1-1, which compares calculated and experimental beam profiles. However, the detector is not linear. The signal S is related to the beam intensity as $S = K I^{\alpha}$, where K is a constant that depends on apparatus parameters, and the exponent α depends on the detector dimensions as well as the beam composition. Typical values of α are 1.2 for CH_3I and 0.9 for argon.

Total collision cross sections have been determined by passing the beam through a chamber containing a scattering gas at a low pressure. The attenuation of the beam is measured as a function of the pressure of the scattering gas, as illustrated in Fig. ID. 1-2. The cross section is calculated from the slope of $\ell n S/S_0$ versus scattering gas pressure, the beam and gas temperatures, and the scattering path length.[4] Provisional values of some cross sections obtained in this way are:

---

[1] K. H. Kingdon, Phys. Rev. 21, 408 (1923); I. Estermann and O. Stern, Z. Physik 85, 135 (1933).

[2] P. R. Brooks and D. R. Herschbach, "The Kingdon Cage as a Molecular Beam Detector," in Inorganic Materials Research Division Annual Report, UCRL-10119, March 1962, and Bull. Am. Phys. Soc. 6, 513 (1961).

[3] The modulation system is due to Kent R. Wilson and will be described by him in a subsequent report.

[4] The method is described, for example, by N. F. Ramsey, Molecular Beams (Clarendon Press, Oxford, 1956), p. 28.

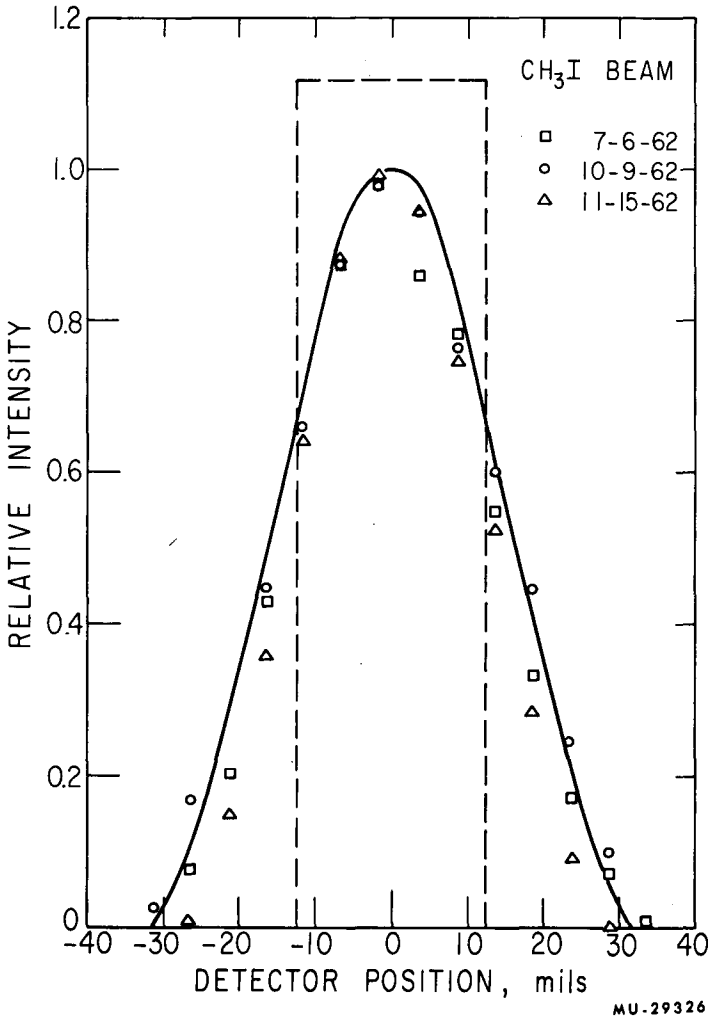

Fig. ID. 1-1. Beam profiles. Dashed curve shows beam shape calculated from slit geometry; solid curve the profile obtained by integration over the detector area (a circular hole 40 mils in diameter); points are experimental.

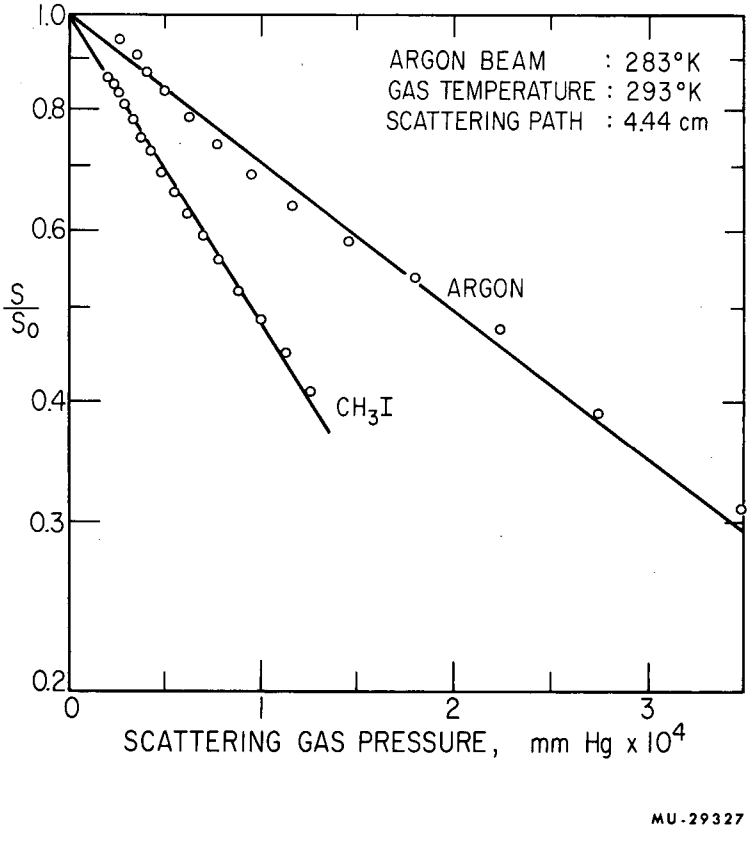

Fig. ID. 1-2. Attenuation of an argon beam as a function of scattering gas pressure.

Argon-argon	220 Å^2
Argon-CH_3I	400 Å^2
CH_3I-CH_3I	370 Å^2

The cross section for argon-argon collisions found here is about one-half that determined by Rothe et al.[5] This may be due to a systematic error in measuring the scattering gas pressure and might be reflected in the other values as well. Experiments in progress are designed to resolve this question.

[5]E. W. Rothe, L. L. Marino, R. H. Neynaber, P. K. Pol, and S. M. Trujillo, Phys. Rev. 126, 598 (1962).

2. CLASSICAL SCATTERING OF ATOMS BY DIATOMIC RIGID ROTOR MOLECULES

R. James Cross Jr., and Dudley R. Herschbach

Several quantum-mechanical treatments of the scattering of a particle by a rigid rotator have been developed,[1-3] although few quantitative applications have been made.[1,4,5] For the simpler problem of elastic atom-atom scattering, however, a semiclassical approximation[6] proves adequate for most purposes. This greatly simplifies the computations and also puts the results in a form that can be more readily visualized. As a step toward an analogous formulation of the scattering of atoms by a diatomic molecule, we have developed a classical treatment for "ellipsoidal" potential functions of the form

$$V = 4\epsilon[(\sigma/y)^{12} - (\sigma/y)^6],$$

where

$$y^2 = r^2 - c^2\cos^2\gamma.$$

[1]K. Takayanagi, Progr. Theoret. Phys. 21, 2045 (1953).

[2]C. F. Curtiss, J. Chem. Phys. 21, 2045 (1953).

[3]A. M. Arthurs and A. Dalgarno, Proc. Royal Soc. (London) A256, 540 (1960).

[4]R. Brout, J. Chem. Phys. 22, 934 (1954).

[5]C. S. Roberts, "Inelastic Scattering from a Diatomic Molecule," MIT Solid-State and Molecular Theory Group Progress Report No. 47, January 1963.

[6]K. W. Ford and J. A. Wheeler, Ann. Phys. 7, 259 (1959).

Here r is the distance between the atom and the center of the molecule, c is an asymmetry parameter, and γ is the angle between r and the axis of the molecule. Hamilton's equations are set up in terms of the known solutions for the central-force case (c = 0, a Lennard-Jones potential with constants ϵ and σ), plus perturbation terms. This yields a set of coupled differential equations in the perturbation terms. An approximate solution can be obtained as a series of iterated integrals which is evaluated by use of an IBM 7090 computer program.

The calculation provides (a) the energy, (b) the angular momentum inelasticity, and (c) the angle of deflection, χ, between the initial and final relative velocity vectors as functions of the potential parameters, the initial and final relative velocity vectors as functions of the potential parameters, the initial relative velocity and impact parameter of the incoming atom, and the initial rotational orientation and angular momentum of the molecule. Thus far numerical results have been obtained only for elastic collisions with a nonrotating molecule. An example is shown in Fig. ID. 2-1. This is further specialized to the case in which the plane of the three particles remains invariant throughout the collision. The values assigned to the other parameters are expected to be roughly appropriate for K + I_2 collisions at an initial relative kinetic energy of E = 1.0 kcal/mole. The most interesting feature of the deflection function is the position of the "rainbow angle," χ_r, at which the curve reaches a minimum. In central-force scattering,[6] the position of χ_r depends almost solely on the ratio E/ϵ. However, for the ellipsoidal potential it is found to vary appreciably with the orientation of the diatomic molecule. This variation is enough to largely "smear out" the "rainbow bumps" that otherwise would appear in the angular distribution.[6] This effect may account for the failure to observe rainbow bumps in the distribution of K atoms elastically scattered from Br_2 molecules.[7]

[7] E. F. Greene and J. Ross (Brown University), private communication, November 1962.

3. ANALYSIS OF REACTIVE SCATTERING IN CROSSED MOLECULAR BEAMS

James A. Norris and Dudley R. Herschbach

An extensive series of crossed-beam studies of the reactions of Na, K, Rb, and Cs atoms with alkyl halides has been essentially completed.[1] In the final analysis of the data the experimental angular distributions have been compared with various theoretical distributions evaluated by means of an IBM 7090 computer program.[2] The computer predicts the laboratory-system

[1] G. H. Kwei, J. A. Norris, J. L. Kinsey, and D. R. Herschbach, J. Chem. Phys. 34, 1842 (1961); Bull. Am. Phys. Soc. 6, 339 (1961); K. R. Wilson and D. R. Herschbach, Bull. Am. Phys. Soc. 7, 497 (1962).

[2] The computer program and comparisons with experimental results will be described in detail in the Ph. D. Thesis of James A. Norris.

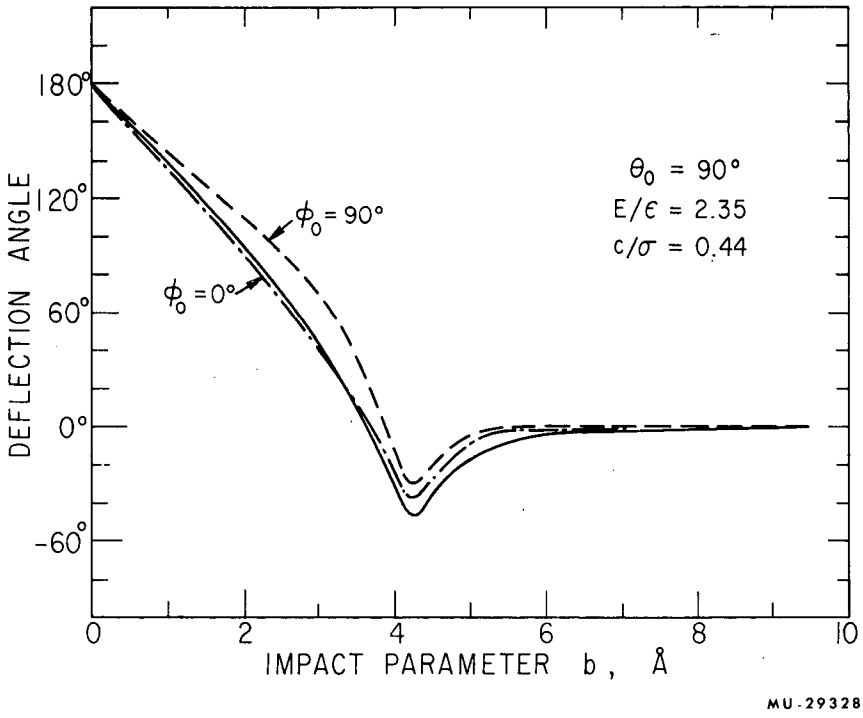

Fig. ID. 2-1. Classical deflection angle as a function of impact parameter for elastic scattering of a particle from a fixed "ellipsoidal" potential. Solid curve refers to central-force scattering with c = 0, σ = 3.0 Å, ϵ = 0.43 kcal/mole; other curves to a noncentral force field with c = 1.33 Å.

angular distributions corresponding to any specified distribution in χ (the angle between the final and initial relative velocity vectors) and Q (the difference between the final and initial values of the relative translational kinetic energy), and also averages over the Maxwell-Boltzmann velocity distribution in the reactant beams.

The qualitative features previously derived[1, 3] have been confirmed:
(a) the final relative velocity vector has a quite anisotropic distribution, peaked about the direction of the initial relative velocity vector;
(b) most of the alkali halide formed recoils "backwards" (in the center-of-mass coordinate system) with respect to the incoming alkali beam; and
(c) most of the energy released in the reaction appears as internal excitation (mainly vibrational) of the products and not as translational energy.
The analysis has also shown, however, that considerably broader distributions of χ and Q are compatible with the data than indicated by our previous analysis.[1, 3]

The computer program is also being applied to a general study of the "resolution" problem involved in deriving the spectrum of recoil velocity vectors in the center-of-mass reference system from the laboratory-system measurements. This has brought out the importance of the "edge effect" illustrated in Fig. ID. 3-1. For a certain class of recoil vectors the transformation from the laboratory to the center-of-mass system becomes singular. The locus of the tips of these recoil vectors is a "singular sphere" with the c. m. vector $\underset{\sim}{c}$ as a diameter, as indicated in the diagram at the top of Fig. ID. 3-1. Recoil vectors terminating on this sphere are perpendicular to the corresponding lab vectors, so that the ratio of solid-angle elements, $d\omega_{c.m.}/d\omega_{lab}$, becomes infinite at all points on the sphere. Those portions of the recoil spectrum which lie on or near the singular sphere are therefore strongly weighted in the observed scattering. Since the singularity is integrable, it is smoothed out by the experimental spread in velocity and beam dimensions. Thus the appropriate weighting factors depend on the velocity and angular resolution of the apparatus. An example illustrating the effect of angular resolution is shown in the lower part of Fig. ID. 3-1. The "edge effect" always appears in reactive scattering (although it may be insignificant if the recoil spectrum is negligible near the singular sphere), and it can also appear in elastic or inelastic scattering. When one or both of the incident beams can be velocity-selected, the "edge effect" offers a very sensitive means for probing the recoil spectrum, since the position of the "singular sphere" can be shifted to various parts of the spectrum by varying the magnitude and intersection angle of $\underset{\sim}{v}_1$ and $\underset{\sim}{v}_2$, the initial velocity vectors.

---

[3] D. R. Herschbach, Disc. Faraday Soc. 33, 149 (1962).

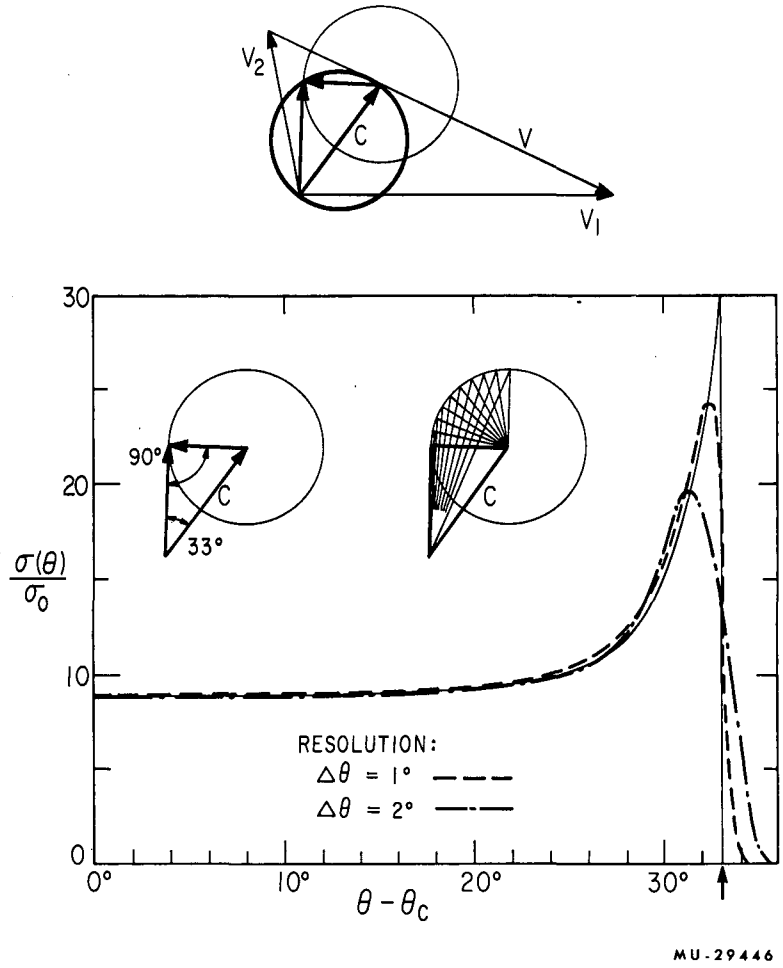

Fig. ID. 3-1. Illustration of the "edge effect." In the topmost velocity vector diagram, the heavy circle indicates the "singular sphere." Lower diagrams show in more detail the edge effect for recoil vectors of the particular length given by the light sphere drawn about the tip of the center-of-mass vector c; in this example the singularity occurs at 33° from the direction of c. The curves show the calculated intensity per unit solid angle in the laboratory system when the intensity in the center-of-mass system is uniformly distributed (differential cross section = σ_0 per steradian). The solid curve corresponds to infinite angular resolution.

4. SURFACE IONIZATION OF ALKALI METALS AND ALKALI HALIDES

Richard J. Ivanetich and Kent R. Wilson

Surface ionization provides an efficient and selective means of detecting atoms with low ionization potentials. Certain molecules containing these atoms may also be surface ionized to give primarily atomic ions, in a process that depends critically on the surface used. Thus by proper choice of surfaces one can differentiate between atoms and molecules containing these atoms. Surface ionization was used to distinguish between the elastically scattered K atoms and the KBr molecules produced in the reaction

$$K + HBr \rightarrow H + KBr$$

when molecular beams of K and HBr were crossed,[1,2] and between Cs and CsI, Rb and RbI, and K and KI when a Cs, Rb, or K beam was crossed with an alkyl iodide beam.[3] In all the above experiments, a W filament was used to ionize both the alkali metal atoms and the alkali halide, and a Pt or Pt-W alloy filament to ionize essentially only the alkali metal atoms.

For experiments involving Na or Li, which have higher ionization potentials, it has been found that Re with its higher work function is more suitable than W.[4]

The ionization of Cs, Rb, K, Na, Li, KF, KCl, KBr, and KI on Pt, Pt-W alloy and W surfaces has been studied by Taylor and Datz.[1] To provide for use of surface ionization more effective in present and future molecular beam experiments, a program to study the ionization of alkali metals and a wider variety of alkali halides on various metal surfaces has been started in this Laboratory. A second aim is to gain an improved understanding of the process of dissociative surface ionization of alkali halide molecules.

The apparatus is shown schematically in Fig. ID. 4-1. A 1440-liter/sec diffusion pump and liquid nitrogen trapping allow rapid pumpdown to pressures in the 10^{-7}-torr range. The oven is a gold-plated stainless steel tube with a slit 1×0.05 cm. The oven unscrews into two sections so that a crucible containing the material to be vaporized may be placed inside.

---

[1] E. H. Taylor and S. Datz, J. Chem. Phys. 23, 1711 (1955); 25, 389 (1956); 25, 395 (1956).

[2] E. F. Greene, R. W. Roberts, and J. Ross, J. Chem. Phys. 32, 940 (1960); D. Beck, E. F. Greene, and J. Ross, J. Chem. Phys. 37, 2895 (1962).

[3] G. H. Kwei, J. A. Norris, J. L. Kinsey, and D. R. Herschbach, in Physics of Electronic and Atomic Collisions (W. A. Benjamin, Inc., New York, 1961) Vol. 2, p. 98; D. R. Herschbach, Disc. Faraday Soc. 33, 149 (1962); D. R. Herschbach, G. H. Kwei, and J. A. Norris, J. Chem. Phys. 34, 1842 (1961).

[4] K. R. Wilson and D. R. Herschbach, Bull. Am. Phys. Soc. 7, 497 (1962).

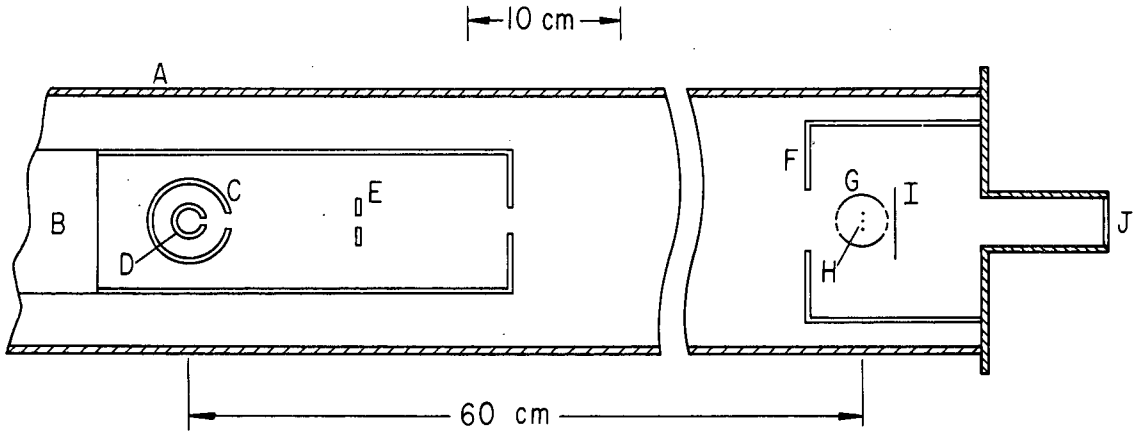

Fig. ID. 4-1. Apparatus for surface ionization studies. (The slit sizes are exaggerated for clarity.)

A- Vacuum envelope.
B- Liquid nitrogen trap around oven.
C- Water-cooled oven shield.
D- Direct resistance oven
E- Movable beam flag.
F- Detector shield.
G- Ion collector plate.
H- Surface ionization filaments.
I- Horizontal temperature calibration filament.
J- Quartz window for temperature calibration.

Surrounding most of the oven section is a liquid nitrogen trap. A beam flag is mounted in front of the oven to interrupt the beam. A surface ionization detector containing several vertical filaments is mounted within a shield 60 cm from the oven. A horizontal tungsten filament used for temperature calibrations is also mounted within the shield. The ion currents are measured with an electrometer and a recorder.

Figure ID. 4-2 shows some preliminary measurements. The temperatures of the filaments were calibrated against current by comparison, through 0.665-μ filters, of the vertical surface ionization filaments with the horizontal W filament, which was then weighed to determine its diameter. The Jones-Langmuir tables[5] were used, with the proper corrections for the emissivity of Pt, Re, and W.

Several times it was observed that the properties of Re with respect to the ionization of molecules change drastically with its conditioning. As can be seen in Fig. ID. 4-2, the higher the temperature at which the Re was aged (and therefore probably the cleaner the surface) the lower the temperature at the threshold for the ionization of LiI. Such effects were also found for NaI on Re, and a similar effect on Pt-W alloy has been observed by Trischka[6] and in this Laboratory for other alkali halides.

Use of a Paul Massfilter behind the surface ionization detector has confirmed that Li^+ and Na^+ constitute the bulk of the ions produced from ionization of LiI and NaI on Re and W wires.

---

[5] H. A. Jones and I. Langmuir, Gen. Elec. Rev. 30, No. 6, 310 (1927).

[6] T. R. Touw and J. W. Trischka, Bull. Am. Phys. Soc. 8, 77 (1963), also private communication.

5. A MASSFILTER MOLECULAR BEAM DETECTOR

Kent R. Wilson

Chemical reactions in crossed molecular beams yield minute quantities of products: less than 10^{-10} gram/sec or a monolayer/month arrive at the detector in a typical experiment. Thus the main experimental problem, which defines the scope and resolution feasible in beam studies of reactions, is detector sensitivity. Previous work has made use of a simple surface ionization detector employing hot tungsten and platinum filaments and a vibrating-reed electrometer.[1] This proved sufficient for studies of the reactions of Cs, Rb, and K atoms, but is only marginal for Na atoms and becomes inadequate for Li or other atoms with higher ionization potentials, and for experiments in which the intensity is reduced by use of velocity selection, or by magnetic or electric analysis of the primary beam.

---

[1] See references 1-4 of preceding report (ID. 4).

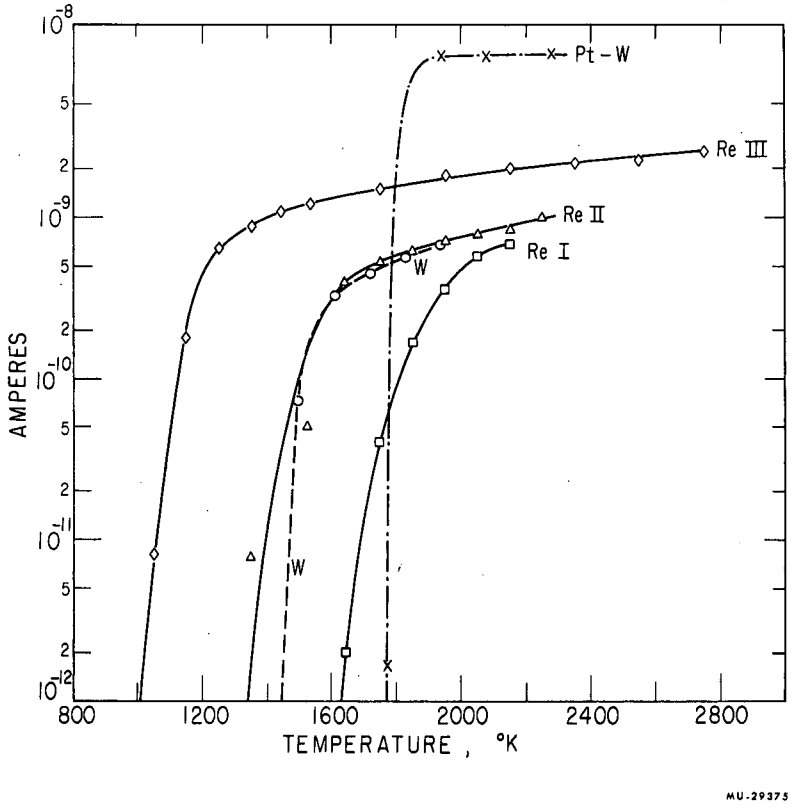

Fig. ID. 4-2. Ion current from LiI vs temperature for 92% Pt-8% W alloy (Sigmund Cohn alloy #479), Re and W filaments.
ReI: Aged 7 hours at 1640°K.
ReII: Aged in addition for several minutes at 2250°K.
ReIII: Aged in addition for several minutes at 2750°K.
Pt-W: Aged 7 hours at 1635°K.
W: Aged 7 hours at 2080°K.

To improve the detector sensitivity, we have constructed the mass-filter detector shown schematically in Fig. ID. 5-1. The reaction products are ionized on a hot wire as before[1, 2] and then passed through a Paul massfilter which eliminates background ions from the hot wire at unwanted mass numbers. The transmitted ions strike an electron multiplier. The amplified current from the multiplier may be measured with either an electrometer or a lock-in amplifier system, or counted as bursts of electrons corresponding to the individual ions. The massfilter and electron multiplier assembly is mounted within a vacuum envelope of 2.5-in. (i.d.) stainless steel tubing which can either be attached to a test stand for calibration with known beams, or mounted on a side flange of the main apparatus. The tube is tilted so that the direct beam cannot contaminate the interior.

The Paul massfilter[3, 4] employs only electric fields. Radiofrequency (rf) and constant (dc) fields are applied to quadrupole electrodes and ions are injected along the axis. The ions follow oscillatory trajectories given by solutions to a Mathieu differential equation. A path will be a stable oscillation and permit the ion to pass through the massfilter only if the mass-to-charge ratio of the ion falls within a certain range determined by the distance between the electrodes, the rf frequency and voltage, and the dc voltage. The ions having other charge-to-mass ratios oscillate with greater and greater amplitude until they strike one of the electrodes. In comparison with conventional magnetic mass spectrometers, the Paul massfilter offers the advantages of wide acceptance aperture, high transmission, small size and weight, and simplicity of operation. In contrast to magnetic mass spectrometers, the massfilter may be varied from high resolution and lower transmission to lower resolution and high transmission merely by adjusting the potentiometer controlling the ratio of dc and rf voltages.

The mass peaks that have been observed are shown in Fig. ID. 5-2. (The Li peaks are at such low voltages on the 1-Mc range of the instrument that they fall in the region where the rf voltage is no longer proportional to plate voltage. They are thus ordinarily observed on the 4-Mc range, at higher voltages.)

An example of a mass peak is given in Fig. ID. 5-3. The Rb^{85} peak height is approximately 1×10^{-11} ampere. The dip on the low-voltage side of the peaks is probably caused by imperfection in the quadrupole symmetry.[3] Mass resolution of 1/150 can be achieved.

---

[2] An electron bombardment ionizer attachment is presently being designed by Dr. Malcolm Fluendy.

[3] W. Paul and H. Steinwedel, Z. Naturforsch. 8a, 448 (1953).
W. Paul, H. P. Reinhard, and V. von Zahn, Z. Physik 152, 143 (1958);
F. V. Busch and W. Paul, Z. Physik 164, 588 (1961).

[4] The massfilter has been employed as a molecular beam detector by at least two other research groups. At Bonn University, where it was invented, the massfilter has been used with surface ionization; see, for example H. G. Bennewitz, K. Kramer, and J. P. Toennies, in Physics of Electronic and Atomic Collisions (W. A. Benjamin, Inc., New York, 1961), Vol. 2, p. 113
Many of the features of the apparatus described in this report are copied from a massfilter detector used to detect already ionized products and designed by G. O. Brink, (UCRL-6669), whose good advice contributed greatly to the success of the present project.

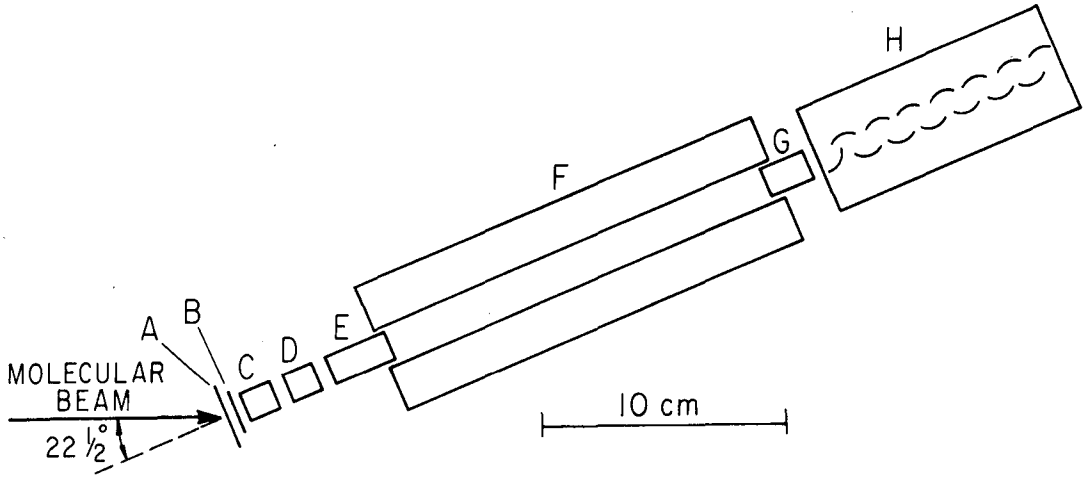

Fig. ID. 5-1. Massfilter.
A- Slotted disk entrance electrode.
B- Surface ionization wire.
C, D- Focusing electrodes.
E- Entrance electrode.
F- Quadrupole electrodes.
G- Exit electrode.
H- 14-Stage electron multiplier.

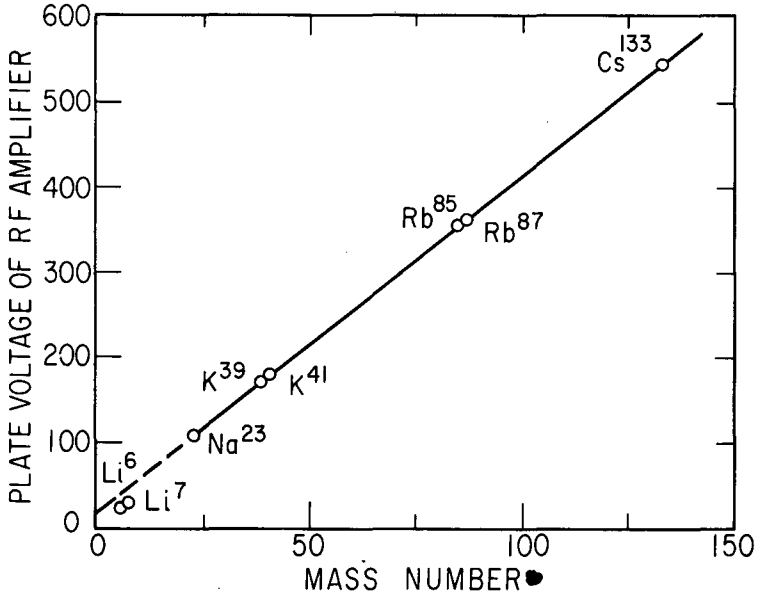

Fig. ID. 5-2. Mass peaks observed with 1-Mc rf.

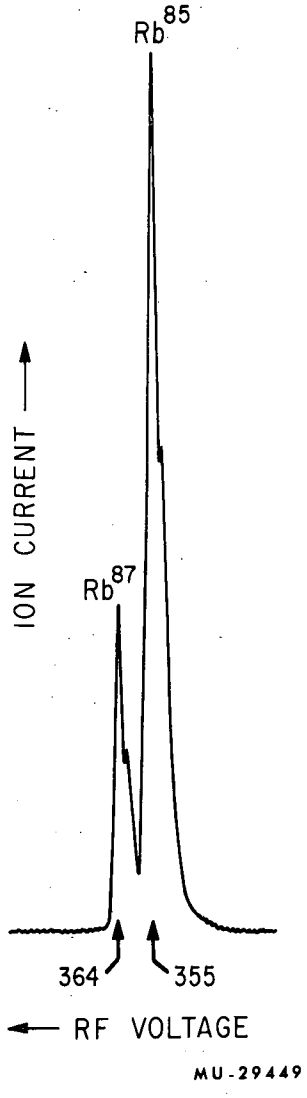

Fig. ID. 5-3. Rb isotope peaks.

Surface ionization studies and scattering experiments have been performed with the massfilter. With the wide range of usable intensity of the massfilter detector (more than 8 decades) simultaneous beams of all the alkali metals can be observed from the same oven. The oven is charged with a mixture of Li, Na, K, Rb, and Cs and the mixed beam is crossed with a beam of CH_3I. The massfilter then sorts out the various alkali metals and alkali halides. In this way the relative total collision cross sections for the alkali metals with methyl iodide have been measured. These decrease in order from Cs to Li, in rough agreement with the expected values.[5]

Similar work is in progress to study the angular distributions of the scattered alkali metal atoms and alkali halide molecules.

[5] E. W. Rothe and R. B. Bernstein, J. Chem. Phys. 31, 1619 (1959).

6. MAGNETIC ANALYSIS OF ATOMIC AND MOLECULAR BEAMS

Ronald R. Herm and Dudley R. Herschbach

Three small iron-core electromagnets have been constructed for use as deflecting magnets in atomic- and molecular-beam experiments.[1] The overall dimensions of the largest magnet (denoted by A) are about 5×5×5 in. and the air gap is 0.10 in. wide, 0.15 in. high, and 4.5 in. long. The other magnets (B and C) are shorter and have wider air gaps. The pole tips conform to the cylindrical magnetic equipotential surfaces of the field produced by a pair of infinitely long parallel wires carrying equal and opposite currents. Forty-two turns of 0.18-in. i.d. copper tubing carry an energizing current of up to 100 amperes which is provided by a transistorized power supply allowing only 0.2% ripple at 100 A. The efficiency of the magnet design was investigated by measuring the flux through the air gap and various cross sections of the magnet yoke as a function of the energizing current. Magnet A exhibited a peak induction at the midpoint of the gap of about 15 kilogauss, with a transverse gradient of 90 kilogauss/cm. For magnets B and C the peak induction observed was about 10 kilogauss, with a gradient of 30 kilogauss/cm.

A FORTRAN program for the IBM 7090 computer has been prepared and a detailed study is being made of the resolution and transmission attainable when the deflecting magnets are used for velocity selection or for separation of paramagnetic and diamagnetic species in a beam. The program calculates the intensity profile of the deflected beam in the plane of the detector as a function of the displacement of the detector from the undeflected beam position.[2] An integration of the intensity distribution over the detector width is included. A subroutine also provides the percent transmission of a paramagnetic species as a function of the slit geometry and field strength.

[1] R. R. Herm and D. R. Herschbach, Construction and Calibration of Inhomogeneous Deflecting Magents, UCRL-10526, Oct. 1962.

[2] The method of calculation is given by N. F. Ramsey, Molecular Beams (Clarendon Press, Oxford, 1956), p. 90-100.

7. ELECTRIC DEFLECTION OF ATOMIC AND MOLECULAR BEAMS

Dudley R. Herschbach

Inhomogeneous electric deflecting fields have long been used in beam experiments designed to measure molecular dipole moments[1, 2] or atomic polarizabilities.[2, 3] We have constructed the field shown in Fig. ID. 7-1 for an investigation of the distribution of the angular momentum of product molecules formed in chemical reactions in crossed beams. Theoretical considerations[4] indicate that under certain conditions practically all the initial orbital angular momentum, $\vec{L}$, in a reactive collision will appear as rotational momentum, $\vec{J}'$, of a product molecule. This conclusion implies that the rotations will be strongly polarized, with the $\vec{J}'$ vector aligned essentially perpendicular to the initial relative velocity vector. If this alignment actually holds, it should have a pronounced effect on the deflection pattern obtained when the product molecules are made to pass through a sufficiently strong inhomogeneous electric field. The experiment thus should give information about the distribution of $\vec{L}$ in those collisions which lead to reaction.

The electrode configuration shown in Fig. ID. 7-1 has the standard "two-wire" form,[1] which produces a field conjugate to that from two parallel-line charges of opposite sign. This field has the convenient property that both the field intensity and gradient remain practically constant over the vertical dimension of a transmitted molecular beam, so that the whole beam is deflected without appreciable distortion. The electrodes are 6 in. long. Cross-sectional dimensions and spacing of the electrodes are identical to those described by Hebert.[5] The field assembly is mounted within a 4-in. (i. d.) brass tube, which is attached to the main beam apparatus by a rotatable vacuum seal. This permits the angle between the electric vector of the field and the initial relative velocity vector of the colliding beams to be varied. The trough electrode is grounded and the T-bar electrode is charged by a transformer capable of supplying 0 to 50 kilovolts at a current of 5 milliamperes with less than 2% ripple.[6] The field and transverse

---

[1] N. F. Ramsey, Molecular Beams (Clarendon Press, Oxford, 1956), pp. 287-309.

[2] R. G. J. Fraser, Molecular Beams (Methuen, London, 1937), pp. 54-66.

[3] A. Salop, E. Pollack, and B. Bederson, Phys. Rev. 124, 1431 (1961); G. E. Chamberlain and J. C. Zorn, Bull. Am. Phys. Soc. 7, 70 (1962).

[4] D. R. Herschbach, The Vortex 22, 348 (1961); Disc. Faraday Soc. 33, (1962).

[5] A. J. Hebert, A Molecular-Beam Electric Resonance Spectrometer and the Radio-Frequency Spectra of Lithium Fluoride (Thesis), UCRL-10482 (Sept. 1962).

[6] HV Standard Type Power Pack HV 500-502, manufactured by Plastic Capacitors, Inc., 2620 N. Clybourn Avenue, Chicago 14, Illinois.

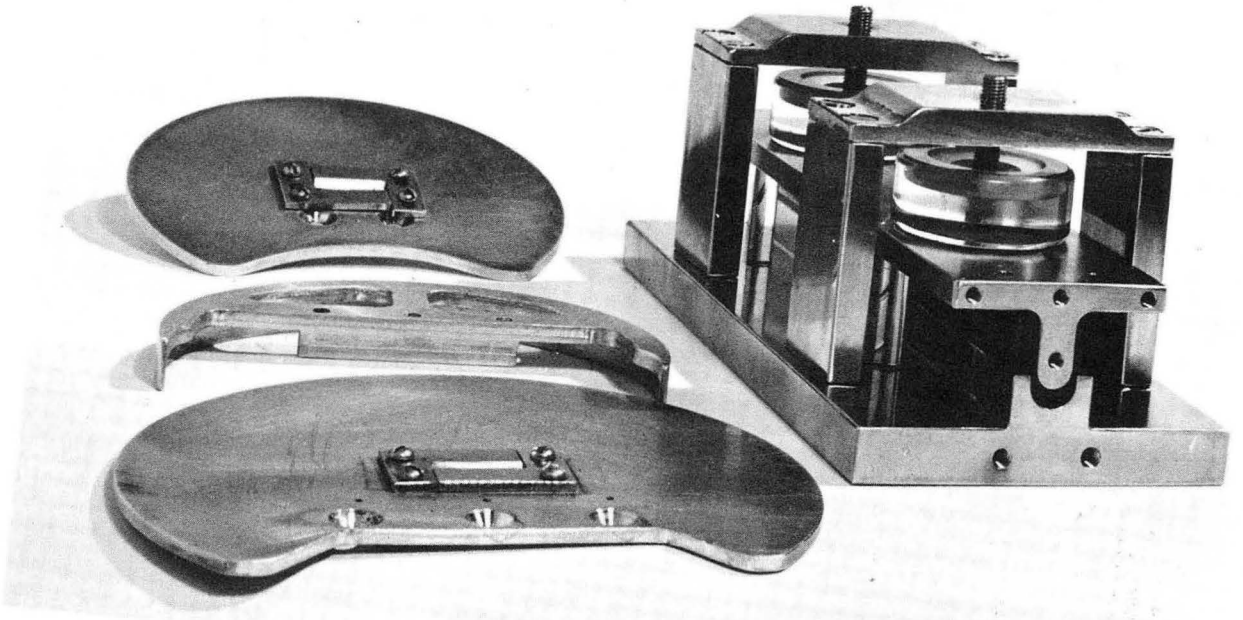

ZN-3609

Fig. ID. 7-1. Deflecting-field assembly.

gradient at the beam position are calculated from the geometry to be

$$E(\text{volts/cm}) = 4.05\ V(\text{kilovolts})$$
$$\partial E/\partial z\ (\text{volts/cm}^2) = 12.5\ V(\text{kilovolts})$$

where V is the electrode potential. Thus at V = 30 kilovolts, $E = 1.25\times10^5$ volts/cm and $\partial E/\partial z = 3.8\times10^5$ volts/cm^2.

The calculated deflecting power of the apparatus has been checked in preliminary experiments with a potassium atomic beam. Examples of the observed deflection patterns are shown in Fig. ID. 7-2. As the deflection is produced by the interaction of the field gradient with the dipole moment induced in the atom by the field, it is a small second-order effect, proportional to the polarizability of the atom. In Fig. ID. 7-2 the deflected beam is seen to be repelled from the charged electrode (as expected for a second-order perturbation) and noticeably broadened by the thermal distribution of velocities. An IBM 7090 computer program prepared by Ronald R. Herm has been used to analyze the deflection patterns. Good agreement is found with the value $\alpha = 37$ Å obtained in previous measurements[3] of the polarizability of the potassium atom.

In crossed-beam experiments the use of electric deflection analysis of dipolar product molecules costs about a factor of 400 in intensity arriving at the detector. However, recent improvements (phase-sensitive detection of modulated beams and mass analysis of detected ions) have offset this loss and make the reaction studies appear feasible.

8. APPARATUS FOR SCATTERING STUDIES WITH VELOCITY-SELECTED MOLECULAR BEAMS

George H. Kwei

A new crossed-molecular-beam apparatus has been constructed which incorporates a mechanical velocity selector. This will be used to measure the energy dependence of the total cross sections and angular distributions for both elastic and reactive scattering. The features of the scattering that provide the most detailed information about the intermolecular forces, such as "rainbow" bumps,[1-3] are velocity-dependent, and without velocity selection are blurred out by averaging over the thermal distributions of velocities in the beams.

---

[1] K. W. Ford and J. A. Wheeler, Ann. Phys. 7, 287 (1959); E. A. Mason, J. Chem. Phys. 26, 667 (1957).

[2] F. A. Morse and R. B. Bernstein, J. Chem. Phys. 37, 2019 (1962).

[3] D. Beck, J. Chem. Phys. 37, 2884 (1962); D. Beck, E. F. Greene, and J. Ross, J. Chem. Phys. 37, 2895 (1962).

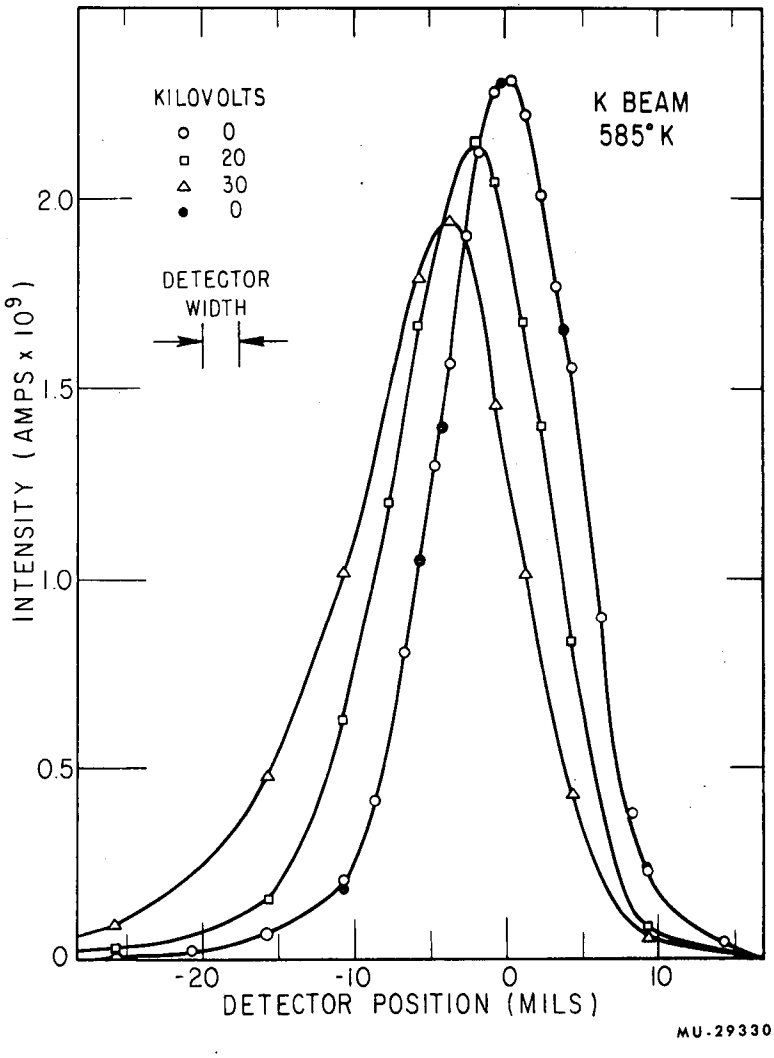

Fig. ID. 7-2. Deflection pattern for atomic potassium beam.

A general view of the apparatus is shown in Fig. ID. 8-1. The apparatus is complementary to the one used in our previous work,[4] in that the detector is pivoted to rotate about the scattering center and the beam sources are placed in stationary, differentially pumped chambers. This allows a vacuum of 2×10^{-7} mm Hg to be maintained in the scattering chamber even when noncondensible beams are used. As before,[4] the beams are formed by effusion from nickel ovens which are heated by radiation from tantalum coils. A two-chamber oven is used for the primary, velocity-selected beam, to permit the beam temperature to be varied independently of beam intensity. The cross-beam oven is designed for use with noncondensible gases. At present a simple surface ionization detector is employed, but the addition of a massfilter and electron multiplier unit and beam modulation is planned.

The velocity selector, shown in Fig. ID. 8-2, is similar to those used by Hostettler and Bernstein and others.[5] Six slotted disks are mounted concentrically on a shaft driven by a hysteresis synchronous motor[6] and a variable-frequency three-phase power supply.[7] Each disk has 240 slots 32 mils wide, and the intermediate disks are spaced in such a way as to block the transmission of any "overtone" velocities. A gear arrangement allows the rotor to be lowered out of the beam path. The selector has a velocity resolution of 0.043 (half-intensity width) and an effective fractional open time to the incident beam of 0.32. At the highest attainable rotor speed (24,000 rpm) the transmitted velocity is 1.2×10^{5} cm/sec.

The apparatus and selector have been tested and some preliminary scattering experiments are in progress.

---

[4] D. R. Herschbach, G. H. Kwei, and J. A. Norris, J. Chem. Phys. 34, 1842 (1961); D. R. Herschbach, Disc. Faraday Soc. 33, 149 (1962).

[5] H. G. Bennewitz, Dissertation (Physical Institute, Bonn, Germany, 1956); H. U. Hostettler and R. B. Bernstein, Rev. Sci. Instr. 31, 872 (1960); S. M. Trujillo, P. K. Rol, and E. W. Rothe, Rev. Sci. Instr. 33, 841 (1962).

[6] Model FF26H67, McLean Suntorque Corp., West Hurley, New York.

[7] Model 1452-C, Communications Measurements Laboratory, Inc., Plainfield, New Jersey.

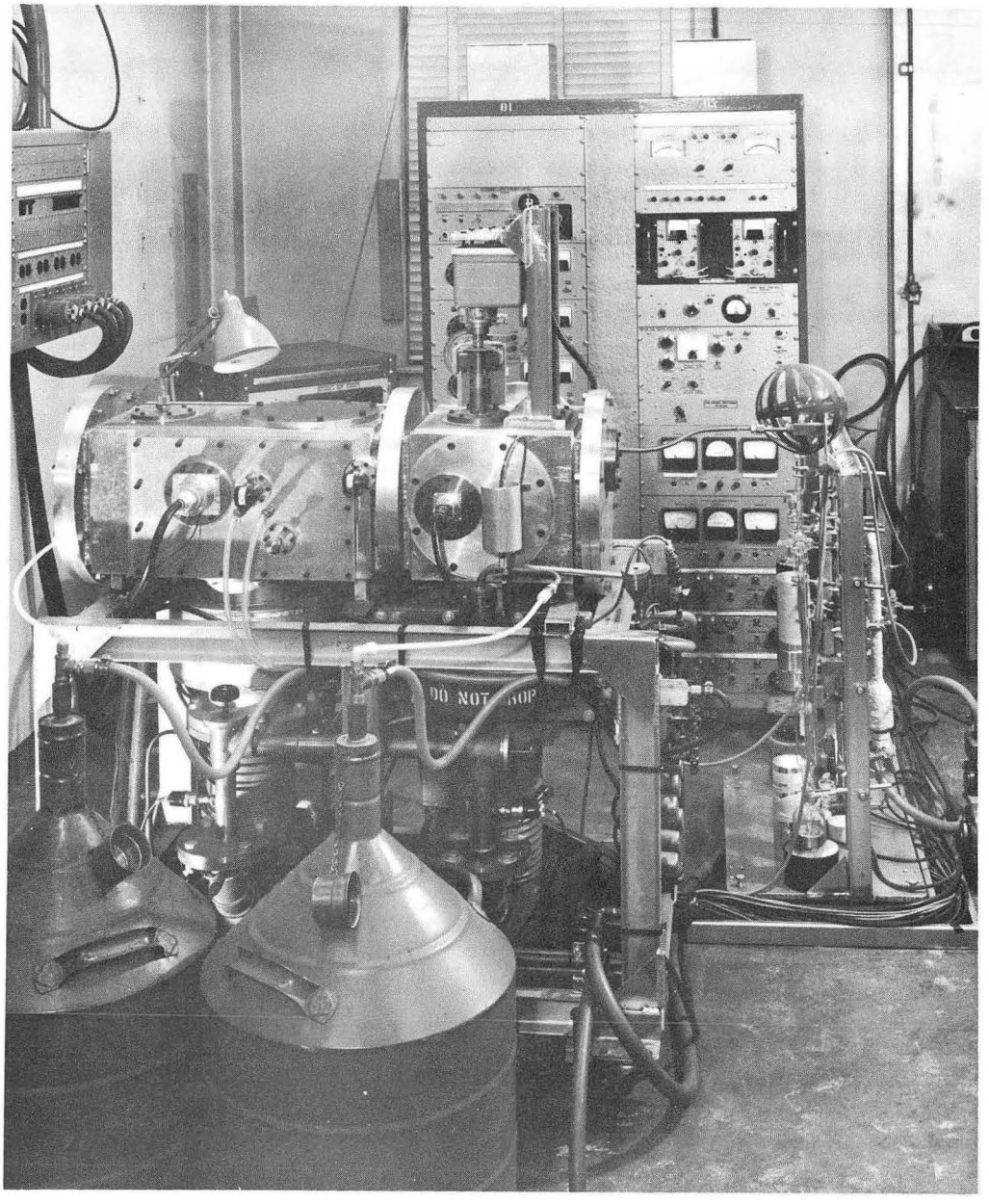

ZN-3610

Fig. ID. 8-1. General view of the apparatus.

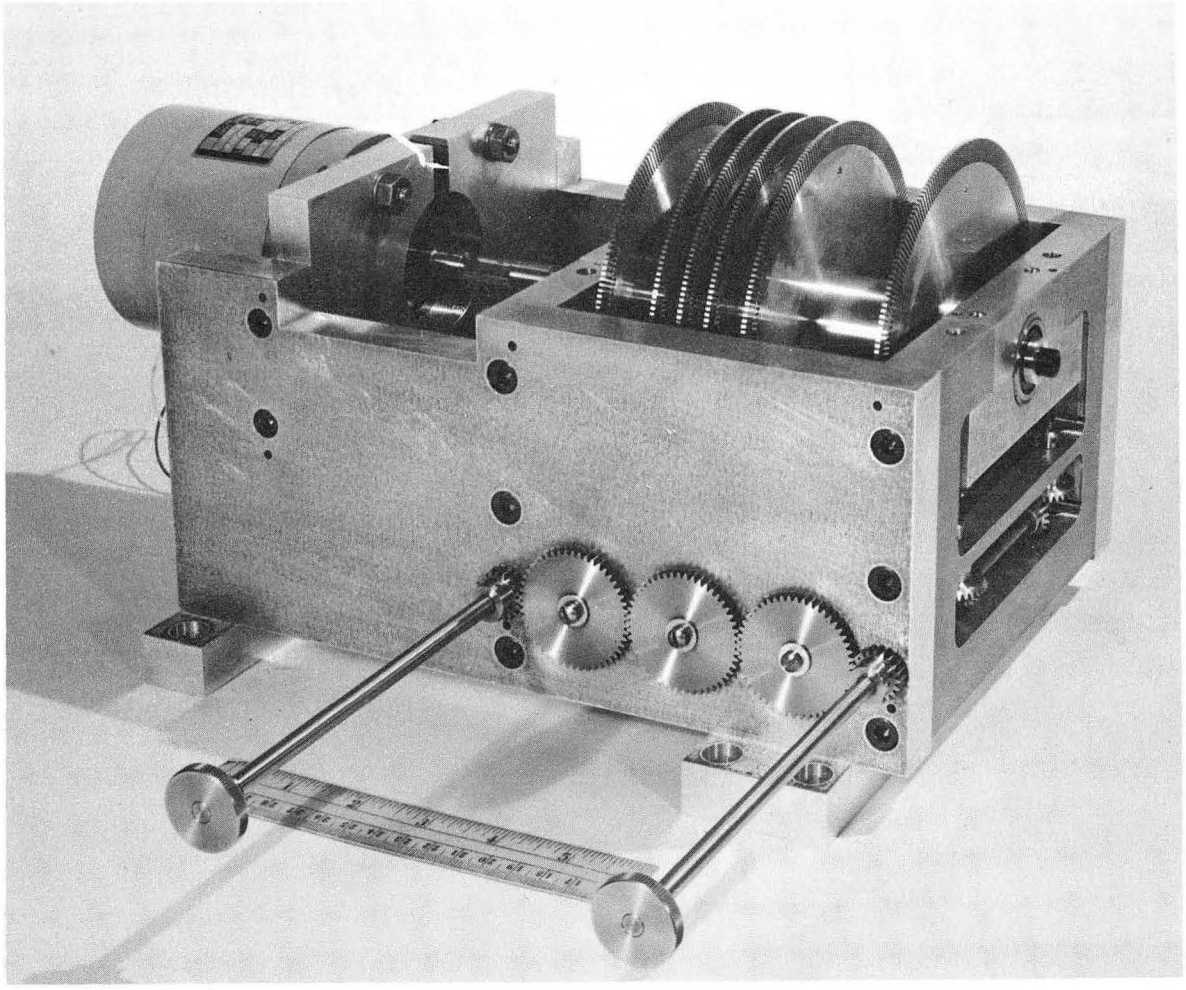

ZN-3608

Fig. ID. 8-2. Molecular beam velocity selector.

9. ELASTIC SCATTERING OF CHEMICALLY REACTIVE MOLECULES

Dudley R. Herschbach and George H. Kwei

Elastic atom-atom collisions have been studied in several recent experiments with velocity-selected beams,[1] with results that fully confirm semiclassical scattering theory.[2] In the thermal energy range the influence of the attractive potential well in the intermolecular potential is dominant, and gives rise to two velocity-dependent effects: (a) the total cross section exhibits undulatory behavior[3] at sufficiently low velocities (long deBroglie wavelengths), in contrast to the monotonic decrease observed at higher velocities; and (b) the angular distribution shows a "rainbow bump" at a scattering angle that corresponds to maximum attractive interaction along a trajectory. The semiclassical analysis of these effects is based on the classical deflection function $\chi(E/\epsilon, \beta)$, which has been tabulated for the customary Lennard-Jones and Exponential-6 potentials as a function of the reduced relative collision energy E/ϵ and the reduced impact parameter $\beta = b/\sigma$, where ϵ is the potential well depth and σ the radius of the repulsive core. The cross-section oscillations (a) primarily involve the velocity dependence of the zero-angle scattering, $\chi(E/\epsilon, \beta) = 0$, and are functions of both ϵ and σ. The rainbow angles (b) appear when $\partial\chi/\partial\beta = 0$ and are essentially functions of E/ϵ only.

In the course of planning experimental studies of elastic scattering of atoms from chemically reactive molecules, we have formulated a semiclassical treatment closely analogous to the atom-atom case. Although a many-dimensional potential surface is involved, for elastic scattering at thermal energies this can be replaced by a suitably defined average potential function. For an A + BC collision, the average potential is given by

$$\mathcal{V}(r) = \int\int V(\xi, a, r) W_{\xi}(\xi, r) W_{a}(a, r) d\xi \, da.$$

Here $V(\xi, a, r)$ denotes the true potential, a function of the translational coordinate r (distance from A to center of mass of BC), the vibrational coordinate ξ of the BC molecule, and the angle a between $\vec{r}$ and $\vec{\xi}$. Throughout practically all the nonreactive collisions the motion in ξ is much higher in frequency than that in r or a, and therefore a Born-Oppenheimer separation is valid. The weightling factor W_{ξ} is the square of the vibrational wave function and depends on r as well as ξ, since the frequency of ξ vibrations varies along the entrance valley of the potential surface. The proper treatment of the average over a and the various rotational terms in the kinetic energy is complicated. However, at large r the W_a factor approaches unity, and at smaller r its detailed form is not

[1] D. Beck, J. Chem. Phys. 37, 2884 (1962); F. A. Morse, R. B. Bernstein, and H. U. Hostettler, ibid. 36, 1947; 37, 2019 (1962); P. K. Rol and E. W. Rothe, Phys. Rev. Letters 9, 494 (1962).

[2] K. W. Ford and J. A. Wheeler, Ann. Phys. 7, 259 (1959).

[3] R. B. Bernstein, J. Chem. Phys. 34, 361 (1961).

crucial if the potential $V(\xi, a, r)$ is assumed to be strongly directional. Furthermore, in most elastic collisions the orbital angular momentum is much larger than the rotational momentum of BC, and the kinetic terms involving BC rotations then cannot greatly perturb the collision trajectories. Thus a calculation using two-body mechanics may reasonably be expected to account for the main features of the elastic scattering of reactive molecules, provided that a qualitatively correct form for $\mathcal{V}(r)$ is chosen.

For exothermic reactions without activation energy, the potential surface $V(\xi, a, r)$ presumably has a rather spacious entrance valley and thus as r decreases $\mathcal{V}(r)$ presents an extended "downhill" slope through much of the region that would comprise the repulsive core in an atom-atom collision. The main effect of this "softness" of $\mathcal{V}(r)$ should be to suppress much of the wide-angle scattering that would appear for collisions of atoms of comparable size. The small-angle scattering should be little affected, as it is almost solely determined by the long-range behavior of the potential.

These features are indeed found in the elastic scattering observed for two reactive systems, K + HBr and K + CH_3Br, in contrast with the scattering of K + Kr. A different interpretation has been proposed by Beck, Greene, and Ross,[4] however; they ascribe the fall-off in wide-angle scattering to depletion by chemical reaction, and assume that otherwise the wide-angle scattering could be predicted from a two-body central force potential such as the Exp-6. The potential parameters are chosen to fit the low-angle scattering, in particular the rainbow bumps. The fractional difference between the calculated and observed intensity in the wide-angle region,

$$\mathcal{P}(E, b) = [I_{calc}(E, \chi) - I_{obs}(e, \chi)]/I_{calc}(E, \chi),$$

then yields the probability of reaction as a function of the initial impact parameter, since b is a single-valued function of χ in the wide-angle region.

In our opinion the Exp-6 potential used by Beck, Greene, and Ross is qualitatively incorrect and is much too "hard" to represent $\mathcal{V}(r)$. The total depletion by reaction derived from their analysis implies reaction cross sections considerably larger than those estimated from measurements of the reactive scattering in this Laboratory and elsewhere[4, 5] (roughly 5 times too large for HBr, 50 times for CH_3Br).

Calculations based on the experimental reaction cross sections indicate that the total depletion by reaction is too small to have a discernible effect on the elastic scattering. Therefore we are attempting to fit the observed scattering with various likely forms of the $\mathcal{V}(r)$ potential. An IBM 7090 computer program has been prepared that can treat any potential function. Preliminary calculations have been completed for the "Bot-s"

---

[4] D. Beck, E. F. Greene, and J. Ross, J. Chem. Phys. 37, 2895 (1962).

[5] E. H. Taylor and S. Datz, J. Chem. Phys. 23, 1711 (1955).

functions, defined by $\mathcal{V}(r) = -\epsilon$ for $r < \sigma$ and $-\epsilon(\sigma/r)^s$ for $r > \sigma$, with $s = 1, 2$. For these the deflection angle can be evaluated analytically. In the literature on atom-atom scattering it is sometimes implied that the cross-section undulations and the rainbow phenomenon appear only for a potential that has both attractive and repulsive branches. However, even a purely attractive potential shows these effects as long as it is finite at the origin. The energy dependence of the rainbow angles for the Bot-s and Exp-6 potentials is compared in Fig. ID. 9-1. It is found that the observed rainbow angles for the K + HBr and K + CH_3Br systems are accurately predicted by the Bot-2 potential, for example, if the ϵ values are chosen to be about twice those inferred for the Exp-6 potential.[4] Likewise, the total cross sections can be fitted by taking σ's for the Bot-2 about half of those for the Exp-6. Of course, the Bot-2 potential is only a crude approximation to a realistic $\mathcal{V}(r)$ function. It will be necessary to add a small repulsive core to account for the weak wide-angle scattering that appears outside the rainbow angle (this is virtually zero for the Bot-2 potential); also, the long-range attractive portion should be adjusted to $s = 6$. These changes will not affect the main qualitative features, however.

The Bot-2 calculations also point to an interesting new phenomenon. For sufficiently low reduced energy, the attraction is strong enough to produce multiple loop trajectories, and the angle of deflection passes several times through 180°, as shown in Fig. ID. 9-2. (This effect is distinct from the familiar orbiting phenomenon, for which χ becomes infinite.) Exploratory calculations indicate that the effect appears for other potentials as well, but it does not occur for the $\alpha = 12$ Exp-6 or the Lennard-Jones potential, for example.

10. A SIMPLE TEST OF THE LONDON-EYRING-POLANYI POTENTIAL SURFACE FOR THE H + H_2 REACTION

J. K. Cashion and Dudley R. Herschbach

Most of the potential surfaces used to describe reactions of the type A + BC → AB + C have been constructed according to the "semi-empirical method" of Eyring and Polanyi. This method utilizes the Heitler-London theory of the covalent bond and London's extension of this to the three- and four-electron cases.[1]

London's energy formula for a system of three s electrons is

$$E = Q \pm \sqrt{1/2}\left\{(\alpha-\beta)^2 + (\alpha-\gamma)^2 + (\beta-\gamma)^2\right\}, \qquad (1)$$

[1] For a full description of the method and the original references, see H. Eyring, J. Walter, and G. E. Kimball, Quantum Chemistry (John Wiley and Sons, New York, 1944), p. 245.

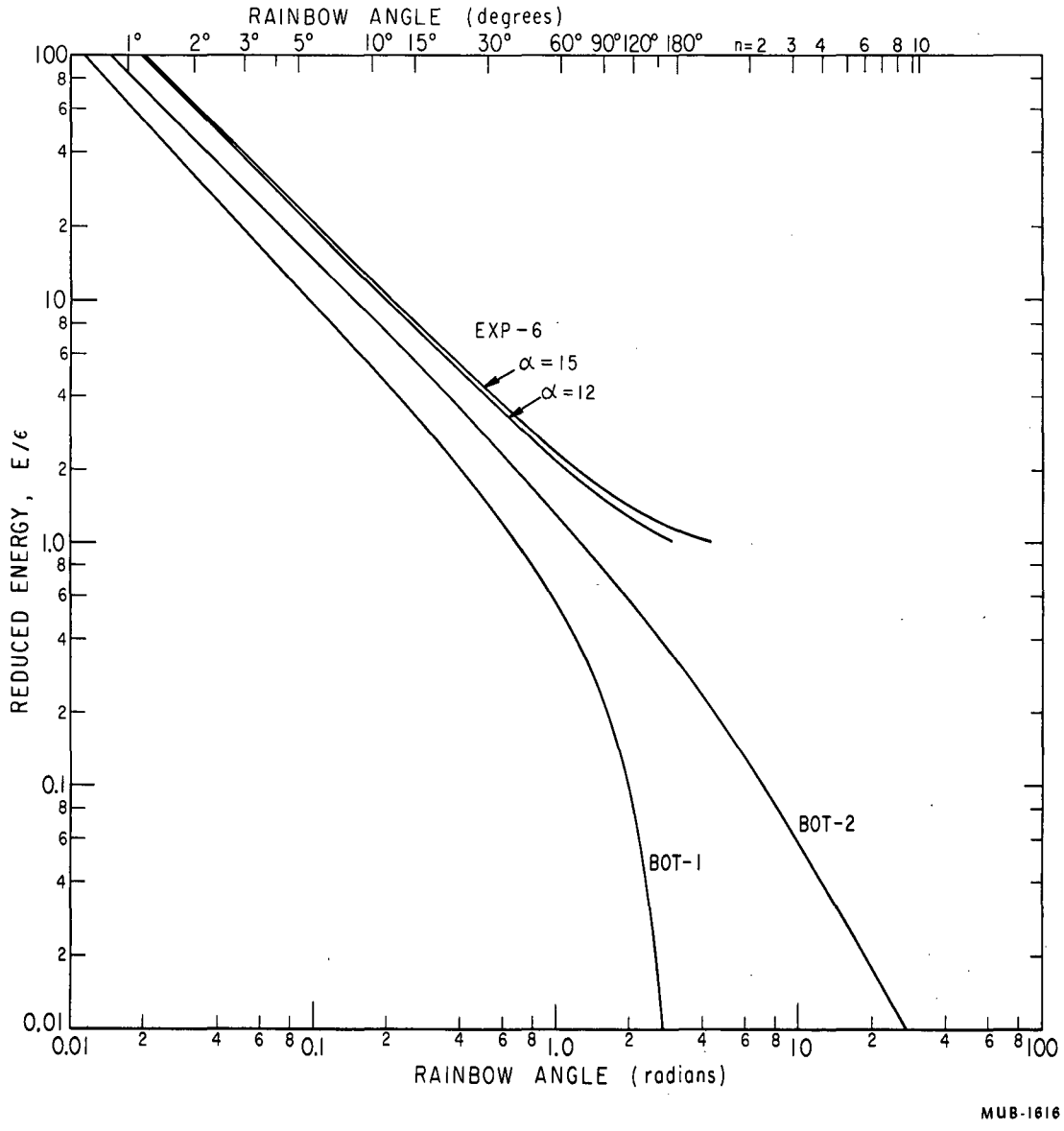

Fig. ID. 9-1. Energy dependence of rainbow angle for various potentials. Curve for a Lennard-Jones (12, 6) potential falls between those for the $\alpha = 12$ and $\alpha = 15$ Exp-6 potentials.

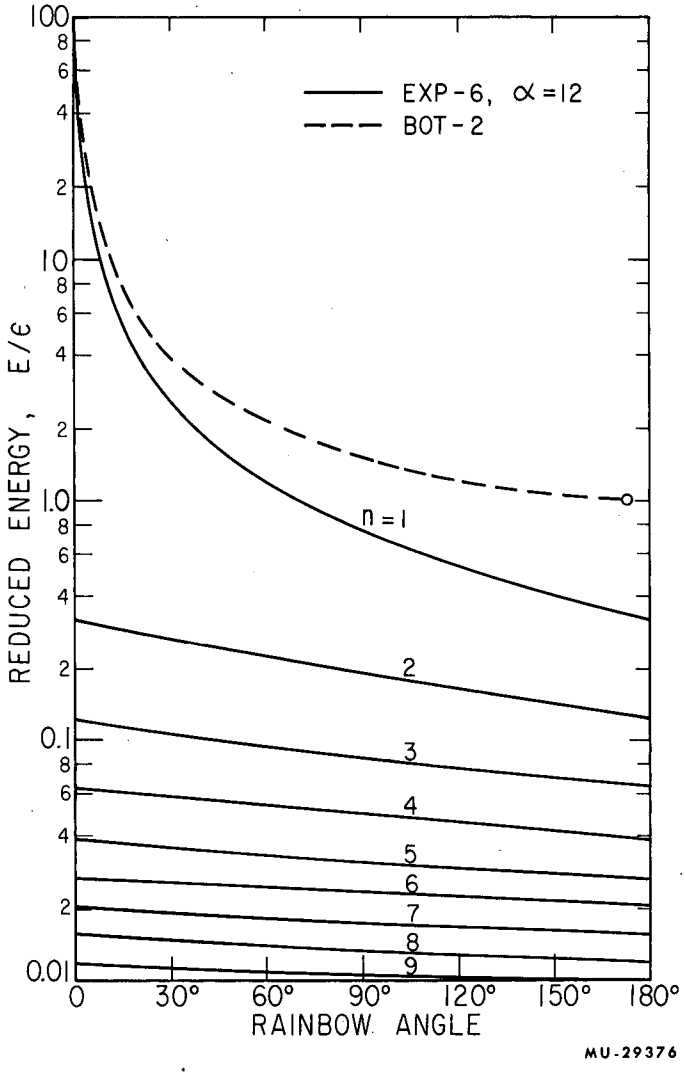

Fig. ID. 9-2. Energy dependence of multiple rainbow angles for the Bot-2 potential. Dashed curve gives result for the α = 12 Exp-6 potential.

where Q is a Coulombic term and α, β, and γ are the so-called exchange terms. In addition to the approximations inherent in the Heitler-London treatment, Eq. (1) involves the assumption that all overlap integrals are zero.

In the Eyring-Polanyi scheme it is further assumed that the energy of any electron-pair bond a-b can be represented by an equation of the form

$$E_{ab} = Q_{ab} + \alpha_{ab}. \tag{2}$$

The value of E_{ab} is determined empirically, usually from the data on the corresponding diatomic molecule. By assuming $Q = \sum_{ij} Q_{ij}$, where Q_{ij} is the Coulombic energy for the two-electron system i-j, Eq. (1) can be evaluated if the ratio Q_{ab}/α_{ab} is known. This ratio is a function of internuclear distance, but could be assumed constant as a first approximation. For the reaction $H + H_2 \rightarrow H_2 + H$ it was found that a surface with the correct activation energy was obtained when the ratio $Q/(\alpha+Q) = Q/{}^1\Sigma$ for H_2 was taken to be 14%. This figure is in reasonable agreement with Sugiura's calculation[2] of the Coulombic exchange terms in the Heitler-London treatment of H_2.

A simple but more severe test of this assumption is now available. The singlet and triplet for the ground electronic state of hydrogen are now known to relatively high accuracy. If Eq. (2) is assumed valid it follows that

$$Q = 1/2\,({}^1\Sigma + {}^3\Sigma) \tag{3a}$$

and

$$\alpha = 1/2\,({}^1\Sigma - {}^3\Sigma). \tag{3b}$$

Hence, the values of ${}^1\Sigma$ and ${}^3\Sigma$ at each value of the internuclear distance can be used to plot a potential surface for the $H + H_2 \rightarrow H_2 + H$ reaction from Eq. (1) without introducing any assumptions about the Q/α ratio. As intermediates in the calculation, Q and α obtained as functions of r and can be used to test the validity of the assumption of a constant ${}^1\Sigma$ ratio.

Figure ID. 10-1 shows the potential surface for the hydrogen exchange reaction derived in this manner. The diatomic potential curves used for this were taken from three sources. For the ${}^1\Sigma$ state the Rydberg-Klein-Rees-type calculations by Tobias and Vanderslice[3] up to about 2 Å were combined with the calculations by Dalgarno and Lynn[4] for larger r. The agreement between the two in their region of overlap is excellent. For the ${}^3\Sigma$ state the Dalgarno and Lynn results were again used for $r \geq 2$ Å, and the calculations by Kolos and Roothaan[5] were employed for lower r values.

[2] Y. Sugiura, Z. Physik 45, 484 (1937).

[3] I. Tobias and J. T. Vanderslice, J. Chem. Phys. 35, 1852 (1961).

[4] A. Dalgarno and N. Lynn, Proc. Phys. Soc. A69, 821 (1956).

[5] W. Kolos and C. C. J. Roothaan, Rev. Mod. Phys. 32, 219 (1960).

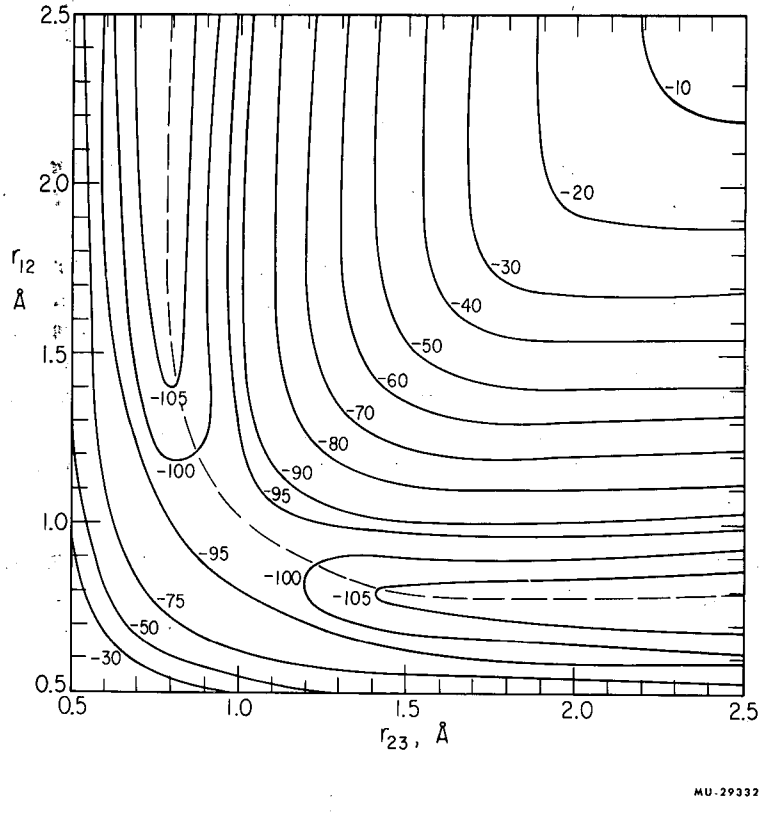

Fig. ID. 10-1. Potential surface for the reaction $H + H_2 \rightarrow H_2 + H$. Energies are in kcal/mole, relative to a zero of energy at infinite separation of all three atoms.

A somewhat arbitrary interpolation was necessary for the region not covered by either calculation (1.5 to 2 Å); several interpolation schemes were tried and gave results in close agreement.

The saddle point of the potential surface occurs at approximately -98 kcal/mole, indicating an activation energy of about 5 ± 2 kcal/mole plus the zero-point vibrational energy of the activated complex, which probably contributes an additional 3 or 4 kcal/mole. The indicated uncertainty arises from the interpolation of the triplet curve. The experimental activation energy[6] is 7.5 ± 1 kcal/mole, in surprisingly good agreement in view of the approximations involved in the London theory.

On combining Eqs. (1) and (3) one finds that the potential energy at the saddle point is given by

$$E_S = \frac{3}{2}\,{}^1\Sigma\,(R) + \frac{1}{2}\,{}^3\Sigma\,(R) + {}^3\Sigma\,(2R) \qquad (4)$$

$$= -140 + 36 + (6\pm2) = -98 \pm 2 \text{ kcal/mole.}$$

In the first two terms, the singlet and triplet energies are evaluated at $r_{12} = r_{23} = R \approx 1.0$ Å and the third triplet term is evaluated at $r_{13} = 2R$. To obtain the activation energy, one must subtract from E_S the (negative) binding energy of the hydrogen molecule, $-D_0 = 103$ kcal/mole, and add the zero-point energy of the activated complex, $E_{\ddagger} \approx 3$ or 4 kcal/mole. This gives

$$E_{act} = E_S + D_0 + E_{\ddagger}$$

$$= -1 + (6 \pm 2) + (3 \text{ or } 4) = 8 \text{ or } 9 \pm 2 \text{ kcal/mole.}$$

The repulsive interaction, ${}^3\Sigma(2R)$, between the outside hydrogen atoms in the complex and the zero-point energy are thus seen to play an important role in determining the activation energy.

Figure ID. 10-2 shows (as the solid curve) the variation of the ratio $Q/{}^1\Sigma$ with r implied by Eq. (2) and the diatomic potential curves used here. The result derived[7] from the Heitler-London-Sugiura approximation is also shown (as the dot-dashed curve). In contrast with the latter approximation, the treatment described here indicates that the assumption of a constant Coulombic ratio is an extremely poor approximation.

---

[6] A. F. Trotman-Dickenson, Gas Kinetics (Butterworths Scientific Publications, London, 1955), p. 169 ff.

[7] J. O. Hirschfelder, J. Chem. Phys. 9, 645 (1941).

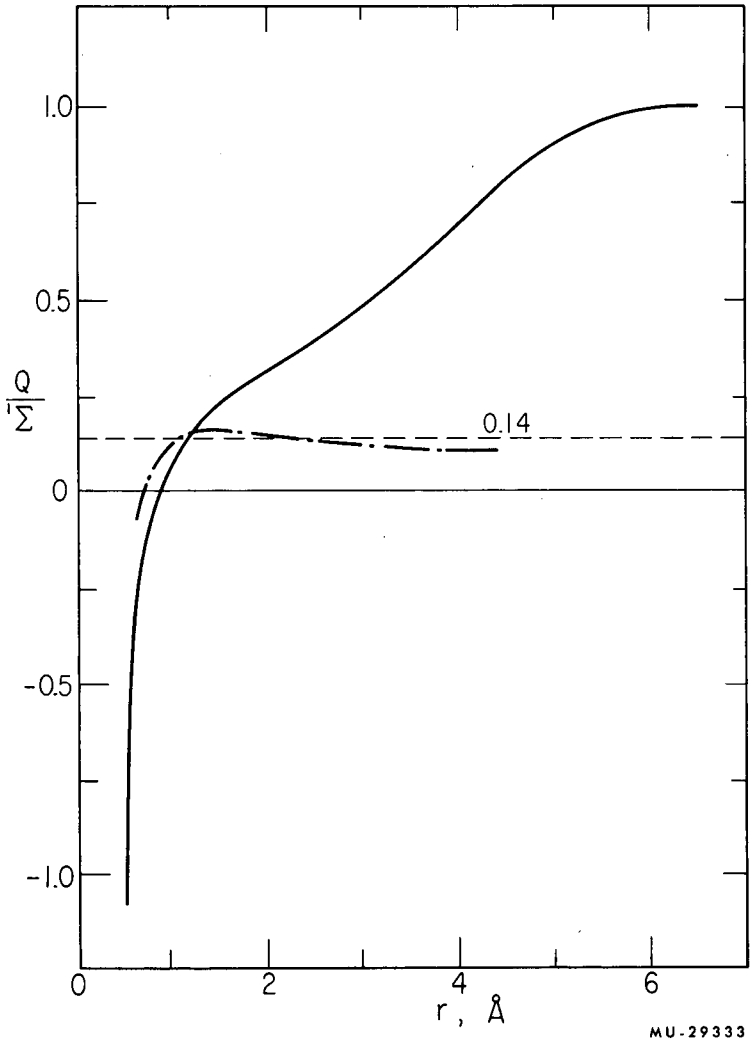

Fig. ID. 10-2. Coulombic fraction of binding energy as a function of internuclear distance. Solid curve derived from this work; dot-dashed curve from Heitler-London-Sugiura approximation. The traditional method for plotting energy surfaces is equivalent to using the dashed line.

11. APPLICATION OF NUMERICAL SOLUTIONS TO THE RADIAL EQUATION FOR DIATOMIC MOLECULES*

J. K. Cashion

Cooley's procedure for solving the Schrödinger radial equation numerically[1] has been found to be highly accurate and efficient. On an IBM 7090 it generates the wave function at 1000 points and corrects the trial eigenvalue in 0.4 second.

Numerical solutions using the Morse potential established that the approximate analytical solution due to Pekeris[2] is highly accurate. An incorrect limit of integration in his development was shown to affect the accuracy of his result by less than one part in 10^7. Quantitative measures were made on the errors resulting from the neglect of high-order terms.

Eigenvalues and eigenfunctions were obtained for the Clinton potential,[3] for which no analytic solutions exist. The potential is markedly inferior to the Morse in predicting vibrational and rotational energy separations.

Vibration-rotation interaction factors were calculated for several molecules using numerically-obtained Morse eigenfuctions. Comparison with the results of Herman, Rothery and Rubin[4] indicated that their approximate formulae for the linear dipole model were accurate to within 1% up to $J = 20$ for $\Delta v = 1$ transitions, but could give errors of several percent for $\Delta v > 1$ transitions.

The effects of neglecting the quadratic and cubic integrals in the expansion for the dipole moment function were examined. Using an approximate method[5] to evaluate the expansion coefficients, the interaction factors were calculated to the quadratic and cubic approximations. It was found that the linear and cubic approximations could differ by a factor of more than three.

---

*Abstract of two papers: J. K. Cashion, Applications of Numerical Solutions to the Radial Equation for Diatomic Molecules; I. Solutions for the Morse and Clinton Potentials Compared with an Approximate Analytical Solution and with Experiment, UCRL-10643, March, 1963; and J. K. Cashion, Applications of Numerical Solutions to the Radial Equation for Diatomic Molecules: II. The Calculation of Vibration-Rotation Interaction Factors, UCRL-10644, March, 1963.

[1] J. W. Cooley, Math. of Computation 15, 363 (1961).

[2] C. L. Pekeris, Phys. Rev. 41, 98 (1934).

[3] W. L. Clinton, J. Chem. Phys. 36, 555 (1962); ibid., 36, 556 (1962).

[4] R. Herman, R. W. Rothery, and R. J. Rubin, J. Mol. Spectroscopy 2, 369 (1958) and ibid. 9, 170 (1962).

[5] J. K. Cashion, A Method for Calculating Vibrational Transition Probabilities, J. Mol. Spectroscopy, in press.

12. CALCULATION OF THE INTENSITY OF MOLECULAR FLUORESCENCE SPECTRA FOR Na_2, RbH, AND I_2

Richard N. Zare

Although the Franck-Condon principle is known to account for the main features of the intensity distribution in an electronic transition, there have been relatively few quantitative comparisons between theory and experiment. In large part this is due to the difficulty of obtaining reliable intensity data and the labor involved in performing a realistic numerical calculation ab initio. The detailed studies of the fluorescence spectra of Na_2 by Brown[1] and of RbH by Gaydon and Pearse[2] provide perhaps the most satisfactory test of the principle.[3] As part of a program of calculations of vibrational transition probabilities, we have recalculated the Na_2 and RbH intensity distributions. The results confirm the earlier calculations, which were based on less exact methods and improve the agreement with experiment.

The intensity $I_{v',v''}$ in emission of the (v', v'') molecular band is given by the well-known expression

$$I_{v',v''} = C \exp(-E_{v'}/kT) E^4_{v',v''} \bar{R}_e^2 \left[\int \psi_{v'} \psi_{v''} dr\right]^2,$$

where C is a constant containing the effects of geometry and conversion factors, $\exp(-E_{v'}/kT)$ is proportional to the population of the v'th level, which has an energy $E_{v'}$; $E_{v',v''}$ is the energy of the (v', v'') transition; $\bar{R}_e$ is the average electronic transition moment, which will be assumed to be independent of the internuclear separation r; and $\psi_{v'}$ and $\psi_{v''}$ respectively are the vibrational wave functions of the upper and lower states connected by the transition. The variation of intensity is predominantly controlled by the square of the overlap integral

$$\int \psi_{v'} \psi_{v''} dr,$$

which is highly sensitive to the phase relation between the initial and final wave functions. The integrand is the product of two oscillatory functions, being positive where the functions are of the same sign and negative where they are of opposite sign. For higher vibrational levels, more nodes and loops appear in the vibrational wave function and the value of the integral depends critically upon the relative phase.

For Na_2, Brown used a complicated algebraic expression derived by E. Hutchisson[4] to obtain the intensity variation for the $v' = 0$ and $v' = 5$ series. Corrections for the anharmonicity were made for each vibrational level.

---

[1] W. G. Brown, Z. Physik 82, 768-775 (1933).

[2] A. G. Gaydon and R. W. B. Pearse, Proc. Roy. Soc. (London) A173, 28-47 (1939).

[3] E. U. Condon, Am. J. Phys. 15, 365-374 (1947).

[4] E. Hutchisson, Phys. Rev. 36, 410 (1930); 37, 45 (1931).

To minimize the computational complexity, Gaydon and Pearse used systematically distorted harmonic oscillator wave functions and calculated the overlap integrals numerically to locate the primary, secondary, and tertiary Condon parabolas for RbH.

In the calculations reported here, and IBM 7090 computer is programmed to solve iteratively Schrödinger's equation for the energy and wave function by the Numerov method for finite-difference equations.[5] The potential is specified at every 0.002-Å interval for a range of about 2Å. For both Na_2 and RbH a Dunham potential was programmed, using the available spectroscopic constants. For Na_2 our calculations compare closely to the previous calculations, and agreement with experiment is good. For RbH, the locations of the primary, secondary, and tertiary parabolas given by our calculation are in better agreement with experiment than the previous calculation.

As pointed out by Condon,[3] a much more severe test of the principle would be a calculation of the intensity fluctuations observed by Wood[6] in the fluorescence spectrum of I_2. On excitation by the Hg green line, I_2 molecules make a transition to the 26th vibrational level of the upper state, from which they emit more than a hundred fluorescence doublets as they fall to the different vibrational levels of the ground state. Intensity estimates for about the first forty doublets have been made by Lenz[7] and Oldenberg.[8]

In calculating overlap integrals for high vibrational quantum numbers v' and v'', the phase relation of the initial and final wave functions is extremely critical. To obtain appropriate wave functions the molecular potential energy curves must be known with precision over a wide range of r. The ground-state potential of I_2 shown in Fig. ID. 12-1 is quite narrow and for $v'' \geq 20$ the average length of a loop in the wave function is about 0.03 Å. The corresponding length for the $v' = 26$ level of the upper state is 0.04 Å. The value of the overlap integral for $v' = 26$, $v'' = 25$ is determined almost entirely in the narrow interval ΔX, which contains about 17 nodes of the upper state and 15 of the lower, as illustrated in Fig. ID. 12-1.

The serious errors that can result from a gradual shift in phase are clearly illustrated in Fig. ID. 12-2. The upper portion of the figure shows the calculated intensity distribution when Morse potentials are used for both upper and lower states. The central portion of the figure shows the experimental distribution. The Morse results are qualitatively correct only up to about $v'' = 10$. At higher v'' agreement would be restored if the calculated

---

[5] J. W. Cooley, Mathematics of Computation 15, 363-374 (1961). N. B.: A SHARE distributed program for the 7090 by Cooley has been corrected and modified. This powerful method is superior for most applications to the slower Runga-Kutta solution which has been used by Hartree and others.

[6] R. W. Wood, Phil. Mag. 35, 236-261 (1918).

[7] W. Lenz; Z. Physik 25, 299-311 (1924).

[8] O. Oldenberg, Z. Physik 45, 451-454 (1927).

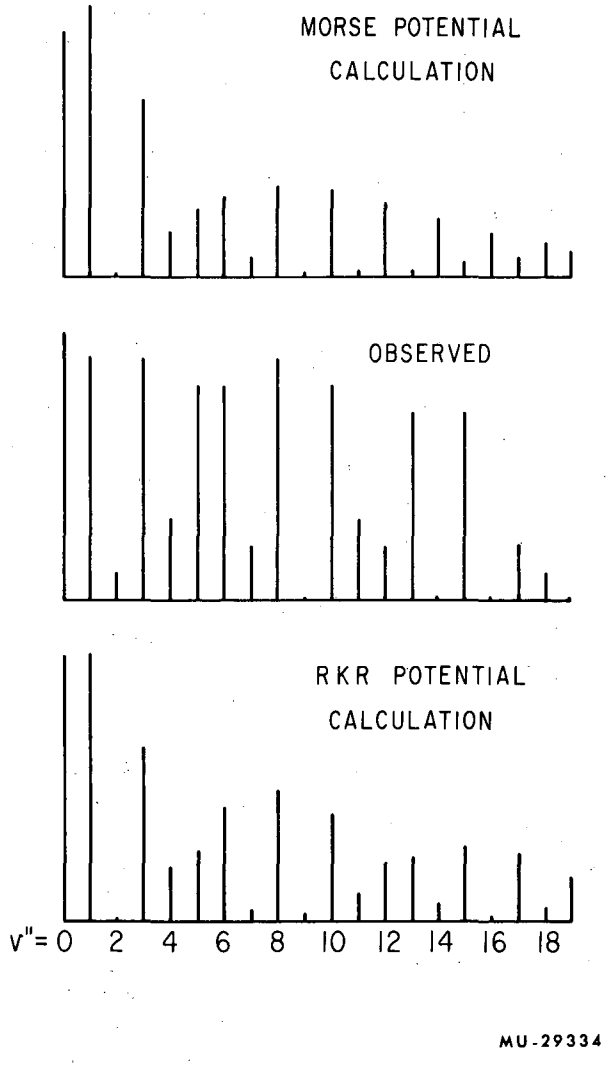

Fig. ID. 12-1. Intensity distribution for I_2 fluorescence, $B^3\Pi_{Ou}^+$ (v' = 26) → $X'\,\Sigma_g^+$. All intensities have been scaled to ten.

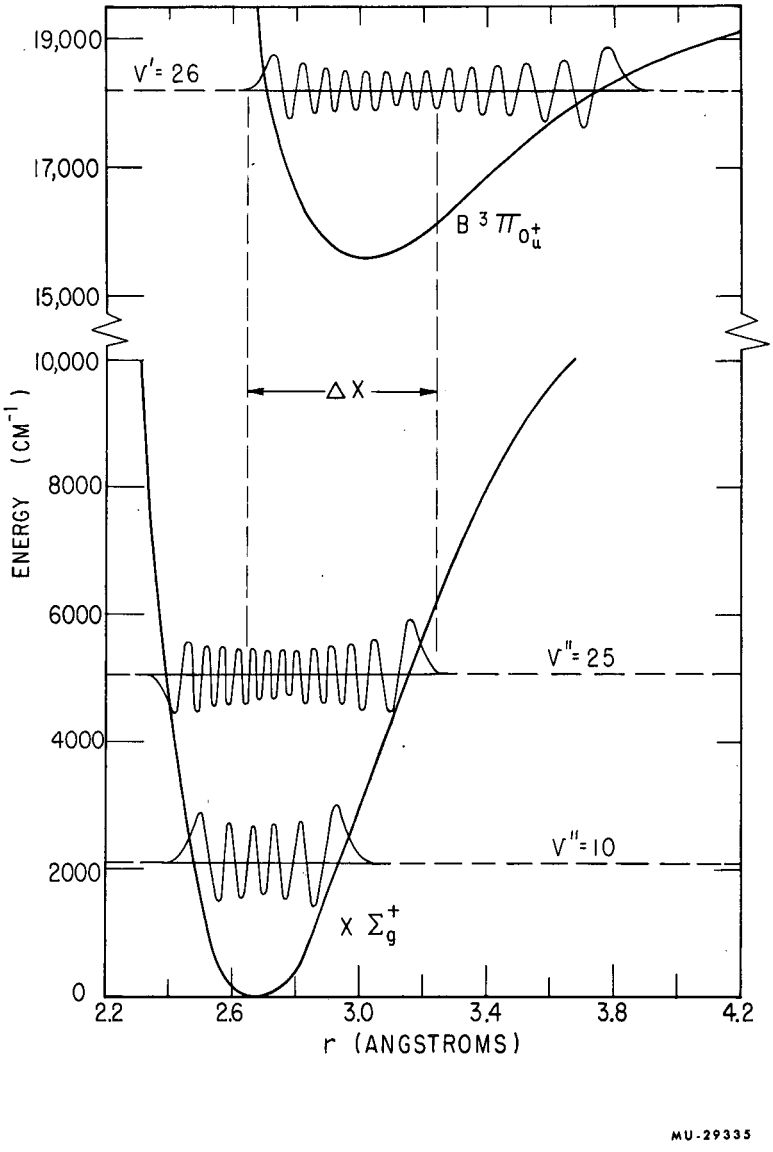

Fig. ID. 12-2. Potential energy diagram for I_2. The wave functions shown have been normalized to unity.

lines were shifted by one unit to the left, e.g., the Morse lines for $v'' = 13$ to 19 reproduce fairly well the pattern of the observed lines $v'' = 12$ to 18.

In the calculations reported here (Fig. ID. 12-2, bottom) this difficulty has been overcome by using "real" potential curves determined from the RKR method. For the ground state the potential is fitted from the turning points determined by Verma,[9] and in the upper state by Mathieson and Rees.[10] The quantitative agreement with experiment is reasonably good, and the qualitative pattern of strong and weak lines is reproduced almost perfectly up to $v'' = 20$. Further work is in progress to attempt to explain the discrepancies and improve the agreement.

---

[9] R. D. Verma, J. Chem. Phys, 32, 738-749 (1960).

[10] Lois Mathieson and A. L. G. Rees, J. Chem. Phys. 25, 753-761 (1956). We thank Dr. Rees for so kindly providing us, through private communication, with the turning points.

13. DOPPLER LINE SHAPE OF ATOMIC FLUORESCENCE EXCITED BY MOLECULAR PHOTODISSOCIATION*

Richard N. Zare and Dudley R. Herschbach

A semiclassical treatment of the photodissociation of a diatomic molecule is developed. It is shown that the angular distribution of products will often be peaked parallel or perpendicular to the direction of the incident light beam. The form of the anisotropy is usually determined just by the orientation of the electronic transition dipole moment within the molecule and the polarization of the exciting light. From the angular distribution, the Doppler line shape of fluorescence emitted by an excited fragment atom is derived by averaging the geometrical factors over the translational velocity distribution of the parent molecules and the distributions in magnitude and angle of the recoil velocity of the excited atoms. A comparison is made with dissociative electron impact processes which show similar features. The photodissociation of NaI is treated in detail, and the factors influencing the fluorescence width are evaluated for possible optical maser systems in which the supply of excited atoms is generated by molecular dissociation.

---

* Abstract of paper published in Proc. I. E. E. E. 51, 173 (1963).

14. INFLUENCE OF VIBRATIONS ON MOLECULAR STRUCTURE DETERMINATIONS

Victor W. Laurie* and Dudley R. Herschbach

The physical interpretation as well as the accuracy of structural parameters derived from spectroscopic effective moments of inertia is limited by vibration-rotation perturbations. It has recently been shown, however, that the effective moments may be converted to the moments of the average molecular configuration by corrections which involve only the harmonic vibrational force constants.[1,2] To a good approximation, the entire effect of anharmonicity is absorbed in displacing the average configuration from the equilibrium one. Formulas have been derived that permit calculation of structural parameters for the average molecular configuration in the ground vibrational state for some simple types of molecules, and about a dozen examples have been treated.[3] Average structures may also be obtained from electron diffraction data. A recent diffraction study of methane[4] has made possible a precise comparison, and the average CH bond lengths derived from the diffraction and spectroscopic results are found to be in excellent agreement.[3,4]

The "inertial defect" observed in planar molecules is a particularly prominent effect of vibration-rotation interaction: the out-of-plane moment of inertia is usually found to be appreciably larger than the sum of the in-plane moments, whereas it would equal this sum if the molecule were rigid. A simple treatment of inertial defects has been formulated in which all but the one or two vibrational modes of lowest frequency are "frozen out." This is found to account for about 90% of the inertial defect in many molecules. Contributions from in-plane vibrations are shown to be positive; those from out-of-plane vibrations to be negative. Methods of estimating the direction and magnitude of related effects that arise in nonplanar molecules are also examined. Examples are given to show that the structural ambiguities caused by these effects can be largely eliminated if the average moments of inertia are used instead of the effective moments.[5]

For all except the simplest molecules, a structure determination requires the use of moments of inertia for several isotopic species. A detailed study[3-6] of the isotopic dependence of the vibration-rotation effects

---

*Presently at Department of Chemistry, Stanford University, Stanford, California.

[1] T. Oka, J. Phys. Soc. Japan 15, 2274 (1960); Y. Morino, K. Kuchitsu, and T. Oka, J. Chem. Phys. 36, 1108 (1962).

[2] D. R. Herschbach and V. W. Laurie, Bull. Am. Phys. Soc. 5, 500 (1960); J. Chem. Phys. 37, 1668 (1962).

[3] V. W. Laurie and D. R. Herschbach, J. Chem. Phys. 37, 1687 (1962).

[4] L. S. Bartell, K. Kuchitsu, and P. J. de Neui, J. Chm. Phys. 35, 1211 (1961).

[5] V. W. Laurie and D. R. Herschbach, Inertial Defects, J. Chem. Phys. (to be published, 1963).

[6] V. W. Laurie and D. R. Herschbach, The Determination of Molecular Structure from Rotational Spectra, UCRL-10377, July 1962.

has shown that in most cases the main contribution appears in the isotopic variation of the average molecular configuration. The variations are largest for deuterium substitution, which usually shrinks the average bond length by 0.003 to 0.005 Å. For heavier atoms the isotopic variations are much smaller, of the order of 0.0001 Å or less. These slight isotopic changes in the actual average parameters can give rise to much larger errors in the calculated parameters, however, as the usual methods of structure analysis magnify the effect of isotopic variations. The formulas used in the "substitution method" of structure determination[7] have been generalized to include explicitly the isotopic variations. Although lack of information about the anharmonic vibrational force constants precludes a theoretical evaluation of the isotopic variations, it is found that an empirical treatment, based largely on data for diatomic molecules, accounts for many anomalies and inconsistencies in published structure studies.[6]

[7] J. Kraitchman, Am. J. Phys. 21, 17 (1953); C. C. Costain, J. Chem. Phys. 29, 864 (1958).

15. RESEARCH IN PROGRESS: DUDLEY R. HERSCHBACH

a. The velocity dependence of the total cross section for elastic scattering of Li by CH_3I is being measured by George H. Kwei. For this system, the de Broglie wavelength is sufficiently long to permit observation of quantum undulation effects. This should provide information about the form of the intermolecular potential function in the region where dispersion forces become insignificant and chemical interaction is dominant.

b. The massfilter detector built by Kent R. Wilson has made feasible the study of exchange reactions of alkali metals with alkali halide molecules, $M + M'X \rightarrow MX + M'$. For these reactions the scattering kinematics is particularly favorable for a detailed study of the energy partitioning and angular distributions. Also, since both products can be detected, in the analysis of the scattering considerably higher resolution can be attained than is feasible for other systems.

c. The elastic scattering of velocity-selected alkali atoms by other alkali atoms, $M + M'$, is also being studied in order to evaluate the intermolecular potential parameters from which transport properties for the alkalies can be calculated.

d. A new crossed- molecular-beam apparatus is being assembled by Ronald R. Herm. This can be used with any condensible reactants, and is designed to facilitate work with magnetically analyzed beams. The reactions between alkali metals and halogens, $M + X_2$ and $M_2 + X$, will be studied with the aim of settling the question of the relative proportion of vibrational and electronic excitation in the products.

e. A second new crossed-beams apparatus is being assembled by J. K. Cashion and Malcolm Fluendy. This has a differentially pumped oven chamber, and will be used for experiments with hydrogen atom or halogen atom beams.

f. A semiclassical treatment of rotationally inelastic collisions has been developed by Mark Child and R. James Cross, and an experimental study of the Li + H_2 system is being set up to test predictions of the theory.

16. THE RATE OF COMBINATION OF GASEOUS IONS

Bruce H. Mahan and James C. Person

Using 9.9-eV vacuum ultraviolet radiation, we have produced plasmas of NO^+ and NO_2^- in which the charge concentration is 10^8 to 10^9 ions/cc. By suddenly extinguishing the ionizing radiation, allowing the plasma to decay for a predetermined time, and then withdrawing and measuring the residual charge, we have determined the rate of the mutual neutralization of gaseous ions. The reactions involved in the establishment and decay of the plasma are

$$\begin{aligned} NO + H\gamma &\rightarrow NO^+ + e, \\ NO + e + M &\rightarrow NO^- + M, \\ NO^- + NO_2 &\rightarrow NO_2 + NO, \\ NO^+ + NO^- &\rightarrow \text{neutral fragments.} \end{aligned}$$

Plots of the reciprocal ion concentration as a function of time are linear for at least two or three half-lives, which indicates that the ions disappear by a reaction which is of second order with respect to total charge, or first order with respect to the concentrations of positive and of negative ions. However, as Fig. ID. 16-1 shows, the value of the second-order rate constant α is a function of total pressure.

There are three significant features to this pressure dependence. First, in the limit of zero pressure the rate constant remains finite, which shows that there is a true bimolecular charge-neutralization reaction. Second, at low pressures the combination rate constant increases with pressure, which suggests that there is also a parallel third-order neutralization process. Third, the pressure dependence of the rate constant diminishes at high gas pressure.

These facts are consistent with the following detailed mechanism:

$$\begin{aligned} NO^+ + NO_2^- &\xrightarrow{k_0} \text{neutrals}, \\ NO^+ + NO_2^- &\xrightarrow{k_1} (NO^+NO_2^-)^*, \\ (NO^+NO_2^-)^* &\xrightarrow{k_2} NO^+ + NO_2^-, \\ (NO^+NO_2^-)^* + M &\xrightarrow{k_3} (NO_2 + NO_2^-) + M \rightarrow \text{neutrals}. \end{aligned}$$

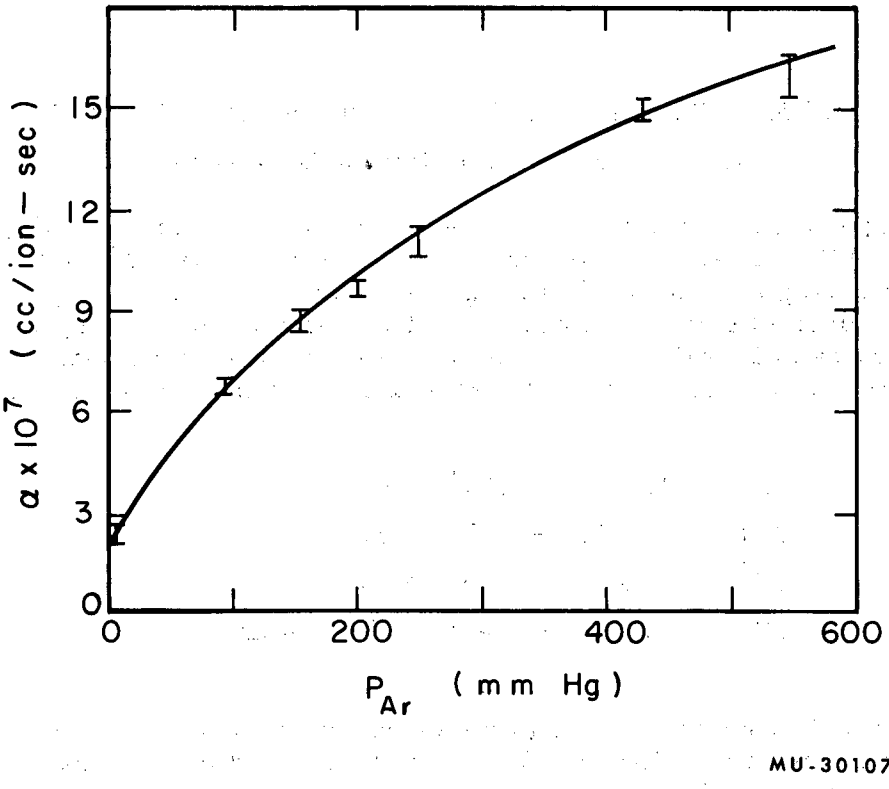

Fig. ID. 16-1. Dependence of recombination coefficient on pressure. NO and Ar.

The complex $(NO^+ NO_2^-)^*$ is an ion pair which upon collision with a neutral molecule M becomes permanently bound. These reactions give the rate law

$$-\frac{dn}{dt}/(NO^+)(NO_2^-) = k_0 + \frac{k_1 k_3(M)}{k_3(M)+k_2},$$

which is consistent with our data. The value of k_0 is 1.7×10^{-7} cc per molecule sec, which shows that the two ions need only come to within 10 Å of each other to effect electron transfer. The value of k_1 is 1.8×10^{-6} cc per molecule sec, so that any pair of ions closer than 150 Å may be deactivated to form a bound pair. The relative values of k_2 for various gases are He, 1; N_2, 4; Ar, 4.5; Xe, 13.

17. RESEARCH IN PROGRESS: BRUCE H. MAHAN

a. A microwave-detection cavity which can be used to measure electron concentrations as a function of time has been built. Preliminary experiments now being done will eventually yield rate constants for the reactions of thermal electron with molecules and molecular ions.

b. The photosensitized ionization of cesium is being studied. When cesium atoms absorb a light quantum and are excited to a discrete state near the ionization limit, the reaction

$$Cs^* + Cs \rightarrow Cs_2 + e$$

occurs. The threshold for this process is a measure of the bond energy of Cs_2^+, which older work indicates is 1 eV, twice as great as the bond energy in Cs_2. This work is being repeated and extended to the other alkali metal molecules.

c. An apparatus for measuring dielectric constants as a function of time at 100 Mc/sec is being completed. This will allow precise determinations of ion-ion neutralization rates in low-pressure gases.

d. In collaboration with Professor Rollie Myers, we are constructing an apparatus to measure by means of paramagnetic resonance the rates of hydrogen and oxygen atom reactions.

18. THE KINETICS OF THE COORDINATION OF Cl^- AND $SO_4^=$ WITH Mn^{++} AS DETERMINED BY PARAMAGNETIC RESONANCE*

Robert G. Hayes, William Sherwood, and Rollie J. Myers

The measurement of paramagnetic resonance line widths should be an excellent method for the determination of very short lifetimes. If transition metal ions and complexes are being formed and decomposed in times shorter than 10^{-7} second it should, in most cases, be possible to measure this process by paramagnetic resonance. Most chemical reactions are not this fast, however, and one could expect to measure only special reactions. The formation of simple complex ions with small ligands should be fast enough for this technique.

The paramagnetic resonance line width for Mn^{++} in aqueous solutions containing Cl^- goes through some interesting changes as the temperature is raised. Between 20°C and 80°C the line width drops with increasing temperature and it changes little with the Cl^- concentration. Above 100°C the line width can rise rapidly with temperature and it is a critical function of the Cl^- concentration. A graph of this behavior is shown in Fig. ID. 18-1.

This behavior can be explained if it is assumed that the Cl^- enters the coordination sphere of Mn^{++} and that this complex ion has a short paramagnetic relaxation time. Since the line width due to coordination increases with temperature, the rate of formation of the complex must be the limiting rate process. This is confirmed by the finding that a log plot of the excess width due to Cl^- against 1/T gives an activation energy of 9.4 kcal/mole and a rate constant $k(25°C) = 1.5 \times 10^6$ sec^{-1} M^{-1}. This large activation energy must be associated with the formation of a first-coordination-sphere complex.

The results for $SO_4^=$ are more complicated. The line width near room temperature is changed by $SO_4^=$ ion, but again at high temperatures there is a rapid increase in line width with temperature. The difference between $SO_4^=$ and Cl^- arises because the equilibrium constants for coordination of $SO_4^=$ around Mn^{++} are in the range of 100 at room temperature. At the concentrations used in our work an appreciable fraction of Mn^{++} is coordinated with $SO_4^=$ at all times. The observed line widths are then the expected average width for Mn^{++} and for the Mn^{++} - $SO_4^=$ complexes. It seems most likely that the formation of the second-coordination-sphere complexes is sufficiently fast so that the line width is a simple average of the Mn^{++} and the outer-sphere $SO_4^=$ complexes. As in the Cl^- case, however, the formation of the first-coordination-sphere complex is the limiting rate, and it should be possible to obtain this rate from the data. The calculation is much more difficult than for the Cl^- case, since the equilibrium constant for the formation of the outer-sphere complex and its line width must also be obtained from the data. The values that we have obtained from the data are in agreement with those of Eigen and Tamm obtained for $MnSO_4$ by ultrasonic relaxation.[1]

---

*To be submitted to J. Chem. Phys., and to be presented in part at the American Chemical Society Meeting in September 1963.

[1] M. Eigen and K. Tamm, Z. Elektrochem. 66, 107 (1962).

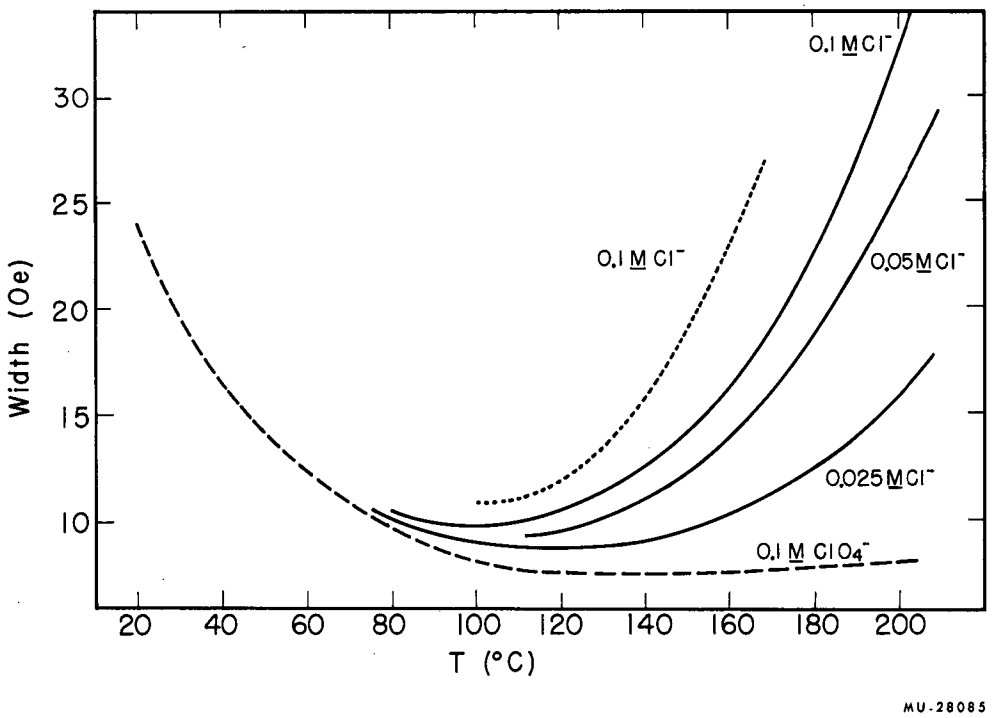

Fig. ID. 18-1. The solid lines show the effect on the paramagnetic line width of adding NaCl to a 0.05 M $Mn(ClO_4)_2$ solution. The dashed line is the line width of a 0.05 M $MnCl_2$ solution.

The Cl^- data were obtained by adding NaCl to a 0.05 M $Mn(ClO_4)_2$ solution. In this case the excess line width is very nearly first order in the Cl^- concentration. If on the other hand, one dilutes a $MnCl_2$ solution it is found that the excess line width is not proportional to the Cl^- concentration. The rate constant for the formation of the Mn^{++} complex with Cl^- appears to increase considerably as the solution is diluted. This is quite clearly an ionic strength effect and it qualitatively follows the expected behavior. In the $SO_4^=$ case since the ionic strength was far from constant when Na_2SO_4 was added to $Mn(ClO_4)_2$ the data obtained so far for $SO_4^=$ can only be treated qualitatively. Further work is being done on this ionic strength effect.

19. THE KINETICS OF THE SLOW EXCHANGE OF CN^- WITH $Cr(NO)(CN)_5^{-3}$ AS FOLLOWED BY PARAMAGNETIC RESONANCE*

J. Brook Spencer and Rollie J. Myers

The paramagnetic resonance of $Cr(NO)(CN)_5^{-3}$ has been reported by Bernal and Harrison.[1] From a variety of evidence it is concluded that the NO is essentially NO^+ and therefore the chromium is present as Cr^{+1} surrounded by six isoelectric ligands. The resonance lines in this complex are only a few gauss wide and the hyperfine interactions of $N^{14}O^+$ and Cr^{53} (9.5%) are clearly resolved.

Hayes has shown that C^{13} in natural abundance can also be detected in the hyperfine splitting.[2] We have followed quantitatively the formation of $Cr(NO)(CN)_5^{-3}$ containing $C^{13}N^-$ by exchange in aqueous solution, utilizing NaCN enriched to 50% in C^{13}. The measurements were made by directly following the formation of $Cr(NO)C^{13}N(CN)_4^{-3}$ while the samples were heated in glass tubes placed inside the paramagnetic resonance spectrometer. Below 100°C no net decomposition of the complex could be observed, but decomposition was detected above this temperature.

The reaction was assumed to be over-all second order, and both the initial rate and the integrated rate were used to determine the rate constant for exchange. The activation energy was calculated to be 23±2 kcal/mole.

During the exchange it was observed that hyperfine interaction was produced which corresponded to two and more equivalent $C^{13}N^-$ in the complex. Since $Cr(NO)(CN)_5^{-3}$ has most certainly C_{4v} symmetry, the observation of two magnetically equivalent CN^- must mean that the observed rate of exchange is not simply the rate of exchange of the axial CN^-. From intensity

*A report of this work is being presented at the American Chemical Society Meeting in Los Angeles in April 1963.

[1] I. Bernal and S. E. Harrison, J. Chem. Phys. 34, 102 (1961).

[2] Robert G. Hayes, Electron Spin Resonance Line Widths of Transition Metal Ions and Complexes in Solution (thesis) (UCRL-9873, Sept. 1961), J. Chem. Phys. (to be published).

measurements with C^{13} in natural abundance Hayes has concluded that the observed hyperfine coupling corresponds to either four or five magnetically equivalent CN^- sites.[2] Since we have been unable to observe a unique set of hyperfine lines that can be ascribed to the axial CN^-, there are several possible situations.

If all five of the CN^- are magnetically equivalent they may have very similar rates of chemical exchange. In this case we would be unable to differentiate between the axial and equatorial CN^-. If only the four equatorial CN^- are magnetically equivalent, either the axial CN^- has a much slower rate of exchange, so that we have not been able to enrich this position, or its hyperfine interaction is particularly small, so that we have not been able to detect it.

Since the NO^+ and CN^- are isoelectronic, one might expect a similar unpaired spin density on the N^{14} and C^{13}, and the observed hyperfine interaction constants are in agreement with this expectation. It is thus quite possible that all five CN^- are magnetically equivalent and that the axial and equatorial CN^- may exchange at the same rate. Further experiments are being done to check this point.

20. RESEARCH IN PROGRESS: ROLLIE J. MYERS

a. High-Temperature Microwave Spectroscopy

A ceramic and platinium high-temperature microwave cell designed by John Howe has been assembled and tested. The cell has been repeatedly heated to 1000°C, and microwave transmission has been retained with only one failure. After additional testing our first work will be on AgCl.

b. Power Saturation in Paramagnetic Resonance

A 200-watt S-band spectrometer is being assembled. Lack of space for the magnet has delayed this project. After testing on both high and low power levels this apparatus will be used to determine the spin-lattice relaxation times (T_1) for $Cr(NO)(CN)_5^{-3}$ and other transition metal ions in solution. These data can be of considerable value to Robert E. Connick in his work on O^{17} NMR line widths in solutions containing transition metal ions.

c. Paramagnetic Resonance of Free Radicals

The formation of free electrons and other free radicals in liquid ammonia by electrolysis has been studied. Some interesting results have been obtained both with NaI and with $(CH_3)_4$ NI used as solutes. The NaI results seem to confirm William L. Jolly's observation of a shift in the infrared absorption when NaI is added to Na dissolved in liquid ammonia. The preparation of other free radicals by electrolysis in liquid ammonia will be continued. We also plan to restudy the calcite resonances on which we worked earlier and to try to determine the occurrence of triplet states in inorganic molecules.

E. ELECTROCHEMISTRY

1. NUMERICAL EVALUATION OF CURRENT DISTRIBUTION IN ELECTRODE SYSTEMS*

Donald N. Hanson and Charles W. Tobias

In homogeneous and isotropic conducting media, in the absence of space charge, the distribution of electric potential in a regime enclosed by electrodes and insulators satisfies the Laplace equation.

Analytical solution of the Laplace equation is possible only in a few relatively simple geometries and when the boundary conditions describing the relation between potential and flux are linear. Even when general solutions are available, it is often difficult and tedious to translate these into particular, numerical answers. The various analog techniques usually employed to evaluate the approximate current distribution are cumbersome and inaccurate.

In recent years numerical solutions of the finite-difference form of the Laplace equation according to the interpolation method ("the method of squares") have been perfected and widely used to solve problems in electrostatics, heat conduction, and hydrodynamics.

It is shown that the "method of squares" is ideally suited for evaluation of current distribution in electrode systems of more than trivial geometry. This technique allows realistic consideration of the nonlinear overvoltage characteristics of electrode processes.

The precision of the numerical solutions is limited only by that of input parameters used to describe the system.

Although calculations may be readily made by desk calculators, the method is ideally suited for programming onto high-speed computing machines.

Figures IE. 1-1, through IE. 1-4 show the variation of local current density, i, in relation to the average current density, i_{av}, in two commonly occurring electrode arrangements. Figure IE. 1-3 demonstrates the effect of logarithmic (Tafel) polarization on the primary distribution; while in Fig. IE. 1-4 the limitations of the linear polarization approximation are shown.

---

*Abstract of an invited address given before the 13th annual meeting of the Comite International de Thermodynamique et de Cinetique Electrochimiques in Rome, September 28, 1962, by Charles W. Tobias.

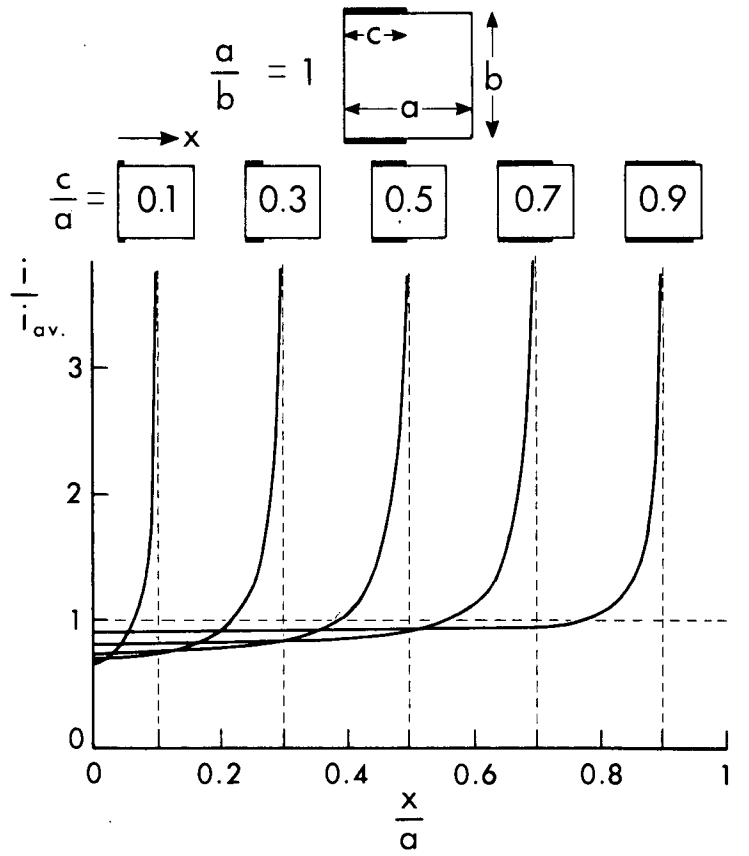

Fig. IE. 1-1. Primary distribution of current on stopped-off electrons in rectangular enclosure.

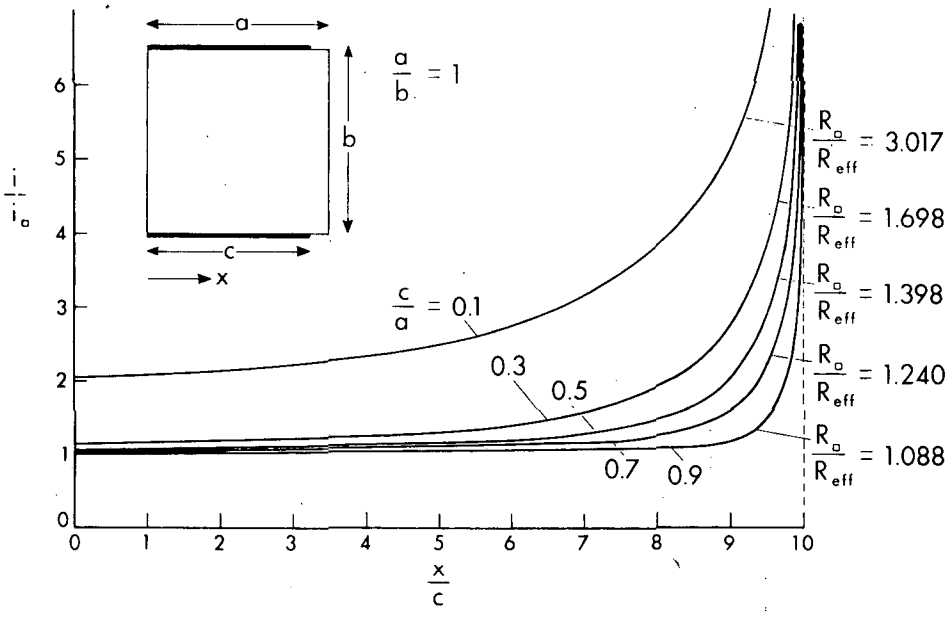

MU-29694

Fig. IE. 1-2. Relation of effective resistance, R_{eff}, between stopped-off electrodes and resistance when full-end electrodes are used, $R_{\square}$.

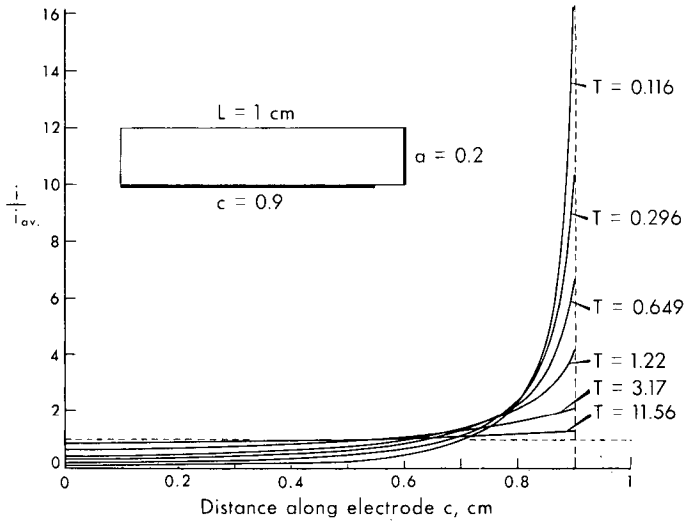

Fig. IE. 1-3. Effect of Tafel polarization on current distribution.
$T = \frac{k \cdot \beta}{L \cdot i}$, where K = conductance ($ohm^{-1}cm^{-1}$),
β = Tafel slope (volts),
i = average current density (A/cm^2).

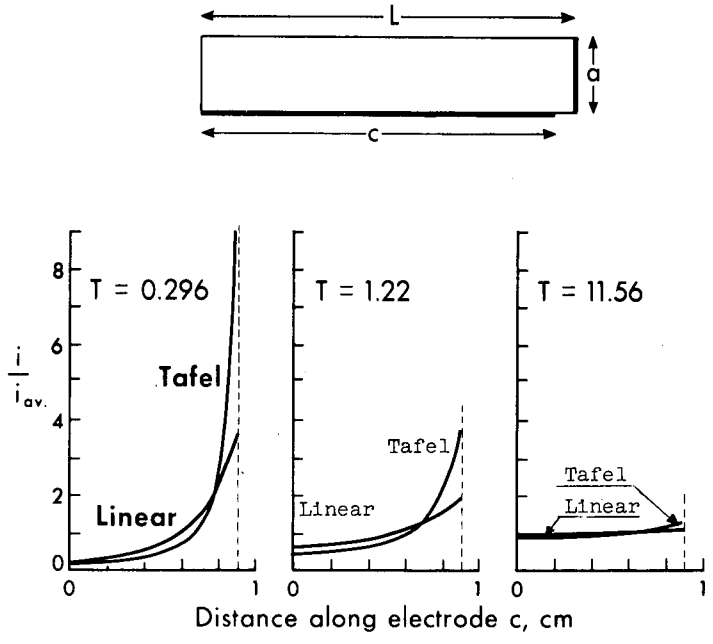

Figure 17. MU-29696

Fig. IE. 1-4. Comparison of influence of Tafel and linear polarization.

2. CONCENTRATION CELLS IN LIQUID AMMONIA

Rolf H. Muller and Charles W. Tobias

The reversible behavior of lead electrodes immersed in 0.01 to 0.1 molal solutions of lead nitrate and lead thiocyanate in anhydrous ammonia containing 5 mole % or more of ammonium or potassium thiocyanate or ammonium or sodium nitrate has been confirmed by potential measurements of concentration cells over an extended range of compositions. Thus, the earlier suggested use[1] of such electrodes as references for potential measurements in liquid ammonia has been corroborated.

[1] R. H. Muller, G. D. Snider, and C. W. Tobias, Reference Electrodes in Liquid Ammonia, submitted to J. Electrochem. Soc.

3. RESEARCH IN PROGRESS: CHARLES W. TOBIAS

a. Distribution of Current into a Fissure-like Pore

Recent advances in the theory of porous electrodes[1] require careful experimental checks on critical assumptions made in the theoretical models. Measurements on scaled-up models would be rather simple to obtain; however, it is not possible to assure dynamic similarity between model and prototype when the size difference is significant. To allow measurement of the distribution of current into a pore, a segmented microfissure has been constructed. Two segmented flat electrodes, facing each other at distances typical of pores (of the order of 10 microns), are assembled to form a fissure. Each electrode surface is 5 cm wide and 1 cm deep and divided (in the 1-cm direction) into ten electrically insulated sections from which branch currents can be measured. The small dimensions of the fissure opening make it necessary that the two opposing electrode surfaces be optically flat. Pure nickel was chosen as an inert electrode material for use with aqueous redox systems, and the electrically insulated sections were obtained by bonding stacks of 1-mm-thick nickel sheets alternating with 1-mil Mylar insulators. Grinding and polishing of the front side of these stacks proved to be very difficult because of the softness of the metal, and technique had to be developed to maintain the separation between sections while attaining a smooth, flat surface. Figure IE.3-1 shows four polished electrodes consisting of ten sections each, contained in a holder used for their preparation. Figure IE.3-2 is a photomicrograph showing the well-defined separation between sections after polishing. The electrodes will be incorporated in an electrolytic cell assembly for the measurement of current-distribution patterns under various combinations of parameters. (With Rolf H. Muller and Edward A. Grens)

[1] John S. Newman and Charles W. Tobias, Theoretical Analysis of Current Distribution in Porous Electrodes, J. Electrochem. Soc. 109, 1183-91 (1962).

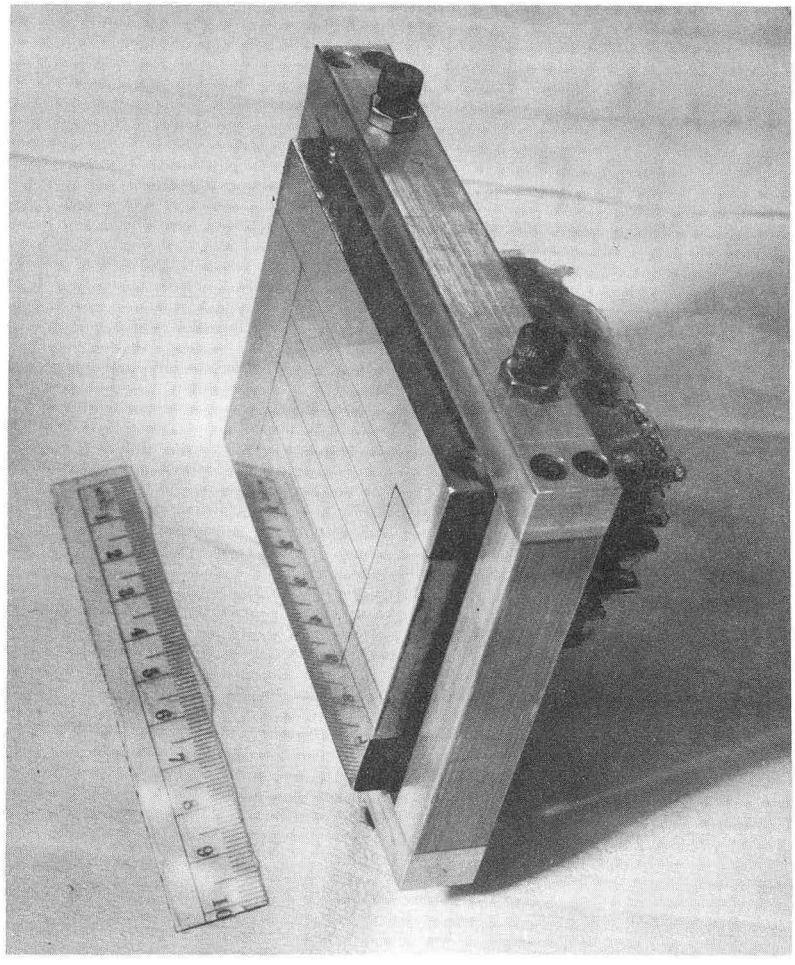

ZN-3639

Fig. IE. 3-1. Four segmented electrodes held in jig for surface polishing.

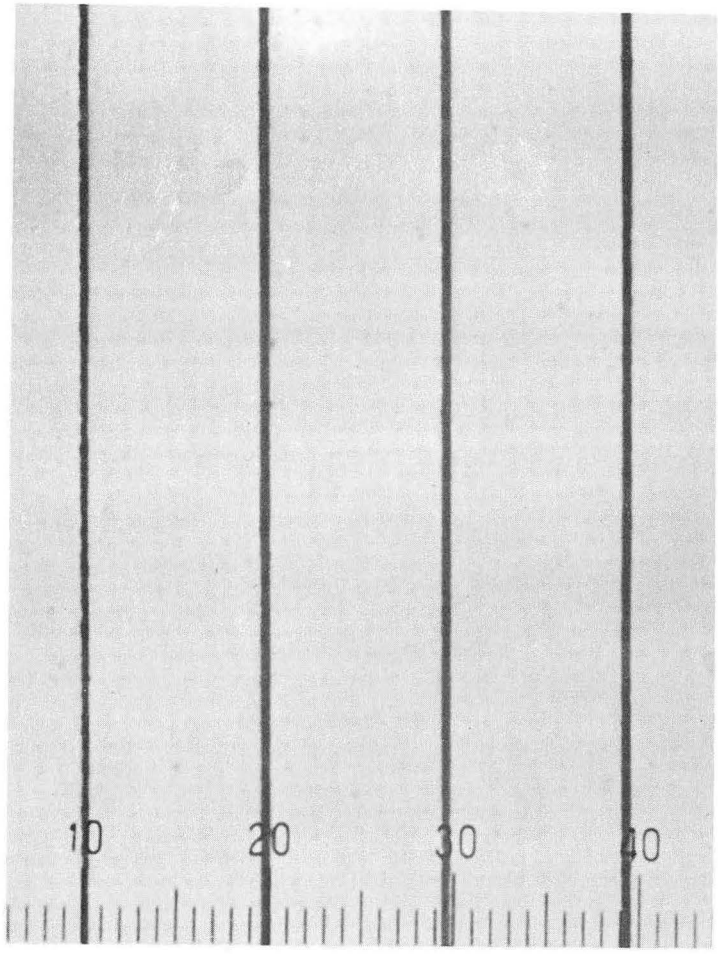

ZN-3640

Fig. IE. 3-2. Polished electrode surface with "Mylar" separators (1 division = 101 microns).

b. Electrochemical Oxidation of Phosphorus

Phosphorus and phosphorus compounds have been studied rather extensively from both thermodynamic and systematic chemistry standpoints; however, apparently very little work has been done to characterize the electrochemical behavior of phosphorus. Aside from purely theoretical aspects, the direct oxidation of phosphorus in an electrochemical cell might be of great interest both as an energy-source device for space technology applications and as a manufacturing process in the phosphoric acid industry. For these reasons, a study is being made of the electrochemical oxidation of phosphorus and simple phosphorus compounds.

The experimental program for this work consists essentially of measuring equilibrium potentials and polarization, or kinetic parameters for the various oxidation states of phosphorus. The phosphorus electrode consists of a porous plate of an inert metal saturated with phosphorus and immersed in an electrolyte. Potentials are measured between the phosphorus–phosphorus oxide electrode and a suitable reference electrode, such as mercury–mercuric oxide or calomel. The polarization is determined by passing a small current between the phosphorus electrode and a platinum disk that serves as a counter electrode.

Preliminary measurements have shown that although the half-cell potentials of liquid phosphorus in various electrolytes are within the range of interest for energy-source devices, they have not approached the expected equilibrium values and have been unstable with respect to passage of small currents. Possible reasons for this behavior may be the appearance of a mixed potential (i.e., simultaneous oxidation of phosphorus to two or more oxidation states), or direct hydrolysis and disproportionation of phosphorus to form phosphine, hydrogen, and various phosphorus-oxygen acids, followed by simultaneous oxidation of these compounds.

Current research indicates that the problem of providing suitable phosphorus-metal-electrolyte contact can be solved by using mercury (which is preferentially wetted by phosphorus in contact with aqueous solutions) in a porous silver amalgam electrode. The problem of mixed potentials may be resolved by measuring equilibrium potentials and polarization characteristics between different oxidation states and comparing these with the known rates of hydrolysis and disproportionation of phosphorus to these states. (With Michael L. Barry)

c. Numerical Evaluation of Current Distribution in Electrode Systems

The purpose of this study is to provide accurate and rapid methods for the evaluation of current distribution on electrodes in realistic geometric configurations. The "method of squares" has been successfully adapted in this Laboratory for the treatment of two-dimensional rectangular enclosures in which the electrodes – and insulators – coincide with the walls. At present the following programs are being perfected:

(i) Rectangular enclosures: electrodes and insulators are placed inside the field. (Multiply connected regions.)

(ii) Polygonal enclosures involving only right angles (both concave and convex corners). Electrodes and insulators coincide with boundaries.

(iii) Trapezoidal enclosures. Electrodes and insulators coincide with boundaries.

In addition to the basic, four-point method, large molecules are also used to improve inherent accuracy, and to reduce computational time. The effects of sequence of iteration and of overrelaxation also are considered.

The polarization behavior of the electrodes is described by the "full" polarization equation, involving two exponential terms. (With Ray N. Fleck and Donald N. Hanson)

4. OPTICAL STUDY OF GAS-ELECTROLYTE-ELECTRODE INTERFACES

Rolf H. Muller

Preliminary data on the current distribution at a gas-solid-liquid interface indicate the importance of the liquid film adhering to the solid wall. Optical means are being investigated to precisely define the extent and thickness of this film. Also, an attempt is made to characterize the concentration distribution in the film by a schlieren-optical technique modified for such a study. (Rolf H. Muller)

5. CRITICAL PROPERTIES OF MIXTURES AND THE EQUATION OF BENEDICT, WEBB, AND RUBIN*

Frank J. Ackerman and Otto Redlich

The critical lines of a binary fluid mixture (critical temperature and critical pressure as functions of the composition) are of some interest in the technology of gaseous reactions as well as in the application of thermodynamic functions to vapor-liquid equilibria. In principle, equations for the critical lines can be derived from an equation of state, but the problem is far too complicated for a complete explicit solution. However, rigorous relations for the limiting slopes of the critical lines have been derived,[1] and a fair approximation of the critical lines is obtained by a suitable interpolation. The quality of the results is therefore determined practically only by the accuracy of the equation of state on which the computation is based.

*A paper on this subject is scheduled to appear in J. Chem. Phys., May 1963.

[1] O. Redlich and A. T. Kister, J. Chem. Phys. 36, 2002 (1962).

A two-parameter equation[2] furnished fairly satisfactory results.[1] But it was obvious that one should expect the often and sucessfully used equation of Benedict, Webb, and Rubin,[3] containing eight parameters, to result in a much better representation of the critical lines. With the aid of automatic computation the use of this equation of state presents no serious difficulties. Various sets of values for the eight coefficients of several gases have been computed by different authors before.

The results of an application of Benedict's equation to the thermodynamic relation for the limiting critical slopes were surprising. It is obvious that the sixteen parameters of a binary mixture could always be adjusted to fit the critical points of the pure components and the limiting slopes of the critical lines. But the purpose of an equation of state is, of course, the prediction of thermodynamic properties on the basis of coefficients derived beforehand from other data. With the various sets of coefficients published in the literature, the limiting slopes of the critical pressure computed from Benedict's equation were sometimes good, sometimes fair, in a few cases entirely wrong. In comparison, the two-parameter equation of Redlich and Kwong furnished fewer good approximations but is never as far wrong as the more complicated relation.

The limiting slopes of the critical temperature lines are very well represented by either equation of state.

The general conclusion may be drawn that considerable caution is indicated in the use of a relation containing a large number of individual coefficients. Benedict's equation can be relied upon only in the range in which the coefficients have been determined. For the purpose of orientation in a range in which data are lacking, a less elaborate equation appears to be preferable.

---

[2] O. Redlich and J. N. S. Kwong, Chem. Revs. 44, 233 (1949).

[3] M. Benedict, J. B. Webb, and L. C. Rubin, J. Chem. Phys. 8, 334 (1940); 10, 747 (1942); Chem. Eng. Progr. 47, 419 (1951).

6. THE MOLAL VOLUME OF ELECTROLYTES*

Otto Redlich

As derived from the theory of Debye and Hückel, the apparent molal volume of an electrolyte in dilute solution depends linearly on the square root of the ionic strength.[1] The coefficient k depends only on the valency of the electrolyte and on properties of the solvent--in particular, on the pressure dependence dD/dP of its dielectric constant.

---

* A note on this subject is scheduled to appear in J. Phys. Chem., February 1963.

[1] O. Redlich and P. Rosenfeld, Z. Physik. Chem. A155, 65 (1931); Z. Elektrochem. 37, 705 (1931).

The numerical value of the coefficient has been repeatedly discussed since 1931 because available data for dD/dP were contradictory. A survey[2] of accurate determinations of the molal volume led to

$$k = 1.86 \pm 0.02, \qquad (25°C)$$

in satisfactory agreement with the results for dD/dP obtained by Falckenberg.[3] On the other hand, Owen and Brinkley[4] believed that the value

$$k = 2.517 \qquad (25°C)$$

following from Kyropoulos's measurements[5] should be adopted, and attempted to impose this value on the molal volume data by assuming large deviations from the limiting law at very low concentrations.

Recent measurements of dD/dP by Owen et al.[6] lead to

$$k = 1.884, \qquad (25°C)$$

so that any artificial assumptions concerning deviations from the limiting law at low concentrations are unnecessary.

---

[2] O. Redlich, J. Phys. Chem. 44, 619 (1940).

[3] G. Falckenberg, Ann. Physik 61, 145 (1920).

[4] B. B. Owen and S. R. Brinkley, Jr., Ann. N. Y. Acad. Sci. 51, 753 (1949).

[5] S. Kyropoulos, Z. Physik 40, 507 (1926).

[6] B. B. Owen, R. C. Miller, C. E. Milner, and H. L. Cogan, J. Phys. Chem. 65, 2065 (1961).

7. RESEARCH IN PROGRESS: OTTO REDLICH

The Molecular State of Rare Earth Chlorides in Aqueous Solution
(with Diane D. Monahan)

There is a wide difference in our knowledge of the molecular states of uni-univalent strong electrolytes and of multivalent electrolytes. It is clear by now that such salts as sodium nitrate are completely dissociated and that the concentration of undissociated molecules in concentrated acids can be quantitatively determined.[1] Results from various authors on the sulfates of divalent metals appear to indicate incomplete dissociation, while salts with larger divalent ions such as sulfonates probably are completely dissociated. In some cases complexes are known for salts with tervalent ions.[2] Extensive measurements by Spedding and his co-workers, especially the peculiar results for molal volumes, can be explained by electrostatic interaction as well as by formation of intermediate or complex ions. A clarification would be of interest not only in the interpretation of the properties of rare earths but also for the better understanding of ionic interaction.

The primary and most promising method to be used for the present problem is the determination of extinction spectra. For neodymium chloride, Jorgensen indeed found variations in the extinction at about 4250 Å in concentrated solutions of hydrochloric acid.[3] He ascribes them to an intermediate ion $NdCl^{++}$. So far it can be concluded from concordant results at 5600 to 6000 Å, 4950 to 5400 Å, and at about 4250 Å that, in addition to Nd^{+++}, two absorbing species exist.

For the interpretation of the spectra, automatic computer programs have been developed which derive the concentrations of two or three absorbing species and extinction-peak data from measurements of the extinction of several solutions.

In addition to extinction, some other independent methods such as NMR measurements, Raman spectra, and potentiometric titration may be useful. At present, NMR measurements are carried out in cooperation with Dr. Charles H. Holm, Shell Development Company, Emeryville.

---

[1] O. Redlich and J. Bigeleisen, J. Am. Chem. Soc. 65, 1883 (1943);
G. C. Hood, O. Redlich, and C. A. Reilly, J. Chem. Phys. 22, 2067 (1954);
O. Redlich, Monatsh. Chem. 86, 329 (1955);
O. Redlich and G. C. Hood, Disc. Faraday Soc. 24, 87 (1957);
T. F. Young, L. F. Maranville, and M. B. Smith in of Structure of Electrolytic Solutions, edited by W. J. Hamer (John Wiley & Sons, Inc., New York, 1959) Chapt. 4;
G. C. Hood and C. A. Reilly, J. Chem. Phys. 32, 127 (1960).

[2] For example, fluorides of iron (R. E. Connick et al., J. Am. Chem. Soc. 78, 1827, 1956), $GaCl_4^-$, and $FeCl_4^-$ (K. Schug and L. I. Kalzin, J. Phys. Chem. 66, 6007, 1962).

[3] C. K. Jorgensen, Kgl. Danske Videnskab. Selskab Mat.-Fys. Medd. 30, No. 22 (1956); Absorption Spectra and Chemical Bonding in Complexes (Pergamon Press, Oxford, 1962), p. 268.

II. METALLURGY AND CERAMICS

A. SUBMICROSCOPIC STRUCTURE

1. DISLOCATION SUBSTRUCTURES, STACKING-FAULT ENERGIES, AND YIELD STRESSES OF α BRASSES*

Gareth Thomas

The effect of zinc concentration on the dislocation arrangements, stacking-fault energies, and yield stresses of deformed α brasses has been investigated by transmission electron microscopy. With increasing percentage of zinc the apparent stacking fault energy, γ, (the term "apparent" is used to indicate that γ has been estimated from the curvature of extended nodes,[1]) decreases up to 30% Zn, above which γ rises or falls depending upon heat treatment. This effect is shown in Fig. IIA. 1-1 together with previous measurements made by Howie and Swann.[1] Above 25% Zn the dislocations are observed to be paired. Most of these are of opposite sign, giving rise to piled-up groups of dipoles (see report IIA. 2). In slowly cooled specimens or in specimens quenched-aged at 200°C, some pairs may be of the same sign. At first it was thought that this phenomenon indicated the existence of long-range order (LRO), particularly as the calculated spacings between pairs (assuming LRO) were in good agreement with the observed spacings. Now, since the critical temperature is below 100°C,[2,3] quenched specimens and specimens aged above 100°C should be disordered. However, the existence of pairs of the same sign in material aged to 200°C suggests that they are due to short-range order (SRO) only [Fig. IIA. 2(e)]. Furthermore, LRO has never been observed in α brass by other workers.

The changes in dislocation arrangements with increasing zinc content are typical of materials that show decreases in γ with increasing percentage of solute.[4] These changes are illustrated in Fig. IIA. 1-2. It can be seen that the tendency to form dislocation cells and tangles decreases with increasing percentage of zinc. For $\gamma < 4$ ergs/cm^2, cells are not observed because dislocations tend to remain in their slip planes as piled-up groups. The dislocation density for the same strain was found to be independent of the concentration of the alloy. It was also found that the yield strengths of the alloys varied inversely with γ. Thus the strength of the alloys can be understood in terms of γ and the increased difficulty of cross-slip as γ decreases.

---

*Brief version of paer to be presented at the International Conference: "Relation between Structure and Properties," Melbourne, Australia, May 1963 (UCRL-10488, Oct. 1962). (For J. Australian Inst. Metals.)

[1] A. Howie and P. R. Swann, Phil. Mag. 6, 1215 (1961).

[2] L. M. Clarebrough, M. E. Hargreaves, and M. H. Loretto, Proc. Roy. Soc. (London) A257, 326 (1960); A261, 500 (1961).

[3] D. T. Keating, Acta Met. 2, 885 (1954).

[4] See, e.g., P. R. Swann, Electron Microscopy and Strength of Crystals, Eds. G. Thomas and J. Washburn (Interscience Publishers, Inc., New York, 1962), p. 131.

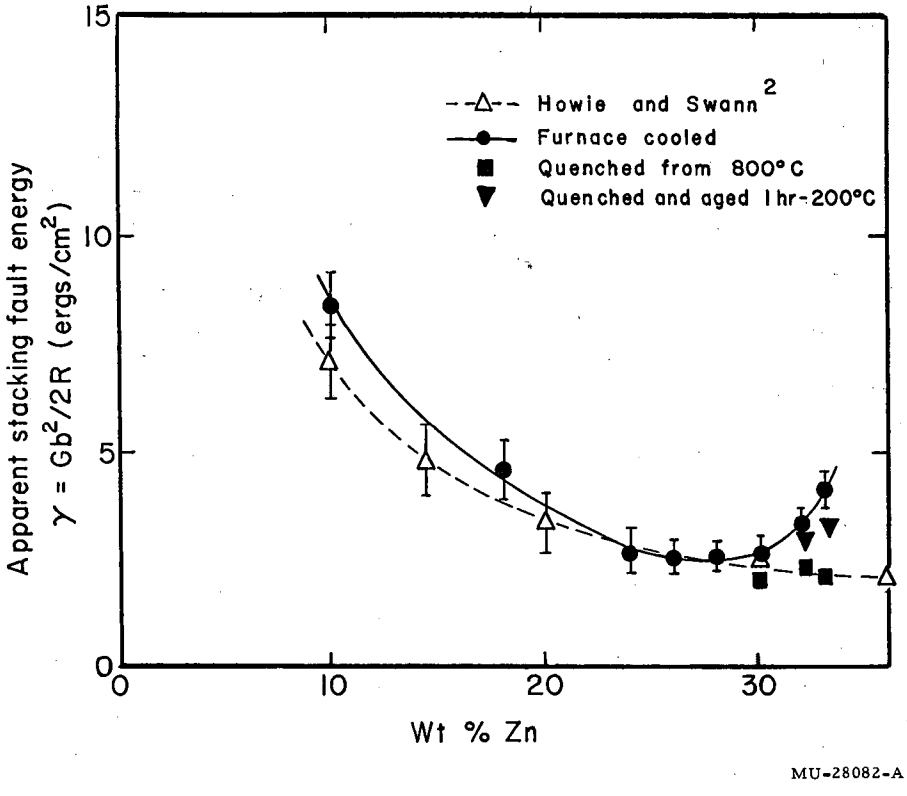

Fig. IIA. 1-1. The stacking-fault energies of α-phase Cu-Zn alloys, deformed 4% after various heat treatments.

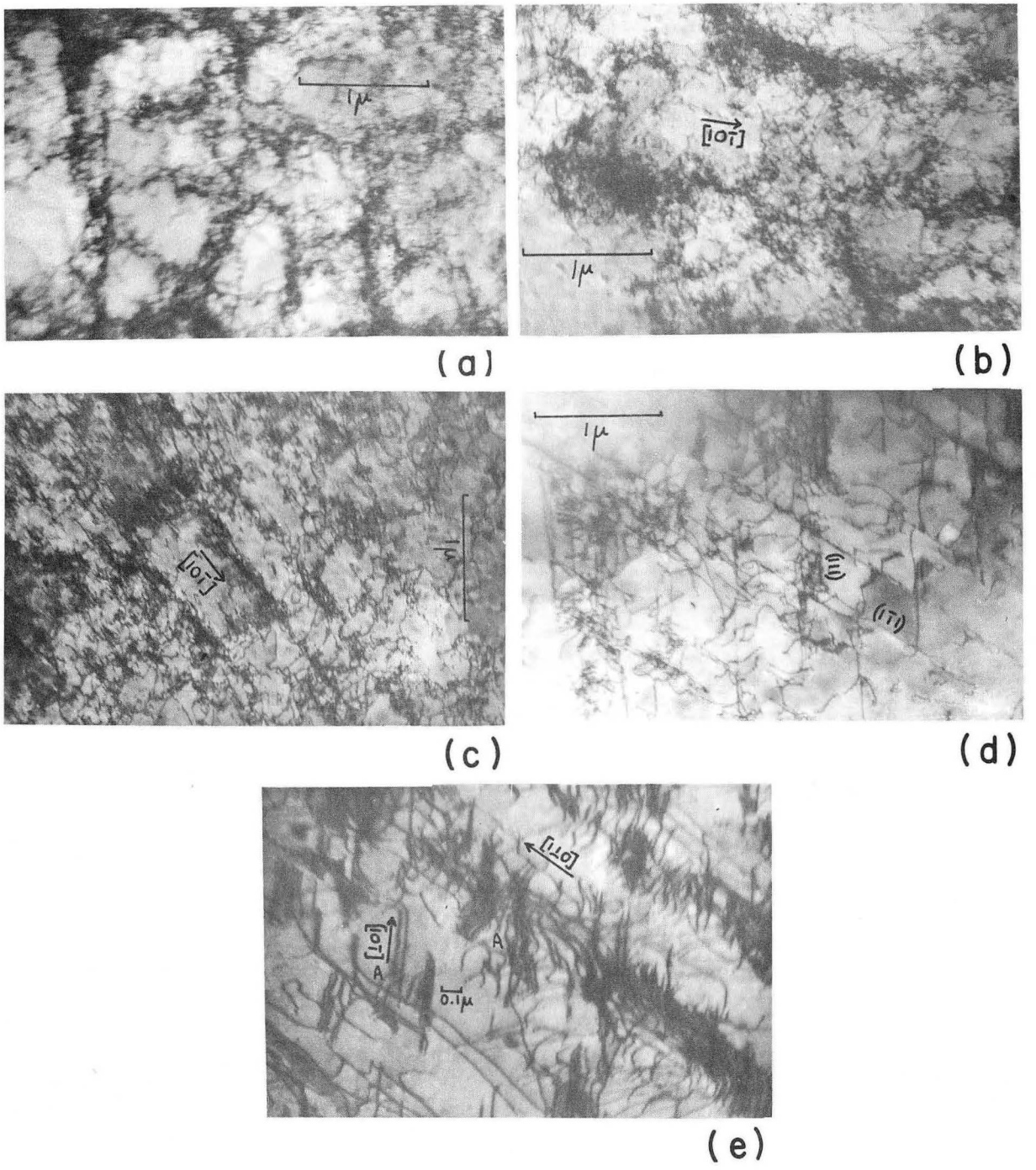

ZN-3550

Fig. IIA. 1-2. Effect of % Zn on dislocation arrangements in furnace-cooled α brasses. All alloys deformed 10% in tension at 273°K. (a) 4% Zn, (b) 8% Zn, (c) 16% Zn, (d) 24% Zn, and (e) 33.5% Zn. All micrographs in [101] orientation.

The strong temperature dependence of the yield strength can be understood as resulting from thermally activated processes such as that of overcoming SRO and of thermally activated cross-slip. Both these processes become more difficult with decreasing temperature, and as γ decreases--i.e., as the percentage of zinc in the alloy is increased.

I wish to acknowledge invaluable help with the experimental part of the project from Mr. Walter Bell and Mr. George Blank.

2. HETEROGENEOUS PRECIPITATION IN AUSTENITIC STEELS*

Gareth Thomas

Swann and Louat have recently made some very important observations regarding contrast effects in copper alloys of relatively low stacking-fault energies.[1] These workers showed that in many cases fringe contrast, similar to that for stacking faults and Moiré images, actually arises from groups of dislocation dipoles, so that previous interpretations of stacking-fault and Moiré contrast effects may be incorrect.[2,3] For example, the so-called Moiré fringes do not necessarily indicate segregation of solute atoms at faults. Our work on stainless steels has shown that the phenomenon discussed by Swan and Louat is not confined to copper alloys, and this discussion is presented to demonstrate that precipitation in stainless steels may not occur at stacking faults.[3]

We have examined a range of austenitic stainless steels (e.g., 18/8 and 20/10 to 20/40 Fe/Cr/Ni alloys) and have observed that increasing the nickel content increases the apparent stacking-fault energy (as determined from nodes), but in all cases dislocations tend to remain in their slip planes. Upon plastic deformation of annealed alloys many dislocation dipoles are observed. These are produced when edge (or nearly edge) dislocations of opposite sign on nearby parallel slip planes try to pass each other. Consequently, piled-up groups of dipoles may be formed; an example is shown in Fig. IIA. 2-1. That dislocations are of opposite sign can be deduced from the appearance of fringes at opposite sides of the dislocations,[4] e.g., at A, B. Because of the extinction phenomenon,[5] contrast effects similar to (but not) Moiré fringes can be observed in Fig. IIA. 2-1. In certain orientations the dipoles also give rise to pseudo-stacking-fault fringe contrast which is also due to extinction effects along the lengths of the inclined dipoles. Figure IIA. 2-2 shows an example for a case in which the foil is tilted so as to reveal dipoles A, pseudo-fault contrast B, and pseudo-Moiré contrast C.

---

*Written discussion to N. P. L. International Conference, January 1963 (Teddington, England).

[1] P. R. Swann and N. Louat, J. Inst. Metals, in press.

[2] P. R. Swann and J. Nutting, J. Inst. Metals, 50, 133 (1961-62).

[3] J. S. T. Van Aswegan and R. W. K. Honeycombe, Acta Met. 10(3), 262 (1962).

[4] A. Howie and M. J. Whelan, Proc. Roy. Soc. (London) A267, 206 (1962).

[5] P. B. Hirsch, A. Howie, and M. J. Whelan, Phil. Trans. Roy. Soc. (London) A252, 499 (1960).

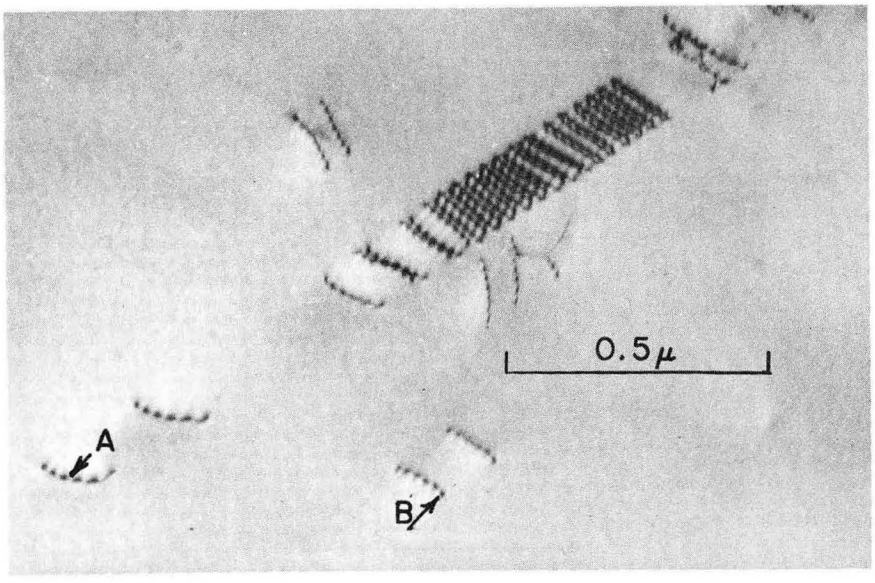

ZN-3644

Fig. IIA. 2-1. Fe-18% Cr-36% Ni-0.04% C alloy annealed 1/2 hour at 1100°C, deformed 10%, showing formation of piled-up dipoles from (nearly edge) dislocations of opposite sign on nearby parallel slip planes. The dislocations are of opposite sign, since fringes appear on opposite sides of dislocations on parallel planes (Ref. 5), e. g., at A and B. Notice pseudo-Moiré fringes in the piled-up group. Orientation [110].

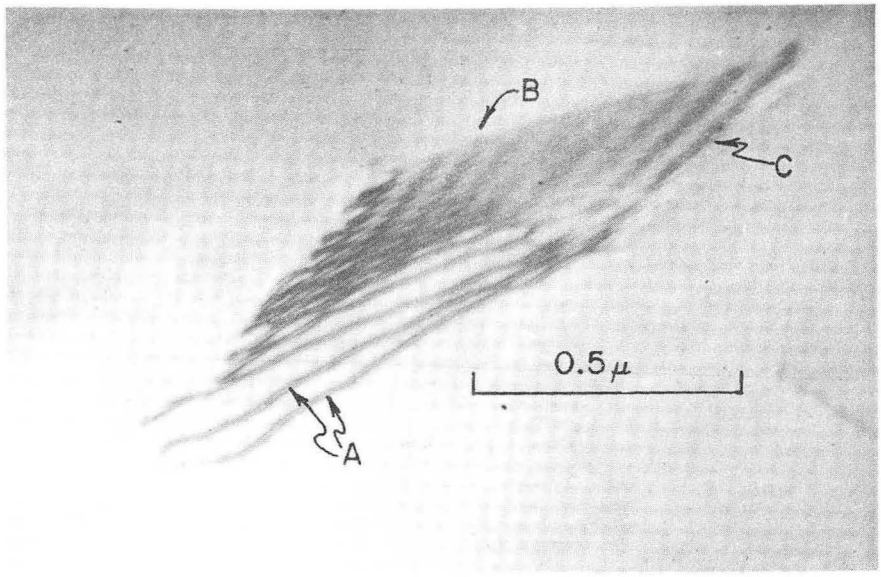

ZN-3645

Fig. IIA. 2-2. Similar region in [211] orientation with a group of dipoles A tilted so as to show pseudo-stacking-fault fringes B and pseudo-Moiré fringes C.

These effects are exactly like those described for copper alloys.[1] All these results show that unless careful tilting experiments are done during electron microscopy, the appearance of such fringe contrast effects does not necessarily imply the existence of stacking faults or segregation of solute atoms at faults (Moiré fringes). Furthermore, upon aging of the austenitic steels, precipitation occurs preferentially on the dipoles and at piled-up groups (Fig. IIA. 2-3). We have never observed precipitation on stacking faults. Also, dipoles are even more favorable nucleation sites than single edge dislocations (Fig. IIA. 2-3).

I am grateful to Dr. Swann and Dr. Louat for providing me with their results prior to publication.

3. STACKING-FAULT ENERGIES ORDERING AND TRANSGRANULAR STRESS-CORROSION CRACKING IN AUSTENITIC ALLOYS*

Walter R. Roser and Gareth Thomas

It has been found that stainless steels, in general, fail in a transgranular manner when subjected to stress-corroding conditions.[1] It is the purpose of this investigation to determine the mechanism responsible for this phenomenon.

Robertson and Tetelman have shown that the tendency to transgranular failure increases in alloys with lower stacking-fault energies (SFE).[2] Their theory postulates that in alloys having low stacking-fault energy, dislocations are widely dissociated and therefore form pile-ups because cross-slip cannot take place. The pile-ups thus formed provide sites for preferred chemical attack because of the locally high strain energy present. Besides the strain energy factor, there is reason to believe that impurity segregation to faults is also important. For example, Swann and Nutting have published electron micrographs of copper alloys wherein stacking faults have not dissolved with the matrix,[3] suggesting that segregation to stacking faults occurs. However, there is little other support for this suggestion.

---

*Condensed form of paper presented at Second International Congress on Corrosion, New York, March 11-15, 1963.

[1] J. J. Harwood, "The Phenomena and Mechanism of Stress Corrosion Cracking," in Stress Corrosion Cracking and Embrittlement Symposium, Boston, 1954 (John Wiley & Sons, New York, 1956), p. 1.

[2] W. D. Robertson and A. S. Tetelman, "A Unified Structural Mechanism for Intergranular and Transgranular Corrosion Cracking," in Strengthening Mechanisms in Solids (American Society for Metals, 1962), p. 217.

[3] P. R. Swann and J. Nutting, J. Inst. Metals 88, 478 (1960).

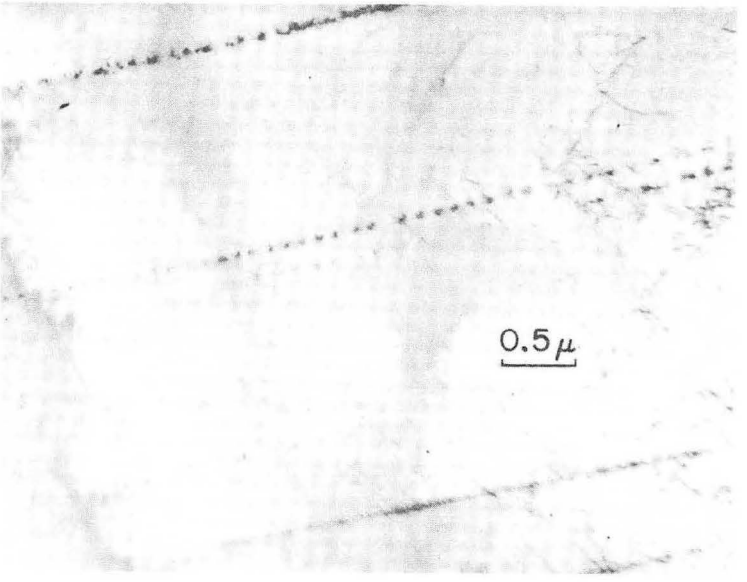

ZN-3646

Fig. IIA. 2-3. As in Fig. IIA. 2-2, after aging 24 hours at 190°C, showing precipitation of carbide particles on dislocations. Foil tilted to show strong precipitate, but weak dislocation, contrast. Orientation [110].

In this investigation, the SFE is being determined directly from the radii of curvature of extended dislocation nodes for Fe-Ni-Cr alloys of various compositions.

Specimens are prepared by straining to 5 to 10% plastic deformation, aging the strained samples at 500°C for 1 to 2 hours, and then electropolishing to obtain a thin foil for transmission investigation.

The relationship of SFE to radius of curvature of extended nodes is given by[4]

$$\gamma_{SF} = \frac{Gb^2}{2\pi KR} \ln \frac{R}{b} ,$$

where

γ_{SF} = stacking-fault energy,

G = shear modulus,

b = Burger's vector of partial dislocation,

R = radius of curvature,

K = constant $\approx 5/6$.

Figure IIA. 3-1 is a typical example of extended nodes found in 304 stainless steel. Uhlig and White have shown that nickel increases the resistance to corrosion cracking whereas nitrogen seriously impairs the corrosion resistance.[5]

Results from the determinations of stacking-fault energy indicate that the SFE does in fact increase with increasing nickel content. The value for the SFE for 304 stainless steel (9.4% Ni) was determined to be 16 ergs/cm^2, while the SFE for the Fe–20 Cr–40 Ni alloy was estimated to be 60 ergs/cm^2. It should be noted that the latter value is probably somewhat low, since the only nodes were found in networks and therefore were subjected to other dislocation stress fields. Since the above formula for SFE neglects the repulsive interactions between the other partial dislocations in the node, very small nodes will give a low estimate of the stacking-fault energy. In the other compositions examined, the SFE is sufficiently high that no measurable nodes were found.

---

[4] P. R. Swann and A. Howie, Phil. Mag. 6, 1215 (1961).

[5] H. H. Uhlig and R. A. White, "Some Metallurgical Factors Affecting Stress Corrosion Cracking of Austenitic Stainless Steels," Trans. Am. Soc. Metals 52, 830 (1960).

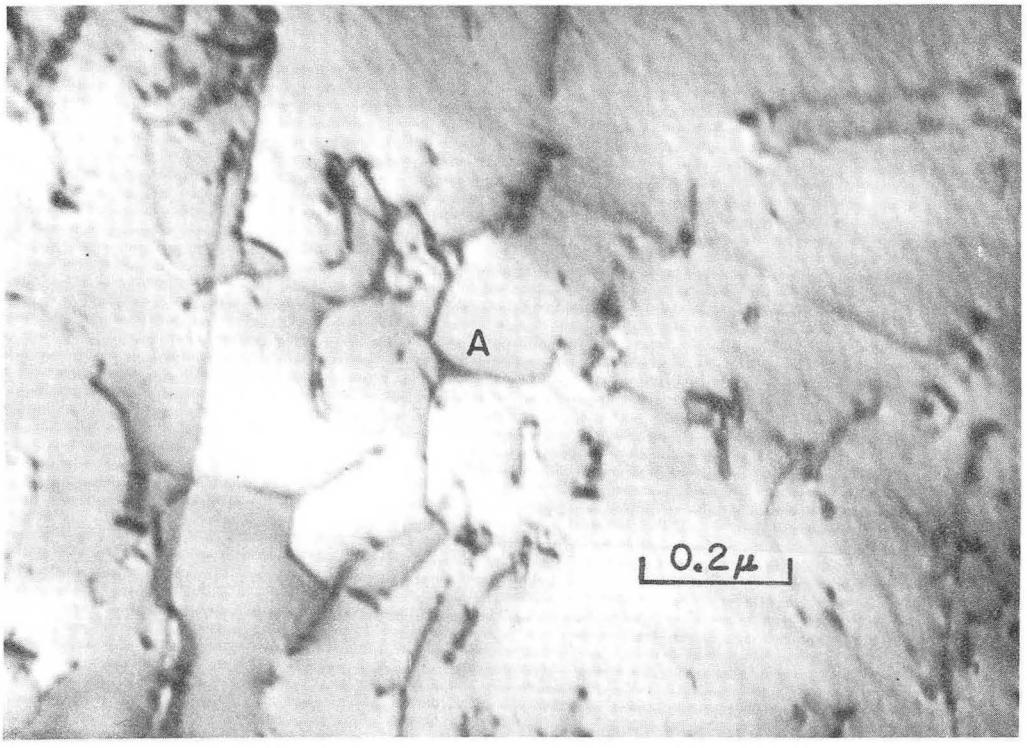

ZN-3647

Fig. IIA. 3-1. Extended node (A) in 304 stainless steel.

Nitrogen has apparently very little effect on the stacking-fault energy. Two Fe-20 Cr-40 Ni alloys containing 60 ppm and 200 ppm did not exhibit any measurable nodes (i.e., the SFE was very high). Chromium, niobium, and titanium, however, all lower the SFE in austenitic alloys.

The results have shown that transgranular susceptibility is always found in alloys where dislocations are arranged in coplanar groups. Coplanar arrays are usually due to the low SFE effect, except in high-nickel nitrogen-containing alloys. Figure IIA. 3-2 is an example of coplanar arrays in Fe-20 Cr-40 Ni-0.05N deformed 10%, but the SFE in this alloy is large. By analogy with the results reported for brass (see Paper IIA. 1), it is suggested that short-range order is responsible for coplanar arrays in alloys of high SFE. Nichrome V has a low SFE ($\approx$ 16 ergs/cm^2), but this alloy is not susceptible. Hence, a low SFE alone cannot be responsible for transgranular stress corrosion cracking. In pure metals and alloys where easy cross-slip and dislocation tangling occur, no transgranular susceptibility is found.

It is proposed that destruction of strong short-range order by plastic deformation is responsible for localized chemical attack when dislocation movement is restricted to the original slip plane. As dislocations cut through the ordered regions, localized galvanic action is made possible, since the number of unlike bonds is reduced. A crack once opened is then restricted to the slip plane. However, if cross-slip occurs, the tendency for preferential chemical or electrochemical attack is reduced.

4. THE STRUCTURE AND PROPERTIES OF SHOCK-LOADED NICKEL

Richard L. Nolder and Gareth Thomas

Under the conditions of plane-wave explosive detonation, a shock-loaded metal specimen attains a high degree of hardening without much macroscopic deformation or grain distortion.[1] Because of the growing commercial use of explosive forming and shock hardening, it is of interest to understand what is the structure of shock-hardened metal and how it differs from that resulting from other methods of hardening, such as low-strain-rate compressive or tensile testing.

In this work, thin foils were prepared from the deformed samples (0.25-in.-thick, 1-in. radium discs) by means of spark erosion cutting followed by electropolishing. Examination of annealed specimens prepared in the same way showed that the damage done to the specimens by the spark erosion cutting was negligible and therefore had little or no effect on the dislocation substructures induced by explosive, compressive, or tensile deformation.

[1] P. G. Shewman and V. F. Zackay, Eds., Response of Metals to High-Velocity Deformation (Interscience Publishers, Inc., New York-London, 1961).

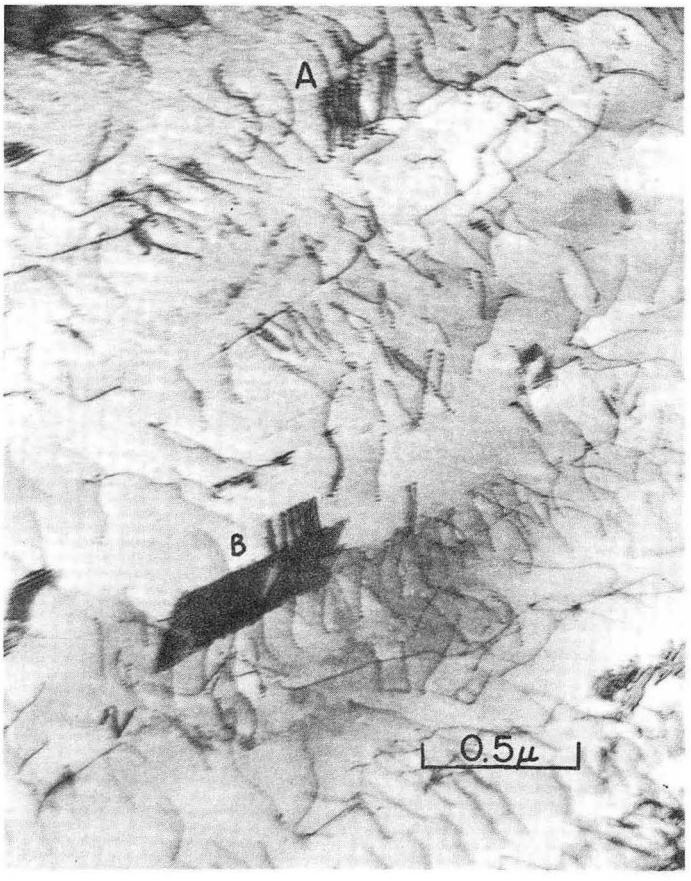

ZN-3649

Fig. IIA. 3-2. Coplanar dislocation arrays in Fe–20 Cr–40 Ni–0.05 N.

It has been found that up to pressures of 250 kilobars the dislocation substructures are similar to those observed after compressive loading in that there are dense dislocation tangles and cell boundaries.

A typical cell structure is illustrated in Fig. IIA. 4-1. The diameters of these cells decrease with increasing applied pressures. In alloy systems deformed by a constant amount, such a trend in cell diameters is also observed as the stacking-fault energy decreases with increasing proportion of solute. For deformation >300 kilobars cell walls are not observed. Instead, packets of narrow twins or slip traces are formed, with a high density of dislocation tangles forming a "background." A typical micrograph of such a structure is shown in Fig. IIA. 4-2. Observation of twinnings is especially interesting, since no mechanical twinning has previously[2] been reported in nickel. In fact, it is commonly believed not to occur.

The structures of specimens compressed at low strain rates have also been studied. The hardness of these specimens was equivalent to that of shock-loaded specimens loaded to less than 300 kilobars. Only cell structures were found in these specimens. Cell diameters were essentially the same for all applied stresses.

An anomaly found in the hardness of shock-loaded specimens is illustrated in Fig. IIA. 4-3. Between 250 and 350 kilobars there is a sudden increase in the hardening rate with increasing pressure. This increase is no doubt associated with the formation of microtwinning above 250-kilobar pressure.

The structure of shock-loaded specimens is currently being compared with that of statically loaded specimens deformed at low temperatures. It has been reported by Haasen that nickel deformed at 20°K and below may contain mechanically twinned structures;[3] however, this evidence is not very convincing. If such a structure exists a comparison with the twinning in shock-loaded nickel should prove interesting.

It is proposed to present a final report of this work at the International Conference on Mechanical Twinning in Florida, March 1963.

---

[2] G. E. Dieter, "Metallurgical Effects of High-Intensity Shock Waves in Metals," in R. G. Shewman and V. F. Zackay, Eds., Response of Metals to High-Velocity Deformation (Interscience Publishers, Inc., New York-London, 1961), p. 409.

[3] P. Haasen, Plastic Deformation of Nickel Single Crystals at Low Temperature, Phil. Mag. 3, 384 (1958).

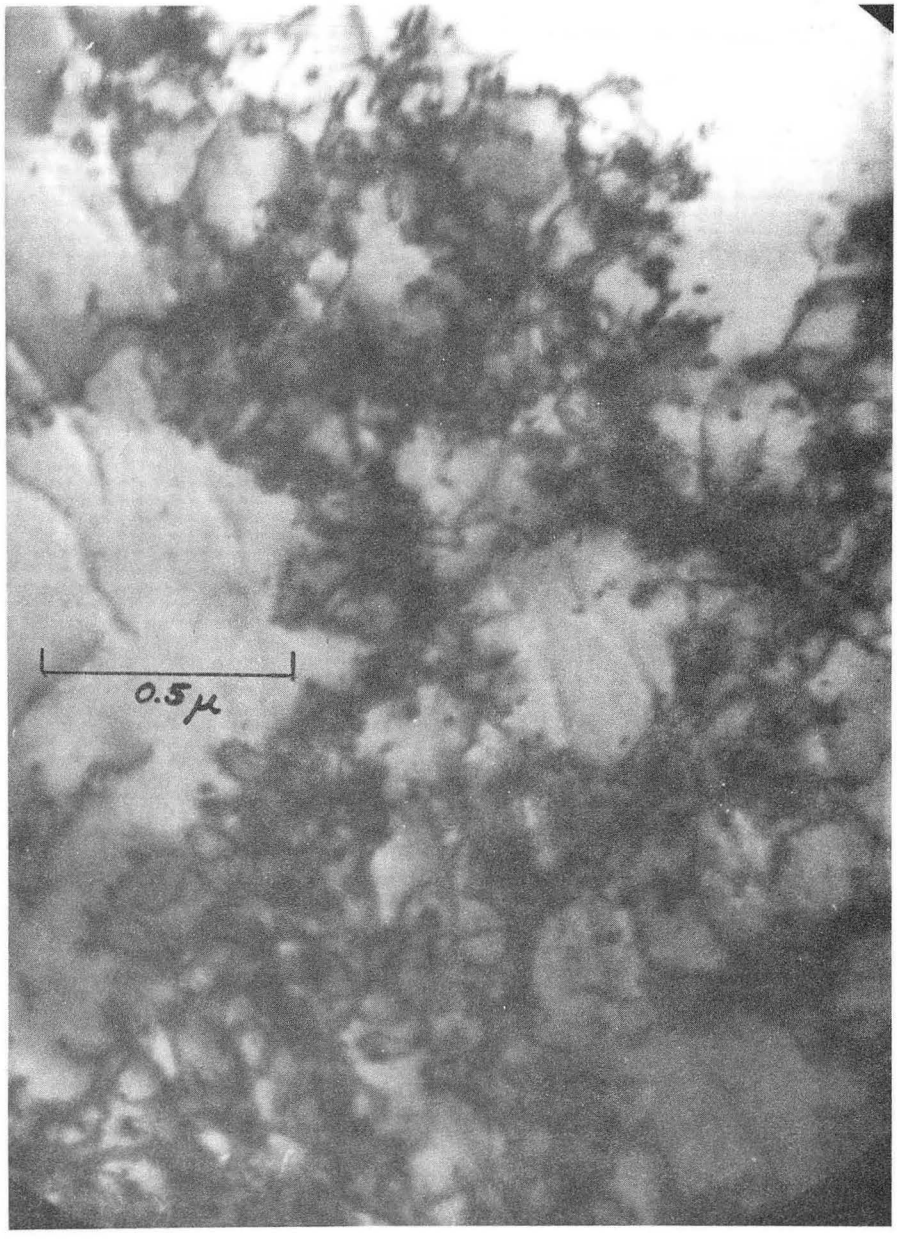

ZN-3650

Fig. IIA. 4-1. 70-kilobar shock-loaded specimen typifying cell structure.

ZN-3648

Fig. IIA. 4-2. 350-kilobar shock-loaded specimen containing microtwinning along two sets of {111} type planes.

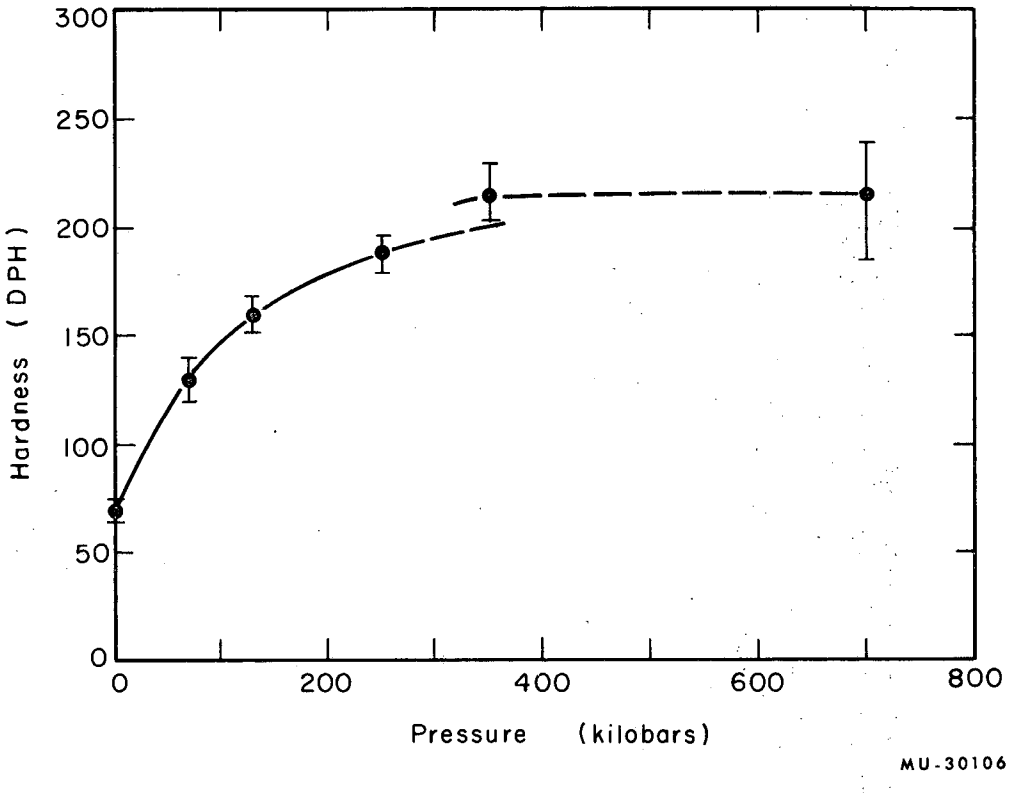

Fig. IIA.4-3. Hardness as a function of pressure for shock-loaded specimens.

5. THE MAGNESIUM-VACANCY BINDING ENERGY IN Al-5 wt % Mg ALLOY

Alf Eikum and Gareth Thomas

Helical dislocations and columns of prismatic loops are found in Al-5 wt % Mg alloy which has been quenched from near the melting temperature and aged at 20°C.[1] Additional annealing at 180°C or higher results in growth of both the helices and loops. The growth in thin foils was observed by using high-temperature electron microscopy, and found to be similar to that which occurs during bulk annealing. An example of loop growth observed in thin foils is shown in Fig. IIA. 5-1.

The magnesium-vacancy binding energy estimated from thin-foil kinetic data is in reasonable agreement with that estimated from bulk annealing experiments. The results have been published,[2] and are summarized as follows:

a. From bulk annealing experiments, E_B(Mg-vac.) = 0.1eV (lower limit).

b. From thin-foil annealing experiments, E_B(Mg-vac.) = 0.17 eV (Fig. IIA. 5-2).

c. The uncounted vacancies after aging at only 20°C are thought to exist as complex magnesium-vacancy clusters.

d. Helices appear to degenerate into columns of prismatic loops without interaction with a second dislocation.

e. Helices and loops were not observed to be preferential sites for precipitation during the aging treatments used.

The bulk-annealing and high-temperature electron-microscopy experiments are continuing with aluminum alloys containing 1, 3, 7, and 10 wt % magnesium.

---

[1] Alf Eikum and Gareth Thomas in Inorganic Materials Research Division Annual Report, 1961, UCRL-10119, March 1962, p. 96.

[2] A. Eikum and G. Thomas, International Conference Proceedings on Crystal Lattice Defects, Kyoto, Japan, 1962, UCRL-10441.

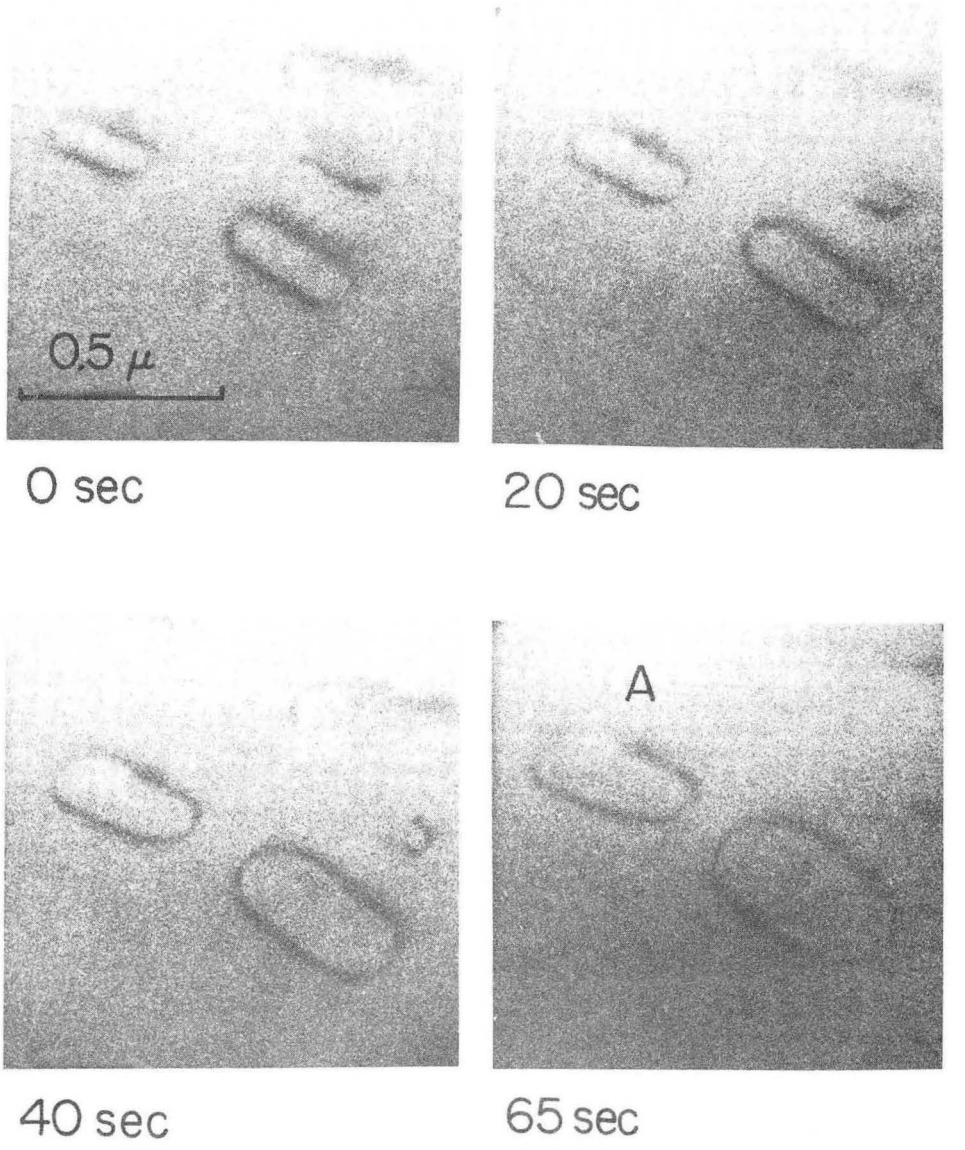

Fig. IIA. 5-1. Heating stage time sequence, showing loops growing in a thin foil at 365°C.

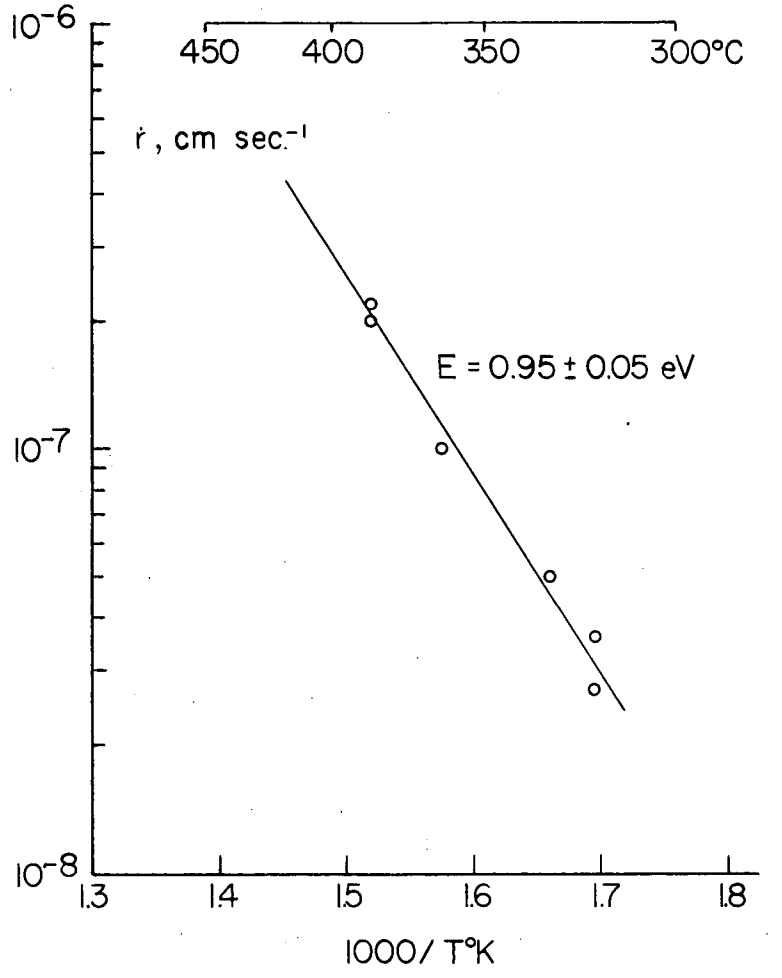

Fig. IIA. 5-2. Rate of increase in loop radius vs reciprocal of the absolute temperature.

6. YIELDING AND PLASTIC FLOW IN NIOBIUM*

Lenon I. Van Torne and Gareth Thomas

The results of this investigation have been reported in detail in a paper submitted to Acta Metallurgica. Our summary and conclusions of the research are as follows.

1. The lower yield stress of impure polycrystalline Nb can be expressed by

$$\tau_{ly} = \tau_f + \tau_{struc} + \tau(\dot{\epsilon})$$

(as plotted in Fig. IIA. 6-1),

where τ_f = friction stress = $(\tau_o + \tau_{soln})$,

τ_o = 0.8 $(\frac{kg}{mm^2})$ (lattice friction stress),

$\tau_{soln} = 0.279 \times 10^3 \times$ (Atom Fraction of Impurities) (that is, friction stress due to impurities atomistically in solution),

τ_{struc} = stress due to (i) dilatations in the crystal from solute atom clusters and precipitates and (ii) dislocation-cluster interactions.

$\tau(\dot{\epsilon})$ = strain-rate dependence of the yield strength.

It is concluded that τ_o is the only thermal contribution to τ_{ly}; thus τ_o may be associated with the Peierls-Nabarro stress. Impurities do not contribute to the temperature dependence of τ_{ly}.

2. The results show that the concept of dislocation unlocking is not necessary to explain the yield drop. Direct evidence has been given to show that the yield drop is accompanied by a large and rapid increase in dislocation density by multiplication. Precipitated impurities are important in increasing the density, probably through cross-slip. Cross-slip is observed to be an easy process in Nb.

3. The strongest barriers to dislocation movement for the purities investigated appear to be solute atom clusters.

4. The relation between flow stress and plastic strain, determined from dislocation-density measurements, correlates with the experimentally observed flow stress–plastic strain relation.

---

*Condensation of paper (UCRL-10515, Nov. 1962) submitted to Acta Met.

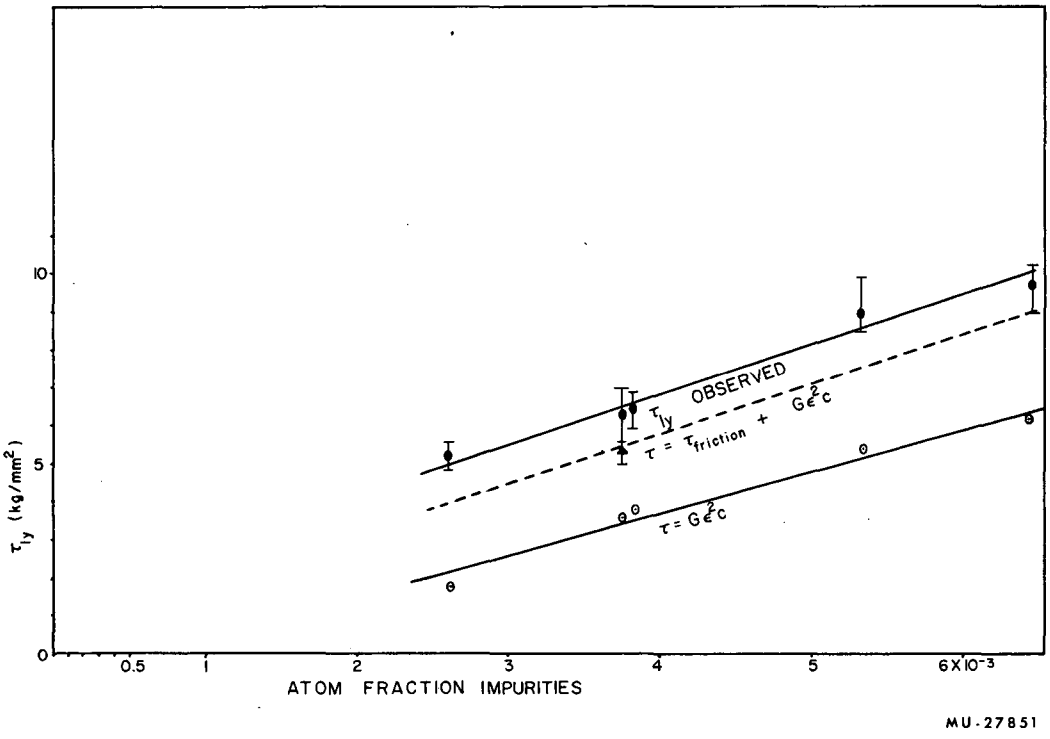

Fig. IIA. 6-1. Effect of impurities on the lower yield stress of Nb. Here τ_f is calculated from dislocation curvatures and τ_f from dilational strain fields of impurity atoms.

5. The flow stress of polycrystalline Nb is markedly influenced by the initial dislocation substructure. The presence of precipitate networks gives rise to cell formation upon plastic deformation (Fig. IIA. 6-2a, b), producing a flow stress-dislocation density dependence of

$$\sigma_f = 0.85\ Gb\sqrt{\rho}\ + \text{constant}, \qquad \text{expressed in kg/cm}^2.$$

The flow stress–dislocation density dependence in fully annealed polycrystalline Nb where cells are not observed (Fig. IIA. 6-2c) is given by

$$\sigma_f = 6.5\times 10^3\ Gb\sqrt{\rho}\ + \text{constant}, \qquad \text{expressed in kg/cm}^2.$$

Thus, the tendency for cell-structure formation depends strongly on the dispersion of impurities. Neither stacking faults nor dislocation pile-ups were observed in this work.

6. The grain size dependence of σ_y and σ_f has been shown to be significant through the dislocation density.

7. From these conclusions, it is possible to predict the lower yield point and flow stress for polycrystalline Nb when the impurity level and annealing conditions are known.

7. RESEARCH IN PROGRESS: GARETH THOMAS

a. Improvements in Thinning Techniques

An ion-bombardment apparatus has been constructed for thinning materials not amenable to chemical or electrolytic techniques (e. g., Al_2O_3). The principle of the method is simply to knock atoms off the surface of the specimen by using ionized air particles. The difficulties are in obtaining the right voltage and leak-rate conditions. The apparatus may also be used for cleaning specimens contaminated by oxidation or by exposure to the electron beam. Attempts to thin nonmetallic crystals are now in progress. We are also giving more attention to chemical polishing methods for thinning single-phase materials. (With William R. Goggin)

b. Grain-Size Effects in Copper

We are investigating the effects of grain size and strain rates on the yield stress and work-hardening rates of pure copper specimens deformed at various temperatures. So far most of the time has been spent in growing single crystals and polycrystals differing in grain sizes by a factor of ten. Part of the deformation program is completed. Structural investigations are in progress. (With Om Johari)

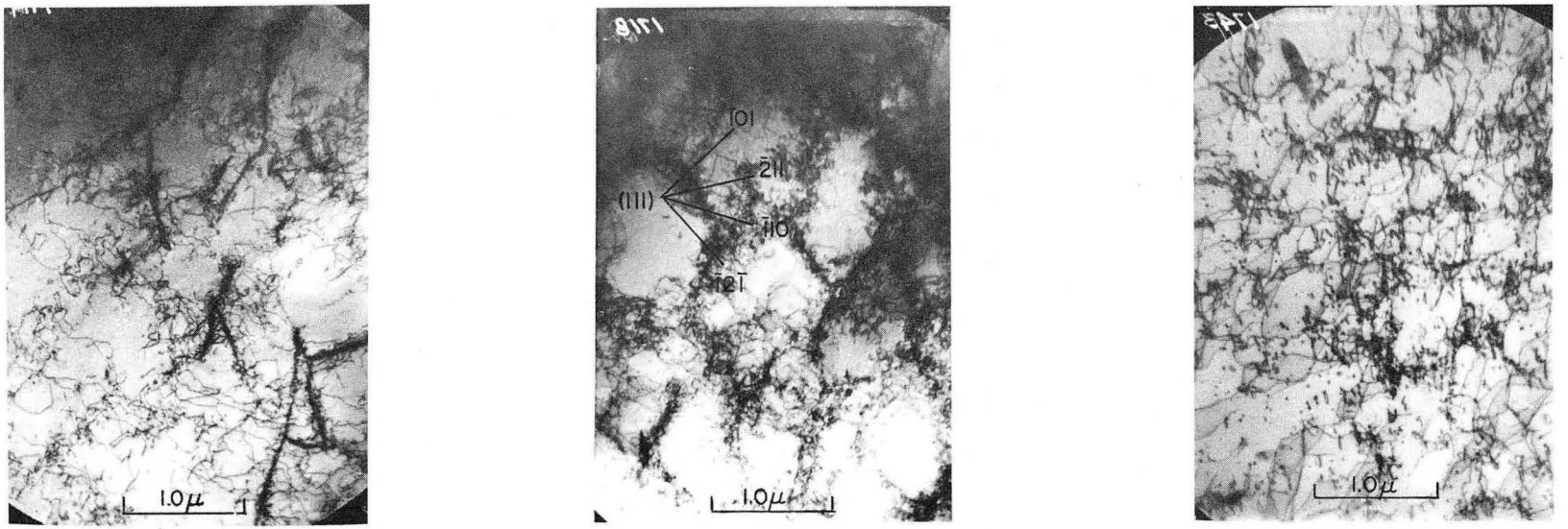

(a) (b) (c)

ZN-3232

Fig. IIA. 6-2. Dislocation substructures in Nb deformed 10% in tension at room temperature.
(a, b) Tangles developed in Nb initially containing precipitates on dislocations.
(c) Absence of tangles in Nb not containing precipitates.

c. Superconductivity

A program has been initiated to study in detail effects of cold work and precipitation upon the superconducting properties of BCC materials and other compounds. Preliminary investigations on Nb seem to be the most promising. Electron microscopy of Nb-Zr alloys has shown they are structurally very complicated. (Group effort)

d. High-Strength Refractory Alloys

A program has been initiated to investigate structure-property relationships in BCC alloy solid solutions and possible dispersion strengthening in BCC alloy systems. Some unusual transformations have been observed in impure Nb (e. g., Fig. IIA. 7-1) during examination in the electron microscope. At present the phenomenon is not well understood, and work on this is proceeding. (With Lenon I. Van Torne)

e. Structure and Properties of Semiconductors

The work on silicon[1] is being extended to investigate effects of impurities on the structure of epitaxial silicon crystals. (With Jack Washburn, in collaboration with Shockley Transistor Company)

f. Vacancy Effects in Alloys

The dislocation loop density observed in copper after quenching and aging at a temperature at which vacancies are mobile is low. Also, the loops found in copper are often associated with dislocation tangles, which might indicate that loops are due to deformation and not vacancy supersaturation per se. The difficulty in forming "quench" loops appears to be general for low-stacking-fault fcc metals.

The prismatic loops found in quenched and aged metals may be grouped according to four major sources:

(a) "Homogeneous" nucleation of loops from vacancy clusters.

(b) Degeneration of helices into loops.

(c) Combination of plus-minus pairs (dislocation dipoles) to form loops.

(d) Punching out of prismatic loops at an impurity particle.

Preliminary experiments on copper-base alloys containing 1/2 and 2 at. % silver have given varied results. Columns of loops, random loops, loops associated with dislocation tangles, and defects showing stacking-fault contrast have been observed. These various arrays indicate that each of the above sources could be operating. The experiments are continuing, with

[1] R. H. Finch, H. J. Queisser, J. Washburn, and G. Thomas, Structure and Origin of Stacking Faults in Epitaxial Silicon, J. Appl. Phys. 34, 406 (1963).

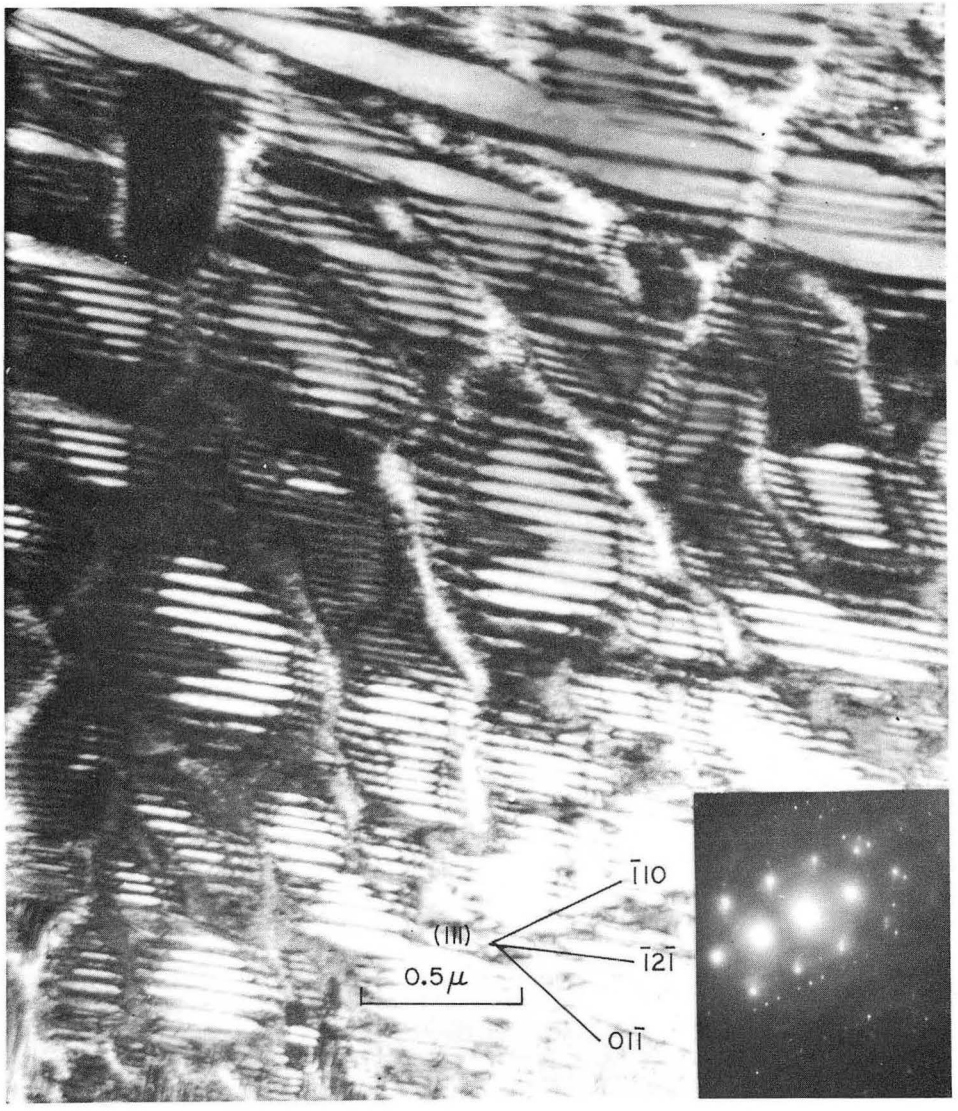

ZN-3642

Fig. IIA. 7-1. Bright-field image and corresponding diffraction pattern of a transformed Nb Foil (~ 2000 Å). Note separation of transformed regions, which implies nucleation of the transformation at several points.

emphasis on more strict control of quenching rate and impurity pick-up.

Copper-base alloys have been chosen to supplement resistivity studies being carried out at other laboratories. (With Alf Eikum and W. Bell)

8. PUBLICATIONS: GARETH THOMAS

Work completed since preliminary report in Annual Report 1961.

J. A. Hren and G. Thomas, Heterogeneous Precipitation in Al-20% Ag Alloy, Proc. 5th International Conference of Electron Microscopy 1962,

J. A. Hren and G. Thomas, Direct Observation of Precipitation in Thin Foils of Al-20% Ag Alloy (UCRL-10198, May 1962), Trans. AIME (in press).

G. Thomas and J. Washburn, Structure and Origin of Growth Faults in Epitaxial Silicon, in Proceedings of AIME Conference on Semiconductors (Interscience Publishers, Inc., New York, in press); also with R. H. Finch and H. J. Queisser, Structure and Origin of Stacking Faults in Epitaxial Silicon, J. Appl. Phys. 34, 406 (1963).

R. Benson, G. Thomas, and J. Washburn, Dislocation Substructures in Deformed and Recovered Molybdenum, in Direct Observations of Imperfections in Crystals (Interscience Publishers, Inc., New York, 1962), p. 375.

Books

1. G. Thomas, Transmission Electron Microscopy of Crystals (John Wiley & Sons, Inc., New York, 1962).
2. G. Thomas and J. Washburn, Editors, Electron Microscopy and Strength of Crystals (Interscience Publishers, Inc., New York, 1962).

9. EFFECT OF VACANCY CLUSTERS ON YIELDING AND STRAIN HARDENING OF COPPER*

James Galligan† and Jack Washburn

Small voids or clusters of vacant lattice sites can be formed by irradiation, by quenching, or by plastic deformation. Very large clusters of vacancies containing 10^4 or more elementary point defects have been shown by transmission electron microscopy to exist as dislocation loops or tetrahedra.

*Abstract of paper, based on Galligan's thesis, being prepared for publication.

†Now at Columbia University, New York.

In quenched copper or aluminum the density of dislocations in the form of small loops a few hundred angstroms in diameter can be as high as 10^{10} cm per cm^3. These loops can account for the experimentally observed hardening. However, a dislocation substructure consisting of small, closed loops is unstable and is swept away by moving dislocations when several slip systems are active.

Rather less is known about the effects due to smaller clusters of vacancies containing ten to a few thousand elementary point defects. In the present experiments electrical resistivity, small-angle x-ray scattering, and stress-strain measurements on quenched pure copper single crystals were employed to study effects due to clusters of vacancies too small to be easily detected by transmission electron microscopy.

This work has led to the following conclusions:

1. Resistivity and small-angle scattering measurements made immediately after quenching revealed that very little clustering took place during the quench. The largest clusters present were probably not over 10 Å in diameter.

2. Decrease in excess resistivity due to quenching and increase of the radius of gyration of the clusters as measured by small-angle x-ray scattering occurred concurrently, and were substantially completed within 2 hours aging time at 20°C.

3. At 20°C, aging for 2 years did not produce clusters or dislocation loops large enough to be studied by transmission electron microscopy.

4. Isolated excess vacancies had no effect on the stress-strain curve. The yield stress and the strain-hardening behavior of as-quenched crystals were the same as those for annealed, slowly cooled crystals when tested at -196°C.

5. Aging at 20°C resulted in an increase in yield stress for crystals of both single-slip and multiple-slip orientations. The greatest changes in yield stress occurred within the first 2 hours of aging, as did the changes in electrical resistivity and x-ray small-angle scattering.

6. The effect of small vacancy clusters on strain-hardening rate depends on the initial orientation of the tensile axis. For single-slip orientations, the strain-hardening rate is increased; no clear easy glide region exists. For the $\langle 111 \rangle$ multiple-slip orientation, no change in work-hardening rate occurs for aging times less than about 10 hours. For longer times, the strain-hardening rate is reduced and the strain preceding fracture is greatly increased relative to annealed crystals.

10. INTERACTION BETWEEN PRISMATIC AND GLISSILE DISLOCATIONS*

V. Georges Saada† and Jack Washburn

A detailed theoretical analysis was made of the interactions between moving dislocations and prismatic dislocation loops in the face-centered cubic structure. Both perfect loops and Frank loops containing a stacking fault were considered.

For perfect loops there are four different kinds of contact interaction depending on the relationship between the Burgers vectors of the loop and the moving dislocation. The intersection of a loop by a moving dislocation can (a) leave the loop essentially unchanged, (b) leave the loop reduced in size while the moving dislocation acquires large jogs, (c) cause rotation of the loop on its glide cylinder toward the plane at right angles to the Burgers vector, (d) result in the formation of two nodes and a segment of dislocation having a Burgers vector equal to the sum of the two original Burgers vectors, (e) cause a change in the Burgers vector of the entire loop.

If the loop originally contains a stacking fault, contact with a moving dislocation can (a) cause the stacking fault to be swept away and the loop to be converted to a perfect loop, or (b) reduce the size of the Frank loop and produce large jogs on the moving dislocation line.

One of the results of this investigation that is of particular interest to the theories of strain hardening, quench hardening, and radiation hardening is that prismatic loops, possibly too small to be easily detected by transmission electron microscopy, may still be important barriers to the motion of dislocations. The results also show how moving dislocations can sweep away the kind of loop substructure that is formed by quenching and aging aluminum.

*Abstract of paper to be published in Proceedings of the Tokyo Symposium on Mechanical Aspects of Lattice Defects, 1962 (Physical Society of Japan, Tokyo).

†Visiting Physicist from Institut de Récherches de la Siderurgie), Paris, France.

11. DISLOCATION MULTIPLICATION*

Jack Washburn

A theoretical study was made of the problem of dislocation multiplication during the plastic deformation of a crystal. New insight into fundamental reasons for differences in plastic properties from one class of materials to another will probably be gained by focusing attention on nucleation and growth of individual slip bands rather than by studying the relationships between average values of strain rate, stress, strain, and work-hardening rate.

*Abstract of paer to be published in Proceedings of the North Carolina State College Research Conference on Structure and Properties of Engineering Materials, 1962.

Some measurements have been made of changes in dislocation velocity accompanying changes in stress. However, these results are not very useful unless the changes in moving dislocation density are also studied. It is important to differentiate between multiplication of shear strain, multiplication of the length of moving dislocation line, and increase in the length of immobile dislocation line. All of these usually occur together during growth of a slip band. For example, etch-pit techniques do not usually give information on the number of moving dislocations. Nearly all the pits may mark immobile dislocations in the form of elongated prismatic loops. The density of pits, also, is not directly related to the shear strain. The shear strain is determined by the number of dislocations that have traversed the glide planes, many of which may have left the crystal at the external surfaces.

Some of the conclusions that can be reached relative to the growth of slip bands are as follows.

(a) Few, if any, metal crystals have been studied that were perfect enough to require the spread of slip from one plane to another by double cross-slip. The presence of small-angle twist boundaries makes it unnecessary.

(b) Even in a crystal perfect enough to contain no twist boundaries and in which all dislocations in the three-dimensional network are immobilized by precipitates, a single moving dislocation, perhaps originating from a surface stress concentration, will probably interact with the network to produce a Frank Read source and, therefore, unlimited shear displacement.

(c) When a crystal contains a network of dislocation tangles of the type observed in cold worked metals by transmission electron microscopy, then slip bands grow by propagation of slip from one subgrain to the next. The critical step is probably the bowing out of a new segment from the opposite side of a dislocation tangle into which a dislocation has moved. Repetition of this process can produce a slip band.

The fundamental reason for the great differences between the kind of damage produced by slip in metals compared and that in ionic crystals such as LiF and MgO may be the marked difference in the ratio between the stress necessary to just move dislocations and the stress needed to form slip bands. This ratio is about 0.1 for copper and about 0.5 for MgO.

12. THE FORMATION OF STACKING-FAULT LOOPS IN QUENCHED PURE ALUMINUM*

Francois Vincotte† and Jack Washburn

The dislocation substructure in quenched pure aluminum was investigated following different rates of quenching and different aging temperatures. Low-magnification (8000×) transmission-electron microscope observations revealed that loops always occurred in colonies separated by loop-free zones (Fig. IIA. 12-1). Dislocation tangles were sometimes present in the loop-free zones, which suggests that they were due to the presence of dislocation

*Abstract of paper, based on Vincotte's M. S. thesis, being prepared for publication.

†Now serving in French Armed Forces.

sinks during quenching. These sinks could have been elements of the network of dislocations present before quenching and dislocations that multiplied owing to quenching stresses. Small amounts of plastic deformation at -20°C immediately after quenching greatly increased the percentage of the volume that was free of loops.

The average size of the irregularly shaped colonies of loops did not depend on the quenching rate. This suggests that no extensive plastic deformation occurred, during quenching, even for the most rapid quench, and that the colony size was related to the scale of the dislocation network existing prior to quenching.

Though the average size of the colonies was the same for all quenching rates and aging temperatures, the sizes of individual loops near the colony borders were not. Increasing the aging temperature caused a decrease in the number and an increase in the average size of the loops near the borders (Fig. IIA. 12-1). The size and density of loops near the centers of the colonies did not vary with aging temperature. This suggests that the density of nuclei is determined by vacancy supersaturation and that loops were not nucleated during the quench. By quenching from a series of temperatures, it was estimated that the critical supersaturation necessary to nucleate loops was about 10^{-6}.

For supersaturations near the critical value, loops were almost all of the Frank sessile or stacking-fault type and were hexagonal in shape (Fig. IIA. 12-2). The $\frac{a}{3}\langle 111\rangle$ dislocations tended to lie along $\langle 110\rangle$ directions. The occurrence of stacking-fault loops in aluminum is of particular interest because it shows that the type of loop that is formed cannot be predicted simply on the basis of stacking-fault energy. The mechanism of nucleation and growth and the mechanism of transformation from imperfect to perfect loops must also be considered. In the centers of colonies the loops may have been of the predicted perfect prismatic type. They did not appear to be hexagonal in shape. However, owing to their small size, a hexagonal shape might not be easy to detect because of electron-diffraction contrast conditions. They were also too small to exhibit fringed stacking-fault contrast. Further experiments are needed to establish whether or not these small loops in pure aluminum are actually of the perfect prismatic type.

13. RESEARCH IN PROGRESS: JACK WASHBURN

a. The dislocation loop substructure produced by quenching or irradiation of face-centered cubic materials is gradually swept away by subsequent plastic deformation. Experiments are in progress to further clarify this phenomenon.

b. The uniformity with which shear strain is distributed in a plastically deformed crystal varies greatly from one material to another. The factors that affect slip distribution in crystals are being investigated.

c. The dislocation-multiplication mechanism that operates during the growth of slip bands in materials of the sodium chloride structure is being studied by use of magnesium oxide single crystals and electron microscope techniques.

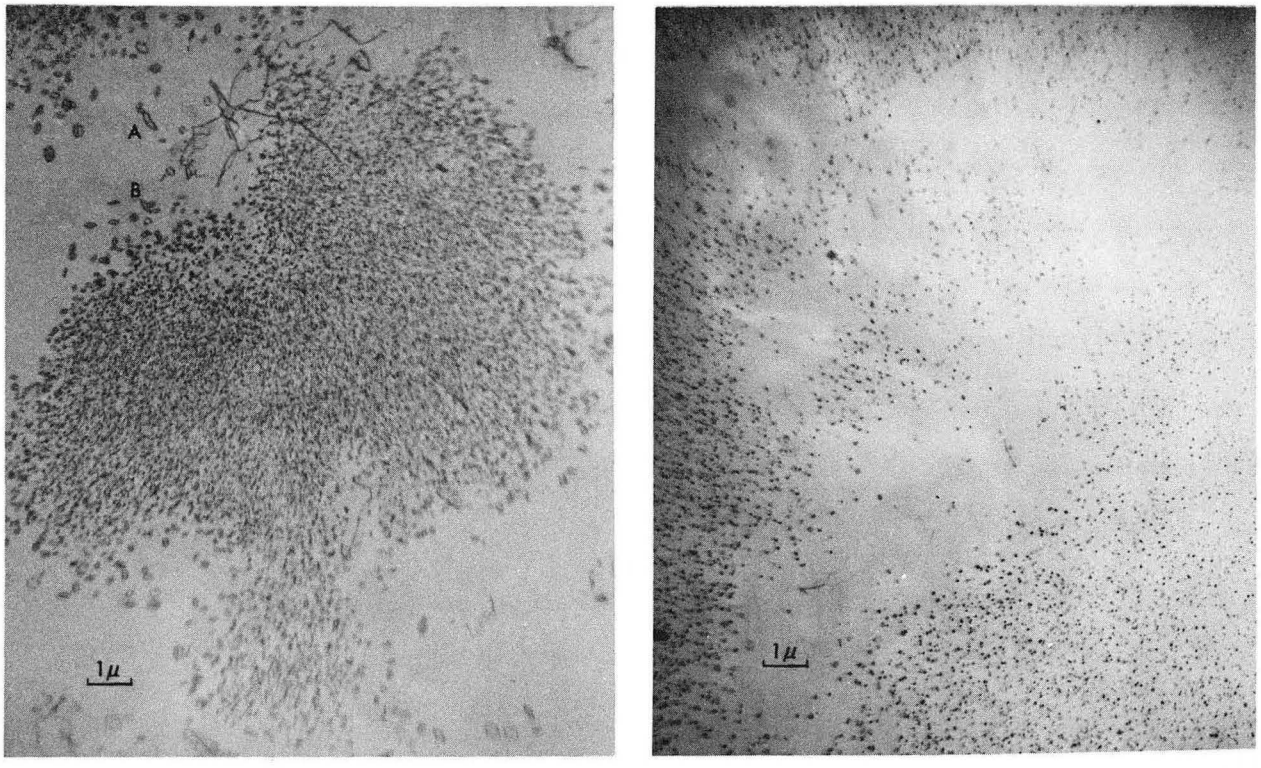

Fig. IIA. 12-1. Colonies of dislocation loops in quenched pure aluminum.

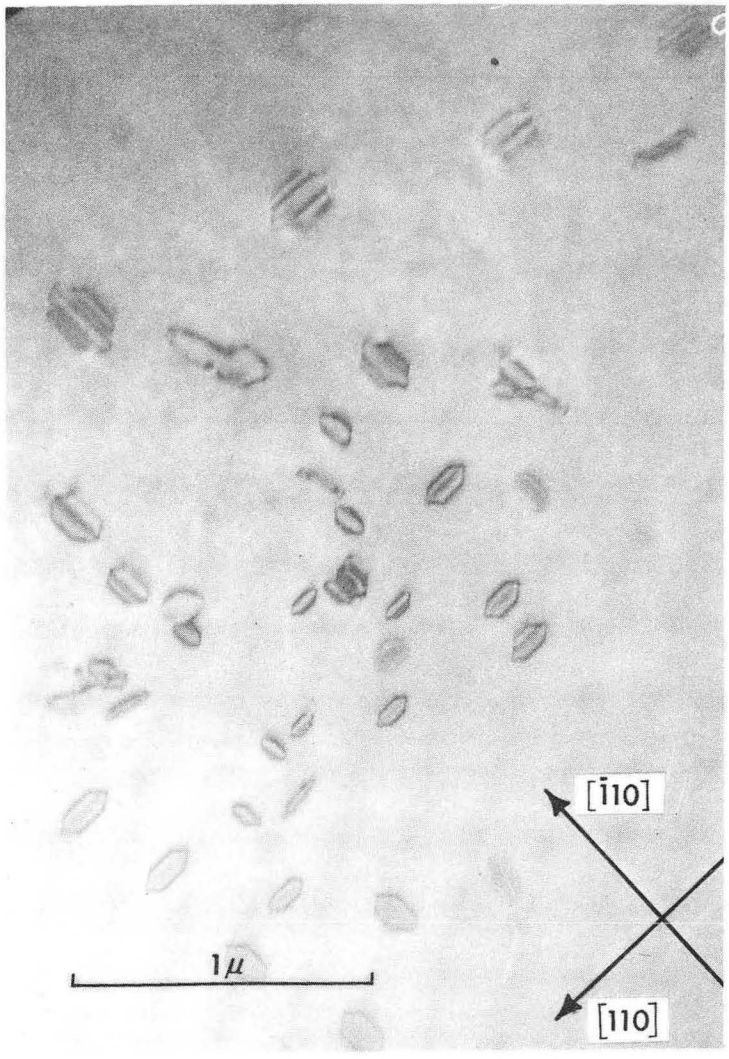

ZN-3651

Fig. IIA. 12-2. Large $\frac{a}{3}\langle 111\rangle$ dislocation loops, showing stacking-fault fringes.

14. A "SPIRAL-RING" MODEL FOR CHARGED PARTICLES

Ira Pratt

The current status of our basic understanding of the electron still rests essentially upon the classical picture--an almost-point spherical charge with a magnetic moment. The charge, mass, and magnetic moment are experimentally well established and useful. The classical radius $r_0 = e^2/mc^2 = 2.82 \times 10^{-13}$ cm is not generally considered to be meaningful. Our knowledge of the proton is hardly in any better shape than our understanding of the electron. In this light, certain charge-distribution models are being considered, i. e., a charged ring and a charged spiral.

What seems to be the prime difficulty in building an acceptable model of a charged "particle" is to account for the cohesion of an extended charge without involving unknown forces.[1] An elementary particle with charge distribution in the form of a ring, with an axial spin ω, would be cohesive if the magnetic field in the immediate vicinity of the loop circumference could be reversed. This may be accomplished by changing the model to a spiral ribbon.

The magnetic field in the immediate vicinity of a simple current loop (not a simple thing to calculate) was computed with the IBM 7040 and experimentally verified. The dotted curve of Fig. IIA. 14-1 indicates the singularity found at the loop circumference. An axially aligned pair of current loops, representing a rotating cylindrical charge distribution, gives a magnetic field which is a continuous function of n, the distance from the axis in radius units. The solid curve of Fig. IIA.13-1 is a plot of the measured field (Hall probe) in a plane centered between two parallel current loops separated by a distance approximately equal to one-fourth their radius. The negative portion of this curve forms a potential well just outside the circumference--an indication of the pitch of a spiral. Beyond n = 2, the measured field for the loop pair essentially coincides with the computer value for a single loop.

Calculation based upon the spiral-ring model--a spiral with an equivalent ring radius r--gives, when Coulomb repulsion is equated with opposing magnetic interaction, a radial velocity

$$r\omega = c. \qquad (1)$$

This relativistic result may seem a bit irregular, but it is consistent with other presentations.[2]

The magnetic moment M = iA of a rotating charge distribution may be written in terms of charge e, effective radius r, and the rate of charge

---

[1] L. Rosenfeld, in Niels Bohr and the Development of Physics, edited by W. Pauli (McGraw-Hill Book Co., Inc., New York, 1955), p. 85.

[2] V. F. Weisskopf, Phys. Rev. 56, 72 (1939).

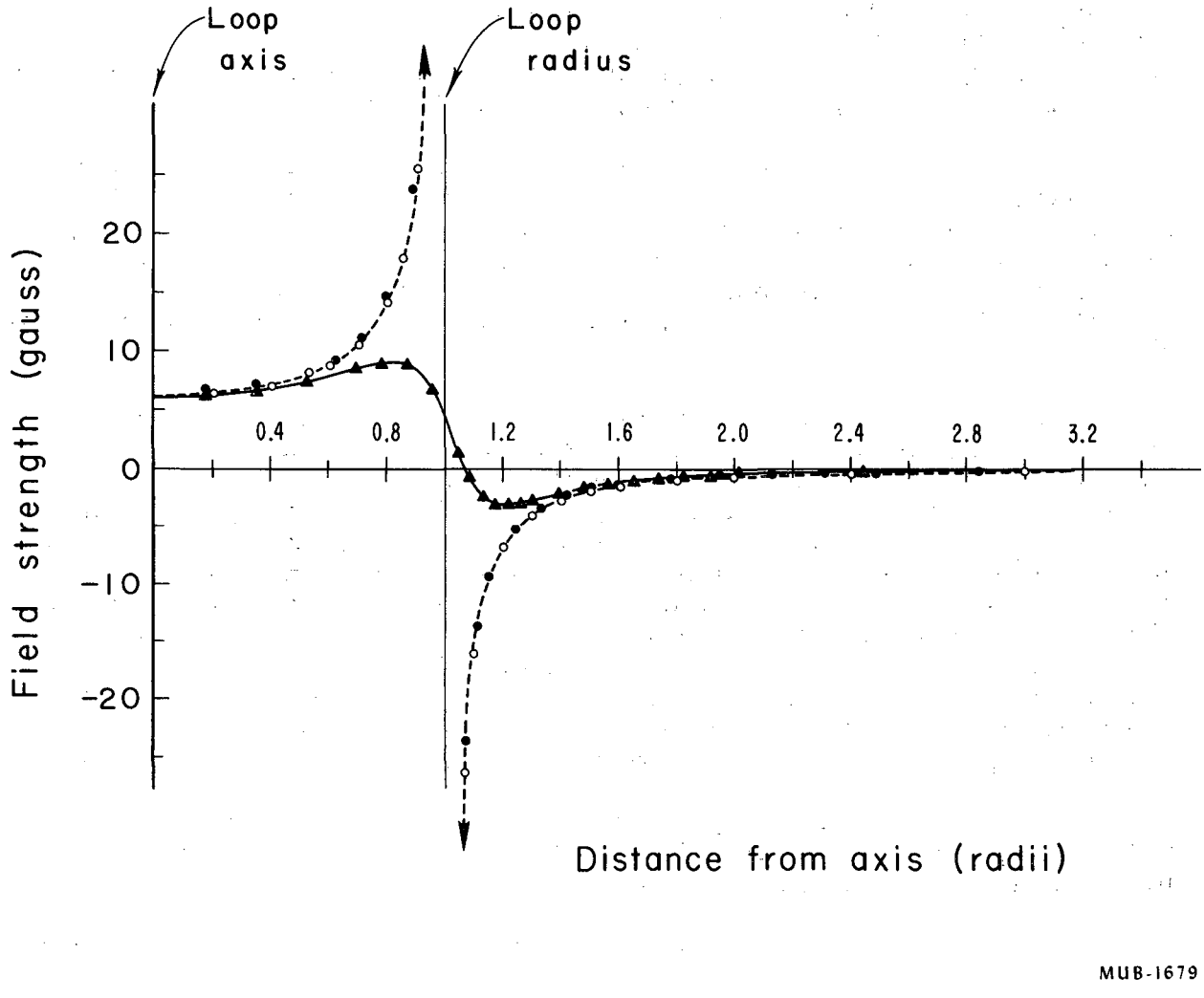

Fig. IIA. 14-1. A plot of field strength in the plane of a current loop (normalized to 1 abampere-turn with 1 cm radius) as a function of the number of radii from the axis.

O calculated, single coil
● experimental, single coil
▲ experimental, double coil

propagation around the loop ω, as

$$M = iA = \frac{er^2\omega}{2c} . \qquad (2)$$

Combining this relation with Eq. (1) and solving for r, we get

$$r = \frac{2M}{e} \qquad (3)$$

for the "size" of a fundamental particle with charge and spin. From known values for the spin magnetic moments of the electron and the proton, and their charge, we can obtain associated radius values. For an electron magnetic moment of $M = 0.9284\times10^{-20}$ erg/gauss, we get an electron radius $r_e = 0.386\times10^{-10}$ cm. For a proton with $M_p = 1.410\times10^{-23}$ erg/gauss, we get a radius value $r_p = 0.587\times10^{-13}$ cm.

No comparable value for the electron radius is available (except the classical radius), but a comparable value for proton size, $r_p \approx 0.8\times10^{-13}$ cm, has been obtained experimentally in high-energy electron-scattering studies of proton size by the Stanford group.[3]

[3] R. Hofstadter, F. Bumiller, and M. R. Yearian, Rev. Mod. Phys. 30, 482 (1958).

15. RESEARCH IN PROGRESS: IRA PRATT

In addition to administrative and technical coordination responsibilities, a modest effort is maintained in the following areas:

a. Equipment designed last year will be assembled to give a pulsed-bremsstrahlung intense ultraviolet source for study of solid-state fluorescence.

b. An electronic beam has been shown by others [J. Appl. Phys. 29, 583(1958)] to follow a slalom orbit in the periodic potential field of a special electron-tube structure. The basic mechanisms of current flow in normal metals and superconductors are being reviewed with an interest toward developing a model for current flow in the solid state similar to that in such a "macroscopic" free-space periodic potential.

B. MICROSTRUCTURE AND PHYSICAL PROPERTIES

1. CRYSTALLIZATION OF ALUMINA

Amio R. Das and Richard M. Fulrath

Spherical single-crystal particles of ceramics in the range of 1 to 100 microns diameter are necessary for extension and verification of many existing theories regarding the mechanical properties of two-phase systems and the mechanism of densification under pressure. An arc plasma torch has been used successfully to produce metal spheres and some ceramic spheres in the above size range. The mechanism of nucleation and crystal growth plays a dominant role in the solidification process.

Crushed and sized single-crystal particles of alumina when fed through an arc plasma torch do not follow the behavior exhibited by metals. The optical transparency of alumina makes heating difficult in the short "residence time" at high temperatures. Adjustment of the plasma gas to increase the surface heat-transfer coefficient can greatly improve the heat transfer and allow melting of larger particles. Large particles of single-crystal alumina partially melted will spheroidize and resolidify as single crystals of α alumina. With complete melting, metastable alumina phases may be crystallized along with the stable α phase. Completely melted particles show spherical or cylindrical holes.

The spheroidization of alumina has been studied by using the arc plasma torch and varying power, residence time in the plasma, and alumina particle size. Microstructural examination, x-ray analysis, and differential thermal analysis have been used to study the spheroidization of alumina and metastable phase formation.

2. STRESS-ENHANCED PERMEATION THROUGH CERAMICS

Orlin M. Stansfield, Perry L. Studt*, and Richard M. Fulrath

Gas permeation through ceramic bodies can drastically limit the utility of ceramics in applications such as nuclear fuel elements or electron-tube envelopes. Normal bulk diffusion or grain-boundary diffusion are high-temperature phenomena; however, at low temperatures microcracks may cause increased permeation if allowed to open and close under cyclic stress. The existence of such cracks in ceramics may be due to the presence of crystals with anisotropic thermal expansion characteristics, due to a thermal expansion mismatch in multiphase ceramics. These thermal expansion characteristics can lead to internal stresses of sufficient magnitude to fracture interfacial bonds. For permeation of noble gases such as helium, a microcrack with a thickness of the order of two atomic diameters would allow increased low-temperature permeation. The nature of the microstructure and

*Now at Aeroject General Nucleonics, San Ramon, California.

the extent to which microcracks join to form continuous channels through a ceramic body, determine the gaseous flow rate. The study of these microcracks by direct methods is impossible with present research tools; however, indirect methods such as gaseous flow rates under cyclic stress coupled with microstructural observations can give informative data.

Work has been completed on a review of permeation of helium and other noble gases through glass,[1] because it is a secondary phase in many commercial ceramics. As a consequence of this review, a new approach to gas permeation through glass has been formulated and an expression developed to incorporate the entropy change of a gaseous atom on entering into solution in a glass. Through this approach the mechanism of gas permeation can be studied more quantitatively.

Four commercial alumina bodies were studied at room temperature to determine the relation of stress-enhanced permeation to microstructure. Ceramics containing a glass phase, and with porosity distributed either as large pores (much greater than the grain size) or as small pores along grain boundaries, showed bursts of gas permeation upon the rapid application or release of a biaxial stress. The bursts could be introduced only with rapid stress application or removal. It is hypothesized that the high stressing rate was more rapid than elastic stress relaxation, and allowed microcrack permeation between pores. These observed bursts decreased in intensity with continued cycling, and channel plugging due to absorption is probably responsible. Bodies containing no porosity or containing a large fraction of the porosity within grains did not show burst phenomena under any of the conditions imposed on the ceramic membrane.

Work is now in progress on glass-bonded "vacuumtight" mullite bodies at room temperature and at elevated temperatures. Enhanced permeation through these bodies has been observed at elevated temperatures. A relationship between the permeation rate under stress and the temperature-compensated applied stress has been determined, as also has the effect of stress on the activation energy for permeation. Additional work on fused silica is being pursued to establish whether or not the enhanced permeation is through microcracks or the glass phase.

---

[1] Perry Louis Studt, Mechanism of Gaseous Permeation Through Glass, Single Crystal Silica, and Germanium; and Stress-Enhanced Gaseous Permeation Through Alumina Bodies (thesis), UCRL-10466, Sept. 1962.

3. DIFFERENTIAL CALORIMETRY

John O. Barner and Richard M. Fulrath

The initial design of a differential calorimeter suitable for measurement of heats of solid-state reactions at high temperatures has been completed and tested. The apparatus consists of two identical sample cells, one empty and the other containing the material to be studied. The environmental temperature is increased with an external furnace. The differential temperature between the two cells is maintained at zero and the differential power

necessary to retain the constant zero differential temperature is recorded as a function of time as the temperature of the calorimeter is increased. Subsequent integration of the curve of differential power vs time yield the heat of transformation.

The endothermic transformations in SiO_2, K_2SO_4, Na_2SO_4-III, and FeS were studied. The results of these experiments are listed in Table I.

Table I.

Material	Heat of transformation (cal/mole) Measured	Published	Difference (%)	Number of runs	Reaction temperature Observed (°K)	Published (°K)
SiO_2	198	290	-31.0	8	848	848
K_2SO_4	2309	2140	+ 7.9	8	856	856
Na_2SO_4	1780	1790	- 0.5	1	553	514
FeS	155	120	+29.2	5	598	598

Although the values differ from the published values by as much as 31%, it is felt by their investigators that the measured values are correct to within ±2%. Heat capacities measured by the differential calorimeter resulted in appreciably high errors (30% to 45%), owing to unequal vertical heat losses in the apparatus. These unequal heat losses were not significant during the reactions, so that any errors in the measured heats of transformations fall well within the ±2% limits.

4. RESEARCH IN PROGRESS: RICHARD M. FULRATH

a. The study of idealized two-phase ceramic systems is continuing. Additional work is being initiated to consider both elastic data and fracture strength in studying the effect of interfacial bonding on the strengthening of brittle matrices by dispersed phases. The problem of differentiating between interfacial bonding and internal stress strengthening will be attacked by using various particle shapes as the dispersed phase.

b. The question of whether densification of ceramics under applied pressure at elevated temperatures proceeds primarily by volume diffusion or by plastic deformation has not been resolved. A study has been initiated using spherical particles and vacuum hot-pressing techniques to investigate this question. Microstructural analysis, supported by directly observed densification rates under pressure, is expected to be the primary method of study.

5. THE MECHANISM OF THE MARTENSITE BURST TRANSFORMATION IN SINGLE CRYSTALS OF IRON CONTAINING 31.7% NICKEL*

Jack C. Bokros† and Earl R. Parker

The strongest metallic materials of general interest are complex alloy steels. In these materials, the reactions that occur during heat treatment have very large effects upon the yield and tensile strengths. The detailed physical processes that occur during heat treatment, and which are the cause of strengthening, are not understood. It is well known that at high temperatures carbides dissolve in the face-centered cubic phase that exists above about 700°C, and that at low temperatures complex carbides precipitate. The crystal structure changes upon quenching from the face-centered cubic to either body-centered cubic or body-centered tetragonal, and the carbon solubility drops to a very low value. In addition, a martensite transformation accompanies the phase change. The role played by the martensite transformation may be one of providing nucleation sites. There is a high degree of lattice disorientation associated with the phase change, and a large number of relatively uniformly spaced carbide nucleation sites may be operating. This hypothesis cannot be checked directly by simple experiments. In ordinary materials, the martensite structure is so fine that the crystallographic relationships between the martensite plates and the austenite crystals in which they form cannot be accurately determined.

This paper describes a study of the nature of the martensite transformation in single-crystal austenite. This carbon-free material, free of grain boundaries, is relatively simple in comparison with the usual martensite structure. High-purity iron-nickel austenitic single crystals were prepared by a vacuum zone-melting technique, and were transformed to martensite under a variety of conditions including various states of plastic strain.

It was found that the morphology of the transformation was greatly simplified in crystals that had been strained plastically prior to transformation. This simplification made possible detailed crystallographic studies of the morphology and transformation. These studies showed that the autocatalysis responsible for the burst transformation had its origin in a mechanical coupling between certain variants of the habit plane that were geometrically oriented in such a way that the stress induced by transformation on one plane aided transformation on others. In both strained and unstrained crystals, the most effective mechanical autocatalysis were observed to be between groups of four nearly parallel planes the poles of which clustered about common $\langle 110 \rangle$ directions. These new observations have helped clarify some of the uncertainties that have been associated with martensite transformations in steel.

---

*An abstract of the Ph. D. Thesis by Dr. Jack C. Bokros (UCRL-10415 Sept. 1962); abbreviated version to be submitted to AIME for publication.

†Now at Ford Scientific Laboratory, Dearborn, Michigan.

6. ULTRAHIGH-STRENGTH MATERIALS

Earl R. Parker and Victor F. Zackay

Precipitated particles in crystalline materials contribute to their strength and hardness. Current studies have indicated that the main factor controlling the strength of a hardened material is the nucleation of precipitates. Theory, based on analysis and observation of dislocation behavior, dictates that precipitated particles should be uniformly dispersed with a spacing of less than 100 Å if high strength is to be obtained. The crystal structure of the precipitate should be such that plastic flow is not possible--except, perhaps, at stress levels above about one-half million pounds per square inch. The required conditions cannot normally be met in useful materials because of the coarse pattern of nucleation sites that invariably develops. For steel, nucleation of the required kind may be provided by the martensite transformation. Consequently, our attention has been focused upon means for introducing finely dispersed nuclei in metals that do not undergo martensite transformations. It may be possible to introduce such nuclei by plastic straining under certain critical conditions. Experiments are currently under way to evaluate these concepts.

A second approach is to control the nucleation state of precipitation by controlling the degree of supersaturation in solution. With a sufficiently high degree of supersaturation, the driving forces for extensive fine-scale nucleation may be high enough to initiate the fine precipitation required for extremely high strength. This is not possible in any known case with standard heat treatments involving quenching from a solid solution range. We are extending the solution range into the liquid state where the degree of supersaturation upon quenching can be made at least an order of magnitude higher than with solid solutions. Tiny spheres of liquid may be quenched at extremely high rates, and their strength changes determined with a microhardness test after aging under various conditions of time and temperature.

7. AN INVESTIGATION OF GRAIN-BOUNDARY ENERGIES

Kurt Kennedy and Earl R. Parker

The important role played by boundaries in mechanical properties has prompted an investigation of room-temperature grain-boundary energy. The existing method of determining such energy uses high-temperature surface diffusion of metal atoms away from the interface creating an energy-determining groove. The approach here involves the use of an equilibrium low-temperature liquid solution to transfer metal from the boundary region to lower-energy surface positions.

First attempts were made with an aqueous solution, limiting the operating temperature to 100°C. Present techniques with grain boundaries in copper make use of a fused salt consisting of 52% $ZnCl_2$, 26% KCl, and 21% CuCl in the temperature range of 200°C to 400°C. The groove angle is measured with an interference microscope. Preliminary results indicate that large-angle tilt boundaries are not one, but two or more boundaries very close to each other.

8. RESEARCH IN PROGRESS: EARL R. PARKER

a. The program described under Ultrahigh-Strength Materials is continuing. If appropriate results are obtained in quench-hardening small spheres, the details of the hardening process will be studied with electron microscope techniques.

b. A program of research on superconducting materials is bein started. Efforts are being concentrated on the effect of processes and fabrication variables on the microstructure of wires containing the superconducting compound Nb_3Sn. It is generally agreed that present techniques are relatively inefficient in that only a small fraction of the volume of the processed material is in the superconducting state. It is believed that a substantial improvement in current-carrying capacity is possible through an increase in volume of the appropriate microstructural constituent. Our studies are being directed toward producing such improvement.

Other work includes the investigation of superconductivity in ternary and more complex alloy systems, which to date have received relatively little attention. The selection of systems is being guided by structural and thermodynamic considerations as outlined in the new theory of metal structures by Dr. Leo Brewer.

c. Investigation of grain-boundary energies will be continued.

9. ALLOY-STRENGTHENING MECHANISMS

Victor F. Zackay*

Understanding of the mechanical properties of metals are greatly accelerated with the advent of dislocation theory. The highly sophisticated development of this concept and the subsequent direct observation of individual dislocations and their interactions have provided materials scientists with a fairly complete understanding of simple solids. Until recently, the bulk of the theoretical and experimental effort has been accomplished with pure metals in the single or polycrystalline form. Since very-high-strength ductile solids are extremely complex in structure, it is natural that few attempts have been made to describe their properties in terms of fundamental theory. Several years ago, it became apparent that attempts might be made to design steels which had strength of nearly one-half million pounds per square inch by the application of the existent knowledge of flow and fracture theory.

---

*Until October, 1962, Dr. Zackay was Assistant Manager of the Applied Science Department at the Ford Motor Company in Michigan. This abstract summarizes a portion of his research while at Ford and is representative of the type of program he plans to carry on in Berkeley.

With the use of steels of appropriate composition, the metallurgical processing variables required to give very high strength were studied. The alloys selected were carbon-containing martensitic steels. Martensite normally forms from a high-temperature face-centered cubic phase called austenite prior to its transformation to martensite, a fine-grained martensite of unusual properties was found. The processing variables studied were the amount and temperature of deformation of the austenite, the carbon content, and tempering temperature of the martensite. The effects of the various mechanical, thermal, and compositional variables on the structure and properties of martensite formed from strain-hardened austenite were thus examined. In addition, these factors were studied on special alloys less complex than the high-strength steels. Interpretation of these experimental results led to conclusions regarding the strengthening mechanisms operative in these very-high-strength materials.

In conformance with dislocation theory, the strengthening mechanism found to be most likely was that of a uniformly fine dispersion of alloy carbide precipitates. The spacing and fineness of this precipitate was apparently sufficient to impede the motion of dislocations to such an extent that yield strengths in excess of 400,000 lb/in.^{2} and ultimate strength of 450,000 lb/in.^{2} were observed. This unique distribution of precipitate particles was apparently due to the nucleation sites found in the strain-hardened austenite prior to transformation to martensite. This structure seems to account for the high strength and ductility, excellent fatigue resistance, and superior elevated-temperature properties of these steels.

10. RESEARCH IN PROGRESS: VICTOR F. ZACKAY

a. High-Strength Ductile Solids

The dislocation theories of flow and fracture and the existing information on the strengthening mechanisms[1] of high-strength solids suggest that a very fine uniformly dispersed precipitate in a ductile matrix might lead to strength levels that are an appreciable fraction of whisker strength. To achieve the dispersion of precipitate required--a spacing of particles with less than 50 Å separation--unusual processing techniques must be employed. One of these techniques, viz., the quenching of molten spheres less than 0.1 mm in diameter, is currently being explored. It is hoped that, by use of this approach and other related ones, nonequilibrium microstructures

[1] Victor F. Zackay presented a paper on this subject, "Structural Aspects and Properties of Martensite of High Strength," at an International Symposium held at the National Physical Laboratory, Teddington, England, in January of this year. The proceedings of the Conference on "The Relations Between the Structure and the Mechanical Properties of Metals" is to be published in the near future.

having a large volume fraction of precipitate and a high density of nucleation sites can be obtained. The structure and properties of these spheres will be established as a function of processing variables. (With Earl R. Parker)

b. Superconducting Alloys

The superconducting properties of solids are a complex function of the electronic and crystal structure. The work of Matthias and his colleagues has shown that certain crystal structures favor superconductivity in solid solutions, intermetallic compounds, and compounds of metals and nonmetals. In an effort to find high-performance superconductors, it is first necessary to predict those alloys and compounds having those favored structures. Recently Leo Brewer of the Chemistry group has shown that certain correlations of crystal structure with electron configuration can be used to predict the occurrence of these favored structures and others in binary and more complex systems. High-purity materials with favored crystal structures will be made. The objective of the research will be to establish a more complete working theory of the structural dependence of superconductivity and, one hopes, to produce superconductors of superior performance. (With Earl R. Parker)

c. The Strain-Hardening Behavior of the Element Iridium

The element iridium of the face-centered-cubic platinum group elements -- Pt, Pd, Rd, and Ir--is characterized by an unusual combination of mechanical and chemical properties. Iridium has the highest modulus of elastically of all face-centered cubic metals (74×10^6 psi). Iridium is chemically inert to virtually all aqueous solvents and most molten salts. It is oxidation-resistant to about 1000°C and at this temperature is as strong as unalloyed molybdenum or tungsten. However, the property of especial interest is its reportedly high rate of strain hardening.

Iridium can be significantly strengthened by relatively small amounts of cold working. Strengths of more than 300,000 psi have been reported for commercially pure iridum deformed 50%.

Current theories of the strain hardening of metals suggests that stacking faults may play an important role. If such be the case for iridium, then an opportunity exists for examining the theoretical concepts in detail. The current experimental program is directed toward examination of the stacking-fault density of iridium foils by transmission electron microscopy, the detailed examination of the stress-strain curve of iridium at very small strains, and the further purification of 99.9% iridium by elevated-temperature treatments of ribbons in very high vacua. (With Jack Washburn and Gareth Thomas)

11. DISLOCATION DAMPING IN HIGH-PURITY SILVER AND DILUTE SILVER ALLOYS

Michael Guinan and Lawrence Himmel

Internal friction and elastic modulus measurements provide a powerful and sensitive tool for studying the nature of dislocations and point defect–dislocation interactions in crystals. Such measurements are currently being carried out on of high purity (99.9999%, $\rho_{296°K}/\rho_{4.2°K} \geq 2000$) oxygen-free (< 1 ppm) single crystals silver, at frequencies of the order of 25 kc by use of the resonant bar technique. Crystals of both [100] and [111] orientations, which have been grown from the melt in vacuum (approx 10^{-6} mm Hg), are being investigated over the temperature range from about 4°K to 900°K. To check various predictions of the vibrating-string model for the damping due to dislocations,[1,2] the following experiments have been initiated:

(a) The temperature dependence of both the background damping and the modulus defect is being measured at constant strain amplitude (approx 10^{-8}) from 4.2°K to about 900°K.

(b) The dependence of the damping on strain amplitude is being studied at various fixed temperatures within this same range.

The damping is known to be extremely sensitive to the presence of relatively long unpinned dislocation loops unavoidably introduced during handling.[3] We have found, for example, that the decrement in silver can be reduced by almost an order of magnitude by annealing a freshly mounted crystal for 2 to 3 hours at about 100°C. Before measurements are made on any crystal, therefore, the specimen is first annealed in situ at temperatures of the order of 700°C ($< 10^{-5}$ mm Hg) after being mounted in the apparatus, and frequent reproducibility checks are made to ensure that no additional changes in the dislocation structure occur once the specimen has been annealed.

Preliminary measurements of the temperature dependence of the background damping in a [111]-oriented crystal indicate that the damping begins to increase exponentially with temperatures above about 300°C. The corresponding activation energy appears to be no higher than about 0.2 to 0.3 eV. This is substantially lower than the value of 0.9 eV found in copper[4] but the data are not yet sufficient to establish the activation energy with good precision.

---

[1] J. S. Koehler, Imperfections in Nearly Perfect Crystals (John Wiley & Sons, Inc., New York, 1952), Ch. VII, p. 197.

[2] A. Granato and K. Lücke, J. Appl. Phys. 27, 583, 789 (1956).

[3] D. H. Niblett and J. Wilks, Advan. Phys. 9, 33 (1960).

[4] L. A. Kamentsky, Thesis, Cornell University, AFOSR-TN-56-425, 1956.

12. THE ANNEALING OF COLD-WORKED SILVER AND INTERNALLY OXIDIZED SILVER ALLOYS

Raymond Busch and Lawrence Himmel

Dispersed particles of a second phase generally act to restrain grain-boundary migration and hence exert a marked influence on the kinetics of recrystallization in cold-worked metals.[1,2] The presence of a dispersed phase often leads to a substantial improvement in the creep resistance at elevated temperatures, which implies that the dispersed particles are effective in inhibiting the climb or rearrangement of dislocations by thermally activated processes.[3,4] However, whether or not second-phase particles also interact strongly with point defects and therefore influence the rate of recovery in cold-worked metals has not been established. To obtain such information, the annealing behavior of a cold-worked silver alloy containing a fine dispersion of magnesium oxide particles is being studied and compared with that of high-purity silver on the one hand and with the annealing behavior of the oxygen-free solid-solution alloy on the other. The dispersed oxide phase is introduced by internal oxidation of a Ag–0.1 at. % Mg alloy at about 600°C.

Polycrystalline wires (0.010 in. diam) of each material are deformed to the same extent (approximately 20% strain) in tension at -195°C and then annealed either isochronally or isothermally at various temperatures between -195°C and +300°C. The kinetics of the annealing process are being followed by measuring both the recovery of the electrical resistivity and the recovery of the flow stress on the same specimen. All resistivity and flow-stress measurements are carried out at -195°C; the specimens are tested in a relatively hard tensile machine at a strain rate of approximately 7×10^{-4}.

The results obtained to date may be summarized briefly as follows:

1. Internal oxidation of the Ag–0.1% Mg alloy raises the flow stress at -195°C by about a factor of about 5.

2. The increase in electrical resistivity, $\Delta\rho$, with the strain, ϵ, can be represented in each case by an expression of the form

$$\Delta\rho = a\epsilon^n,$$

where a and n are constants. For pure silver n is approximately 3/2, but for the oxidized alloy $n \approx 3/4$. This may indicate a higher rate of defect production in the dispersed-phase alloy, but such an interpretation must be regarded as highly tentative at present.

---

[1] J. L. Meijering and M. J. Druyvesteyn, Philips Res. Repts. 81, 81, 260 (1947).

[2] A. Gatti and R. L. Fullman, Trans. AIME 215, 762 (1959).

[3] J. Weertman, J. Appl. Phys. 26, 1213 (1955); ibid. 28, 362 (1957).

[4] J. W. Martin and G. C. Smith, J. Inst. Metals 83, 417 (1955).

3. From a comparison of the isochronal annealing curves (holding time = 1/2 h at each temperature) for pure silver and for the oxidized alloy, it appears that point-defect annealing as well as dislocation annealing are retarded by the presence of the dispersed oxide phase. Identical annealing treatments on these two materials give rise to substantially greater recovery of the electrical resistivity in pure silver than in the oxidized alloy, and this recovery occurs at lower temperatures in pure silver. No recovery of the flow stress has been observed in the oxidized material at temperatures up to 100°C, whereas roughly 50% of the strain hardening in cold-worked high-purity silver can be annealed out in 1/2 h at 100°C.

No detailed interpretation of the results will be attempted until the annealing kinetics and the temperature ranges over which the various annealing stages occur are determined more precisely so that estimates can be obtained for the activation energies associated with these annealing stages.

13. SEARCH FOR A ZENER RELAXATION IN SILVER-MAGNESIUM-OXYGEN ALLOYS

John Papazian and Lawrence Himmel

Any elastically anisotropic defect in a crystal--i.e., one that produces a distortion of lower symmetry than the lattice--tends to reorient itself under the application of a stress in such a way as to minimize the elastic strain energy of the system. Such defects may, therefore, give rise to an internal friction peak when an alternating stress of the proper frequency is applied.[1,2,3] In this case, the frequency at which the relaxation peak occurs at any given temperature is directly related to the appropriate atomic jump frequency for local rearrangement or reorientation of the defect. A search is currently being made for such a relaxation peak associated with the stress-induced ordering of Mg-O atom pairs in a face-centered cubic silver matrix. From the diffusion coefficient for oxygen in silver it is estimated that the internal friction peak, if it exists, will occur near -90°C at a frequency of 1 cps.

In view of the strong binding energy between oxygen and magnesium atoms, the concentration of Mg-O pairs should be quite high even in dilute alloys. The probability of forming such pairs should be further enhanced by introducing oxygen into a dilute Ag-Mg alloy at relatively low temperatures. Any Mg-O pairs so formed should be of the interstitial-substitutional type, since oxygen is believed to dissolve interstitially in silver.

---

[1] C. Zener, Elasticity and Anelasticity of Metals (University of Chicago Press, Chicago, 1948).

[2] A. S. Nowick, Progress Metal Phys. 4, 1 (1953).

[3] B. S. Berry, Acta Met. 10, 271-280 (1962).

An inverted torsion pendulum of the conventional type has been constructed for measuring the internal friction at frequencies near 1 cps and at temperatures from -195° to about 200°C. Provision has been made for direct resistance heating of the specimen after mounting in the grips in order to eliminate damage due to handling. The free decay of the torsional oscillations is observed by means of a long optical lever, and the logarithmic decrement is automatically recorded by using suitably coupled photodiode detectors. The specimens used are in the form of single crystal wires approximately 8 in. long and 1/16 in. in diameter which have been grown from the melt in graphite crucibles.

The apparatus has been assembled and calibrated and a few preliminary runs have been made on a high-purity silver wire which had been deliberately deformed in tension at room temperature. Sharp damping peaks have been observed at approximately -120° and -70°C. These seem to correspond to the deformation-produced damping peaks observed by Hasiguiti and co-workers in cold-rolled silver.[4] In contrast to the behavior reported by Hasiguiti et al., these peaks did not disappear on aging for two days at room temperature; however, they did disappear when the wire was annealed at about 350°C.

[4] R. R. Hasiguiti, N. Igata, and G. Kamoshita, Acta Met. 10, 442 (1962).

14. RESEARCH IN PROGRESS: LAWRENCE HIMMEL

a. The temperature dependence of the flow stress (and of the critical resolved shear stress) is being measured in dilute Ag-Mg and Ag-Cd alloy single crystals both before and after internal oxidation in order to check the predictions made according to various theories of dispersion hardening. Cottrell-Stokes-type experiments are being carried out over the temperature range from 4°K to approximately 400°K. (With S. Gupta)

b. The changes in the dislocation structure which are produced by tensile deformation of Ag-Mg and Ag-Cd alloy single crystals in both the unoxidized and oxidized condition are being followed by electron-transmission microscopy and correlated with the macroscopic stress-strain behavior. (With Subash Gupta, William R. Goggin, and Gareth Thomas)

c. Bordini damping in the kilocycle region is being studied in high-purity silver single crystals and in crystals doped with known concentrations of substitutional (Mg, Al, Cd) and interstitial (oxygen) impurities. (With Michael Guinan)

d. The temperature dependence of the elastic constants of copper, silver, and gold are being measured from room temperature to approximately 500°C using the ultrasonic pulse-echo technique. (With Y. A. Chang)

e. The variation in the room temperature elastic constants of silver-aluminum alloys with composition (0-10 at. % Al) is being determined. (With Y. Austin Chang)

f. The self-diffusion coefficient of silver is being measured in internally oxidized Ag-Mg alloys over the temperature range from about 400° to 800°C in order to determine whether or not the presence of MgO particles or clusters (together with the associated elastic strain in the silver matrix) has any appreciable influence. (With Richard J. Borg, Livermore)

g. The nature of the defects introduced into silver by quenching is being investigated by transmission electron microscopy. (With Dennis Maher)

15. EFFECT OF TEMPERATURE ON THE PLASTICITY OF POLYCRYSTALLINE LITHIUM FLUORIDE*

D. W. Budworth and Joseph A. Pask

Stress-strain curves have been obtained in four-point bending at temperatures up to 500°C for large-grained specimens of polycrystalline lithium fluoride (Fig. IIB. 15-1). A marked increase in ductility and decrease of work hardening were observed to occur between 350°C and 400°C, and to coincide with the appearance of wavy slip lines on the specimen surface. A change in the curve for yield stress vs temperature also occurred in this temperature range (Fig. IIB. 15-2). It is suggested that these changes are due to the additional movement on $\{100\}\langle 110\rangle$ slip planes in this temperature range, supplementing the movement on the $\{110\}\langle 100\rangle$ planes. Failure above 400°C was of the grain-boundary type, whereas at lower temperatures it was principally of the cleavage type. It is suggested that this difference is due to the decreased ease of cleavage at the higher temperatures.

*Brief of paper presented at British Ceramic Society, October 1962 (UCRL-10490, Oct. 1962).

16. DEFORMATION OF MAGNESIA SINGLE-CRYSTAL AND POLYCRYSTALLINE SAMPLES

Stephen M. Copley and Joseph A. Pask

Numerous investigations have been made of the plastic deformation and fracture of magnesia single crystals. However, none of these investigations has included data at temperatures exceeding 1200°C. In this investigation, stress-strain curves were obtained at temperatures ranging from 1000 to 1500°C. Single-crystal samples were compressed in the [001] direction at a constant loading rate of 20 psi/sec.

Between 1000 and 1500°C the yield stress of magnesia remains constant and corresponds to a resolved shear stress of 2000 psi on the active $\{110\}\langle 110\rangle$ slip systems. The initial work hardening, defined as the slope of the first linear part of the stress-strain curve following the yield, reaches a maximum of 1200 psi per % strain at 1100°C and then decreases rapidly to a value of 200 psi per % strain at 1500°C. At 1200°C and higher, the disappearance of a sharp yield, characterized by a rapid decrease of $\frac{d\sigma}{d\epsilon}$ with

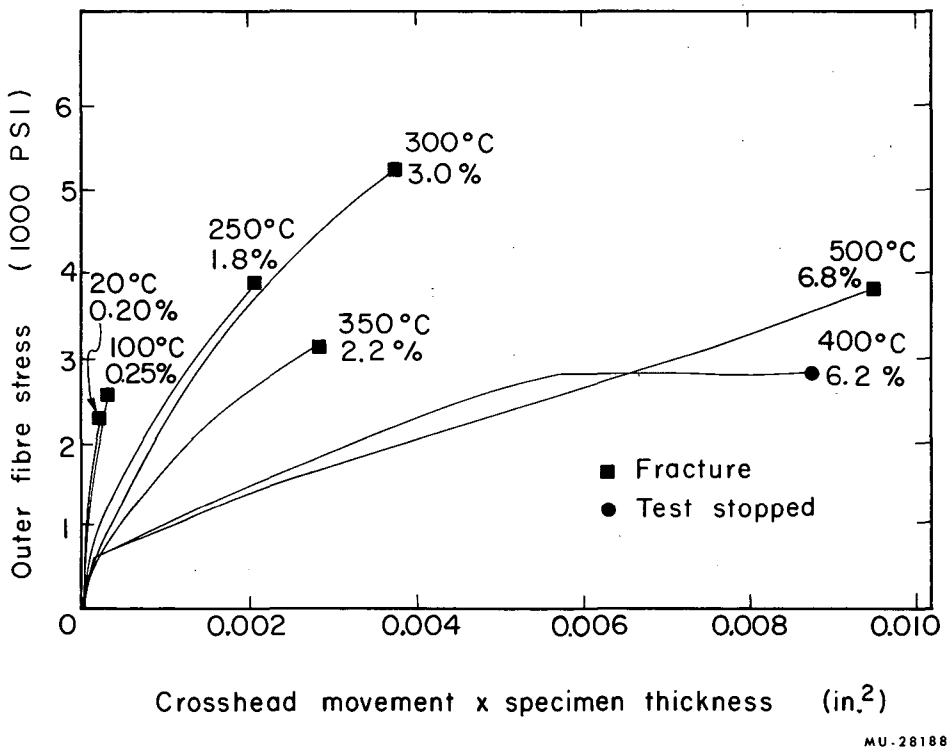

Fig. IIB. 15-1. Stress-strain curves for polycrystalline lithium fluoride.

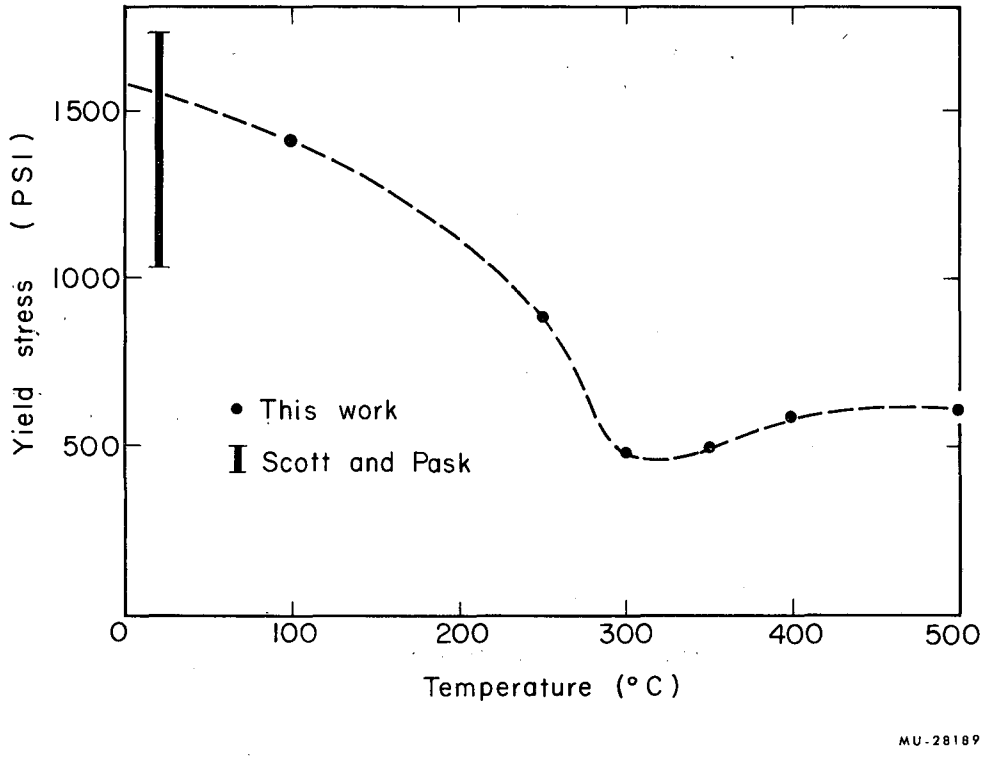

Fig. IIB. 15-2. Yield stresses for polycrystalline lithium fluoride.

increasing ϵ, was observed.

Several stress-strain curves were obtained at 1300°C at loading rates of 200 and 2 psi/sec. At 200 psi/sec an increase in yield stress and an increase in initial work hardening was observed. At 2 psi/sec an increase in yield stress and a decrease in initial work hardening was observed. The reason for the increase in yield stress at 2 psi/sec is not apparent, and further experiments are planned.

A reduced tendency for cleavage fracture was noticed above 1200°C, and at 1500°C one sample strained 30% without fracture. Examination of deformed samples indicates that intersection of dislocations moving on {110} ⟨110⟩ planes inclined at 60 deg to one another does not easily occur even at 1500°C.

17. MECHANICAL BEHAVIOR OF SINGLE-CRYSTAL AND POLYCRYSTALLINE CESIUM BROMIDE*

Lawrence D. Johnson and Joseph A. Pask

Plastic-deformation experiments were conducted on cesium bromide, a material that lacks cleavage planes, to study the effect of the absence of cleavage on the mechanical behavior.

Single-crystal cesium bromide was found to be soft and ductile if it was favorably oriented relative to the loading axis to activate the {110} ⟨100⟩ slip systems. Kink bands were formed by directing a compression load normal to the {100} system of planes. Cross-slip was found to occur during deformation at all test temperatures from room temperature to 250°C. Tensile and bending loads directed normal to {100} and {110} planes caused fracture on {110} planes, whereas compressive loads normal to {100} planes forced fracture on {112} planes rather than {110} planes.

The ductility of polycrystalline cesium bromide was found to decrease for samples with smaller grain sizes. The absence of a sufficient number of slip systems in the specimens may have been responsible for this plastic behavior. The mechanism of fracture was intergranular in polycrystalline cesium bromide.

*Abstract of Johnson's Ph. D. Thesis (UCRL-10468, September 12, 1962).

18. RESEARCH IN PROGRESS: JOSEPH A. PASK

a. Studies on the kinetics and mechanism of the anatase-rutile transformation are being continued. Powders from several sources are being used. Causes for variations in the rate constants and activation energies and the effects of additives on the transformation rates will be explored.

b. The kinetics of the high-temperature hydrolysis of magnesium fluoride are under study. Specific data are being obtained on the effect of water vapor pressure and temperature on the rate of reaction. Attempts will be made to determine the mechanism of the reaction.

c. The diffusion of iron into single-crystal MgO will be studied. The source of iron in the first experiments will be metallic iron. Diffusion profiles will be measured.

d. Studies are being continued on the solution of the different iron oxides in sodium disilicate glass and on the nature of diffusion. Attempts will be made to determine relative rates of diffusion for ferrous and ferric ions.

e. Studies on the plastic deformation of single-crystal and polycrystalline LiF at elevated temperatures will be continued. Relationships of single-crystal behavior to polycrystalline behavior will be determined.

f. Attempts are continuing to prepare completely dense and transparent polycrystalline MgO with controlled grain size. The plastic deformation of such samples will be studied up to 1600°C.

g. The plastic anisotropy of single crystals of MgO up to 1600°C is being studied. Specific studies will be made on the plastic deformation due to flow in the $\{100\}\langle 110\rangle$ slip system.

h. Studies will be started on the nature of viscous flow in fused silica in the transformation temperature range.

i. The rheological behavior of nonideal dispersed systems will be studied.

C. KINETICS OF DISLOCATION MECHANISMS

1. ENERGETICS IN DISLOCATION MECHANICS

John E. Dorn

A major objective of the research in mechanical behavior at the Lawrence Radiation Laboratory concerns the determination of the various dislocation mechanisms responsible for the plastic behavior of crystalline materials. This study requires consideration and development of suitable theories for dislocation mechanics, critical investigations of mechanical behavior of crystalline materials (particularly the determination of activation energies and volumes for deformation) coupled with auxiliary x-ray, metallographic, and electron-microscopic evidence so directed as to provide documentation and identification of the strain-rate controlling mechanisms. A summary of the present status of the theory with extensive examples of LRL contributions to this subject[1] was presented at the National Research Council Seminar on "Energetics of Metallurgical Phenomena" at the University of Denver in July 1962.

[1] John E. Dorn, Energetics in Dislocation Mechanics (to be published under the Transactions of the National Research Council Seminar on Energetics in Metallurgical Phenomena) Denver, 1962.

2. ON THE NATURE OF STRAIN HARDENING IN POLYCRYSTALLINE ALUMINUM AND ALUMINUM-MAGNESIUM ALLOYS*

Sandip K. Mitra and John E. Dorn

By applying experimental techniques involving changes in temperature and strain rate during the low-temperature plastic deformation of polycrystalline Al and several Al-Mg α solid solutions, it was possible to deduce--from an appropriate extension of Seeger's theory for thermally activated intersection of dislocations--the mean force-displacement diagram for the thermally activated intersection, the mean distance between the dislocations being intersected, and the contribution of the athermal processes to the flow stress.[1] The force-displacement diagram for pure polycrystalline Al agreed precisely with that previously obtained for pure single Al crystals, revealing that intersection is the rate-controlling mechanism.[2,3] Whereas the initial effective

*Description of work reported in published paper of same title.

[1] Sandip K. Mitra and John E. Dorn, On the Nature of Strain Hardening in Polycrystalline Aluminum and Aluminum-Magnesium Alloys, J. Met. Soc. AIME, 1963.

[2] Sandip K. Mitra and John E. Dorn, On the Nature of Strain Hardening in Face-Centered Cubic Metals, Trans. Met. Soc. AIME 224, 1062-1071 (1962).

[3] Sandip K. Mitra, P. W. Osborne, and John E. Dorn, On the Intersection Mechanism of Plastic Deformation in Aluminum Single Crystals, Trans. Met. Soc. AIME 221, 1206-1214 (1961).

dislocation spacing was found to be identical in polycrystalline Al and in single crystals of Al, the dislocation density increased much more rapidly with straining in the polycrystalline material. This was attributed to the polyslip that must take place when polycrystalline metals are deformed. Furthermore, in the polycrystalline metal, the athermal contributions to the flow stress increased much more rapidly with strain. The principal factor causing this was shown to be the greater long-range back stresses due to blockage of dislocations at the grain boundary. The theoretical ratio calculation predicting that the flow stress of a polycrystalline aggregate is 3.10 times the resolved shear stress for slip as suggested originally by G. I. Taylor, was not confirmed. When the strains were identical, the ratio did hold if the effective dislocation density was the same in the polycrystalline and single-crystal specimen.

Theoretically, many factors such as short-range-order hardening (Fisher), dislocation–solute atom locking (Cottroll), and chemical interaction due to stacking faults (Suzuki), can account for a solid-solution strengthening. In this investigation it was found that the thermally activated mechanism for deformation of Mg a solid solutions of Al was also ascribable to intersection. The force-displacement diagram deduced from the plastic behavior was only slightly different from that for pure Al, as expected when the stacking-fault energy is decreased slightly. The major factor, however, in accounting for the increased strength on alloying was the greater initial density of dislocation and the more rapid increase in dislocation density with strain. The back stress due to various athermal processes was also increased as a result of alloying. Undoubtedly the various locking mechanisms are responsible for the retention of high dislocation densities following annealing of the cold-worked specimens. This effect of alloying on increasing the density of dislocations was overlooked in all previous investigations on solute-atom strengthening. Since this effect was observed to be much greater than those attributed to the Fisher, Cottrell, and Suzuki contributions to alloy hardening, the entire field of solid solution strengthening should be re-explored.

3. DISPERSED-PARTICLE STRENGTHENING AT LOW TEMPERATURES

Jack B. Mitchell, Sandip K. Mitra, and John E. Dorn

Current thoughts on the effect of dispersion strengthening are based on the Fisher-Hart-Pry extension of Orowan's concept that dislocations can extrude past particles spaced a distance λ apart when the applied stress is $\tau = 2\Gamma/b\lambda$, where Γ is the line energy and b is the Burgers vector. Fisher, Hart, and Pry suggested that the dislocation loops left around the particles provide high back stresses that are responsible for the high rates of strain hardening observed in the initial stages of straining. Finally, fracturing of the dispersed phase as a result of the high stress concentration due to the dislocation loops results in very low final rates of strain hardening.

By use of the same techniques as described in the preceding investigation, it was shown that the thermally activated mechanism of plastic deformation in polycrystalline aggregates of Al containing dispersions of $CuAl_2$ is again intersection of dislocations.[1] The force-displacement diagrams for intersection of dislocations in these alloys differed only slightly from those for pure Al, in a manner suggesting that the alloys had a slightly lower stacking-fault energy than pure Al. The great increase in flow stress in the early stages of deformation was principally attributable to the great increase in dislocation density. The mean dislocation spacing deduced from the mechanical data coincided closely with that observed in the entanglements by transmission-electron microscopy. No circular dislocation loops as postulated by Fisher, Hart, and Pry were observed. This suggests that the dislocation mechanics for dispersion-hardened alloys are similar to those of a solid solutions. Extensive polyslip and cross-slip in the vicinity of the particles causes the formation of high-density entanglements rather than loops. The low rates of strain hardening after extensive deformation were not due to fracturing of the precipitate, and probably are ascribable to cross-slip.

[1] Jack B. Mitchell, Sandip K. Mitra, and John E. Dorn, Dispersed-Particle Strengthening at Low Temperatures, Trans. Am. Soc. Metals (to be published, 1963).

4. ON THE PLASTIC BEHAVIOR OF POLYCRYSTALLINE AGGREGATES

John E. Dorn and Jim D. Mote

The current status and recent research on the plastic behavior of polycrystalline aggregates,[1] illustrated and documented in part by research at Lawrence Radiation Laboratory, was presented at Conference on Materials Science (sponsored by the Department of Defense) at North Carolina University, July 5-8, 1962.

[1] John E. Dorn and Jim D. Mote, "On the Plastic Behavior of Polycrystalline Aggregates" (to be published in the proceedings of the conference, 1963).

5. RECENT PROGRESS IN UNDERSTANDING HIGH-TEMPERATURE CREEP

John E. Dorn

This report, which reviews much of the research done at the University of California on creep at high temperatures, constitutes the 1962 Horace W. Gillett Memorial Lecture of the American Society for Testing Materials.[1]

[1] John E. Dorn, The Horace W. Gillett Memorial Lecture of the American Society for Testing Materials, "Recent Progress in Understanding High Temperature Creep" (to be published in the 1962 Transactions of ASTM).

6. PHYSICAL ASPECTS OF CREEP

John E. Dorn and Jim D. Mote

This paper[1] constitutes a summary and analysis of the physical theories and pertinent experiments on high-temperature creep for presentation at the International Conference on Elevated Temperature Structural Mechanics at the third of the Symposia on Naval Structural Mechanics, sponsored by the Office of Naval Research. In addition to a detailed illustration of the status of current theory on creep, several new concepts were developed in this report:

1. Whereas Nabarro and Herring assumed that creep in polycrystalline aggregates occurs by stress-directed diffusion of vacancies through the volume of the grain, there is a finite probability that this diffusion may occur preferentially in the grain boundary. An approximate kinetic analysis was made that suggests that for

$$\frac{g_f - g_{f_b} + g_m}{kT} < 30$$

the diffusion preferentially occurs in the grain boundary. The values of g_f, g_{f_b}, and g_m refer to the free energy of formation of a vacancy in the volume of a crystal (f), the free energy of formation of a vacancy in the grain boundary (fb), and the free energy of activation of a vacancy for motion (m), respectively, where kT has its usual meaning. This suggests that volume diffusion will be the preferred mechanism in most metals, whereas grain-boundary diffusion may predominate in some ceramic materials. The equation for creep by grain-boundary diffusion of vacancies was also developed. Whereas the appropriate experimental creep data for Al_2O_3 suggest that Nabarro creep is controlled by anion volume diffusion, data for BeO and UO_2 suggest the process may be controlled by anion grain-boundary diffusion.

2. Although experimental results on dislocation-promoted creep revealed that high-temperature creep results from the formation and migration of vacancies, no completely satisfactory formulation of the theory matured. We have shown in this report that the creep of bcc and fcc metals with high-stacking-fault energy can be well rationalized in terms of the motion of jogged screw dislocations. The critical issue concerns the fact that the distance between jogs in these metals is very small and therefore the activation energy is only mildly reduced as a result of the stress. The short jog length arises from facile cross-slip of screw segments. Therefore the observed activation energy for creep coincides well, as we have shown experimentally, with that for self-diffusion. This fact also accounts for the insensitivity of the activation volume with the temperature. A second major issue concerns the fact that dipoles, entanglements, and subgrains are formed during primary creep. The entire change in creep rate over the primary stage can be ascribed to the decreasing density of moving jogged screw dislocations.

3. The secondary creep rate was assumed to arise when the generation of dislocations by climb from dipoles and entanglements equals the rate of formation of these substructural details as controlled by the motion of jogged screw dislocation. Thus the creep in this region can be analyzed by either the motion of jogged screw dislocations or the climb of edge dislocations.

[1] John E. Dorn and Jim D. Mote, Physical Aspects of Creep (to be published as part of the Proceedings of the Third International Symposium on Naval Structural Mechanics, 1963).

4. The major advantage of this theory is that for the first time it can explain, in at least some detail, the primary stage of creep. It follows from the theory that the total creep strain γ can be given by $\dot{\gamma} = f(te^{-\frac{\Delta H_d}{RT}})$, which has been experimentally established at the University of California, where t = duration of the test and ΔH_d is the enthalpy for self-diffusion.

5. A more accurate equilibrium distribution of solute atoms in a Cottrell atmosphere was developed, taking into consideration the problem of occupancy of lattice sites and, for the first time, the effect of nonideality of the solution.

6. The qualitative formulation for a better theory of creep in dispersion-strengthened alloys was also presented.

7. CREEP BY PRISMATIC SLIP IN THE HEXAGONAL Ag-Al INTERMEDIATE PHASE

Eugenia M. Howard, Willis L. Barmore, Jim D. Mote, and John E. Dorn

Previous research revealed that prismatic slip of Ag-Al (33 at.%) hexagonal intermediate phase from 170° to 475°K was athermal and could be ascribed only to short-range-order strengthening.[1,2] From the mechanical data and assuming chemical equilibrium at 475°K, the short-range order energy was determined to be 730 cal/mole, and Cowley's degree of order was about $\chi = 0.30$. Above 475°K, however, thermally activated creep was observed.

In this investigation both the activation energy for creep (thesis by Willis L. Barmore) and the stress laws for creep (thesis by Eugenia M. Howard) were determined in the order to assist in identifying the thermally activated mechanism for creep.[3] Following a short inverted transient, a steady-state creep rate, $\dot{\gamma}$, given by

$$\dot{\gamma} = 1.4\tau^{3.6} e^{-33,000/RT},$$

---

[1] Jim D. Mote, K. Tanaka, and John E. Dorn, Effect of Temperature on Yielding in Single Crystals of the Hexagonal Ag-Al Intermetallic Phase, Trans. AIME 221, 858 (1961).

[2] K. Tanaka and Jim D. Mote, The Effect of Temperature on the Yield Strength of Polycrystalline Hexagonal Ag-Al Intermetallic Phase (UCRL-9992, Dec. 1961)(submitted for publication Trans. ASM, currently under revision).

[3] Eugenia M. Howard, Willis L. Barmore, Jim D. Mote, and John E. Dorn, On the Thermally Activated Mechanism of Prismatic Slip in the Ag-Al Hexagonal Intermediate Phase, Trans. AIME (to be published).

where τ is the applied shear stress, was obtained. The activation energy of 33,000 cal/mole was independent of the applied stress and about equal to the estimated value for diffusion. Since the stress level for creep was much below that necessary to overcome short-range ordering, the process could not be ascribed to either the motion of jogged screw dislocations or the climb of edge dislocations. Equally it could not be ascribed to viscous drag of a Cottrell atmosphere, since such an atmosphere does not form in this alloy because of the identity of the atomic radii of Ag and Al. A theory in qualitative agreement with the facts was proposed, based on local disordering by diffusion due to relaxation in the near vicinity of the cores of moving dislocations.

8. THERMODYNAMICS OF STACKING FAULTS IN BINARY ALLOYS*

John E. Dorn

Distribution of solute atoms between the matrix and stacking faults is significant to the mechanical behavior of alloys as a result of Suzuki locking of dislocations. A more complete and sophisticated analysis of the distribution coefficient was established by use of classical thermodynamics, for any solid solution (not just regular solutions) and the final results were expressed in terms of experimentally measurable quantities.

*Brief of paper accepted for publication in Acta Metallurgica, 1963.

9. DYNAMIC BEHAVIOR OF CRYSTALLINE MATERIALS AND PLASTIC WAVE THEORY

Frank Hauser, Ted Larsen, Stanley Rajnak, and John E. Dorn

Perhaps the least well understood area of plastic deformation of crystalline materials concerns the behavior of high-speed dislocations and the implication of these effects in plastic wave theory. Over the past year, since Lawrence Radiation Laboratory undertook sponsorship of this project, several interesting results have matured. The experimental technique being employed at LRL and illustrative data were reported at the ASTM Symposium on Dynamic Behavior of Materials at the University of New Mexico.[1] A summary of some of our research in this area was reported at the Symposium on Structural Dynamics sponsored by NASA and WADD in Dayton, Ohio, in September, 1962.[2]

[1] Stanley Rajnak and Frank Hauser, Plastic Wave Propagation in Rods, ASTM Symposium on Dynamic Behavior of Materials, University of New Mexico, Albuquerque, Sept. 27, 1962 (to be published as a special technical publication).

[2] John E. Dorn and F. Hauser, Dislocation Concepts of Strain-Rate Effects, given at the Symposium of Structural Dynamics under High Impulsive Loading, Dayton, Ohio, on September 17, 1962.

These data will also be discussed at a Tripartite (U. S., Canada and Great Britain) Special Meeting at the Aberdeen Proving Grounds, Md., January 30-31, 1963. A detailed report on the dynamic behavior of single crystals of the Ag-Al (33 atomic percent) hexagonal intermediate phase under dynamic conditions is being prepared for publication.[3] Our results have also been summarized for presentation at the International Conference on Production Engineering Research to be held in Pittsburgh, Pennsylvania, September 9-12, 1963.[4]

a. Von Karman and Taylor's assumption that a shock in plastic strain accompanies a shock in stress is theoretically untenable because, as shown by Frank, dislocations have inerta as given by the relativistic equation $\Gamma = \Gamma_0 \{1 - (\frac{v}{c})^2\}^{1/2}$ where Γ is the energy of a dislocation moving with velocity, v, Γ_0 is its rest energy and c is the velocity of sound in the material. But the accelerative period is short because of the low inertia of dislocations.

b. At high stress levels the velocity of dislocations should not exceed the velocity of sound. We have found, however, that at the lower ranges of temperatures and stress we can predict the dynamic behavior of polycrystalline Al from low tension or creep data, assuming the velocity of dislocations is determined by the thermally activated intersection of dislocations. At higher stress levels, just at the point where the prediction reveals that mechanically applied force is great enough to cause intersection without waiting for a thermal fluctuation, the strain rate dependence on the flow stress changes from almost exponential to almost linear. Analyses revealed that the moving dislocations have velocities several orders of magnitude below the velocity of sound. As shown by applying Leibfried's analysis the viscous restraint on the motion of the dislocation is much greater than can be accounted for in terms of interaction of phonons with moving dislocations. Some yet unknown process is responsible for the rather large viscous drag on fast dislocations. In any event, in this material the plastic wave phenomenon cannot be that suggested by the von Karman and Taylor theory. We have shown that the actual propagation obtained experimentally in Al can be predicted by introducing the experimentally determined dependence of stress on strain rate as well as strain in terms of a quasi-viscous theory of plastic behavior.

c. Dynamic behavior of single crystals of the Ag-Al (33 at. %) hexagonal phase oriented for basal slip gave yield strengths that are insensitive to the strain rate and increase somewhat with temperature even as the temperature approaches the melting point. This athermal process has been shown to be due to the Suzuki locking of dislocations. The increase in flow stress with temperature was much greater than could be accounted for in terms of interactions

---

[3] T. Larsen, S. Rajnak, F. Hauser, and John E. Dorn, Effect of Strain Rate and Temperature on the Yield Strength of Ag-Al Hexagonal Single Crystals (to be prepared for publication).

[4] John E. Dorn and S. L. Rajnak, Dislocations and Plastic Waves, UCRL-10627, to be presented at the International Conference on Production Engineering Research, Pittsburgh, Pa., September 9-12, 1963.

between phonons and high speed dislocations. It could be accounted for exclusively in terms of Suzuki locking provided the difference in stacking fault energy of pure hexagonal and Ag-Al has a small linear increase with temperature. The stacking fault energies deduced from the mechanical data were small, (100 to 200 ergs/cm^2 which are very reasonable values). In this instance the von Karman and Taylor assumptions appear to be valid. This arises because the least count of the experimental set up is about 10^{-6} seconds, whereas the accelerative period for dislocations is about 10^{-11} second. Thus if the strain rate were very high at first and then decreased as a result of strain hardening to a very low value, it would appear experimentally that over the interval from 10^{-11} to 10^{-6} second, a shock in strain $[\gamma] = \int \dot{\gamma}\, dt$ was obtained. Thus the constitutive equations to be used in plastic wave propagation must be adjusted to the time intervals and plastic strains that are significant.

d. Prismatic slip of Ag-Al (33 at. %) under dynamic conditions revealed flow stresses that were 25 or more times as great as those for slow deformation at temperatures above 500°K. This reveals that the previously discussed diffusion controlled processes for slow deformation are replaced by other mechanisms when the strain rate is so high that diffusion can no longer play a significant role in the mechanism. The same yield stress at the absolute zero was approached under dynamic and slow tension tests suggesting that the dynamic process was also controlled by the thermally activated Peierls mechanism previously shown to be valid for the slow tests. But predictions of the dynamic test data in terms of the Peierls mechanism gave much lower flow stresses, particularly in the higher temperature range, than those observed experimentally. Modification of the simple Peierls theory by taking into consideration phonon interactions with moving dislocations and alternately thermal activation of the motion of kinks failed to give sufficiently high flow stresses at the higher temperatures to account for the experimental data. Again some yet unknown strong viscous drag appears to be restraining the velocity of high speed dislocations.

10. EFFECT OF STRAIN RATE ON THE DIFFUSIVITY OF Ni^{63} INTO SINGLE Ni CRYSTALS*

Frank Wazzan and John E. Dorn

Enhanced diffusivity is obtained as a result of plastic straining. The increase in the diffusivity is directly proportional to the strain rate. Analyses reveal that these results cannot be attributed to excess vacancies produced either by motion of jogged screw dislocations or by climb of edge dislocations. Analyses of the data suggest that rapid pipe diffusion along moving dislocations is responsible for the observed effect. This report is based on analyses of data given in Wazzan's thesis.[1]

*Brief of paper being prepared for publication.

[1]Ahmed Rassem (Frank) Wazzan, Analysis of Enhanced Diffusivity in Nickel (Ph. D. thesis), UCRL-10457, Aug. 1962.

11. RESEARCH IN PROGRESS: JOHN E. DORN

a. Determination of Short-Range Order in Hexagonal Ag-Al Intermediate phase

Previous investigations have shown that the athermal deformation of Ag-Al (33 at. %) by prismatic slip over the temperature range 170°K to 475°K could be ascribed only to short-range-order strengthening. From the mechanical data it was deduced that the ordering energy was about 730 cal/mole and Cowley's degree of order at 475°K was $\alpha \approx 0.30$. This investigation was then undertaken to determine the degree of order in the Ag-Al hexagonal phase. One preliminary paper has resulted,[1] and the equipment necessary to survey quantitatively x-ray intensities over the entire reciprocal lattice (in order to determine the degree of short-range order) has been completed. This investigation should be completed by next August. (With Joachim P. Neumann)

[1] J. P. Neumann, On the Order in the Hexagonal ζ - Phase in the System Silver-Aluminum, Acta Met. 10, 984 (1962).

b. Mechanism of Prismatic Slip in the Ag-Al (33 at. %) Hexagonal Intermediate Phase

The low-temperature prismatic slip in Ag-Al (33 at. %) was previously ascribed to the operation of the Peierls mechanism. The present investigation plans a broader study of the behavior of this alloy, with more detailed information on the activation energy and volume as a function of temperature and with wide ranges in strain rate in order to provide the data necessary for a better check on the theory (which is yet under discussion for revision). Some of the required oriented single crystals have been prepared. Experimental work and analyses will be started in about one month. (With Abraham Rosen and Jim D. Mote)

c. Mechanism of Deformation in the Ag-Mg Intermetallic Compound

As a step in our effort to unravel the detailed mechanisms of deformation of intermetallic phases we have selected, as representative of the CsCl lattice type, the Ag-Mg intermetallic phase. Thus far we have learned how to make single crystals of this material. It is shown that polycrystalline Ag-Mg is ductile, at least down to room temperatures, but there is no information at present on the possible rate-controlling dislocation mechanisms. (With Amiya K. Mukherjee)

d. Recovery of Cold-Worked Polycrystalline Aluminum

The techniques developed by Mitra and Dorn for analyzing the structural details of dislocation spacing L and the athermal back stresses in the intersection mechanism permit, for the first time, a more detailed study of factors involved in recovery. High-purity polycrystalline aluminum prestrained to a stress of 12,000 psi at 77°K was used in the recovery investigation. Dislocation spacings during intersection were deduced from the activation

volume, and the change in this spacing following recovery was measured. The recovery of the dislocation spacing over the range of 300° to 377°K increases as the stress during recovery increases from 0 to 4,680 psi. (Higher stresses were not used because creep attended the recovery.) The activation energy for recovery, however, was independent of the dislocation spacing, the stress and the temperature of recovery being about 12,000 cal/mole. Although the mechanism for recovery has not yet been established, since the 12,000-cal/mole value is much greater than that calculated for intersection and much less than that estimated for cross-slip, with investigation reveals for the first time that the major factor for low-temperature recovery of the mechanical behavior of aluminum (and presumably other fcc metals) is the dislocation spacing. Other interesting and significant features will be included in a report now being prepared for publication. (With Abraham Rosen)

e. Effect of Crystal orientation on Strain Hardening

The rate of strain hardening of single fcc crystals increases as the orientation approaches that for duplex slip. Higher rates of strain hardening are also obtained for orientations that promote the operation of two, four, six, and eight slip systems simultaneously. No detailed investigation has hitherto been made of such observations in terms of dislocation mechanisms. By use of the techniques previously developed by Mitra and Dorn for analyzing the factors pertinent to the intersection mechanism, it should be possible to shed more light on strain hardening as deduced from orientation effects in fcc metals. A series of single crystals of Al has been prepared and several orientations have been examined. (With Amiya K. Mukherjee and Jim D. Mote)

f. Mechanism of Low-Temperature Prismatic Slip in Alpha Solid Solutions of Li in Mg

Previous investigations have shown that of all the elements soluble in Mg only Li provides good low-temperature ductility in Mg solid solutions. This is because Li in solution permits prismatic slip in addition to basal slip. It has recently been shown that prismatic slip of Mg takes place as a result of thermally activated cross-slip at temperatures above 450°K. But a lower temperatures, single crystals oriented for prismatic slip either twin or fracture, the resolved shear stress for low-temperature prismatic slip being very high. A recent report showed that Li additions increased the shear stress for low-temperature basal slip.[1] Data now being gathered on specially oriented single crystals of Li in Mg show that Li additions reduce the resolved shear stress for prismatic slip. Current evidence on the activation volume suggests that the active process is the Peierls mechanism. More complete data covering various compositions of Li are being gathered to determine how Li might reduce the Peierls stress. (With Aziz Ahmadieh)

---

[1] F. E. Hauser, P. R. Landon, and J. E. Dorn, Fracture of Magnesium Alloys at Low Temperatures, Trans. AIME 206, 589 (1956).

g. Theory for Deformation by the Peierls Mechanism

The Peierls mechanism for deformation, which appears to be rate-controlling for low-temperature deformation of all bcc metals and for prismatic slip in Ag-Al (33 at. %) and Li solid solutions in Mg (and perhaps other crystals, particularly those containing some eovalent bonding), is not yet well formulated. Seegar's analyses and those of Lothe and Hirth are directed more at elucidating damping capacity and the Bordoni peaks. A more accurate theoretical approach to determining the kink energy and the activation energy for the formation of a stable dislocation loop under applied stresses over the saddle point of the reaction path has been calculated. Additional theoretical advances relative to formulation of the strain-rate laws as a function of stress and temperature will be attempted. The theory will be checked with experimental evidence. (With Stanley Rajnak)

h. Dynamic Behavior of Dislocations

As described in the preceding sections, a new viscous-drag mechanism on moving dislocations, giving greater restraining forces than can be accounted for by phonon-dislocation interactions, has been shown to be operative at high stresses and high dislocation velocities. More accurate data will be obtained to ascertain how this effect varies with strain rate and temperature in polycrystalline pure Al, in an attempt to arrive at the physical origin of this mechanism. (With Frank E. Hauser, Mahadeo Patell, and Jim D. Mote)

i. Low-Temperature Dynamic Recovery

Inorder to shed more light on the cold-worked state of metals, the effect of creep straining at low temperatures on the recovery of severely cold-worked polycrystalline Al will be studied. (With Abraham Rosen)

j. Recovery of Creep-Induced Substructures

The present contract under Wright Air Development Division will be transferred to LRL (AEC sponsorship) on March 31, 1963. Several reports have already been submitted on this contract. At present two additional reports are being prepared. At high stresses the recovery of the creep behavior in the cross-slip region has an activation energy of 28,000 cal/mole, which equals that for creep by cross-slip. Recovery under low stresses during which no measurable creep takes place occurs by some alternative process that has an activation energy of about 70,000 cal/mole. Similarly, in the higher temperature region where creep takes place by the motion of jogged screw dislocations and the climb of edge dislocations, the recovery of the substructure under the higher stress ranges has a value of 35,000 cal/mole just as for the creep itself. But when the stress is so low that no detectable creep accompanies recovery, the activation energy for recovery equals again about 70,000 cal/mole. The low-stress recovery has an activation energy that is about twice that for self-diffusion, but it is not yet certain whether or not a double-vacancy mechanism is responsible for this recovery. The extension of these investigations will involve uncovering more details on the recovery, also electron-microscopic investigations of the substructure. (With Lou Raymond, Nissen Jaffe, and Howard Bell)

k. Intermetallic Compounds

Dislocation mechanisms of deformation will be investigated for other intermetallic compounds, perhaps representative Laves phases, as soon as the investigations on Ag_2Al and AgMg are completed. (With Amiya Mukherjee)

l. Dynamic Behavior of Dislocations

Because of the great interest in progress achieved thus far, additional studies designed to unravel the dynamic behavior of dislocations will be planned. (With Frank E. Hauser and Jim D. Mote)

D. HIGH-TEMPERATURE REACTIONS

1. THE KINETICS AND MECHANISM OF THE ANATASE-RUTILE TRANSFORMATION

Robert D. Shannon and Joseph A. Pask

Last year it was found that the anatase-rutile transformation was accompanied by a loss of SO_3. The possibility existed that this SO_3 was in solid solution in the TiO_2 and that its evolution somehow controlled the rate of transformation. In order to test this hypothesis, the gas evolved in the early and later stages of transformation was collected and analyzed by means of a mass spectrometer. SO_3 was found in the early period but only a trace remained in the later period. This indicated that the SO_3 was merely adsorbed and in all probability played no role in the transformation. This conclusion was later confirmed by Sullivan and Coleman,[1] who measured the kinetics of the loss of SO_3 and found no relation between these and the kinetics of the transformation. The gas analysis is given below and the presence of CO_2 and H_2O will be noted. The presence of these adsorbed gases at temperatures as high as 1000°C has been observed by other investigators, also.[2-4]

Gases evolved in early stages		Gases evolved in later stages	
H_2O	40%	H_2O	75%
CO_2	14%	CO_2	24.8%
SO_2	35%	SO_2	0.1%

A study of the orientation effects accompanying the anatase transformation indicated that the transformation takes place as an interface reaction, i.e., the reaction proceeds from the surface of a crystal toward the center. The kinetics of the reaction would ideally be determined on single crystals, but no crystals of high purity or quality were available. The presence of the interface reaction and the fact that commercial polycrystalline anatase exists in the shape of almost spherical particles suggested the study of the kinetics of various commercial powders.

---

[1] W. F. Sullivan and J. R. Coleman, Effect of Sulfur Trioxide on the Anatase-Rutile Transformation, in Abstracts of Scientific Papers Presented at the XVIIIth International Congress of Pure and Applied Chemistry, Montreal, Canada, 1961, p. 90.

[2] D. J. C. Yates, Infrared Studies of the Surface Hydroxyl Groups on Titanium Dioxide and of the Chemisorption of Carbon Monoxide and Carbon Dioxide, J. Phys. Chem. 65, 746 (1961).

[3] R. S. McDonald, J. Phys. Chem. 62, 1168 (1958).

[4] J. B. Peri, paper presented at the International Congress on Catalysis, Paris (July 1960).

The kinetics of the transformation have been determined by Sullivan and Cole[5] and Rao.[6] Sullivan and Cole studied colloidal titania produced by a commercial process and concluded that the transformation was a first-order process with an activation energy of 100 to 110 kcal. Rao prepared highly purified anatase and also found a first-order kinetic law but accompanied by an activation energy of 80 kcal. Neither investigator included an attempt to interpret the data in terms of the geometry of the crystals or to suggest a mechanism. It has long been recognized that solid-state reactions, typically represented by sigmoid α-t curves, cannot be considered apart from the geometry of the particles undergoing reaction and the type of nucleation that occurs. Garner has discussed the various possibilities at length.[7]

Numerous authors have also described the effects of impurities on the transformation, some ions being found to inhibit the transformation and others to accelerate it.[8-10] In particular, CuO was found by Ozaki and Iida to lower the effective transformation temperature by 200° to 300°C.[11] The same investigators found that a reducing or vacuum atmosphere greatly accelerated the transformation.

Consequently, a study of the kinetics of the transformation of several commercial powders has been carried out for two purposes: (a) to make a test of various rate laws assuming spherical particles and (b) to provide a basis for studying the effects of CuO and nonoxidizing atmospheres on the rate of transformation.

Three commercial varieties of anatase were obtained: (a) Baker and Adamson, reagent TiO_2, lot R163; (b) The Glidden Co., Zopaque SD, lot 1-K-1; and (c) The American Cyanamid Co., Unitane 0-110, lot 401887. Some of the properties of these materials are summarized in Table I.

---

[5] W. F. Sullivan and Sandford S. Cole, Thermal Chemistry of Colloidal Titanium Dioxide, J. Am. Ceram. Soc. 42, 3, 127-133 (1959).

[6] C. N. R. Rao, Kinetics and Thermodynamics of the Crystal Structure Transformation of Spectroscopically Pure Anatase to Rutile, Can. J. Chem. 39, 498-500 (1961).

[7] P. W. M. Jacobs and F. C. Tompkins, Classification and Theory of Solid Reactions, W. E. Garner, in Chemistry of the Solid State (Butterworths, London, 1955).

[8] C. N. R. Rao, A. Turner, and J. M. Honig, Some Observations Concerning the Effect of Impurities on the Anatase-Rutile Transition, Phys. Chem. Solids 11, 173-175 (1959).

[9] H. Knoll and U. Kühnhold, On the Stability of Anatase, Naturwissenschaften 44, 394 (1957).

[10] C. N. R. Rao and M. P. Lewis, Impurity Effects on the Anatase-Rutile Transformation, Current Sci. (India), 29, 52 (1960).

[11] H. E. Swanson and E. Tatge, "Standard X-Ray Diffraction Powder Patterns," NBS Circular 1, 539 (1953).

Table I. Properties of commercial anatase.

Type	TiO_2 (%)	Anatase (%)	Particle size (μ)	Method of preparation
B&A R163	99.0	99.0	--	--
Zopaque SD	97.3-99.2	100	--	hydrolysis of titanium sulfate solution
Unitane 0-110	99.4	99.7	0.25-0.30	

The samples were prepared by heating in a tube furnace in small platinum crucibles. Material heated in platinum crucibles transformed at the same rate as that in alumina crucibles, showing that no catalytic effects were present.

Analysis of the extent of transformation was performed according to a standard x-ray-diffraction method using integrated peak heights and described fully in Klug and Alexander.[12] A rotating sample holder was used to minimize possible orientation effects. It was not possible to avoid orientation of the long needlelike rutile crystals; thus it was necessary to base the analysis on the anatase content.

Typical sigmoid curves of percent transformation (α) vs time were obtained. The acceleratory period was described by

$$\alpha = Ae^{kt}, \qquad (1)$$

and was valid from $\alpha = 0.0$ to $\alpha \approx 0.50$. This exponential law is derived by Garner by assuming the growth of linear, branching chains of nuclei. The deceleratory period is described reasonably well by several additional expressions,

$$(1 - \alpha)^{1/3} = kt + c, \qquad (2)$$

$$\ln (1 - \alpha) = kt + c, \qquad (3)$$

and

$$[\ln(1 - \alpha)]^{1/3} = kt + c. \qquad (4)$$

[12] H. P. Klug and L. E. Alexander, X-Ray Diffraction Procedures for Polycrystalline and Amorphous Materials (John Wiley & Sons, Inc., New York, 1954).

The data for two of the powders were evaluated by each of these expressions, and the results are presented in Table II. The data for the transformation of the Zopaque SD titania have not yet been evaluated.

Table II. Kinetic data for anatase → rutile transformation.

Anatase source	Expression	Region of validity	E
U-110	ln a = kt + c (1)	0.0-0.5	148 kcal
	(2)	0.5-0.9	186 kcal
	(3)	0.3-0.9	194 kcal
	(4)	0.3-1.0	204 kcal
R 163	(1)	0.0-0.5	109 kcal
	(2)	0.45-0.90	94.6 kcal
	(3)	0.45-1.00	101 kcal
	(4)	0.70-1.00	108 kcal

It does not appear possible to identify the correct rate law from Expressions (2), (3), and (4), since the experimental points fits each expression equally well. This situation is an inherent difficulty in studying powder reactions, particularly those in which the geometry of the crystals is not certain and the particle size is not entirely uniform. However, the fact that the rate expressions allow an ambiguous interpretation of the mechanism does not prevent these reaction curves from being used to study the effects of other variables on the rate.

Electron micrographs will be made on samples at various stages of the transformation. The causes for the variation in activation energies between samples will be explored. The effect of various amounts of CuO on the transformation rates and on the effective transformation temperature will be studied both by the method already employed and by differential thermal analysis. Finally the effect of a nonoxidizing atmosphere on the rate constants will be determined.

2. KINETICS OF THE HIGH-TEMPERATURE HYDROLYSIS OF MAGNESIUM FLUORIDE

Donald R. Messier and Joseph A. Pask

During the past year, work was continued on the determination of the kinetics and mechanism of the high-temperature hydrolysis of magnesium fluoride,

$$MgF_2(c) + H_2O(g) = MgO(c) + 2HF(g).$$

A high-temperature weight-loss apparatus was constructed that is capable of determining weight changes with a precision of better than ± 0.1 mg under vacuum or controlled pressure conditions at temperatures up to 1200°C. Experiments concerning the selection of suitable MgF_2 test specimens were carried out. In addition, an investigation of the dependence of the reaction rate on water vapor pressure was begun.

Previous experiments showed that the hydrolysis of MgF_2 proceeds by reaction at the MgF_2 surface with the subsequent formation of a porous, adherent MgO product layer.[1] The reaction rate thus depends upon the area of the MgF_2 specimen, and it is required that this area be accurately known or at least reproducible from one specimen to the next. In addition, the specimens must be dense and uniform and should be made from high-purity material.

Test reaction runs were made to assess the effects of sample type, surface preparation, and thermal history. An additional objective was to establish the reproducibility of the experimental technique. Hot pressed material supplied by the Bausch and Lomb Optical Company proved satisfactory except for showing a tendency to bloat, blister, and crack when heated rapidly to temperatures above about 800°C. It was decided to determine if this effect could be eliminated by vacuum heat treatment of the sample before reaction, to distill trapped gases. A sample heated from 750°C to 940°C at a rate of 0.5°C per minute showed no visible evidence of bloating. The sample was then reacted at 805°C. The reaction rate was in reasonable agreement with that obtained on a sample not previously heat-treated. This result indicated that neither the heat treatment nor the presence of trapped gases in the untreated sample influenced the reaction rate. Furthermore, it shows that preheat treatment should overcome the bloating problem and allow samples to be reacted at temperatures greater than 805°C. Samples ground with 400-mesh silicon carbide gave rates two or three times the rates for highly polished samples. This was attributed to the greater area of the rough surface.

Examination of the surface of a single-crystal specimen from which the MgO had been removed by treatment with dilute HCl solution showed that substantial surface roughening had occurred during reaction. Re-reaction without repolishing gave a rate higher than the original one. Re-reaction after repolishing gave a rate in agreement with the original one.

The surface roughening may have been a result of an orientation effect whereby the reaction would proceed faster in certain crystallographic directions than in others. Further experiments on samples known to be of different orientation should give evidence of the possible presence and magnitude of such an effect.

Hot pressed specimens were reacted at 805°C at six water vapor pressures ranging from about 2 to 15 mm. The reproducibility was good. The

[1] Donald R. Messier, Kinetics of the Oxidation of Magnesium Fluoride (Ph. D. Thesis), UCRL-9821, Aug. 1961.

rate showed a pressure dependence which could be correlated with the Langmuir adsorption isotherm. This isotherm may be expressed as

$$P = P\theta + k.$$

The θ, which represents the fraction of the surface covered by adsorbed molecules, was replaced by the reaction rate. A plot of P vs P/rate then gave a straight line, indicating that the rate is proportional to the fraction of surface covered.

One might assume that the reaction proceeds by the adsorption of a water molecule followed by its reaction with the MgF_2 surface. Since the adsorption isotherm represents an equilibrium situtation, the above behavior implies that the adsorption step is in equilibrium, and that the rate-determining step is reaction at the surface.

In order to obtain an activation energy for the reaction, rates must be found at several different temperatures and at the same concentration of water vapor. If the above analysis is correct, it indicates that the effective water vapor concentration depends upon surface coverage and not merely pressure. Therefore, the activation energy will have to be obtained from runs at equal surface coverages rather than equal pressure.

In summary it may be concluded that:

(a) The Bausch and Lomb hot pressed material with suitable heat treatment will be satisfactory for future work.

(b) Barring unaccountable orientation effects, the single-crystal material should also be suitable.

(c) The reaction rate is dependent upon the surface polishing procedure. Because a truly smooth surface is impossible to obtain, it was decided to employ the most convenient polishing procedure in order to at least get reproducible surface areas as determined from the external dimensions of the samples.

(d) The pressure dependence appears to follow a Langmuir adsorption isotherm relationship. This result may indicate only that the results fit an equation of this type. Therefore, the present effort is being directed toward obtaining more data on the pressure dependence at different temperatures in order to gain more insight into the reaction mechanism.

3. DIFFUSION OF IRON INTO SINGLE-CRYSTAL MgO

Stuart L. Blank and Joseph A. Pask

The purpose of this study is to determine the reaction and diffusion mechanism involved when powdered iron is in contact with single-crystal MgO. Preliminary diffusion runs were made by heating cleaved crystals of magnesium oxide while in contact with metallic iron. Samples have been

heated in air and vacuo at constant temperatures, in the range of 1000 to 1375°C. The diffusion profile will be determined by use of an electron microprobe analyzer. A high-temperature vacuum furnace is being designed to allow greater accuracy and precision in controlling the time, the temperature, and the atmosphere over the reacting substances.

4. DIFFUSION OF IRON INTO SODIUM DISILICATE GLASS

Marcus P. Borom and Joseph A. Pask

The purpose of this study is to obtain information on the kinetics of the reactions and the solution and diffusion processes that occur at glass-metal and glass-metal oxide interfaces at elevated temperatures. To achieve this goal, systems of sodium disilicate glass in contact with elemental iron and in contact with the various oxides of iron will be investigated under varying conditions of time, temperature, and atmosphere. Electron probe and spectrophotometric techniques are to be employed in analyzing the glass-substrate interface.

A controlled run in argon has been completed with a vacuum-melted cylinder of sodium disilicate glass in contact with wuestite. There is a strong indication that the reaction:

$$Fe^{+2} + Na^{+} = Fe^{+3} + Na(g)$$

occurs in the bulk of the glass.

Future efforts will be directed toward the development of further glass-iron or glass–iron oxide interfaces and their analysis by the aforementioned techniques.

5. GLASS-METAL "INTERFACES" AND BONDING

Joseph A. Pask

Studies on glass-metal bonding based on sessile-drop and adherence types of experiments were completed during the early part of the year. Two papers have been published during the year.[1,2] A chapter entitled "Glass-Metal Interfaces and Bonding" has been submitted for publication in the third

[1] Joseph A. Pask and Richard M. Fulrath, Fundamentals of Glass-to-Metal Bonding: VIII. Nature of Wetting and Adherence, J. Am. Ceram. Soc. 45, 592-596 (1962).

[2] Frances D. Gaidos and Joseph A. Pask, Effect of Glass Composition on the Glass-Iron Interface, Chapter in Advances in Glass Technology, VI International Glass Congress, Washington, D. C., July 1962 (Plenum Press, New York, 1962), pp. 548-565 (UCRL-9956, Jan. 1962).

volume of Modern Aspects of the Vitreous State.[3] It presents a detailed discussion of the broad concepts of a therory on glass-metal bonding that has developed as a result of these studies. A research study is now in progress on the diffusion of iron and iron oxide in sodium disilicate glass.

[3] Joseph A. Pask, Glass-Metal "Interfaces" and Bonding, UCRL-10611, Jan. 1963.

6. RESEARCH IN PROGRESS: JOSEPH A. PASK

See also Section IIB.

7. KINETICS OF THE REACTIONS BETWEEN TUNGSTEN AT HIGH TEMPERATURES AND OXYGEN OR NITRIC OXIDE AT LOW PRESSURES*

Harlan U. Anderson and Alan W. Searcy

The kinetics of gas-solid reactions is not as well understood for low pressures and high temperatures as for more conventional conditions. In the gas-solid reactions usually studied, the rate-determining step is commonly passage of a reactant or product through a surface layer. For tungsten, molybdenum, rhenium, and the platinum metals, however, the oxidation products are relatively volatile. Under low pressures and high temperatures the rate-controlling reaction for such metals must become condensation of the gaseous reactant, formation of a surface complex, or evaporation of a reaction product. In this work low-pressure-high-temperature studies of the reaction of hot tungsten with cold oxygen and nitric oxide are reported.

Samples of tungsten metal in the form of filaments were brought to temperature (1950 to 2600°K) by resistance heating. The known dependence[1] of resistivity on temperature was used to determine the temperature. The pressure range was 10^{-8} to 10^{-6} atm. The gases were passed at a known pressure in the range 10^{-8} to 10^{-6} atm into an evacuated reaction vessel of fixed wall temperature. With the design used, a gas molecule strikes the filament only once before again striking the cold reaction vessel wall, i.e., the gas is at wall temperature. The collision frequency of gas molecules with the filament and the reaction probability per collision could be calculated. The flow of gas was metered by a device designed by Ehler.[2] The rate of oxidation of the filament could be calculated from the rate of weight loss, which in turn could be calculated from the electrical properties with tabulated data of Jones and Langmuir.[1]

The rate of reaction of tungsten with oxygen gas was found to decrease with increasing temperature in the range 2150 to 2600°K, and was found to depend upon the approx 1.26th power of the oxygen pressure in the range 10^{-8} to 10^{-6} atm. In the temperature range 1950 to 2050°K, the reaction probability was independent of pressure, whereas the average rates of disappearance of oxygen molecules and tungsten atoms depended linearly upon the pressure of oxygen gas over the entire pressure range. The reaction probability was found to vary from 0.01 to 0.06 and the reaction rate from 10^{13} to 10^{16} molecules/sec/cm^2. The ratio of the average loss rates of oxygen molecules vs tungsten atoms was pressure-independent, and increased from 1.5 at 1950°K to 2 at 2400°K. Mass-spectrometer experiments indicate the major tungsten oxide gas product to be WO_2.[3] The oxygen disappearance in excess of that

---

*Abstracted from Harlan U. Anderson, Kinetic Studies of the Reactions Occurring Between Tungsten and Gases at Low Pressures and High Temperatures (Ph. D. thesis), UCRL-10135, April 1962. The earlier phases of the research were supported by the Missile and Ordinance Department of the General Electric Company, by the Office of Naval Research, and by the Advanced Projects Research Agency.

[1] H. A. Jones and I. Langmuir, Gen. Elec. Rev. 30, 310, 354, 408 (1927).

[2] R. W. Ehlers, Rev. Sci. Instr. 29, 72 (1958).

[3] J. B. Berkowitz-Mattuck (Arthur D. Little Co., Cambridge, Mass.), private communication, 1962.

required for WO_2 production is believed to reflect emission of oxygen atoms that are consumed by reactions at the cold walls.

The rate of tungsten loss, or WO_2 formation, is

$$R_w = 6.7\times10^{22}\ P^{(1.5-\theta/2)} \exp\left[-\frac{(37.6\theta - 27.6)\times10^3}{RT}\right]$$

in the temperature and pressure ranges of the investigation. This expression simplified to the relationships deduced by Becker et al.[4] at low and at high coverage.

A tungsten filament was heated to more than 2800°K in a pressure of nitrogen at 10^{-6} atm pressure. No evidence of reaction was detected. This result places the limit of reaction at less than 10^{13} molecules/sec/cm^2 in the pressure range of 10^{-8} to 10^{-6} atm of nitrogen and at temperatures up to 2800°K.

The tungsten–nitric oxide reaction is more complicated than the tungsten-oxygen reaction because three gases are present in the reaction vessel (NO, O_2, and N_2). The tungsten surface adsorbs both oxygen and nitrogen atoms. The reaction was separated into two parts: dissociation of nitric oxide, and oxidation of tungsten by nitric oxide or by the oxygen produced by the nitric oxide. Table I shows how the apparent activation energies were found to depend upon the pressure. For nitric oxide decomposition the values are constant (35.2±1.2 kcal/mole). The reaction probability was found to decrease as the pressure increased. This seemed to indicate that the number of sites at the surface available for decomposition depends on the pressure. The observed high rate of WO_2 formation is consistent with the assumption that the surface is completely covered by at least one layer of adsorbed atoms at all temperatures and pressures of the study. More atomic oxygen is evolved by the nitric oxide–tungsten reaction than by the oxygen-tungsten reaction because nitric oxide decomposes much more completely than does oxygen gas. The evolution of atomic oxygen is negligible with either gas below 2000°K. At about 2600°K the rate is about four times as high for the NO-W reaction as for the O_2-W reaction. The rate of decomposition of nitric oxide on tungsten is controlled by the adsorption of nitric oxide molecules on the surface and is given by

$$R_{30} = 4.44\times10^{26}\ P(1-624\ P^{1/2})\ \exp[-35{,}200/RT].$$

The rate of weight loss by tungsten filaments or rate of WO_2 gas formation is controlled by the concentration of oxygen atoms on the surface, and can be represented by

$$R_w(\text{net}) = 8.5\times10^{21}\ P^a \exp\left[-\frac{(1-a)\ 75{,}000}{RT}\right],$$

[4] J. A. Becker, E. J. Becker, and R. G. Brandes, J. Applied Phys. 32, 411 (1961).

Table I. Apparent activation energies for the tungsten-nitric oxide reaction as a function of pressure.

Nitric oxide pressure (atm)	Apparent activation energy (kcal/mole) R_{30}	ϵ	R_{32} (net)	R_W (net)
10^{-6}	36.5	35.1	4.95	0
10^{-7}	37.8	34.7	9.3(2050-2335°K) 30.8(2335-2600°K)	6.2
10^{-8}	33.5	35.1	12.5(2050-2230°K) 37.1(2230-2600°K)	0(2050-2335°K) 22.5(2335-2600°K)
10^{-9}	33.9	---	12.5(2050-2230°K) 51.5(2230-2600°K)	0(2050-2335°K) 54 (2335-2600°K)

R_{30} = rate of disappearance of nitric oxide due to reaction.

R_{32}(net) = average rate of disappearance of oxygen molecules due only to nitric oxide.

R_W(net) = average loss rate of tungsten atoms due only to nitric oxide reaction.

ϵ = reaction probability of a molecule striking the tungsten filament.

where α is the coverage factor.

The activation energy for tungsten oxide solution is dependent upon concentration of atoms on the surface. After Becker et al. we have assumed the activation energy to obey the equation $\Delta H = 75(1-\alpha)$kcal/mole, where $\alpha = 0.15 \exp[8000/RT]$, and 75 kcal/mole is the activation energy for a complete first-layer and negligible second-layer coverage. The rate of tungsten loss from nitric oxide attack is about three times that for the corresponding pressure of oxygen.

8. DEMONSTRATION OF SOME UNRECOGNIZED CHARACTERISTICS OF GAS FLOW THROUGH ORIFICES*

Alan W. Searcy and David A. Schulz

We have completed measurements, by the torsion-effusion method,[1] of the force exerted by tin vapor as it effused from graphite cells at temperatures between 1150°K and 2120°K. The apparent vapor pressure of tin increased with temperature from below 10^{-8} to above 10^{-2} atms. A factor f derived by Freeman and Searcy to correct for the effect of finite lengths of the orifice channel in the range of tin vapor pressures below 10^{-5} atms does bring into agreement, generally to within ± 5%, pressures calculated from forces measured with a variety of orifice diameters and lengths.[2,3] But at higher pressures, the factor no longer brings the measurements into agreement either with each other or with a third-law extrapolation of the low-pressure curve. The divergence presumably occurs because the vapor no longer obeys molecular flow equations.

Over the range 10^{-4} to 10^{-3} atms, the uncorrected pressures show a new, but well-defined, dependence on orifice geometry. Division of each apparent pressure by an empirical constant f' yields the true pressure curve over this range. The data collected for this pressure range demonstrate previously unrecognized gas flow characteristics. The factor f' for these pressures depends only on the orifice length ℓ and not upon the orifice diameter, provided that the diameter is smaller than a critical value d_c. The data fit the equation $(1 - f') = 1.6\ell^{0.7}$.

We conclude that a true pressure can be calculated from the force exerted by a vapor or gas that effuses under these flow conditions by either of two means: An orifice of short channel length may be used, in which case f' becomes nearly unity; or an orifice with finite ℓ and diameter greater than d_c may be used, in which case the data can be corrected by use of the factor of Freeman and Searcy.

---

*Brief of published paper, J. Chem. Phys. 38, 772 (1963).

[1] M. Volmer, Z. Physik Chem. Bodenstein Festband, 863 (1931).

[2] R. D. Freeman and A. W. Searcy, J. Chem. Phys. 22, 762 (1954).

[3] D. A. Schulz and A. W. Searcy, J. Chem. Phys. 36, 3099 (1962).

9. DETERMINATION OF IONIZATION PRESSURE GAUGE SENSITIVITIES WITH A MASS SPECTROMETER*

Harlan U. Anderson

A new method has been devised to calibrate ionization pressure gauges for measurements of pressures of gases other than nitrogen. A mass-spectrometer signal is obtained as a function of the apparent (uncorrected) pressures recorded by an ionization gauge. Since the ionization gauge reads correctly only for nitrogen, the mass-spectrometer signal corresponds to a known pressure at the ionization gauge only for nitrogen. If, however, a high-pressure mixture of nitrogen and some other gas, whose partial pressure has been determined with a manometer or other high-pressure gauge, is allowed to leak into the system to establish a steady-state pressure, the mass spectrometer yields intensities that then correspond to the relative pressures of the two gases. A previous calibration of the mass-spectrometer intensity against pressure for nitrogen makes the absolute nitrogen pressure at the ionization gauge known. The pressure of the second gas then can be determined from the known composition of the mixture. (The pressure ratio of the gauge must be corrected by the ratio of the square roots of the molecular weights of the two gases to correct for their differences in diffusion rates.) The true pressure of this second gas at the ionization gauge relative to the mass-spectrometer signal is therefore known.

The method was tested at pressures near 10^{-4} mm for a Veeco Type RG 21A hot-filament ionization gauge with an RG 75K ionization tube. The results showed rather good agreement with previous determinations of ionization gauge sensitivities.[1,2,3]

*Abstracted from Harlan U. Anderson, Kinetic Studies of the Reactions Occurring Between Tungsten and Gases at Low Pressures and High Temperatures (Ph. D. thesis), UCRL-10135, April 1962, pp. 25-34. Submitted as a Note to Rev. Sci. Instru.

[1]S. Dushman and A. H. Young, Phys. Rev. 68, 278 (1945).

[2]S. Wagener and C. B. Johnson, J. Sci. Instr. 28, 278 (1951).

[3]G. J. Schulz, J. Appl. Phys. 28, 1149 (1957).

10. CALCULATION OF INTEGRAL AND PARTIAL THERMODYNAMIC FUNCTIONS FOR SOLIDS FROM DISSOCIATION PRESSURE DATA*

David J. Meschi and Alan W. Searcy

Thermodynamic stabilities of binary inorganic solids are often determined from dissociation pressure measurements, from partition-function measurements, or from other measurements of the activity of one of the solid-phase components. In calculations of integral free energies ΔG, integral heats of formation ΔH, and integral entropies of formation ΔS from such experimental data for inorganic solids, solid-solution regions are usually assumed to be narrow and phase-boundary compositions are usually assumed not to vary with temperature. However, many inorganic solids of high-temperature interest

*Shortened version of paper (UCRL-10189, April 23, 1962) published in Thermodynamics of Nuclear Materials (International Atomic Energy Commission, Vienna, Austria, 1962), pp. 131-142.

have wide solid-solution ranges whose boundaries vary extensively with temperature so that data obtained from use of these assumptions are of questionable exactness. Fortunately, available data make the assumption unnecessary for a number of metal hydride phases and for some metal oxide and metal nitride phases. Proper treatment of the data yields not only integral thermodynamic quantities as functions of composition, but also partial molal thermodynamic quantities for the second component. This additional information makes possible both more complete understanding of the bonding forces of the phases studied and more precise predictions of chemical behavior. Illustrative calculations were carried out for the uranium-hydrogen and the zirconium-hydrogen systems.

Properties calculated from the data were partial molal Gibbs free energies $\overline{G}_i$, enthalpies $\overline{H}_i$, and entropies $\overline{S}_i$ for each component i, activities and activity coefficients, and the relative Gibbs free energy ΔG^M, the relative enthalypy ΔH^M, and the relative entropy ΔS^M. These relative quantities are the free energy, enthalpy, and entropy of formation, respectively, of 1 gram atom of total material. The pure condensed-phase metals were chosen as standard states for uranium and zirconium. The diatomic gas at 1 atm pressure was chosen as the standard state for hydrogen, but activities were discussed in terms of hydrogen atoms rather than molecules.

Dissociation pressure data for the U-H and Zr-H systems were obtained from various published papers.[1-6] From the dissociation pressures, the activities of the metallic components were calculated by means of a form of the Gibbs-Duhem equation,

$$\ell n\, a_m(B) = \ell n\, a_m(A) - \int_A^B \frac{X_H}{X_m}\, d\, \ell n\, a_H,$$

where a_m and a_H are the activities of metal and hydrogen, respectively, A and B are the two different phase compositions, and X_m and X_H are the mole fractions of metal and hydrogen, respectively. Integration was performed graphically. From the activities, ΔG^M was calculated as a function of composition for both systems at 50-degree intervals from 450 to 650°C. The ΔG^M for the Zr-H system at 600°C is shown in Fig. IID. 10-1. For both systems the relative enthalpies ΔH^M and entropies ΔS^M were then calculated from the ΔG^M values. Both the entropies and enthalpies were found to be essentially independent of temperature in the range under consideration, but strongly dependent on composition, as is shown for the Zr-H system in Fig. IID. 10-1.

---

[1] G. G. Libowitz and T. R. P. Gibb, J. Phys. Chem. 61, 793 (1957).

[2] B. M. Abraham and H. E. Flotow, J. Am. Chem. Soc. 77, 1446 (1955).

[3] E. A. Gulbransen and K. F. Andrew, J. Metals, Jan. 1955, p. 3.

[4] C. E. Ells and A. D. McQuillan, J. Inst. Metals 85, 89 (1956-57).

[5] G. G. Libowitz, J. Nucl. Mater. (to be published).

[6] A. W. Searcy, in Progress in Inorganic Chemistry, Vol. III, F. A. Cotton, Ed. (Interscience Publishers, Inc., New York, 1962), pp. 49-127.

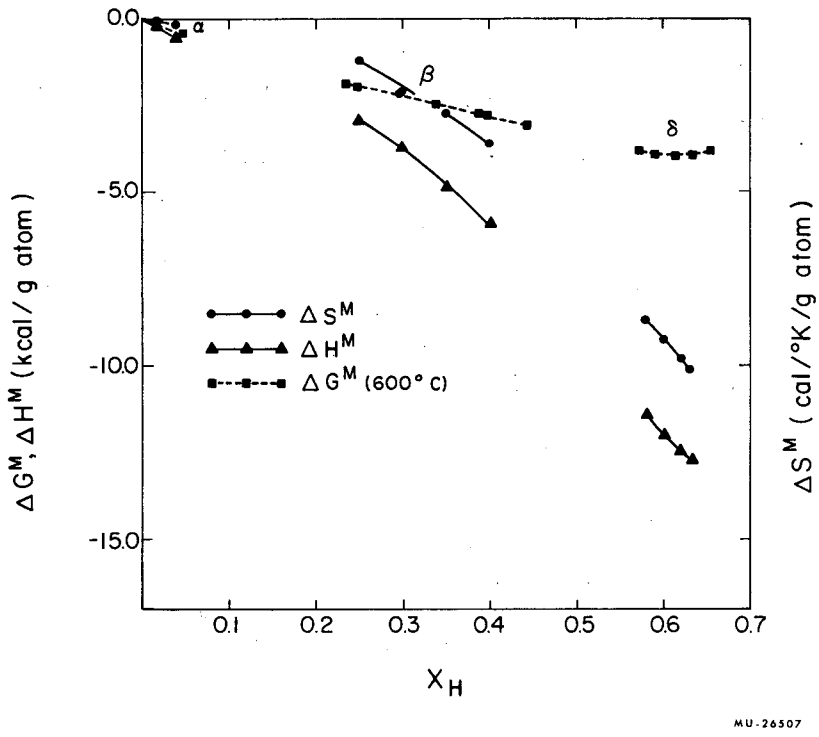

Fig. IID. 10-1. ΔG^M(600°C), ΔS^M, and ΔH^M for the Zr-H system.

The values of ΔH^M for both systems were easily fitted by a quadratic expression. This could not be done with the entropy ΔS^M for the Zr-H system. It was possible, however, to divide ΔS^M into two components, one of which arose from the random occupation of the interstices in the Zr lattice by the H atoms, this part labeled ΔS^p, and the other of which was the residue or "excess" term, labeled ΔS^e. The component ΔS^p was evaluated by the assumption of completely random mixing of vacant interstitial sites and H atoms. The residue or excess term ΔS^e showed the same variation with composition as ΔH^M and could therefore also be expressed by means of a quadratic function.

For each of these metal-hydrogen systems the composition that shows the maximum stability per gram atom relative to the elements in their standard states was found to shift toward lower hydrogen content as the temperature was raised. This shift reflects the increased importance of ΔS^p.

The most striking feature of plots of integral free energies, heats, and entropies of formation per gram atom vs composition for the Zr-H system (Fig. IID. 10-1) is that they closely resemble similar plots for metal-metal systems with intermediate phases of similar solubility ranges. In metal-metal systems, the free energies change so slowly as functions of composition that the curvature that distinguishes single-phase regions from two-phase regions is scarcely perceptible. Although the magnitude of the free-energy change is greater in the zirconium hydrides, the general form of stability variation is similar. The integral heats and entropies change less smoothly from phase to phase, but these thermodynamic quantities appear to reflect mainly the relative quantities of the components combined and only secondarily the structure and bonding characteristics of particular phases. Values of activities or related partial molar quantities, on the other hand, are much more sensitive to phase changes than are integral thermodynamic quantities.

The activities for zirconium and hydrogen have been presented in Fig. IID. 10-2. Examination of activity coefficients reveals what is at first surprising--that Henry's law is a better approximation to describe the activity of hydrogen for the β phase than for the α phase. In the α phase the activity coefficient γ_H varies from 0.25 to 0.36 at 600°C and γ_{Zr} varies from 1 to 0.98. In the β phase over a composition range more than four times as wide, γ_H varies from 7.2×10^{-2} to 6.4×10^{-2} and γ_{Zr} varies from 1.23 to 1.30.

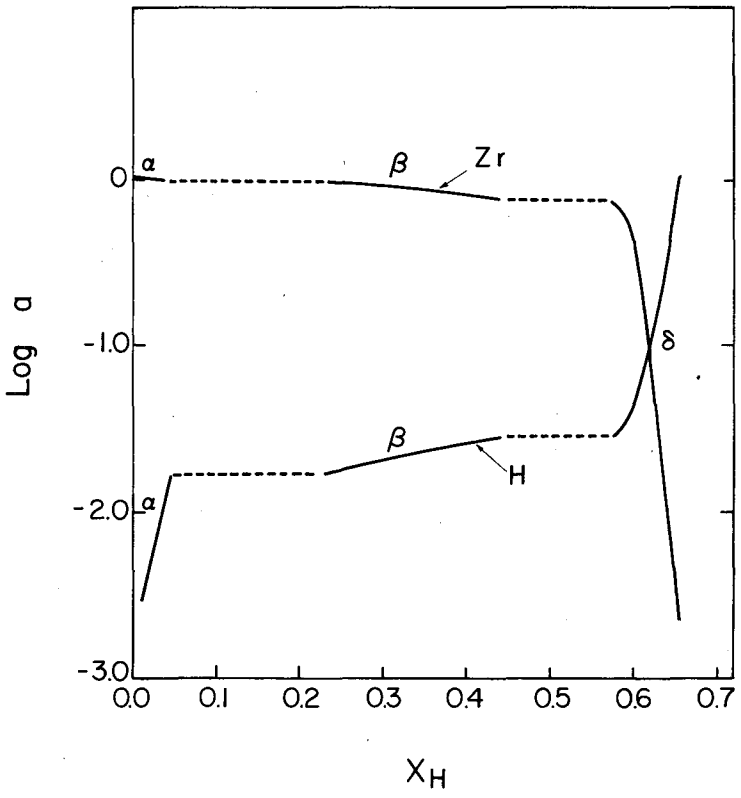

Fig. IID.10-2. Activities of H and Zr in Zr-H system at 600°C.

11. THE PREDICTION OF ACTIVATION ENERGIES FOR SELF-DIFFUSION AND FOR DIFFUSION OF INDIVIDUAL COMPONENTS IN BINARY SOLUTIONS

Louis E. Toth and Alan W. Searcy

Introduction

A general method for predicting activation energies in diffusion in alloys of variable concentration has been developed. The activation energies for self-diffusion and infinitely dilute solute diffusion are treated as limiting cases of the more general case of alloy diffusion. No new empirical constants or principles are introduced in changing from one class of diffusion to the other. This approach differs from previous works on the subject, which usually are limited to correlating experimental data either for self-diffusion or for solute diffusion at very low concentrations and which cannot explain diffusion in concentrated solutions. The results of the method presented here usually agree with the experimental results to within the probable experimental error.

Development of the Equation for Self-Diffusion

For self-diffusion proceeding by a vacancy mechanism the total activation energy for diffusion Q_d is generally accepted to be the sum of the activation energy for motion of the vacancy Q_m and the activation energy for the formation of the vacancy Q_f. The reasonably good agreement between experimental and calculated values with the use of one-parameter equations used in previous correlations implies that Q_f and Q_m are approximately proportional to each other. Treating Q_f and Q_m as separate terms, however, improves the agreement between experimental and calculated values of Q_d and gives better insight into the nature of diffusion.

Determination of the Energy of Movement

We consider Le Claire's expression[1] for the activation energy of vacancy formation,

$$Q_f = k_1 L_s , \qquad (1)$$

to be the most satisfactory for use in correlation of energies of vacancy formation. The expression is reasonable because the heat of sublimation is a measure of the bond strengths. Vacancy formation requires that an atom be transferred from the bulk of the solid to the surface. This process results in a decrease in the number of bonds and in a displacement toward the vacancy of the atoms adjacent to the vacancy. For metals of a given crystal structure, the net energy changes should be a nearly fixed fraction of the energy of sublimation. We still must analyze the relationship of Q_m to measurable thermodynamic or mechanical properties.

[1] A. D. Le Claire, Progr. Metal Phys. 4, 307 (1953).

When an atom and a vacancy exchange positions, or when a group of atoms coordinate their motions to allow a vacancy to migrate, the individual bonds are compressed or extended. The assumption is here made that the potential which governs the motion of the atoms can be approximated by a function symmetric about the mean-relaxed-rest position of the atom. This assumption avoids the difficulties of assigning positions to the atoms surrounding a vacancy, of fixing the direction of their movement, and of distributing the strains among all the processes contributing to vacancy migration.

Starting with the equation for the energy of compression,

$$E_c = - \int P dV,$$

and expressing P in terms of the bulk modulus B_s,

$$dP = - B_s/V dV,$$

we obtain, upon integration,

$$E_c = V_0 B_s [V_f/V_0 - V_f/V_0 \ln V_f/V_0].$$

Here V_0 is a generalized initial volume of all the atoms involved in a particular vacancy migration and V_f is a generalized volume of the same atoms at the point of maximum distortion. The ratio of V_f/V_0 should simply reflect the distortion necessary to move an atom through the position of maximum distortion in the diffusion process. This ratio should be essentially a function of the crystal geometry, and should be constant for a given type of crystal structure. Thus, we can write

$$Q_m = E_c = K_2 V_0 B_s . \qquad (2)$$

The proportionality constant K_2 is dependent upon crystal structure and is adjusted so that V_0 is now the atomic volume.

Another correlation can be found by showing that Q_m and T_m are proportional to each other, so that $Q_m = K_2' T_m$.

Relationship Between Q_m, Q_f, and Q_d

The entire expression for the activation energy of diffusion can now be written as

$$Q_d = k_2 V_0 B_s + k_1 L_s$$

and

$$Q_d = k_2' T_m + k_1 L_s .$$

In order to determine k_1, k_2, and k_2', independent measurements of Q_f and Q_m should be used. Accordingly, k_1 was evaluated from the ratio of the experimental values of Q_f/L_s and a mean value of 0.27 was found for fcc (hcp) elements, and the same value was found for the bcc elements. Similarly, for the fcc elements, k_2' was evaluated from the experimental values of Q_m/T_m and a mean value of 16.0 was found. Since no experimental values for Q_m in bcc elements were available, k_2' for these elements was evaluated from the experimental values of $\frac{Q_d - 0.27\,L_s}{T_m}$ and a mean value of 14.7 was found. The experimental values of $\frac{Q_d - 0.27\,L_s}{B_s V_0}$ were used to determine k_2 in fcc(hcp) and bcc elements, and mean values of 22.6 and 23.8 were found, respectively, when V_0 was taken as the atomic volume expressed in units cm^3/mole and B_s was in $kg/cm^2 \times 10^{-7}$.

Determination of Q_d for Alloys

To discuss alloy diffusion we need only to make the one additional assumption that the strength of the bond connecting atoms A and B is the arithmetic mean of the strength of the bonds found in the pure metals A and B. No new empirical coefficients need be introduced.

Consider an alloy for which X_A and X_B are the mole fractions of A and B atoms, respectively, and z is the coordination number of any atom. The number of A-A bonds for the average A atom will be zX_A, and the number of A-B bonds will be zX_B. Similarly, the number of B-B bonds for the average B atom will be zX_B and the number of A-B bonds, zX_A. The assumption is made that the bond strength is proportional to the heat of sublimation and that the number of vacancies formed by removing A and B atoms from the interior of the crystal and placing them on the surface is proportional to X_A and X_B, respectively. The activation energy needed to form vacancies is then proportional to

$$Z(X_A^2 L_s^A + 2X_A X_B L_s^{AB} + X_B^2 L_s^B),$$

where L_s^{AB} is the arithmetic mean of L_s^A and L_s^B.

When an A atom exchanges places with a vacancy, the number of A-A bonds distorted is $X_A(z-1)$ and the number of A-B bonds distorted is $X_B(z-1)$. As in the case for self-diffusion, we may correlate A-A with $(B_s V_0)_A$ or equivalently with T_m^A, and A-B with $(B_s V_0)_{AB}$ or T_m^{AB}, the arithmetic mean of these quantities for the pure metals A and B. The activation energy for vacancy migration in fcc metals can be expressed for A as

$$Q_m^A = 22.6 \left(X_A (B_s V_0)_A + X_B (B_s V_0)_{AB} \right) \qquad (3a)$$

or

$$Q_m^A = 16.0 \left(X_A T_m^A + X_B T_m^{AB} \right), \qquad (3b)$$

with a similar expression for B. The activation energy is then

$$Q_d^A = 22.6\left(X_A(B_s V_0)_A + X_B(B_s V_0)_{AB}\right) + 0.27\left(X_A^2 L_S^A + 2X_A X_B L_S^{AB} + X_B^2 L_S^B\right)$$

or

$$Q_d^A = \left(16.0\ X_A T_m^A + X_B T_m^{AB}\right) + 0.27\left(X_A^2 L_S^A + 2X_A X_B L_S^{AB} + X_B^2 L_S^B\right),$$

and a similar equation is obtained for the activation energy of the atom B in the alloy.

These correlations have been compared with experimental data for self-diffusion in metals and for alloy diffusion.

The most severe test of the correlations is provided by the data for concentrated solutions. In Table I calculated differences ΔQ between the activation energy for diffusion and activation energies for solvent self-diffusion are listed for silver alloys to illustrate the extent of agreement.

Table I. Comparison of theoretical and experimental values for $\Delta\Omega$ in alloy systems of varied composition (all energies in kcal/mole).

Solvent (at. %)	Solute (at. %)	Tracer	$\Delta\Omega_{calc.}$ [a]	$\Delta\Omega_{calc.}$ [b]	$\Delta\Omega_{exptl.}$
90.5 Ag	9.5 Al	Ag^{110}	- 0.3	- 0.5	- 1.2
93.5 Ag	6.5 Cd	Ag^{110}	- 1.4	- 1.1	- 1.5
		Cd^{115}	- 6.1	- 6.2	- 3.6
72.0 Ag	28.0 Cd	Ag^{110}	- 4.9	- 4.6	- 6.8
		Cd^{115}	-10.0	- 9.7	- 8.2
98.2 Ag	1.8 Cu	Ag^{110}	- 0.3	+ 0.1	+ 0.7
98.5 Ag	1.5 Ge	Ag^{110}	- 0.1	+ 0.2	- 0.1
95.6 Ag	4.4 In	Ag^{110}	- 1.4	- 0.4	- 1.5
		In^{114}	- 5.1	- 6.9	- 3.8
83.3 Ag	16.7 In	Ag^{110}	- 1.5	- 1.2	- 7.9
		In^{114}	- 6.0	- 8.0	- 7.5
99.3 Ag	0.7 Pb	Ag^{110}	- 0.3	0.0	+ 0.6
99.5 Ag	0.5 Pb	Pb^{210}	- 3.3	- 5.1	- 5.4
90.2 Ag	9.8 Pd	Ag^{110}	+ 1.1	+ 1.1	- 0.4
99.1 Ag	0.9 Sb	Ag^{110}	- 0.4	0.0	- 1.6
		Sb^{124}	- 4.3	- 4.3	- 5.8
70.0 Ag	30.0 Zn	Ag^{110}	- 4.8	- 4.3	- 8.1
		Zn^{65}	-10.5	- 8.6	- 8.9

[a] Calculated according to Eq. (3a).

[b] Calculated according to Eq. (3b).

12. ENERGY EXCHANGE BETWEEN COLD GAS MOLECULES AND A HOT TUNGSTEN SURFACE*

Gerald L. De Poorter and Alan W. Searcy

Most kinetic studies of gas-solid reactions at high temperatures and low pressures are conducted with only the solid directly heated and with the bulk of the gas at room temperature. This procedure is adopted because of the experimental difficulty of heating the gas. Unfortunately, the usual assumption that the effective temperature of the gas is that of the solid may be incorrect. The effective temperature of the gas when it reacts with the solid is unknown. Also unknown is the fraction of gas molecules that may revaporize from the surface before reaching a temperature high enough to permit reaction.

Studies of the energy exchange between hot metals and cold, nonreactive gases may reduce the uncertainty on these points by establishing the average energy per molecule--and thus the average effective temperature--acquired before the molecules revaporize.

The object of this investigation was to study the energy exchange between cold gas molecules and a hot tungsten surface. The average temperature reached by the gas molecules before revaporization was calculated from measurements of energy exchanged.

Apparatus and Experimental Methods

A 5-mil tungsten filament was suspended in the form of a loop in an evacuated vessel with a background pressure of 2×10^{-6} mm Hg. Filament temperatures between 1700 and 2500°K were obtained by resistance heating. Temperatures were determined from the electrical properties of tungsten. The interaction of the tungsten surface with helium, neon, argon, nitrogen, carbon dioxide, and oxygen was studied at 0.1 to 10 μ pressure.

The amount of energy exchanged was determined by measuring the power loss from the filament to the gases. From this information, the thermal accommodation coefficients of the gases were calculated.

Results and Conclusions

The experimental results showed that: (a) the power loss to the gas molecule is proportional to the gas pressure, and (b) the power loss is nearly independent of the filament temperature over the range studied.

The results can be interpreted in terms of a process suggested by Gomer and Meyer[1] to explain interaction of gases with graphite. The impinging gas molecules are first physically adsorbed, then heated until they gain sufficient thermal energy to overcome the attractive forces of the tungsten surface. On the average, the gas molecules then "desorb" at a certain

*Abstracted from De Poorter's M. S. Thesis, UCRL-10504, Nov. 1962.

[1]R. Gomer and L. Meyer, J. Chem. Phys. 28, 617 (1958).

"critical" temperature that is independent of the filament temperature. The critical temperatures calculated for the gases used in this investigation are 356°K for helium, 386°K for neon, 442°K for argon, 449°K for nitrogen, and 520°K for carbon dioxide. The variation in critical temperature is consistent with the expected variation in van der Waals attractions of the gases for the surface.

13. RESEARCH IN PROGRESS: ALAN W. SEARCY

a. An experimental study of the kinetics and thermodynamics of sublimation of zinc oxide, with and without zinc vapor present, has been completed and the data are being evaluated. (With Donald F. Anthrop)

b. An experimental study of the kinetics and thermodynamics of gallium nitride sublimation has been completed and an analysis of the data is in progress. (With Zuhair A. Munir)

c. A study of the thermodynamics and kinetics of evaporation of indium sesquisulfide has been completed. A mass spectrometer has been used to measure the partial pressures of the principal vapor species, In_2S and S_2, as functions of temperature and composition in the In_2S_3 phase solid solution. Data are being analyzed. (With Alan R. Miller)

d. An experimental study of the evaporation of stannic oxide is nearing completion and preliminary work has been initiated on the study of kinetics and thermodynamics of evaporation of beryllium nitride. (With Clarence L. Hoenig)

e. A study of the dissociation pressure of aluminum phosphate is nearing completion. Additional mass spectrometer work must be done to evaluate the relative importance of the variety of phosphorous oxide vapor species that have been observed . (With Lies N. Finnie)

f. Modification of three different systems for measurements of vapor pressures by the torsion-effusion method has been completed. Two of these systems will be used initially to measure the vapor pressures of strontium and barium fluorides. The third will be used for thermodynamic and kinetic measurements on solids whose sublimation behavior is proved interesting by preliminary screening experiments. (With Lies N. Finnie, Bruce A. Boyer, Patrick E. Hart, and Bette Blank)

g. A mass spectrometer study of vapor species significant to the metallurgy of steels has been initiated. An attempt to improve the thermodynamic data for CS and HS will be made. (With John Chipman, David J. Meschi, and Charles Washburn)

h. The equipment for use in studies of the kinetics of reaction of metals at high temperatures with gases at low pressures is being rebuilt. The apparatus will be used to study the kinetics of reaction of reaction of rhenium with oxygen

and probably with nitric oxide. (With Gerald L. De Poorter)

i. A theoretical study is being made of partial molal quantities in solid phases of several metal oxide systems. (With Lies N. Finnie)

E. THERMODYNAMICS OF METALS AND ALLOYS

1. EVALUATION OF THERMODYNAMIC DATA FOR METALS AND ALLOYS

Ralph Hultgren and Raymond L. Orr

The compilation and critical evaluation of all published thermodynamic data for metallic elements and binary alloy systems have been completed. This project has been in progress for several years, with support provided by grants from the AEC as well as from a number of industrial sponsors prior to assumption of support by the IMRD. The goal of this effort has been the critical evaluation of all pertinent available data, eliminating those which were demonstrably incorrect and presenting the apparently valid data in an easily usable form. For many alloy systems the reinterpretation of available data has made a more substantial contribution to existing knowledge than could have been made in a more expensive or time-consuming experimental study.

A book, Selected Values for the Thermodynamic Properties of Metals and Alloys, incorporating the results of the evaluations, is scheduled for publication in April 1963 by John Wiley & Sons. Tables of selected values with estimated uncertainty limits, together with discussions and analyses of the experimental data, are given for 63 metallic elements and 168 binary alloys, in 942 pages of text.

For the elements, the following properties are tabulated as completely as the available data permit:

Low-Temperature Data: C_P from 0° to 298.15°K, including data for the superconducting state and the electronic contribution; $H_{298}-H_0$ and S_{298} for both the condensed and gas phases at 298.15°K.

High-Temperature Data: C_P, H_T-H_{298}, S_T-S_{298}, and $(F_T-H_{298})/T$ from 298.15°K to the boiling temperature for the condensed and gas phases; values of T, ΔH, and ΔS for all allotropic transformations and for fusion.

Vapor Pressure Data: Values of $\Delta H_{V\,298}$ calculated from each investigation and the selected value; values of the equilibrium vapor pressure, P, and of ΔF and ΔH of vaporization from 298.15°K to the boiling temperature.

The properties generally tabulated for each alloy phase are the integral free energy (ΔF), heat (ΔH), entropy (ΔS), excess free energy (ΔF^{xs}) and excess entropy (ΔS^{xs}) of formation, and the associated relative partial molar properties ($\Delta \bar{F}_i$, $\Delta \bar{H}_i$, $\Delta \bar{S}_i$, $\Delta \bar{F}_i^{xs}$ and $\Delta \bar{S}_i^{xs}$) for each component. Activities (a_i) and activity coefficients (γ_i) are also tabulated for convenience. Where the data permit, values of ΔC_P and $\Delta \bar{C}_{Pi}$ are given. Additional properties such as heat contents (H_T-H_{298}), entropies (S_T-S_{298}), and heats of fusion or transformation are given where they are known.

The evaluation project will be continued, and reevaluation and extension of the selected values will be a continuing process as new data become

available. A new Termatrex system of bibliography coding and searching is now being installed, which will greatly improve the efficiency of these operations in future work.

2. HEATS OF FORMATION OF ALLOYS

Ralph Hultgren and Raymond L. Orr

A project for the study of alloy thermochemistry has been under way for several years with the support of the U. S. Army Research Office (formerly the Office of Ordnance Research). This work is being continued under IMRD support. The basic aim of this program is the measurement and interpretation of thermodynamic data for representative alloy systems in an attempt to draw conclusions of general validity on metallic bonding in alloys. The primary experimental effort has been directed towards the measurement of heats of formation of binary alloys, as this property provides a direct measure of the difference between bonding energy in the alloy and that in the pure metals from which it was formed. A liquid tin solution calorimetric designed to make such measurements has been developed into an extremely reliable and precise apparatus, and studies have been conducted on a large number of representative alloy phases. Two papers pertaining to thermodynamic aspects of the gold-nickel system[1] and the silver-zinc system[2] were published in the past year.

[1] Gene F. Day and Ralph Hultgren, J. Phys. Chem. 66, 1532 (1962).

[2] R. L. Orr and J. Ravel, Acta Met. 10, 935 (1962).

3. VAPOR PRESSURE MEASUREMENTS ON ALLOYS

Ralph Hultgren and Prodyot Roy

An apparatus has been developed for measuring the equilibrium vapor pressures of solid and liquid metals up to 1900°K by the Knudsen technique for the purpose of determining the activities of alloy components. Preliminary measurements on several pure metals have proved successful. Measurements are now being made of the vapor pressures of Mn in a series of Fe-Mn alloys from X_{Mn} = 0.0 to 1.0 at 1200° to 1400°K in order to determine the activity of Mn as a function of composition and temperature. The initial results for X_{Mn} = 0.09 and 0.19 show the activity of Mn in these alloys to be virtually ideal at 1400°K and to have only a small negative deviation from ideality at 1200° to 1300°K.

This work has been supported by the U. S. Army Research Office and will be continued under the IMRD.

4. HEAT CAPACITY OF LIQUID METALS AND ALLOYS

Ralph Hultgren and Raymond L. Orr

The purpose of this project is to determine accurately the heat capacities of representative liquid metals and alloys. Such data will contribute to the present meager knowledge of the behavior of the liquid metallic state and should aid in interpretations of liquid metal structures. A particularly simple method of making these usually difficult measurements has been developed, using the slightly modified liquid tin solution calorimeter. Data have been obtained for liquid Bi, In, and Sn, and a paper giving the results for a liquid In-Sn alloy was published in the past year.[1] Similar measurements are now in progress on the equatomic Bi-In alloy.

This work has been supported by the U. S. Office of Naval Research and will be continued under the IMRD.

[1] Raymond L. Orr, Henri J. Giraud, and Ralph Hultgren, Trans. Am. Soc. Metals 55, 853 (1962).

5. HEAT CONTENT MEASUREMENTS

Ralph Hultgren and Raymond L. Orr

A Bunsen type calorimeter using diphenyl ether as the working substance is being used to measure high temperature heat contents of metals and alloys from 300° to 1400°K. Such heat content and derived heat capacity data are necessary for extending values of other thermodynamic properties measured at a single temperature to other temperatures of interest. The data are also often of interest in themselves in studies of many phenomena characteristic of alloys. Data have been obtained for a large number of metals and alloys. Two papers published in the past year resolved previous uncertainties in the thermal properties of Fe[1] and Pt[2]. Measurements have just been completed for Hf, for which no previous heat content data existed.

This work has been supported by the U. S. Air Force Office of Scientific Research and will be continued under the IMRD.

[1] Philip D. Anderson and Ralph Hultgren, Trans. AIME 224, 842 (1962).

[2] W. B. Kendall, R. L. Orr, and Ralph Hultgren, J. Chem. Eng. Data 7, 516 (1962).

6. DILATIONAL CONTRIBUTION TO HEAT CAPACITY

Ralph Hultgren and Y. S. Austin Chang

Heat capacities of solids and liquids are measured at constant pressure (Cp), while theories of heat capacity (Debye, electronic, etc.) apply to heat capacity at constant volume (Cv). The difference in the two quantities, the dilation contribution,

$$Cp - Cv = 9\alpha^2 VT/K,$$

where

α = linear coefficient of expansion,

V = volume,

T = temperature, °K,

K = compressibility,

is small below room temperature, but becomes important at elevated temperatures.

Because K is not known above room temperature for most metals and alloys, the value of Cp - Cv is hard to estimate.

Experiments have been completed under sponsorship of the Office of Scientific Research of the U. S. Air Force whereby longitudinal and transverse velocities of sound in copper and alpha brasses have been measured up to about 500°C by means of a sonic echo device. From these values the compressibility can be calculated, and Cp-Cv has been found to be as much as 18% of the total heat capacity at the highest temperatures of measurement.

7. RESEARCH IN PROGRESS: RALPH HULTGREN

Thermodynamics of Semiconducting Compounds

a. Thermodynamic properties of binary alloy systems involving semiconducting intermediate phases are to be determined. Measurements of heat contents, heats of fusion, and heats of formation of solid and liquid phases present in the systems In-Sb, Ga-Sb, Al-Sb, In-Bi, In-As, and In-P will be undertaken. These data, supplemented by measurements of electrical conductivity, will be interpreted in terms of existing models in the theory of alloy phases, and new models, characteristic of semiconducting systems, will be derived.

b. A diphenyl ether calorimeter is available for measurements on solid phases with low vapor pressure. Construction of a second diphenyl ether calorimeter, for measurements on liquid phases and on solid phases with high vapor pressures, is nearing completion.

c. The studies of the dilational contribution to the heat capacities of solids, using sonic technique, will be continued.

III. REACTOR MATERIALS ENGINEERING

1. DIFFUSION OF FISSION GASES IN CERAMIC FUEL BODIES

Stephen Lowe, Donald R. Olander, Thomas H. Pigford, Firooz Rufeh, and Hagai Shaked

Part 1

The lattice diffusion coefficient of Xe^{133} in cast uranium monocarbide was measured in postirradiation anneal experiments in the temperature range 1000°C to 2000°C.[1] Cylindrical specimens, 5×5 mm in size, were irradiated in evacuated pyrex capsules in the Livermore pool type reactor. Irradiation levels ranged between 6×10^{14} and 3×10^{15} n/cm^2. The irradiated specimen contained in a tungsten cup was annealed isothermally in an evacuated induction chamber for about 12 hours. Xe^{133} released from the annealed specimen was adsorbed on charcoal at liquid nitrogen temperature. The charcoal was continuously monitored with a scintillation detector during the anneal. Total Xe^{133} content of the specimen was determined by melting the specimen and collecting the xenon on the charcoal trap. From these data fractional release was computed as a function of time.

In calculating D, the "conventional" analysis which has been applied in previous experiments[2,3,4] and in which a uniform concentration of Xe^{133} at the start of the anneal is assumed, was replaced by a new analysis. In the new analysis account was taken of the nonuniformity in the concentration of Xe^{133} at the start of the anneal due to the recoil release during irradiation prior to the anneal.

This was the first time that the diffusion coefficient of Xe^{133} in UC was measured above 1400°C, and it was found that the diffusion coefficient of specimens consisting of large grains (700 to 1000 microns) and for the range 1000°C to 2000°C was best approximated by

$$D = (1.17 \pm 0.16)\ 10^{-6} \exp\left(-\frac{54900 \pm 1200}{RT}\right),$$

where the units of D are cm^2/sec and RT is in cal/mole. Specimens with small grains (20 to 150 μ) exhibited the same diffusion coefficient above 1500°C. Below 1500°C results varied widely, with the latter specimens indicating dependence on grain size and hence existence of appreciable grain-boundary diffusion.

---

[1] Hagai Shaked, Diffusion of Xenon in Uranium Monocarbide (Thesis), UCRL-10462, Dec. 1962.

[2] Allan Auskern and Yasutaka Osawa, Xenon Diffusion in Uranium Carbide Powder, BNL-6012, Ed., 1960.

[3] J. Belle, Uranium Dioxide; Properties and Nuclear Applications, (Division of Reactor Development, AEC, Washington, 1961).

[4] R. Lindner and H. Matzke, Z. Naturforsch. 14a, 1074 (1959).

Results of this experiment (as represented by the above equation) are one order of magnitude lower than those obtained by Lindner and Matzke[3] for UC particles, and two-and-a-half to three orders of magnitude higher than those obtained by Auskern and Osawa for UC powders.[2] Values of D obtained here are of the same order of magnitude as obtained for the diffusion of Xe^{133} in urania.[3,4]

Part 2

In a postirradiation anneal experiment[1, 3] one measures the rate of release of a specified fission gas, which is referred to in this paper as the "tracer." The measured quantity is the fractional release f, and is

$$f = \int \vec{dr}[C(\vec{r}, 0) - C(\vec{r}, t)] / \int \vec{dr}\, C(\vec{r}, 0), \qquad (1)$$

where integration is carried over the volume of the solid specimen. The concentration of tracer atoms, C(r, t), in a solid of an arbitrary shape is given by

$$\frac{\partial C}{\partial t} = D\nabla^2 C, \qquad \text{for } t < 0, \qquad (2a)$$

$$C(\vec{r}, t)\big|_{\text{surface}} = 0, \qquad \text{for } t \geq 0, \qquad (2b)$$

$$C(\vec{r}, 0) = S(\vec{r}), \qquad (2c)$$

where D is the diffusion coefficient. An important property of the solution of Eq. (2) is that it depends on the time variable through the product Dt. The term $(Dt)^{1/2}$ has the dimensions of length and is called the diffusion length.

Asymptotic expansion of C(r, t) for small t may be obtained from a term-by-term inversion of the proper infinite-series expansion of the Laplace transformation of C(r, t). The asymtotic expansion converges quickly if the diffusion length is small compared with the dimensions of the solid. Berthier[5] used this method to solve Eqs. (2) in the special case S(r) = constant, and obtained for the fractional release

$$f = \frac{2}{\sqrt{\pi}} \frac{F}{V} (Dt)^{1/2}, \qquad (3)$$

where terms of the order of $[\frac{2F}{V}\sqrt{Dt}]^2$ were neglected. This solution has been used in analyzing many other postirradiation anneal experiments.[3]

During irradiation of a solid specimen of fuel fission recoil occurs, and a region that is below the surface by the distance of one recoil range appears depleted of tracer atoms. When diffusion length is large compared with the recoil range the assumption S(r) = constant still yields a good approximation (in calculating f). But when diffusion length is of the order of magnitude

[5] G. Berthier, J. Chim. Phys. 49, 527 (1952).

of the recoil range or less this assumption yields a poor approximation.

The correct distribution of tracer atoms at the end of irradiation (assuming no diffusion) near a flat surface[1] is

$$\begin{aligned} S(z) &= \frac{C_o}{2\mu}(\mu+z) && \text{for } 0 < z < \mu, \\ &= C_o && \text{for } \mu < z . \end{aligned} \tag{4}$$

where the origin is assumed to be at the surface and μ is the recoil range.

If we restrict the solids to those of such surface that the radius of curvature is large compared with both the recoil range and the diffusion length, we may then apply the flat-surface condition to the solid as follows: The solid with surface area F and volume V is replaced by an equivalent slab with a thickness equal to 2V/F. Equations (2) and (4) are solved in slab geometry and the fractional release is found to be[1] (for a solid of arbitrary shape except for the above restrictions)

$$f \approx \psi \frac{2F}{V}\frac{1}{\sqrt{\pi}}(Dt)^{1/2}, \tag{5}$$

where

$$\psi = \frac{1}{2}\left[1 + \frac{\sqrt{\pi}}{\mu/2\sqrt{Dt}}\left(\frac{1}{4} - i^2\mathrm{erfc}\frac{\mu}{2\sqrt{Dt}}\right)\right], \tag{6}$$

and terms of the order of $(\frac{2F}{V}\sqrt{Dt})^2$ are neglected. Here ψ is the function by which the fractional release in which recoil was neglected has to be multiplied in order to obtain the fractional release in which recoil was taken into account. The integral error function $i^2\mathrm{erfc}(x)$ is tabulated in Reference 6.

Inthoff and Zimen proposed an approximate numerical solution.[7] Using their method, we obtained a correction function equivalent to ψ which was smaller than ψ by a factor of $\sqrt{\pi}/2$ throughout the range of $\mu/2\sqrt{Dt}$. In the limits:

$$\frac{\mu}{2\sqrt{Dt}} \to 0 \qquad \psi \to 1$$

$$\frac{\mu}{2\sqrt{Dt}} \to \infty \qquad \psi \to \frac{1}{2}$$

In both limits f becomes identical with the solutions of Bertheir.[1, 5]

---

[6] H. S. Carlshaw and J. C. Jaeger, "Conduction of Heat in Solids", 2nd ed., 485, Oxford (1959).

[7] K. Inthoff and K. E. Zimen, Trans. Chalmers Univ., Gothenburg, No. 176, 1956.

2. LIFETIME AND BURNUP OF NUCLEAR FUELS*

J. R. L. de Ladonchamps and Thomas H. Pigford

Analytic methods have been developed for predicting the reactivity lifetime and burnup of nuclear fuels.

The analysis applies to those nuclear fuels whose changes in composition with time are due solely to neutron-absorption processes, so that the composition of any fuel species is a function only of the integrated flux time of its irradiation exposure. Reactivity lifetime can then be expressed as a function of the appropriate average flux time of the fuel at the end of the irradiation. Local and average burnup of the irradiated fuel can then be calculated without necessarily specifying the magnitude of the irradiation flux or the power program of irradiation.

A generalized perturbation method is developed which allows the calculation of the above results, taking into account spatial variation in neutron flux within the reactor and changes in this spatial variation during irradiation as a result of changes in fuel composition. Tabulated functions allow hand computations for the batch irradiation of fixed fuel in cylindrical or spherical reactors with uniform initial fuel loading. Such functions also apply to radial mixing and graded irradiation.

The perturbation method is most easily applied to the one-group diffusion model, but it is extended to the multigroup model with only slight modification for reactors with energy-independent boundary conditions.

An exact analytical solution for the reactivity lifetime and fuel burnup has been developed which can be used for continuous fueling schemes, provided the one-group model applies and provided the characteristic excess neutron production of the fuel varies as a quadratic function of the flux time of irradiation exposure. A comparative study of various continuous fueling schemes has been made for a fuel with typical properties.

The validity of the approximate solutions is determined by comparing results of the second-order perturbation method with the exact solutions of the corresponding equations. Numerical computations on high-speed digital computers have been used to obtain exact solutions of those equations which could not be solved analytically by means of elliptic functions.

The computational procedure here developed allows survey studies comparing the performances of various fuels and various reactor designs. Also, it predicts the magnitude of the errors to be expected when we use various models of neutron behavior (one-group, two-group, continuous slowing down) in more elaborate computations on high-speed digital computers.

---

*Abstract of J. R. Lefevre de Ladonchamps, Reactivity Lifetime and Burnup in Nuclear Fuels (thesis), UCRL-10614, Jan. 1963.

3. RESEARCH IN PROGRESS: THOMAS H. PIGFORD

a. Particle-Voltaic Effect in Semiconductors

The conversion of kinetic energy of heavy charged particles to electrical energy by interaction with semiconductor junction diodes is under investigation. Analytical studies of the excitation of electrons and ionization resulting from α particles have led to a prediction of the operating characteristics of an alpha-voltaic device. The energy-conversion efficiency depends primarily upon the ratio of the average energy ϵ used in producing an electron-hole pair to the energy gap of the semiconductor. Experimental and theoretical determination of ϵ for Si and GaAs are under way. The effects of radiation damage upon these properties are also being studied. (With John Poksheva and Lawrence Posey)

b. Thermionic Emission by Refractory Materials

Glass cells are being used to evaluate the effectiveness of cesium, rubidium, and potassium for neutralizing the electron space charge between the electrodes of a thermionic converter. The average work function of the polycrystalline tungsten emitter is large enough to insure surface ionization for each of the three gases.

Variable-spacing flat-plate diodes are being used to study the thermionic-emission and surface-ionization properties as a function of crystallographic orientation. Techniques have been developed for bonding single crystals of tungsten to tantalum cathode cylinders. The bond has been tested at 2500°C through several thermal cycles. (With Homer C. Carney, Osama Dabbousi, Daniel Koenig, and Ronald Wichner)

MUTUAL DIFFUSION IN DILUTE BINARY SYSTEM*

Donald R. Olander

The absolute-reaction-rate theory of liquid diffusion has been amended to account for the effects of solute-solvent interaction. This requires estimation of the difference between the free energies of activation for the viscous and the mutual diffusion processes. The mechanisms of these two processes are subdivided into volumetric and kinetic contributions, the former involving hole formation in the solvent, and the latter involving the motion of the diffusing species from its equilibrium site. Examination of published mutual diffusion data indicates that the total activation energy is approximately equally divided between these two steps. The method results in a correction to standard absolute-rate theory which significantly improves the theory for use in predicting the diffusion coefficient from solvent and solute viscosities and molar volumes.

*Brief of a published paper, A. I. Ch. E. Journal 9, 207 (1963).

5. A HYDRODYNAMIC MODEL OF MASS TRANSFER IN A STIRRED VESSEL EXTRACTOR*

Donald R. Olander

The flow patterns generated by the rotation of stirrer bars in the two immiscible liquids in a stirred vessel extractor have been approximated by a simplified model. Each phase was divided into two regions: the core region, which is the cylindrical volume swept out by the stirrer bars, and the outer annular region, which comprises the remainder of the phase. The flow in the core region has been assumed to be equivalent to that generated by an infinite body of fluid in solid-body rotation over a surface rotating at a slower rate. The axial velocity in the outer annulus is then obtained by a simple material balance. Knowledge of the velocity profile in this latter region permitted a direct solution of the diffusion equation, which in turn resulted in a purely theoretical mass-transfer correlation for this extraction device.

Comparison of the experimental data and the theoretical predictions showed the latter to be approximately 35 to 50% too low; this was considered sufficiently close agreement, however, to warrant tentative acceptance of the flow model upon which the theoretical predictions were based. Two important conclusions that follow from the model are: (a) a turbulent transport mechanism need not be postulated for extraction in a stirred vessel of the type considered here, since a purely laminar flow model comes quite close to reproducing the observed extraction rates; and (b) rippling of the interface does not result in pronounced increases in the mass-transfer coefficient, since the flow model was based upon a planar interface, and the experimental data represent various degrees of interfacial rippling.

*Abstract of a published article, Chem. Eng. Sci. 18, 123 (1963).

6. ANALYSIS OF LIQUID DIFFUSIVITY MEASUREMENTS TO ACCOUNT FOR VOLUME CHANGES ON MIXING--THE DIAPHRAGM CELL*

Donald R. Olander

The method of computing differential diffusion coefficients in liquids from diaphragm cell data has been reexamined to allow for volume changes upon mixing. The diffusion coefficient upon which the new calculation method is based is of greater theoretical interest than the common Fick diffusivity. The difference between the two is usually small in diaphragm cell work, but deviations as large as 6% have been found for the ethanol-water system.

*Abstract of a paper to be published in J. Phys. Chem.

7. RESEARCH IN PROGRESS: DONALD R. OLANDER

a. An investigation of the graphite-hydrogen reaction at elevated temperatures has been begun. A molecular beam of hydrogen will be directed at a hot graphite slab, and the gasified products analyzed mass spectrometrically. Mass analysis will be employed to identify the primary carbon-hydrogen species resulting from the surface reaction.

b. A study of gas-phase radiation chemistry will be started. The reactant gas will be bombarded with α particles or fission fragments, and the free radicals produced will be measured by electron spin resonance, molecular beam separation in an inhomogeneous magnetic field, or mass spectrometry of a beam effusing from the reaction chamber. The first system to be studied is the reaction NH_3 → hydrazine.

IV. PUBLICATIONS, 1962

Publications of the staff members of the Inorganic Materials Research Division that appeared during the 1962 calendar year are listed below. Most, but not all, of these publications received primary financial support from the Atomic Energy Commission.

Brewer and Associates

Brewer, Leo, "Comments On The Publication Explosion Forum," Bull. Atomic Scientists, 18, No. 4, 36 (1962).

Brewer, Leo, Book review on The Determination of Stability Constants and Other Equilibrium Constants in Solution, by Francis J. C. Rosotti and Hazel Rosotti (McGraw-Hill, New York, 1961), Science 136, 643 (1962).

Brewer, Leo, "Thermodynamic Stability and Bond Character in Relation to Electronic Structure and Crystal Structure" in the book Electronic Structure and Alloy Chemistry of Transition Elements, edited by P. A. Beck (Interscience Publishers, Division of John Wiley & Sons, New York, 1962).

Brewer, Leo, W. T. Hicks, and O. H. Krikorian, "Heat of Sublimation and Dissociation Energy of Gaseous C_2," J. Chem. Phys. 36, 182-186 (1962).

Brewer, Leo and J. Engelke, "Spectrum of C_3," J. Chem. Phys. 36, 992-998 (1962).

Brewer, Leo and S. Trajmar, "Ultraviolet Bands of Magnesium Hydroxide and Oxide," J. Chem. Phys. 36, 1586-1587 (1962).

Brewer, Leo, S. Trajmar, and R. A. Berg, "Analysis of the Ultraviolet System of Magnesium Oxide," Astrophys. J. 135, 955-962 (1962).

Brewer, Leo, C. G. James, R. A. Berg, R. G. Brewer, F. E. Stafford, and G. M. Rosenblatt, "Phase Fluorometer to Measure Radiative Lifetime of 10^{-5} to 10^{-9} Second," Rev. Sci. Instr. 33, 14-50 (1962).

Berg, Robert A., "Measurements of Radiative Lifetimes" (Ph. D. Thesis), UCRL-9954, March 1962.

Meyer, C. B., "The Vibration Spectrum of Trapped S_2," J. Chem. Phys. 37, 1577 (1962).

Connick and Associates

Connick, Robert, with T. Swift, "NMR Relaxation Mechanism of O^{17} in Aqueous Solutions of Paramagnetic Cations and the Lifetime of Water Molecules in the First Coordination Sphere," J. Chem. Phys. 37, 307 (1962).

Swift, Terrence J., "The NMR Relaxation Mechanisms of O^{17} in Aqueous Solutions of Paramagnetic Cations and the Lifetime of Water Molecules in the First Coordination Sphere" (Ph. D. Thesis), UCRL-10274, May 1962.

Dorn and Associates

Dorn, John with S. Mitra, "On the Nature of Strain Hardening in Polycrystal Al and Al-Mg Alloys," Trans. Met. Soc. AIME 224, 1062-1071 (1962)

Dorn, John with R. M. Quimby and J. Mote, "Yield Point Phenomena in Magnesium Lithium Single Crystals," Trans. Quarterly 55, 149-157 (1962).

Wazzan, Ahmed R., "Analysis of Enhanced Diffusivity in Nickel" (Ph. D. Thesis), UCRL-10457, Aug. 1962.

Neumann, J. P., "On the Order in the Hexagonal ζ Phase in the System Silver-Aluminum," Acta Met. 10, 984-5 (1962).

Fulrath and Associates

Fulrath, R. M., and P. L. Studt, "Mechanical Properties and Chemical Reactivity in Mullite-Glass Systems," J. Am. Ceram. Soc. 45, 182-188 (1962).

Fulrath, R. M., and J. A. Pask, "Fundamentals of Glass-to-Metal Bonding: VIII, Nature of Wetting and Adherence," J. Am. Ceram. Soc. 45, 592-596 (1962).

Studt, Perry L., "Mechanism of Gaseous Permeation through Glass, Single-Crystal Silicon and Germanium; and Stress-Enhanced Gaseous Permeation through Alumina Bodies" (Ph. D. Thesis), UCRL-10466, Sept. 1962.

Herschbach and Associates

Herschbach, D. R., "Reactive Collisions in Crossed Molecular Beams," Disc. Faraday Soc. 33, 149 (1962).

Herschbach, D. R., "Comments on Inelastic Collisions," Disc. Faraday Soc. 33, (1962).

Herschbach, D. R., "Internal Rotation and Microwave Spectroscopy," Paper C401, International Symposium on Molecular Structure and Spectroscopy, Tokyo, September, 1962.

Herschbach, D. R., and V. W. Laurie, "Influence of Vibrations on Molecular Structure Determinations. I. General Formulation of Vibration-Rotation Interactions," J. Chem. Phys. 37, 1668 (1962).

Herschbach, D. R., and V. W. Laurie, "Influence of Vibrations on Molecular Structure Determinations. II. Average Structures Derived from Spectroscopic Data," J. Chem. Phys. 37, 1687 (1962).

Herschbach, D. R., and V. W. Laurie, "The Determination of Molecular Structure from Rotational Spectra," Paper C309, International Symposium on Molecular Structure and Spectroscopy, Tokyo, September, 1962.

Herschbach, D. R., and K. R. Wilson, "Reactive Scattering in Crossed Molecular Beams: Na Atoms with Methyl Iodide," Bull. Am. Phys. Soc. 7, 497 (1962).

Herschbach, D. R., and R. N. Zare, "Angular Distribution of Products in Molecular Photodissociation," Bull. Am. Phys. Soc. 7, 458 (1962).

Herschbach, D. R., and R. N. Zare, "Doppler Line Shape of Atomic Fluorescence Excited by Molecular Photodissociation," Bull. Am. Phys. Soc. 7, 553 (1962).

Himmel and Associates

Maher, Dennis, "Formation of Porosity During Diffusion Processes in Metals" (Master's Thesis), UCRL-10383, Sept. 1962.

Jolly and Associates

Jolly, W. L., "Inorganic Chemistry of Qualitative Analysis," J. Chem. Educ. 39, 53 (1962).

Jolly, W. L., "The Use of Electric Discharges in Chemical Synthesis," Chapter in The Technique of Inorganic Chemistry, H. Jonassen, editor (Interscience Publishers, New York, 1962).

Jolly, W. L., "Transparencies by Photographic Reversal," J. Chem. Educ. 39, 83 (1962).

Jolly, W. L., with J. Drake, "Hydrides of Germanium," J. Chem. Soc. 1962, 2807 (UCRL-10013).

Jolly, W. L., and M. Becke-Goehring, "The Synthesis of Tetrasulfur Tetranitride and Trisulfur Dinitrogen Dioxide," Inorg. Chem. 1, 76-78 (1962).

Jolly, W. L., and J. Drake, "Hydrides of Germanium, Tin, Arsenic and Antimony," Inorg. Syn. 7, p. 34 (1962).

Jolly, W. L., with R. Mesmer, "The Exchange of Deuterium with Solid Potassium Hydroborate," J. Am. Chem. Soc. 84, 2039 (1962).

Jolly, W. L., with M. Gold and K. Pitzer, "A Revised Model for Ammonia Solutions of Alkali Metals," J. A. Chem. Soc. 84, 2264 (1962).

Jolly, W. L., and R. Mesmer, "The Hydrolysis of Aqueous Hydroborate," Inorg. Chem. 1, 608 (1962).

Jolly, W. L., with J. Drake, "Preparation of Mixed Hydrides of Silicon, Germanium, Phosphorus, and Arsenic," Chem. Ind. (London) 1962, 1470.

Jolly, W. L., and M. Gold, "Absorption Spectra of Metal-Ammonia Solutions," Inorg. Chem. 1, 818 (1962).

Jolly, W. L., C. Lindahl and R. Kopp, "Electric Discharge Reactions of Phosphorus Trichloride and Germanium Tetrachloride," Inorg. Chem. 1, 958 (1962).

Gold, Marvin, "Infrared Absorption Spectra of Metal-Ammonia Solutions" (Ph. D. Thesis), UCRL-10062, Feb. 1962.

Kopp, Richard, "The Chemistry of Hexachlorodigermane" (Master's Thesis), UCRL-10437, Sept. 1962.

Jura and Associates

Jura, George, and H. Stromberg, "Four Lead Electrical Resistance," Science 138, 1344-1345 (1962).

Mahan and Associates

Mahan, Bruce, with J. P. Doering, "Photoionization of Nitric Oxide," J. Chem. Phys. 36, 669-674 (1962).

Mahan, Bruce, and J. P. Doering, "Photolysis of Nitrous Oxide. II. 1470 and 1830 Å," J. Chem. Phys. 36, 1682 (1962).

Mahan, Bruce, and J. Mandel, "Vacuum Ultraviolet Photolysis of Methane," J. Chem. Phys. 37, 207 (1962).

Myers and Associates

Myers, R. J., and M. D. Harmony, "Infrared Spectrum and Thermodynamic Functions of the NF_2 Radical," J. Chem. Phys. 37, 636 (1962).

Edelstein, Norman M., "A Study of the Kinetics of the Reaction H + 0_2 by Paramagnetic Resonance" (Ph. D. Thesis), UCRL-10108, April 1962.

Muirhead, J. S., and J. A. Howe, "Near-Ultraviolet Absorption Spectrum of Tetrolaldehyde," J. Chem. Phys. 36, 2316-19 (1962).

Olander and Associates

Olander, Donald, "Rotating Disk Flow and Mass Transfer," J. of Heat Transfer 84C, 185 (1962).

Olander, Donald, "The Influence of Physical Property Variations on Liquid-Phase Mass Transfer for Various Laminar Flows," Intern. J. Heat Mass Transfer 5, 765 (1962).

Olander, Donald, "Unsteady State Heat and Mass Transfer in the Rotating Disk - Revolving Fluid System," Intern. J. Heat Mass Transfer 5, 825 (1962).

Olander, Donald, J. T. Holmes, and C. R. Wilke, "Diffusion in Mixed Solvents," A.I. Ch.E. J. 8, 646 (1962).

Olander, Donald, and M. Benedict, "The Mechanism of Extraction by Tributyl Phosphate-n-Hexane Solvents. Part I - Water Extraction," Nucl. Sci. Eng. 14, 287 (1962).

Parker and Associates

Bokros, Jack C., "The Mechanism of the Martensite Burst Transformation in Single Crystal of Iron Containing 31.7% Nickel" (Ph. D. Thesis), UCRL-10415, Sept. 1962.

Parker, Earl R., with S. Feuerstein, "The Effect of Grain Boundaries on the Mechanical Properties of Ionic Crystals," Technical Report No. 5, Series 150, Issue No. 5, Contract AF 49(638) 601, January 1962.

Pask and Associates

Pask, J. A., with F. D. Gaidos, "Effect of Glass Composition on Glass-Iron Interface" in Advances in Glass Technology, VI International Glass Congress, Washington, D. C., July 1962 (Plenum Press, New York, 1962), pp. 548-565.

Pask, J. A., and W. D. Scott, "Purification, Growth of Single Crystals, and Selected Properties of MgF_2," J. Am. Ceram. Soc. 45, 586-7 (1962).

Pask, J. A., and R. M. Fulrath, "Fundamentals of Glass-to-Metal Bonding: VIII, Nature of Wetting and Adherence," J. Am. Ceram. Soc. 45, 592-6 (1962).

Scott, William D., "Deformation and Fracture of Polycrystalline Lithium Fluoride" (Ph. D. Thesis), UCRL-10435, Sept. 1962.

Johnson, Lawrence D., "The Mechanical Behavior of Single and Polycrystalline Lithium Fluoride" (Ph. D. Thesis), UCRL-10468, Sept. 1962.

Pitzer and Associates

Pitzer, Kenneth S., with F. Danon, "Corresponding States Theory for Argon and Xenon," J. Phys. Chem. 66, 583-585 (1962).

Pitzer, Kenneth S., with F. Danon, "Volumetric and Thermodynamic Properties of Fluids. VI. Relationship of Molecular Properties to Acentric Factor," J. Chem. Phys. 36, 425-430 (1962).

Pitzer, Kenneth S., and J. Acrivos, "Temperature Dependence of the Knight Shift," J. Chem. Phys. 66, 1693-98 (1962).

Pitzer, Kenneth S., and R. Gerken, "Silver Oxide: The Heat Capacity of Large Crystals from 14 to 300°K," J. Am. Chem. Soc. 84, 2662 (1962).

Pitzer, Kenneth S., and L. Gregor, "The Silver-Silver Oxide Electrodes; the Entropy of Mercuric Oxide," J. Am. Chem. Soc. 84, 2671 (1962).

Acrivos, J., "Application of the Sideband Technique to Wide-Line NMR Spectra," J. Chem. Phys. 36, 1097-1098 (1962).

Acrivos, J., "Analysis of the $A_3(X_3)_3$ Nuclear Spin System and π-electron Coupled with Hyperfine Splitting Constants in Aromatic Hydrocarbon," J. Mol. Phys. 5, 1-14 (1962).

Acrivos, J., Hyperfine Splitting in Aromatic Free Radicals, Chapter in Electron Spin Resonance, edited by J. Wertz (Reinhold Publishing Corp., New York).

McNamee, Raymond, "Matrix Isolation Studies of High-Temperature Species Group II Chlorides" (Ph. D. Thesis), UCRL-10451, Sept. 1962.

Rajnak, Katheryn E., "Configuration Interaction in the Rare Earths and Its Effect on the Stark Levels of $PrCl_3$ and $GdCl_3 \cdot H_2O$" (Ph. D. Thesis) UCRL-10460, Nov. 1962.

Howe, J. A., with J. S. Muirhead, "Near-Ultraviolet Absorption Spectrum of Tetrolaldehyde," J. Chem. Phys. 36, 2316-19 (1962).

Phillips and Associates

Phillips, Norman, with E. Catalano, "The Low-Temperature Heat Capacities of Antiferromagnetic MnF_2 and CoF_2," J. Phys. Soc. Japan 17, 527 (1962).

Searcy and Associates

Searcy, Alan W., "High Temperature Inorganic Chemistry," in Progress in Inorganic Chemistry, Vol. III, F. A. Cotton, Ed. (Interscience Publishers, Inc., New York, 1962), p. 49-127.

Searcy, Alan W., with David A. Schulz, "Effect of Channel Length on the Force Exerted by Effusing Vapors," J. Chem. Phys. 36, 3099 (1962).

Searcy, Alan W., and L. N. Finnie, "Stability of Solid Phases in the Ternary Systems of Silicon and Carbon with Rhenium and the Six Platinum Metals," J. Am. Ceram. Soc. 45, 268 (1962).

Searcy, Alan W., and David J. Meschi, "Calculation of Integral and Partial Thermodynamic Functions for Solids from Dissociation Pressure Data," in Thermodynamics of Nuclear Materials (International Atomic Energy Agency, Vienna, (1962), p. 131-142.

Searcy, Alan W., and Ray S. Newbury, "The Composition and Properties of the Solid Produced by Reaction of Thorium with Hydrochloric Acid," J. Inorg. Chem. 1, 794 (1962).

Finnie, Lies N., "Structures and Compositions of the Silicides of Ruthenium, Osmium, Rhodium, and Iridium," J. Less-Common Metals 4, 24-34 (1962).

Anderson, Harlan U., "Kinetic Studies of the Reactions Occurring Between Tungsten and Gases at Low Pressures and High Temperatures," (Ph. D. Thesis), UCRL-10135, April 1962.

De Poorter, Gerald L., "Energy Exchange Between Cold Gas Molecules and a Hot Tungsten Surface" (Master's Thesis) UCRL-10504, Nov. 1962.

Sederholm and Associates

Sederholm, Charles H., Richard A. Newmaker and Douglas S. Thompson, "Potential Energy as a Function of CfClBr-CFClBr NMR Measurements," J. Chem. Phys., 37, 411 (1962).

Sederholm, Charles H., with L. Petrakis, "Remarks on J. I. Musher's Comments on Our Paper," J. Chem. Phys. 36, 1087 (1962).

Tobias and Associates

Tobias, Charles, and John S. Newman, "Theoretical Analysis of Current Distribution in Porous Electrodes," J. Electrochem. Soc. 109, 1183 (1962).

Tobias, Charles, and Robert E. Meredith, "Conductance in Heterogeneous Systems," in Advances in Electrochemistry and Electrochemical Engineering, edited by Charles W. Tobias (Interscience Publishers, Division of John Wiley & Sons, New York, 1962) Vol. 2, p. 15, Electrochem Eng.

Thomas and Associates

Thomas, Gareth, with R. Benson and J. Washburn, "Dislocation Substructures in Deformed and Recovered Molybdenum," in Direct Observation of Imperfections in Crystals, edited by Newkirk and Wernick (Interscience Publishers, Division of John Wiley & Sons, New York, 1961).

Van Torne, Lenon I., "Yielding and Plastic Flow in Polycrystalline Niobium" (Master's Thesis), UCRL-10356, Aug. 1962.

Washburn and Associates

Washburn, Jack, with H. J. Queisser and R. H. Finch, "Stacking Faults in Epitaxial Silicon," J. Appl. Phys. 33, 1536-7 (1962).

Washburn, Jack, with R. Benson and G. Thomas, "Dislocation Substructures in Deformed and Recovered Molybdenum," in Direct Observation of Imperfections in Crystals, edited by Newkirk and Wernick (Interscience Publishers, a Division of John Wiley & Sons, New York, 1961).

Saada, George, "On the Stability of Quenched Dislocation Loops in Aluminum," Acta Met. 10, 985-986 (1962).